[illegible] 6

National Library of Canada
Canadian Theses Division
Ottawa, Canada
K1A 0N4

Bibliothèque nationale du Canada
Division des thèses canadiennes

51610

PERMISSION TO MICROFILM — AUTORISATION DE MICROFILMER

- Please print or type — Écrire en lettres moulées ou dactylographier

Full Name of Author — Nom complet de l'auteur
RICHARD WRIGHT

Date of Birth — Date de naissance
17th JULY 1955

Country of Birth — Lieu de naissance
ENGLAND

Permanent Address — Résidence fixe
6 GAZELEY RD, ASHLEY NEWMARKET SUFFOLK CB8 9EF,
ENGLAND

Title of Thesis — Titre de la thèse
"STABILITY ANALYSIS IN ROOM AND PILLAR
COAL MINING"

University — Université
UNIVERSITY OF ALBERTA

Degree for which thesis was presented — Grade pour lequel cette thèse fut présentée
MASTER OF SCIENCE

Year this degree conferred — Année d'obtention de ce grade
1981

Name of Supervisor — Nom du directeur de thèse
DR. M.L. JEREMIC

Permission is hereby granted to the NATIONAL LIBRARY OF CANADA to microfilm this thesis and to lend or sell copies of the film.

The author reserves other publication rights, and neither the thesis nor extensive extracts from it may be printed or otherwise reproduced without the author's written permission.

L'autorisation est, par la présente, accordée à la BIBLIOTHÈQUE NATIONALE DU CANADA de microfilmer cette thèse et de prêter ou de vendre des exemplaires du film.

L'auteur se réserve les autres droits de publication; ni la thèse ni de longs extraits de celle-ci ne doivent être imprimés ou autrement reproduits sans l'autorisation écrite de l'auteur.

Date
7th April 1981

Signature
RWright

NL-91 (4/77)

National Library of Canada
Collections Development Branch

Canadian Theses on
Microfiche Service

Bibliothèque nationale du Canada
Direction du développement des collections

Service des thèses canadiennes
sur microfiche

NOTICE

The quality of this microfiche is heavily dependent upon the quality of the original thesis submitted for microfilming. Every effort has been made to ensure the highest quality of reproduction possible.

If pages are missing, contact the university which granted the degree.

Some pages may have indistinct print especially if the original pages were typed with a poor typewriter ribbon or if the university sent us a poor photocopy.

Previously copyrighted materials (journal articles, published tests, etc.) are not filmed.

Reproduction in full or in part of this film is governed by the Canadian Copyright Act, R.S.C. 1970, c. C-30. Please read the authorization forms which accompany this thesis.

THIS DISSERTATION
HAS BEEN MICROFILMED
EXACTLY AS RECEIVED

AVIS

La qualité de cette microfiche dépend grandement de la qualité de la thèse soumise au microfilmage. Nous avons tout fait pour assurer une qualité supérieure de reproduction.

S'il manque des pages, veuillez communiquer avec l'université qui a conféré le grade.

La qualité d'impression de certaines pages peut laisser à désirer, surtout si les pages originales ont été dactylographiées à l'aide d'un ruban usé ou si l'université nous a fait parvenir une photocopie de mauvaise qualité.

Les documents qui font déjà l'objet d'un droit d'auteur (articles de revue, examens publiés, etc.) ne sont pas microfilmés.

La reproduction, même partielle, de ce microfilm est soumise à la Loi canadienne sur le droit d'auteur, SRC 1970, c. C-30. Veuillez prendre connaissance des formules d'autorisation qui accompagnent cette thèse.

LA THÈSE A ÉTÉ
MICROFILMÉE TELLE QUE
NOUS L'AVONS REÇUE

Ottawa, Canada
K1A 0N4

THE UNIVERSITY OF ALBERTA

STABILITY ANALYSIS IN ROOM AND PILLAR COAL MINING

by

© RICHARD WRIGHT

A THESIS

SUBMITTED TO THE FACULTY OF GRADUATE STUDIES AND RESEARCH

IN PARTIAL FULFILMENT OF THE REQUIREMENTS FOR THE DEGREE

OF MASTER OF SCIENCE

IN

MINING ENGINEERING

MINERAL ENGINEERING DEPARTMENT

EDMONTON, ALBERTA

SPRING 1981

THE UNIVERSITY OF ALBERTA

RELEASE FORM

NAME OF AUTHOR RICHARD WRIGHT

TITLE OF THESIS STABILITY ANALYSIS IN ROOM AND PILLAR COAL MINING

DEGREE FOR WHICH THESIS WAS PRESENTED MASTER OF SCIENCE

YEAR THIS DEGREE GRANTED SPRING 1981

Permission is hereby granted to THE UNIVERSITY OF ALBERTA LIBRARY to reproduce single copies of this thesis and to lend or sell such copies for private, scholarly or scientific research purposes only.

The author reserves other publication rights, and neither the thesis nor extensive extracts from it may be printed or otherwise reproduced without the author's written permission.

(SIGNED) ....

PERMANENT ADDRESS:

4 GAZELEY RD.,
ASHLEY, NEWMARKET,
SUFFOLK CB8 9EF,
ENGLAND

DATED 7th April 1981

THE UNIVERSITY OF ALBERTA

FACULTY OF GRADUATE STUDIES AND RESEARCH

The undersigned certify that they have read, and recommend to the Faculty of Graduate Studies and Research, for acceptance, a thesis entitled STABILITY ANALYSIS IN ROOM AND PILLAR COAL MINING submitted by RICHARD WRIGHT in partial fulfilment of the requirements for the degree of MASTER OF SCIENCE in MINING ENGINEERING.

M. Jeremic
Supervisor

Date March 20, 1981

To Ellen and Harold

Creation is the source of All things

Abstract

The research presented in this study is primarily concerned with the application of numerical modelling techniques to the stability analysis of coal mine structures. The work has been limited to room and pillar coal mining of flat and gently dipping (below 20°) seams.

Conventional analytic techniques are described, together with numerical and physical modelling techniques that are presently available. The boundary element computer program (DDSEAMS) which has been used in this analysis is described in detail, and the results of limited testing of the program are included. A stress analysis design concept is presented, which includes the development of a stress criterion for stability at a point.

Comparisons are made between the numerical model, a 3-D physical model, a base friction model and an underground phenomenological study at Grande Cache, Alberta.

An illustration of the stress analysis design concept is included, with reference to a proposed mine at Coal Valley, Alberta. This includes a detailed geotechnical testing program, and the analysis of a number of alternative mine geometries.

The major conclusions are:

* Improved stress analysis, compared to conventional methods, are obtained by using the numerical model presented.

* Definition of a stress criterion is useful for the

prediction of over-stressed regions that are potentially unstable.

- Where strata stress conditions or pillar safety factors indicate that failure will take place, the use of elastic analysis techniques is not adequate for the definition of the overall stability.
- The 3-D physical modelling qualitatively simulates pillar failures observed in the underground phenomenological study at Grande Cache
- Initial analysis indicates that extraction ratios greater than 50% may be possible by the "punch" mining method proposed at Coal Valley.

ACKNOWLEDGEMENTS

I would like to thank all those people who assisted me with help, guidance and encouragement during the course of this study. In particular I would like to give special thanks to the following:

Professor M.L. Jeremic whose guidance and encouragement provided the main foundation for this study.

The departmental technical staff, especially M. Gendron and L. Ding, for their invaluable assistance.

My fellow peers within the Rock Mechanics Department, especially C. Acott, A. Dhar, Z. Felbinger, H. Lutley, H. Soderberg and K. Williams, who endured my idiosyncrasies and pushed me on towards greater deeds.

The personnel of Luscar Ltd. and Luscar Sterco (1977) Ltd., who provided the information and drill core for the mine simulation study

The personnel of McIntyre Mines Ltd. for their help in the underground phenomenological study.

Luscar Ltd. for the financial support provided by the Luscar Scholarship, which enabled me devote more time to this study.

Table of Contents

Chapter Page

1. INTRODUCTION 1

2. CONVENTIONAL DESIGN ANALYSES 4

2.1 Pillar Stability Analyses 4

2.1.1 Pillar Load Estimation 4

2.1.2 Pillar Strength Criteria 7

2.2 Opening Span Stabilities 10

2.2.1 Roof Stability 11

2.2.2 Floor Stability 12

3. MODELLING TECHNIQUES 14

3.1 Numerical Modelling Techniques 14

3.1.1 Finite Element Method 14

3.1.2 Boundary Element Method 16

3.1.3 Block Models 16

3.2 Numerical Program (DDSEAMS) Adopted 17

3.2.1 Analytical Solution Comparisons 17

3.2.2 Program Optimisation 21

3.2.3 Simplified Mine Layouts 22

3.2.4 False Roof Tests 25

3.2.5 Multiple Seam Problems 27

3.3 Physical Modelling 28

3.3.1 Model Materials 28

3.3.2 Loading Conditions 29

3.3.3 Scaling Factors 30

4. STABILITY DESIGN CONCEPT ADOPTED 32

4.1 Stress Distributions 32
4.2 Pillar Stability 33
4.3 Strata Stress Criterion 33
4.4 Discussion of Design Concept Limitations 35

5. MULTI-SEAM STUDIES 38
5.1 Numerical Model 38
5.2 Base Friction Model 41
5.3 3-D Physical Model 43
5.4 Underground Phenomenological Study 44
5.5 Comparison of results 46

6. MINE DESIGN SIMULATION 51
6.1 Geology 51
6.1.1 Structure 51
6.1.2 Stratigraphy 52
6.2 Geotechnical Testing Program 52
6.2.1 Uniaxial Compression 53
6.2.2 Brazilian Disc 54
6.2.3 Triaxial Compression 55
6.2.4 Direct Shear 56
6.2.5 Slake Durability 56
6.2.6 Swelling Index 57
6.3 Rock Mass Parameters 57
6.4 Proposed Mining Method 60
6.5 Stability Analysis 60
6.5.1 Coal Pillar Strength 61
6.5.2 Numerical Analysis 63
6.6 Discussion of Results 64

6.6.1 Pillar Stability 65
6.6.2 Opening Stability 66
7. CONCLUSIONS 69
7.1 Modelling Techniques 69
7.2 Multi-Seam Studies 70
7.3 Mine Design Simulation 70
8. RECOMMENDATIONS 75
8.1 Modelling Techniques 75
8.2 Multi-Seam Studies 77
8.3 Mine Design Simulation 77
Bibliography 128
APPENDIX 1 (DDSEAMS PROGRAM DESCRIPTION)..........................137
APPENDIX 2 (CRACK PROGRAM)..........................193
APPENDIX 3 (PSTRESS PROGRAM)..........................196
APPENDIX 4 (DDSEAMS PROGRAM TESTING RESULTS)..........................200
APPENDIX 5 (GEOTECHNICAL CORE LOGS)..........................236
APPENDIX 6 (GEOTECHNICAL TESTING PROCEDURES)..........................258
APPENDIX 7 (GEOTECHNICAL TEST RESULTS)..........................265
APPENDIX 8 (MINE SIMULATION RESULTS)..........................277

LIST OF FIGURES

2.1 Square pillar layout plan 79

3.1 Configuration of flat elliptical crack 80

3.2 Analytical/Numerical vertical stress comparison 81

3.3 Simplified mine layout 82

3.4 Table of major parameters for runs 06 to 11 83

3.5 Stress results for run 08 84

3.6 Tabulated comparison of simplified layout 85

3.7 Pillar vertical stresses - Runs 14 & 15 86

3.8 Pillar vertical stresses - Runs 17 & 18 87

4.1 Mohr/Coulomb failure criterion 88

5.1 Mine layout for Run 19 89

5.2 Numerical results for upper seam (Run 19) 90

5.3 Numerical results for lower seam (Run 19) 91

5.4 Vertical stress (Run 19) 92

5.5 Horizontal stress (Run 19) 93

5.6 Major principal stress (Run 19) 94

5.7 Minor principal stress (Run 19) 95

5.8 Maximum shear stress (Run 19) 96

5.9 Stress Criterion (Run 19) 97

5.10 Base friction model layout 98

5.11 3-D physical model layout plan 99

5.12 Numerical/3-D physical model comparison (opening2) . 100

6.1 Sandstone triaxial test results 101

6.2 Mudstone triaxial test results 102

6.3 Coal triaxial test results 103

6.4 Pillar strength as a function of width.............104
6.5 Mine simulation layouts & pillar vertical stresses.105
6.6 Mine simulation layouts & pillar safety factors....106
6.7 Stress Criterion (0.75m into floor)................107

LIST OF PLATES

1. Base friction apparatus 108
2. MTS servo controlled stiff testing machine 108
3. 3-D model in compression frame 109
4. Base friction model - caving initiated 110
5. Base friction model - final cave 111
6. 3-D model (run1)-yield state 112
7. 3-D model (run1,opening 2)-yield state 113
8. 3-D model (run1,plan view,upper seam)-after test 114
9. 3-D model (run2,lower seam)-before test 115
10. 3-D model (run2,upper seam)-before test 115
11. 3-D model (run2,side view)-before test 116
12. 3-D model (run2,side view)-0.78 MN/m² 117
13. 3-D model (run2,side view)-yield state 118
14. 3-D model (run2,plan view,lower seam)-after test 119
15. 3-D model (run2,plan view,upper seam)-after test 120
16. Newly exposed pillar side and supports 121
17. Pillar expansion near roof 122
18. Pillar fracturing 123
19. Pillar expansion and failure of supports 124
20. Pillar expansion, floor heave and support failure... 25
21. Caved area and floor heave 126
22. Cave of immediate roof beds 127

1. INTRODUCTION

The object of this research was to demonstrate the application of a particular numerical analysis technique for assessing the stability of mining structures in room and pillar coal mining. A boundary element computer program (DDSEAMS) has been used, which is simple and inexpensive to operate, but which does have limitations in its applicability. These limitations are not restricted by current knowledge, but by the time required to develop suitable program packages for commercial use.

Room and pillar coal mining is a method whereby sections are developed on advance, usually consisting of parallel drives (rooms), and connected at frequent intervals to delineate rectangular coal pillars. In partial extraction the pillars are left to support the overburden. When complete extraction is performed, these pillars are extracted on retreat, and the roof strata are allowed to cave. The method is usually applicable to flat and gently dipping seams (dips less than 20°).

A major factor in the choice of mining method and mine layout, is the stability of the openings and pillars that are formed during extraction of the coal. This study is primarily concerned with the stability of pillars in room and pillar coal mining. However, the stability of openings cannot be ignored, as they interact with pillars in mine structures. Portions of the analysis will only be applicable to room and pillar coal mining of flat and gently dipping seams, but the methods adopted are applicable to many other mining methods which require openings and pillars.

A stress analysis approach, that is suitable for solution by numerical methods, has been adopted. Numerical problems are ideal for solution by digital computers, which are rapidly becoming faster, more powerful and inexpensive. It is probable that the future trend will be for every mine to have a small computer facility, or a communications link to a larger computer. Complex mine stability analyses are expensive, therefore they are currently beyond the finance and expertise of small mines. They are usually restricted to a small number of alternative geometries and conditions. In the future it is probable that stress analysis techniques may be used as routine mine design tools. They enable many alternative layouts to be analysed quickly and inexpensively, with a minimum of input data preparation.

Any engineering analysis requires that certain simplifications be made in the modelling of the real situation, in order to obtain a solution. Thus the simulations required are seldom perfect, and this is especially true for rock materials. The analysis is further complicated by the limited knowledge of the true rock mass behaviour, when it is subjected to complex loading conditions, common in mining situations. Therefore, assumptions have to be made in defining the rock mass behaviour, which are often further simplified for analysis purposes. This produces an element of uncertainty in the solution that can only be reduced by comparison with the real mining conditions. Real behaviour is difficult and expensive to determine comprehensively. Therefore the knowledge of the pre-mining stress field, and the stresses and displacements induced by mining, are seldom complete.

An attempt has been made to compare the stress analysis technique adopted in this study with physical models and an underground phenomenological study.

A mine design simulation study of a mine property at Coal Valley, Alberta, was undertaken. A limited number of possible mine geometries were analysed. The rock mass parameters were estimated from geotechnical testing of drill core from the proposed site.

2. CONVENTIONAL DESIGN ANALYSES

Conventional methods of analysing the stability of mine pillars and openings will be defined as those methods which do not require the use of digital computers in their routine solution. Numerical analysis techniques which require the use of computers for their solution will be described in the next chapter. The analysis methods have been divided into the methods that concern pillar stability and those that concern opening stability. This division is made for simplification purposes, but in reality pillars and openings interact in a complex manner. Only techniques that are applicable to flat and gently dipping seams (dip less than 20°) will be described.

2.1 Pillar Stability Analyses

In the analysis of pillar stability, the load that will be imposed on the pillar is estimated, and then this is compared with the strength of the pillar. From this comparison, safety factors for the stability of the pillars can be derived.

2.1.1 Pillar Load Estimation

Three methods for estimating the loads on pillars are presented. These methods are briefly described:

Tributary Area Theory

This is the simplest analytic technique, utilising the assumption that each pillar is loaded by the vertical column of overburden that is tributary to that pillar. The load is calculated as an average pillar stress, therefore the stress variation within the pillar is not accounted for. An example calculation for the square pillar layout in Figure 2.1 is shown below:

$$\sigma_{pa} = \sigma_v((Wo+Wp)/Wp)^2$$

σ_{pa} = Average pillar stress

σ_v = Pre-mining vertical stress

Wo = Width of opening

Wp = Width of pillar

This equation is a simple force balance for use in flat seams where the vertical normal stress is a principal stress direction [illegible] should not be used for workings that do not extend over [illegible] sufficient lateral extent, relative to depth (such that a [illegible] effects to the abutments are present), or for pillars [illegible] close proximity to large abutment pillars.

Beam Deflection Theories

Beam theories should be used when a roof arching effect is present. They also enable the non-uniform stress distribution across the pillar to be calculated.

The immediate roof strata are assumed to consist of one or more elastic beams (two-dimensional problem), which span the area of interest. In three-dimensional analysis the beams are replaced by plates, but the theory is similar. The beams are loaded by the overburden, which is assumed to provide a uniform load. The load is re-distributed onto the pillars, which are assumed to be elastic. The loading of the beam is transferred to the pillars, producing support reactions. Beam theory is used to obtain stresses, by assuming that the pillars respond in a similar manner to elastic foundations. Two-dimensional analysis is considered to be adequate when the length of the beam in the third dimension is greater than twice the span.

Equations have been developed to satisfy different end constraints, beam interactions and beam thickness. For thick beam analysis (Sheorey & Singh, 1974) the beam thickness is assumed to be greater than one fifth of the span, otherwise thin beam analysis (Stephansson, 1971) is employed.

Beam theory provides a better understanding of pillar stress distributions than the tributary area theory, and should be used when the pillar configurations are not constant. There are many assumptions adopted to define the roof strata beams and their end constraints, which require a high degree of engineering input and experienced judgement, to obtain meaningful results. Beam theory is applicable where roof strata beds are homogeneous, and can withstand tensile stresses. Sedimentary coal measures strata are usually weak, bedded and non-homogeneous (as a result of jointing), which reduces the applicability of beam theory.

Elastic Analysis

There are a number of analytical solutions in the theory of elasticity which can be related to underground openings. They are usually restricted to two-dimensional plane stress or plane strain analysis. The material is usually assumed to be an infinite, homogeneous, isotropic, linear elastic continuum. Simple opening geometries, which are usually aligned with the principal stress field, have been solved. Multiple openings can be simulated by combining results from single openings. The overall stress distribution is produced by summation of the distributions for each individual opening, utilising the principle of superposition. This method can be used to produce 3-D solutions by combining 2-D solutions in transverse planes.

Solutions for simple problems will not be presented as they can be found in many texts on rock mechanics and elastic theory (Timoshenko & Goodier, 1970; Hoek & Brown, 1980 and Coates, 1967).

2.1.2 Pillar Strength Criteria

Prediction of pillar strengths is difficult, primarily because of the non-uniform nature of the pillar loading, resulting in complex failure mechanisms. High stress concentrations on the sides of non-yielding pillars are generally encountered. Local failures are initiated in these regions as a result of low confining stresses. As the perimeter fails, the load is transferred towards the central core, increasing stresses within this region. The central core is more confined than the perimeter, and is therefore able to withstand higher stresses prior to failure. The pillar strength is usually defined as the maximum stress that it can support, and does not account for local failures (Wilson & Ashwin, 1972).

The pillar strength is a function of the material properties, its size, shape, end constraints and loading conditions. The estimation of pillar strength is usually undertaken by loading small pillars to failure, and by applying size and shape correction factors to these results

Pillar Size Factors

Compressive strength results are usually obtained by testing drill core samples or small coal pillars. Core samples are usually taken from the stronger coal seam material, becau of the problems associated with the preparation and handling of the weaker portions. These samples have fewer weakness planes and discontinuities than the real pillar, and therefore tend to have a higher strength.

Much work has been done in attempting to define the relationship between size and strength. These results have been summarized by Hustrulid (1976), and a formula has been derived which seems to fit the available data quite well. For model pillars less than 3ft. (0.91m) in height:

$$\sigma_c = k/\sqrt{H}$$

σ_c = Cube compressive strength
k = Constant for each coal
(compressive strength of a 1 inch cube)
H = Pillar height (inches)

For pillars with dimensions greater than 3ft. (0.91m), the cube compressive strength is essentially constant and is defined by:

$$\sigma_c = k/6$$

Therefore the pillar cube strength can be defined as one sixth of the compressive strength of a one inch cube, as mine pillars always have dimensions greater than 3ft.(0.91m).

Pillar Shape Factors

The compressive strength of rectangular pillars have been investigated, and found to be a function of their shape. Consequently, the relationships derived have been defined with respect to the width and height of the pillar. The majority of results indicate that there is a linear relationship between the pillar compressive strength and its width to height ratio. Hustrulid (1975) has analysed these results and found that one equation can be used which gives a reasonable fit to the majority of available data:

$$\sigma_p = \sigma_c(0.778 + 0.222\ W/H)$$

σ_p = Pillar compressive strength
σ_c = Cube compressive strength
H = Height of pillar
W = Width of pillar

These results indicate that mine pillar compressive strength for a particular coal is linearly dependent upon the shape factor alone, as the cube compressive strength of mine pillars may often be assumed to be constant. Most of the studies have been undertaken on small samples, which may not necessarily reflect the relationship for the real mine pillars.

2.2 Opening Span Stabilities

In room and pillar mining the pillars are delineated by the openings, consequently the sides of the openings are also the sides of the pillars. Therefore this description will only address the stability of the roof and floor strata, as the pillar stability has already been discussed. Only rectangular openings will be considered, as they are common to room and pillar coal mining. If the span is found to be unstable, then support must be installed to maintain stability.

2.2.1 Roof Stability.

Roof strata can be analysed by using beam theory, as described previously for pillar load calculations. The analysis can be simplified, as failure is expected to be initiated at the centre or abutments of each span. Therefore only the stresses and displacements at these points are required. Expressions for the maximum normal and shear stresses are given by Duvall (1976) for a gravity loaded beam clamped at both ends. For beams with a span to thickness ratio greater than five the maximum tensile stress is more than three times the maximum shear stress. The tensile strength of rock is usually much less than the compressive and shear strengths, and therefore a design formula is derived based on the tensile strength:

$$T = \gamma . F . L^2 / 2 . \sigma_t$$

T = Thickness of beam
γ = Unit weight of rock
F = Safety factor
L = Span length
σ_t = Tensile strength

The safety factor in tension should be between 4 and 8

(Duvall, 1976). From this equation a required roof beam thickness can be calculated, and if this beam is not present, then a composite beam should be formed by bolting rock layers together.

Where high horizontal stresses are present, design on the basis of tensile strength may not be applicable. Tensile stresses will be reduced, and may even be eliminated. In these cases the design should be based on the shear or compressive strength of the strata. Strata failures resulting from high horizontal stresses have been observed by Parker (1973). These include shear failures close to the abutments of the opening, and compressive failures at the centre of spans.

Where analysis of structural geology indicates that jointing may cause problems, it may be necessary to design supports to stabilise any wedges formed in the roof. These wedges can be defined by plotting stereonet projections of joint systems and bedding planes.

2.2.2 Floor Stability

Floor stability problems occur when weak, thinly bedded strata are enountered. The competence of floor beds is usually reduced when water is present. Floor failures usually indicate that high horizontal stresses are causing buckling failures of thin unconfined beds. These failures are enhanced when pillars load the floor strata beyond its bearing capacity. The combined failures result in floor migration into the entry (floor heave). This is usually a time-dependent phenomenon, but in highly stressed regions closure of excavations can take place in a matter of days.

Floor heave is difficult to predict, as it results from both floor beam failures into the opening and floor failures below pillars. The interactions between pillar and floor are not well understood, as complex behavioural mechanisms are present. As a result analysis is usually based on past experience and engineering judgement. Floor heave may be controlled by reinforcement of floor strata (e.g. rock bolting), or by reducing the pillar stresses close to the opening.

3. MODELLING TECHNIQUES

The simulation of reality by various modelling techniques is discussed, together with their applicability to various mine situations. The techniques that will be adopted in this study are described in more detail.

3.1 Numerical Modelling Techniques

Numerical modelling techniques have developed rapidly after the advent of the digital computer, which enables many repetitive computations to be performed on large quantities of data. This allows the simplification of complex problems into a series of discrete units which have known solutions. These discrete units are analytically independent, but are connected to form the complex problem, and a solution is obtained by satisfying defined boundary conditions.

In analysing physical structures in rock the discrete units may be boundary elements, finite elements or blocks. Each element or block is defined as having a prescribed relationship between stress and strain, or load and deformation. The combination of these units simulates the overall mine structure. The approximation introduced by this discretisation is usually adequate for engineering applications.

3.1.1 Finite Element Method

With the finite element method the rock structure is divided into a series of elements which are connected at nodal points to form a framework. In two-dimensional analysis these elements are polygonal (commonly triangles or quadrilaterals), and are assumed to have unit thickness in the third dimension. Forces or displacements applied to the element nodes produce stresses and strains within the element, which are translated into displacements at the nodes. The elements are connected together at the nodes to form a continuous structure. The forces and displacements must be compatible at each node. The relationship between forces and displacements is defined by a series of equations which depend upon the material parameters, the element geometry, and the degree to which the strain is permitted to change across the element. A system of equations is produced which is solved to satisfy the boundary conditions.

The elements should extend beyond the area of interest, such that boundary conditions can be specified that do not interact with the mine structure. Planes of symmetry are often utilised to define boundaries and reduce the number of elements that are required to define the problem area. The method produces continuous variation of stress and strain within elements, but not between elements. In order to model the real situation with sufficient accuracy, a higher element density is required in regions of rapid stress variation, such as excavation boundaries.

The advantage of using a discrete structure is that different parameters can be assigned to each material type, such that the physical structure is more completely defined. More complex rock mass behaviour can be modelled by using special elements (e.g. for joints) or complex material behaviour (non-linear elastic, elasto-plastic, visco-plastic or no-tension analysis) (Zienkiewicz, 1977).

3.1.2 Boundary Element Method

The boundary element method involves the discretisation of the boundary of the excavations alone. Integral equation methods are used to produce a fully continuous solution for the stress distribution over the whole area (closed form solution). This results in a much smaller system of equations than the finite element method and a consequent reduction in computer time and data preparation. The major disadvantage of the boundary element method is that it usually requires the rock mass to be homogeneous, and have linear elastic properties. It is possible to define zones with different physical properties by developing special interface elements (Banerjee, 1976), but the technique requires further development.

3.1.3 Block Models

Block models can be used to simulate blocky or jointed strata as a discrete system of rigid blocks. These blocks interact with one another at edges and corners, where force and displacement conditions are satisfied. The system is solved by analysing the forces, displacements, velocities and accelerations of blocks for incremental time steps until equilibrium is attained.

Cundall (1971) has developed a computer model to solve a class of low stress, strong rock problems; where block internal stresses are not important, and large displacements are to be expected. In reality, blocks delineated by joint systems probably only contact at a few points and thus the analysis of these contact forces have practical validity.

3.2 Numerical Program (DDSEAMS) Adopted

A boundary element program (DDSEAMS) was used in this study (Crouch, 1976), which is described in Appendix 1. The numerical technique involves using displacement discontinuity boundary elements and solving the system of influence coefficients for the defined boundary conditions. The program was tested to ensure that it was operating correctly, before being applied to any mine modelling.

3.2.1 Analytical Solution Comparisons

In order to check the program for any computational errors, and to give an indication of the accuracy of the analysis technique, a simple comparison was carried out between the DDSEAMS program output and the closed form solution for a thin crack in a triaxial stress field.

Closed form solutions for flat cracks (slits), in an infinite, homogeneous, linear elastic, isotropic continuum, exist for various crack geometries and stress conditions.

The solution for a flat elliptical crack was chosen for comparison; The long axis being of infinite length in the z direction (Figure 3.1), in a three-dimensional stress field. This solution simulates the plane strain condition, which is calculated using DDSEAMS with the material parameters chosen to simulate an isotropic continuum. The analytical solution takes the following form (Bray, J.W. unpublished notes):

(a) Along the x axis:

$$\sigma_x = P_y(\lambda_x - 1) + P_x$$

$$\sigma_y = \lambda_x . P_y$$

$$\sigma_z = 2.\nu.P_y(\lambda_x - 1) + P_z$$

$$\tau_{xy} = \lambda_x . P_{xy}$$

$$\tau_{yz} = \lambda_x . P_{yz}$$

$$\tau_{zx} = P_{zx}$$

$$\lambda_x = 1/\sqrt{w^2/4x^2}$$

(b) Along the y axis:

$$\sigma_x = P_y(2.\lambda_y - \lambda_y^3 - 1) + P_x$$

$$\sigma_y = P_y . \lambda_y^3$$

$$\sigma_z = 2.\nu.P_y(\lambda_y - 1) + P_z$$

$$\tau_{xy} = P_{xy}(2.\lambda_y - \lambda_y^3)$$

$$\tau_{yz} = \lambda_y . P_{yz}$$

$$\tau_{zx} = P_{zx}$$

$$\lambda_y = 1/\sqrt{w^2/4y^2}$$

(c) Along roof and floor:

$$\sigma_x = P_x - P_y - \frac{x.y}{|x.y|}\,\frac{2.P_{xy}}{\sqrt{w^2/4x^2 - 1}}$$

$$\sigma_y = 0$$

$$\sigma_z = P_z + \nu(\sigma_x - P_y - P_x)$$

$$\tau_{xy} = 0$$

$$\tau_{yz} = 0$$

$$\tau_{zx} = P_{zx} - \frac{x.y}{|x.y|}.\frac{P_{yz}}{\sqrt{w^2/4x^2 - 1}}$$

(d) At edge of crack (sides):

$$\sigma_x = 0$$

$$\sigma_y = \infty P_y - P_x$$

$$\sigma_z = P_z + \nu(\infty P_y - 2.P_x)$$

$$\tau_{xy} = 0$$

$$\tau_{yz} = \infty P_{yz}$$

$$\tau_{zx} = 0$$

σ_x = Normal stress in x direction

σ_y = Normal stress in y direction

σ_z = Normal stress in z direction

τ_{xy} = Shear stress on x plane in y direction

τ_{yz} = Shear stress on y plane in z direction

τ_{zx} = Shear stress on z plane in x direction

ν = Poisson's Ratio

P_x, P_y P_z = Field normal stresses

P_{xy}, P_{yz}, P_{zx} = Field shear stresses

w = Width of slit

(H/w is assumed to tend to zero)

A simple program has been written to calculate some of the solution results. The listing of program (CRACK) is presented in Appendix 2, together with an example of the output.

A run of DDSEAMS was made, with similar conditions to the analytical solution, using a total of eighty elements (forty for the crack). Isotropic material parameters were used in the solution, and the comparison of results for the vertical stress component (σ_y) is presented graphically in Figure 3.2.

The most important stress component is the vertical stress, as this indicates the pillar and abutment loading. As can be seen from Figure 3.2; deviation of the results from program DDSEAMS and the analytical solution, does not exceed 10%. The greatest deviation occurs close to the opening, where the boundary element approximations will have greatest effect. Considering the engineering applications of program DDSEAMS in mine design, this deviation is acceptable. This program has greatest benefit in providing comparisons between alternative mine layouts.

3.2.2 Program Optimisation

A number of similar runs of program DDSEAMS were made simulating identical single span conditions, but with different numbers of elements defining the spans. The results of these runs are summarised graphically in Appendix 4.

In general the smaller number of elements that are used to define the span, the greater is the over-estimation of stresses and displacements. As the number of elements (NSEG) is reduced from 40 to 10 for the span, there is almost no difference between the results. With a 6 element span the errors are more noticeable, but still within approximately 10% deviation from the 40 element span (these results are presented in Appendix 4 for Run Numbers 1 to 4). This means that for the purposes of mine design a 6 element span is acceptable. For greater accuracy a 10 element span will give results that are very close to the 40 element span results.

The results are only given for x co-ordinates at the centre of each element, as this is the position for which the solution is derived. Greater detail of the stress, strain and displacement distributions requires a larger number of elements, to increase the number of internal points calculated.

3.2.3 Simplified Mine Layouts

This section contains the analysis of a simple mine design problem, The analysis is restricted to the variation of three parameters, to facilitate greater understanding of the problem. In reality a comprehensive design approach would include the analysis of additional parameters, and the use of other analysis methods for comparison.

The particular problem analysed is that of twin headings (rooms) driven parallel to each other for the full height of a flat seam (Figure 3.3). The first four program runs (Runs 06, 07, 08 & 09) investigate the effect of variations in the width of the central pillar on the stresses and displacements (all other parameters held constant). The last two runs (Runs 10 & 11) investigate the effect of variation of elastic parameters for the seam and country rock, with the geometry the same as Run 08. The input data for these runs can be seen in Figure 3.4. The horizontal stress has been assumed to be 1/3 of the vertical stress by considering the elastic material to be loaded by the overburden with lateral constraint preventing horizontal strain. The graphical output from these program runs can be seen in Appendix 4 (note that metric units have been used after Run 06). The stress components for the Run 08 results are presented in Figure 3.5, where they may be compared directly to the physical layout. These diagrams show three of the major parameters of concern; the vertical stress within the seam, the horizontal stress, and the shear stress within the immediate roof span.

Diagram A (Figure 3.5) clearly shows the increase of stress within the central pillar and the span abutments. It is interesting to note that the maximum stress (pre-failure) within the pillar occurrs at its sides, and not at the centre (this has been demonstrated by Wagner, 1974). The average pillar stress is 15.0 MN/m^2 greater than the initial stress state of 25.0 MN/m^2, an increase of the average pillar vertical stress by 60% of its initial state.

Diagram B (Figure 3.5) indicates the reduction of horizontal stresses within the immediate roof (1.5m above the top of the seam), and the appearance of tensile stresses above the pillar. Tensile stresses are very undesirable in mine structures, as most rocks have low tensile strength.

Diagram C (Figure 3.5) shows the shear stress developed within the immediate roof (1.5m above the top of the seam). The maximum values occur above the pillar and side abutments. These are potential roof failure zones (especially with weak, thinly bedded strata), where beam type failures are common. The combination of tensile stresses, together with hig shear stresses above the pillar sides, creates a potential failure zone. The important results from all six runs are tabulated in Figure 3.6.

Analysis of the pillar and abutment stabilities, requires knowledge of the pillar strength characteristics. The vertical stress on the pillar can be compared with its estimated strength to calculate a safety factor. If an acceptable safety factor is not achieved, the pillar will be regarded as being unstable. From physical considerations the small pillar (width 1.5m) in Run 09 would normally be classified as unstable, because of its low width to height ratio (0.5).

The design of stable spans for openings is often undertaken utilising past experience, and observation of experimental openings. These analyses do not take into account the interactions with adjacent openings, as have been investigated here. A simple analysis can be undertaken by estimating the stresses within the immediate roof (1.5m above the top of the seam). The horizontal and shear stresses at the abutments and pillar sides are the major factors for consideration. Where spans are large, the stresses and displacements at the centre of the span may be more important, as there is no vertical support for any failed region. The results in Figure 3.6 indicate that tensile stresses, together with high shear stresses, may create instability around the 3m pillar (Run 08). These tensile stresses are not present in the roof above the 6m pillar (Run 07) and indicates that the 6m pillar may give a satisfactory span stability.

Variation of the elastic moduli of the seam and country rock, were analysed to determine the sensitivity of the mine structure (Run 08 - 3m pillar). The effect on the pillar stability was the same for the two Runs (10 & 11); doubling the country rock stiffness, or halving the seam stiffness, reduced the average pillar stress by 5.4 MN/m^2. The effect on roof span stresses and displacements was very small for the seam stiffness variation, but the increase in country rock stiffness reduced the displacement at the centre of the span by 35%.

This simplified analysis indicates that both pillar and roof span stabilities are influenced by variations in the physical layout. Variations in the material constants have a significant effect on pillar stability and a marginal effect on roof span stability.

3.2.4 False Roof Tests

It has been suggested (Crouch & Fairhurst, 1973) that layered strata with varying mechanical properties, can be modelled with unmined coal seams. Because of the nature of the numerical model used, the validity of this hypothesis in modelling false roof conditions was tested. A false roof refers to the existence of an immediate roof stratum with different mechanical properties than the surrounding rock. The results of Run 16 (identical to Run 08, except that a false roof has been modelled by another seam), can be seen in Appendix 4. Run 16 has a false roof with mechanical properties that are 100 times stiffer than the country rock values.

The particular simulation is of a pillar, delineated by an opening on either side. The creation of these openings increases stresses within the central pillar. These stresses should be reduced in Run 16, as a result of the stiffer roof beam. The investigation of the vertical stresses at the centre of the pillar is adequate, as they are linearly dependent upon the closure between roof and floor. Both sets of results indicate a vertical stress at the centre of the pillar of 39.4 MN/m^2, and hence the modelling of layered strata using coal seams is not a valid practise. Upon studying the nature of the numerical model, these findings can be readily understood. A coal seam is modelled by creating a hypothetical crack that has the top and bottom attached to one another by elastic springs. Upon excavating portions of the seam, these springs are removed, thereby removing the reactions between roof and floor. The induced stress distribution is created by the displacements which take place on these crack surfaces. Therefore the presence of a seam does not change the mechanical properties of the country rock, but only the displacements which take place on the crack surfaces. For a seam which has mechanical properties of infinite magnitude one would expect that no displacements will take place on the crack surfaces, and consequently there will be no induced stresses. The conclusion is that coal seams cannot model strata that are stiffer than the country rock.

3.2.5 Multiple Seam Problems

This section will investigate the interaction between excavations and pillars in two adjacent seams. The results demonstrate the validity of the numerical technique and illustrate simple interactions.

Runs 14 & 15 model two seams which are relatively far apart, each having two openings and one central pillar. The effect of offsetting the pillar in the lower seam is investigated and the graphical results are presented in Appendix 4. The physical positions of these two seams can be seen in Figure 3.7. The in-seam vertical stresses are most sensitive to the interaction mechanism, and are presented in Figure 3.7 for specific positions. It can be seen that the two seams are sufficiently far apart, in comparison to the excavation size, so that vertical stress changes as a result of interactions are small.

The seams were moved closer in Runs 17 & 18 (Results in Appendix 4) to increase the interaction effects. The physical structure, and major vertical stress values for the upper seam are shown in Figure 3.8. The vertical stresses are transferred to the right abutment in the upper seam, as the lower seam openings are moved to the left. This results from the location of the right excavation in the upper seam above the right abutment zone in the lower seam. This increase in the abutment stress is 12.5%, illustrating the adverse effects of offsetting mine structures in contiguous multi-seam mining.

3.3 Physical Modelling

Problems associated with mine structures usually involve some type of rock failure mechanism, that is difficult to simulate with numerical modelling techniques. As in all rock mechanics problems, the most important factors for consideration are the rock mass parameters, and the recognition of the failure mechanisms involved. Sedimentary rock structures are usually discontinuous, because of the presence of bedding and jointing. Physical modelling techniques have been developed to simulate the complex behavioural mechanisms which are associated with these strata types.

In physical modelling there are two basic problems; the simulation of the initial stress state by the loading conditions, and the rock mass behaviour. These two problems are interrelated because of the limitations of some loading methods, especially those involving body forces where the use of weak model materials is necessary. Loading conditions can be simulated by utilising friction, gravity, momentum or direct pressure.

3.3.1 Model Materials

The varieties of model materials are numerous (Stimpson, 1970) and they seldom model the real rock mass behaviour perfectly. The material is usually chosen to model the parameters which are considered to be of major importance. Selection of scaling parameters is dependent upon the predominant behaviour; Young's Modulus and Poisson's Ratio for modelling elastic deformations, compressive and tensile strengths for modelling plastic deformations (and failure), dilatancy and friction angle for modelling discontinuities.

3.3.2 Loading Conditions

Direct pressure is usually employed when biaxial or triaxial conditions are simulated. Difficulty is associated with producing boundary loading conditions that are capable of differential displacements whilst still maintaining uniform loading. This problem arises from the physical limitations of producing a model that has the boundary sufficiently far from the mine structure to avoid interactions.

Body forces provide a means of reducing the effect of the boundary by loading each individual model element in proportion to its mass. Gravitational loading is proportional to density, which is difficult to vary, and usually affects other model parameters. Centrifugal loading involves rotation of the model to induce angular acceleration forces and provides the means of varying the loading conditions independent of the model material. Impulse loading has been used by vibrating the model in a controlled manner, but this produces cyclic loading conditions and is more suitable for earthquake or blasting vibration simulation. Base friction loading is commonly employed as it allows more control over the model material preparation, and the ability to stop and start the model test at any point (Goodman, 1976). The body forces are simulated by the friction between the model material and its base. The friction forces may be varied with material density, base friction factor, or by loading a plate placed over the material.

Special conditions may be simulated by combinations of different loading methods. Models usually simulate two-dimensional plane stress conditions, because of the ease of preparation and observation of the model response.

3.3.3 Scaling Factors

In model studies, it is not only necessary to scale the physical dimensions, but also other independent parameters involved. Based upon dimensional analysis, the following equations can be used to match the scaling factors:

$$(\rho Lg/E)_{\text{model}} = (\rho Lg/E)_{\text{actual}}$$

$$(E/\sigma)_{\text{model}} = (E/\sigma)_{\text{actual}}$$

ρ = Density

L = Characteristic length

g = Gravitational acceleration

E = Young's Modulus

σ = Stress conditions

Strength scaling is usually matched to the geometric scaling, or to the loading conditions. Dynamic similitude is not obtained in base friction modelling, but this is not usually considered to be important in studying excavation stabilities.

4. STABILITY DESIGN CONCEPT ADOPTED

The concept of utilising stability analyses for routine mine design problems is presented together with a discussion on their applicability to real mine situations. Emphasis will be placed on the numerical modelling technique utilised (DDSEAMS program); as such techniques become more powerful, their use as routine design tools will increase. The limitations of this approach will not be overlooked, but the potential for future development should not be clouded with excessive criticism of present capabilities.

4.1 Stress Distributions

Mine geometries can be seldom simplified to apply techniques such as the tributary area theory, especially when multiple seam mining is undertaken. The numerical modelling technique adopted was used to analyse the interactions induced between mine openings. The particular program used is a two-dimensional formulation, but it could be adapted for three-dimensional analysis. Elastic analysis is used, as this allows a boundary element technique for seam modelling. This reduces the input data by one dimension (i.e. the 2-D analysis only requires 1-D input data on opening geometry). The real behaviour of the rock mass is usually unknown, therefore it is not necessary to undertake a more complex analysis.

4.2 Pillar Stability

The pillar stability is a factor of the complete stress/strain (load/displacement) characteristics of the pillar. The numerical model assumes the pillars to be elastic and therefore localised failures resulting in stress re-distributions are not accounted for. Hustrulid (1975) presents pillar compressive strength criteria based on empirically derived size and [illegible] factors (section 2.1.2). The pillar strength is equivalent to the maximum average stress that the pillar is able to withstand, and therefore localised failures are empirically accounted for.

Individual pillar stability can be estimated by assuming that the average stress on the pillar is equal to the average stress predicted by the numerical model. A safety factor is then defined as the pillar strength divided by the average pillar stress. If the safety factor is greater than 1.0 then pillar failure is not predicted to occur. Pillar failure is predicted for safety factors less than 1.0, but then the actual value has no physical meaning. Stress re-distributions in the overall structure occur when pillars fail, and these are not accounted for in the numerical model.

4.3 Strata Stress Criterion

There are a number of failure criteria that define the strength and failure mechanism of competent brittle rock in triaxial compression. The linear Mohr/Coulomb failure theory will be discussed (Kidybinski & Babcock, 1973), as the failure envelope is assumed to have a linear relationship between shear and normal stresses. The stress state can be defined by drawing the Mohr circle intersecting the normal stress axis (zero shear stress) at the major and minor principal stress values. An example of a failure envelope and a stress state can be seen in Figure 4.1. Failure takes place if the Mohr circle intersects or touches the failure envelope. The definition of the relative position of the Mohr circle, with respect to the failure envelope, can be used as a basis for assessing the stability at a point.

In attempting to define the stability of a particular stress state the stress path to failure must be defined (Kidybinski & Babcock, 1973). This path is unknown, and a criterion that involves uniform expansion (or contraction) of the Mohr circle is employed. Thus a stress criterion (SC) was developed from Figure 4.1, given below:

$$SC = (Q-R)/Q = 1 - (\sigma_1-\sigma_3)/\mathrm{Sin}\phi.(\sigma_1+\sigma_3+2.C/\mathrm{Tan}\phi)$$

SC = STRESS CRITERION

Q = Distance from centre of Mohr circle to envelope

R = Radius of Mohr Circle

σ_1 = Major Principal stress

σ_3 = Minor Principal stress

ϕ = Internal friction angle

C = Cohesion

This gives a value of zero when the point of failure is reached, is positive when conditions are stable, and negative when failure has been exceeded.

If a safety factor is required it can be obtained from:

Safety Factor = 1.0 / (1.0 - SC)

The use of the stress criterion derived is adequate for defining stable and unstable conditions at a point. A small computer program (PSTRESS) was developed to read the results from the DDSEAMS program and calculate the principal stresses and stress criterion. The program listing and sample output are presented in Appendix 3.

4.4 Discussion of Design Concept Limitations

Some of the analysis limitations are discussed in the following chapters, together with comparisons between the numerical model, two physical models and an underground phenomenological study. The major limitations and suggestions for avoiding these are presented in this section.

Critical analysis of the adopted approach requires understanding of reality, and relating this to the modelling simplifications. If insufficient data is available on the rock mass parameters and post-failure behaviour, then complex modelling using assumed values is inapplicable. In any analysis the quality of the output can never be better than the quality of the input.

Previous work (Ortlepp & Cook ,1964; Ortlepp & Nicoll, 1964 and Salamon & Oravez, 1970) has indicated that stratified rock masses can be simulated as linear elastic bodies with reasonable accuracy. Starfield & McClain (1973) have investigated non-linear behaviour (creep) in salt pillars, loaded by an elastic rock mass, and achieved acceptable results. These results indicate that if, non-linear behaviour in the proximity of the mine structure is modelled, the remainder of the rock mass can be assumed to be linearly elastic. The remaining problem is to define the non-linear and post-failure behaviour of the rock mass in the vicinity of the mine structure. The modelling of these areas is more suited to finite element techniques (Kidybinski & Babcock, 1973), as different parameters can be allocated to regions according to the pre-defined degrees of failure. The boundary element program formulation may be adapted to model non-linear behaviour within the seam, but the country rock must have a linear elastic behaviour.

The advantage of using the DDSEAMS program is that the sensitivity of the mine structure to parametric and geometric variations can be investigated relatively easily. The choice of a preferred geometry can be made, on the basis of defined factors (e.g. minimising unstable regions), by analysing various mine geometries. If the analysis indicates that failure will occur, then the results will not be a true model of reality. The occurrence of failures involve stress redistributions that are not accounted for in the numerical model. A more accurate prediction can be obtained by finite element analysis or physical modelling with correct similitude.

Back analysis techniques should be used wherever possible to ensure that the model adequately simulates the real rock mass. Where time dependent behaviour is encountered a further dimension is added to the problem, greatly increasing the complexity.

The strata stress criterion only indicates potential failure zones, and not the stability of the overall structure. Therefore it does not define the final failed regions, as stress re-distributions as a result of failure are not accounted for.

Pillar safety factors are adequate for stable conditions (all pillar safety factors greater than 1.0). If any pillars have safety factors less than 1.0, the values for the remainder of the pillars do not account for the stress re-distributions that will occur.

5. MULTI-SEAM STUDIES

A comparative study was undertaken to model more complex multi-seam interactions with the numerical technique and compare the results with two physical models and an underground phenomenological study. No suitable mine data was available, consequently the simulation presented was designed primarily for physical and numerical model comparisons. The layout presented is based upon an operating mine at Grande Cache, Alberta. The upper seam position has been moved closer to the lower seam, to match the dimensions of the physical model apparatus, and to increase the seam interactions. Therefore the model geometry is not a perfect representation of the actual mine situation.

5.1 Numerical Model

The geometric layout for the model is presented in Figure 5.1, where large openings have been excavated in the lower seam to simulate de-pillaring operations. Openings in the upper seam have been introduced to simulate development work concurrent with undermining operations. The results for the two seams are presented graphically in Figure 5.2 and Figure 5.3, together with the input parameters.

A grid system of data points was set up, and the analysis results from these points were used to develop a series of contour plots of major results. These contour plots only depict the results for the country rock. The vertical and horizontal stress contours are presented in Figure 5.4 and Figure 5.5 respectively. The analysis results were used as input data to the PSTRESS program and principal stress, maximum shear stress and stress criterion values were produced. Contour plots of major principal stress, minor principal stress, maximum shear stress and stress criterion values are presented in Figure 5.6, Figure 5.7, Figure 5.8 and Figure 5.9 respectively. A contouring package available at the University of Alberta (Surface II) was used to produce these plots. The smoothness of these plots is a function of the coarse grid pattern adopted. The potentially unstable areas predicted by negative stress criterion values are shaded in Figure 5.9.

The vertical stress contours (Figure 5.4) indicate the induced stresses as a result of excavating the mine openings. The initial vertical stresses at the upper and lower seam depths are 11.5 and 12.5 MN/m^2 respectively. The high stress gradients at the pillar abutments are evident (the smoothness of the stress contours in these regions is reduced because of the contour package used). The vertical stress relief above the openings is more pronounced above opening No.4 in the lower seam, as a result of opening No.1 located above it in the upper seam. The average vertical stress on the pillars (tabulated on page 48) indicates that the small pillar between openings 3 and 4 has an average vertical stress of 33.0 MN/m^2. If this average stress had been estimated by the tributary area theory, then an average stress of 60.4 MN/m^2 would be expected. This indicates the improved stress prediction capabilities of the numerical model which accounts for the proximity of the abutments.

The horizontal stress contours (Figure 5.5) also indicate the stress relief above the openings, but to a lesser degree than the vertical stress relief. High horizontal stress gradients below opening No.1, combined with low vertical stresses, indicate potential instability that is confirmed in the stress criterion contour plot.

The major principal stress contours (Figure 5.6) and minor principal stress contours (Figure 5.7) indicate that the horizontal stress is the major principal stress in zones of vertical stress relief. In zones of high vertical stress the vertical stress is the major principal stress.

The maximum shear stress contours (Figure 5.8) indicate the high shear stress gradients at the corners of openings. These are also predicted by the stress criterion to be areas of potential failure. The stress criterion is based on intact rock shear failure and therefore the maximum shear stress is the major variable which indicates possible failure zones. However, it does not allow for the influence of the principal stresses and therefore does not give a complete indication of the potential for failure.

The stress criterion contours (Figure 5.9) gives a much improved prediction of over-stressed regions. The over-stressed region below opening No.1 is evident, and this region has not been predicted to be over-stressed by the maximum shear stress alone. The small over-stressed zones at the extremities of the upper seam are a result of boundary condition limitations of the numerical model.

The material strength parameters have been simplified to give zero cohesion and internal friction angles given below:

Material	Location	Internal Friction Angle
MUDSTONE	above top seam	30.0°
SILTSTONE	between seams	32.0°
SANDSTONE	below lower seam	35.0°

These assumptions were made on the basis of published data (Hoek & Brown, 1980) for these rock types, as no test data was available. The internal friction angle was taken from the tangent to the failure envelope at a confining stress equal to 50% of the uniaxial compressive strength.

5.2 Base Friction Model

One base friction model run was made, primarily to investigate the caving characteristics of bedded strata. The base friction apparatus consists of an electrically driven sand paper belt (Plate 1). A flour and methanol model material was used, that was easy to prepare and cut. The layout prior to excavation (Figure 5.10) is similar to the numerical model, except that an additional opening was made in the upper seam. The model material is stronger than the stresses imposed by the base friction loading, and therefore failure along discontinuities is predominant. The horizontally bedded strata were modelled by cutting beds at 5.1cm intervals, with two 3.8cm beds above the lower seam, and a seam thickness of 5.1cm. The real height of the opening is 3.5m, representing a geometric scale factor of 1/69. The development openings in the upper seam were excavated first, followed by the two openings on the right hand side of the lower seam. The main openings (No.3 and No.4) in the lower seam were then excavated with no significant displacements till the openings reached their full spans (Plate 4). The initial roof failure occurred above these spans; with the two immediate beds failing and significant bed separation of the two above. The small central pillar in the lower seam was then excavated, to simulate failure, and the resultant cave is shown in Plate 5. Significant bed separation up to six beds above the lower seam was observed, with the subsidence profile in the upper strata well pronounced. A cave angle of approximately 70° was observed at both abutments.

The base friction model is very qualitative and cannot be used to accurately predict the real situation. However, it does serve as a useful model to indicate the behaviour of discontinuous strata around excavations.

5.3 3-D Physical Model

The 3-D physical model was developed to simulate the fracture characteristics of pillars (Szwilski & Whittaker, 1975) and to observe multi-seam interactions qualitatively. The coal pillars are modelled by plaster-of-paris cement and the rock strata by a series of rubber strips. The rubber strips offer a lateral strain effect and a high rubber/pillar (strata/pillar) contact friction factor. The model is loaded uniaxially in a 200 ton compression frame (Plate 3) by a hydraulic ram connected to a braced steel plate 0.91m by 0.61m.

Two models were constructed, Run 1 had 5.1cm thick seams, and run 2 had 3.8cm thick seams.The horizontal scale factor was 1/120 for both runs and the vertical scale factors were 1/60 for Run 1 and 1/90 for Run 2. The plaster mix used had a uniaxial compressive strength of 5.2 MN/m^2. Attempts were made to produce weaker pillars of plaster/sand mixes, but these were abandoned after encountering problems with pouring and handling large pillars. The pillar layouts in the two seams are shown in Figure 5.11 (both runs identical) and the assembly for the Run 2 model is shown in Plates 9, 10 & 11.

The model was progressively loaded and photographs were taken at intervals, until a yield state was reached. The yield state was indicated by the peak load condition, associated with increased displacement of the model. The yield state of Run 1 was at 20 MN/m^2 ram pressure

(0.96 MN/m² average model stress), shown in Plate 6. The deformation of opening No.2 is shown in Plate 7; floor heave, roof sag and pillar slabbing failures were observed.

After failure the model was dismantled and the pillar failures were observed in detail. A plan view of openings No.1 and No.2 in the upper seam is shown in Plate 8. Note that there has been a much greater slabbing failure of pillar sides in opening No.2.

Run 2 was loaded in a similar manner and pictures of model average stresses of 0.78 MN/m² and 0.92 MN/m² (yield state) are shown in Plates 12 & 13 respectively. One of the pillars between openings No.5 and No.6 in the lower seam, shown in Plate 14, illustrates the pillar fractures running parallel to the pillar sides. This pillar failure mode is further emphasized in the upper seam between openings No.1 and No.2 (Plate 15).

5.4 Underground Phenomenological Study

The subject of this study is a coal mine located at Grande Cache, Alberta. The coal measures are Lower Cretacious, occur in the Rocky Mountains, and are situated in a flat-bottomed syncline. The inter-seam strata consists of interbedded sandstones, siltstones and shales. Operations are carried out in the No.4 seam (lower) and the No.11 seam (upper). The intermediate seam (No.10), simulated in the physical and numerical models, has not been represented correctly in the vertical dimension.

Mining is carried out by room and pillar, coal being extracted by continuous miners. Panels are developed on a three entry system, rooms being developed on advance and pillars extracted on retreat. Rooms are 6m wide and 3m high, with the roof supported by bolting on a 1.2m square pattern. Rib-sides are supported by rib posts and lagging. Pillar width depends upon conditions, but is usually 24.4m (30.4m roadway centres).

The initial development in the No.4 seam (6.1m thick) is confined to the upper 3m. However, the lower portion of the seam is removed during de-pillaring operations, and the roof is allowed to cave. Regular roof caving is promoted by avoiding remnant pillars, and maintaining a uniform break line for the cave. Irregular caving is associated with excessive pillar stresses, floor heave and instability of roadway intersections close to the break line.

A newly exposed rib-side, pictured in Plate 16, shows the rib posts, lagging and bolting with wire mesh. The competence of the pillar is noticeable, together with the minor seam irregularities indicated by the roof "roll". The initial indications of high pillar stresses are seen by the pillar expansion along a soft band close to the roof (Plate 17). The next stage in pillar failure is indicated by fractures opening parallel to the pillar sides (Plate 18), causing pillar expansion (Plate 19). Pillar expansion and floor heave lead to failure of rib supports (Plate 20). The floor heave creates closure of the openings and, in order to maintain the working height, the floor has to be excavated (brushing). Floor heave close to the cave line is indicated in Plate 21. Regular caving to the break line reduces pressure on supports, as is shown in Plate 21. The thin layered roof, shown in Plate 22, indicates a cave of the immediate roof at an intersection. It is interesting to observe the failure initiated between roof bolt anchor plates, with few anchor failures. The development opening in the upper portion of the seam, together with the mined lower portion, is shown.

It is clear from this study that the real mine situation exhibits time-dependent pillar and floor failures in highly stressed regions.

5.5 Comparison of results

The vertical stress contour plot (Figure 5.4) illustrates the re-distribution of vertical stresses around the mine openings. Stress concentrations are induced within the pillars, especially those between openings No.3, No.4, No.5 and No.6 in the lower seam. The vertical stress relief above the openings is observed, especially above opening No.4, as a result of the presence of another opening above it. The vertical stress on the coal pillars is taken to be equivalent to the average vertical stress (predicted by the numerical model), uniformly distributed over the pillar. The pillar strength can be estimated (Jeremic, 1979) from the following equations:

$$\sigma_p = c.W/H \quad (W/H < 5)$$

$$\sigma_p = 2.4 + c.W/H \quad (W/H > 5)$$

σ_p = Pillar compressive strength (MN/m^2)

W = Width of pillar

H = Height of pillar

c = Factor depending upon coal
(varies from 1.2 to 1.6 MN/m^2)

A value of 1.5 MN/m^2 was assumed for C in all calculations. Pillar widths are assumed to be 24m along the long axis of the openings, from which the effective width can be calculated:

$$W_e = \sqrt{24.W_t}$$

W_e = Effective pillar width

W_t = Width of pillar transverse to long axis

The following table gives the average pillar vertical stress, effective width, width to height ratio, strength, and safety factor (the pillars being defined with respect to the openings e.g. pillar 1/2 is the pillar between openings No.1 and No.2.):

Pillar	Vertical Stress (MN/m²)	Effective Width (m)	W/H	Strength (MN/m²)	Safety Factor
1/2	12.5	20.8	6.9	12.8	(1.02)*
3/4	33.0	12.0	4.0	6.0	(0.18)*
4/5	19.4	24.0	8.0	14.4	(0.74)*
5/6	21.2	14.7	4.9	7.4	(0.35)*

* The results indicate that progressive failures, resulting in stress re-distributions, will occur. Therefore the safety factors calculated do not represent final values, but only predict instability. It should be noted that the instability in the lower seam is associated with a caving phenomenon, that occurs on retreat, and therefore safety factors below 1.0 would be expected.

It was observed that opening No.2 of the 3-D physical model Run 1 (Plates 6 & 7) had characteristic roof and floor displacements. For a single opening in elastic rock, it would be expected that the roof and floor displacements, causing closure, would be equal and symmetrical. Upon inspection of Plate 7 it was observed that the floor heave was much greater than the roof sag. The numerical model has much stiffer elastic constants than the rubber, but a comparison between the two was made by applying horizontal and vertical scale factors. The numerical model displacements were scaled to match the outline of the physical model (Figure 5.12). This qualitative comparison indicates that the numerical model also predicts that the floor heave is greater than the roof sag, but to a lesser degree than the physical model. Close inspection of Plate 6 indicates bed separation occurring in the floor of the model opening, accounting for the increase in floor displacements.

The contour diagram of stress criterion (Figure 5.9) is most informative, as it combines all the data on the major principal stress (Figure 5.6), minor principal stress (Figure 5.7) and maximum shear stress (Figure 5.8), together with the strength properties of the material. The instability of opening No.2 is clearly indicated by the shaded zones in Figure 5.9, and the physical model (Plates 6 & 8) demonstrates the pillar slabbing along this opening.

The mechanism of pillar failures by fracturing parallel to pillar sides is shown in Plates 14 & 15, with the constrained pillar core providing most of the support. The underground photographs show a similar failure mechanism (Plates 18 & 20).

Opening stability is primarily concerned with roof span failures, with roof support by rock bolting being commonly used in room and pillar mining. The existence of layered strata in the immediate roof of the underground mine (Plate 22), indicates that the analysis of stability should be undertaken assuming that bolting forms a composite roof beam. It is interesting to note that the majority of the roof cave depicted (Plate 22) has been caused by rock failure between bolt anchor plates. If roof support produces very competent roof beams it may have a detrimental effect on the mine conditions during full extraction, as regular caving may be prevented.

6. MINE DESIGN SIMULATION

A mine design simulation was undertaken using data from proposed [illegible] mining of the Silkstone seam at Coal Valley, [illegible] study is intended to illustrate the applica[illegible] mine design concept adopted and is too limited in information and scope to be regarded as a comprehensive stability analysis.

Information on structural geology was obtained from the mine personnel and rock mass parameters were estimated from a geotechnical testing program on drill core from the proposed site.

6.1 Geology

Only a brief summary will be presented here as the limited nature of this study does not warrant a detailed description.

6.1.1 Structure

In the proposed area the predominant feature is a broad syncline with dips varying from 4° to 18°, with an average of 10°, towards the southwest. The area is bounded by major fault systems with faulting dividing the area into five offset blocks. The Silkstone seam outcrops along the northeast limb of this syncline, which plunges towards the southeast. Previous drilling has not indicated the predominance of minor faulting and seam "rolls", but this may be due to the low density of drilling. The area is bounded on the down-dip side by an undefined fault (approx 1500m from the outcrop), where the seam is at a depth of approximately 150m.

6.1.2 Stratigraphy

The Silkstone coal measures consist of two seams, the upper denoted as the Wee and the lower as the Bourne, separated by approximately 9m of silty mudstones. The Bourne seam averages only 0.9m in thickness and is not considered to be economically recoverable. The average normal thickness of the Wee seam is 3m, but varies from 1.5m to 5.8m. In places the seam is divided by a carbonaceous shale and mudstone parting which sometimes exceeds 0.6m. The strata above the Wee seam consists mainly of massive sandstone and siltstone beds. In the eastern portion, close to the outcrop (where three of the four core holes were located), the roof strata is predominantly interbedded siltstones and mudstones.

The coal is ranked as High Volatile Bituminous C by the ASTM classification.

6.2 Geotechnical Testing Program

Geotechnical testing of core from four drill holes was undertaken to define the rock mass parameters and other properties which relate to the mine environment. The core was obtained for shallow seam conditions, as it was proposed to initially undertake underground exploration. Conditions at greater depth may be different, but no core was available for testing.

The diamond drilling for 2.6 inch diameter core was carried out using water flush and a triple barrel. Runs were of approximately 7 ft. and the core was immediately sealed in the plastic inner tubing. The sealed core tubes were transported to the laboratory where geotechnical logging and sampling was carried out. Upon exposure to the atmosphere the samples were sealed and placed in a humid environment until they were opened for preparation and testing. The geotechnical core logs for the four holes can be seen in Appendix 5. A detailed description of the testing procedure is presented in Appendix 6, and the detailed testing results are presented in Appendix 7. A summary of the test results follows:

6.2.1 Uniaxial Compression

Samples of the full core diameter were tested in uniaxial compression (with strain gauges attached), however, no suitable coal samples were available for this test. The results obtained were used to estimate the Young's Modulus, Poisson's Ratio and uniaxial compressive strength. Six samples were tested and the average results are tabulated overleaf:

	Young's Modulus (MN/m²)	Poisson's Ratio	Compressive Strength (MN/m²)
SANDSTONE (3 samples)	1.36×10^4	0.267	73.9
SILTSTONE (2 samples)	1.00×10^4	0.288	66.2
MUDSTONE (1 sample)	8.62×10^3	0.172	70.2
COAL * (1 sample)	1.92×10^3	-	15.6

* undercored sample (no strain gauges attached)

6.2.2 Brazilian Disc

Disc samples (thickness approximately half of the diameter) of both 1.6 inch and 2.6 inch diameter were used in the indirect tensile strength Brazilian tests. The average results from 35 tests are tabulated below:

SANDSTONE (14 samples) = 2.29 MN/m^2
SILTSTONE (6 samples) = 3.47 MN/m^2
MUDSTONE (11 samples) = 3.97 MN/m^2
COAL (4 samples) = 0.91 MN/m^2

6.2.3 Triaxial Compression

In order to investigate the compressive strength under confined conditions, and to develop a Mohr/Coulomb failure envelope, 21 samples were tested in triaxial compression. Core samples were prepared by undercoring to 1.6 inch diameter to fit the triaxial cell, and the in situ moisture content was preserved as much as possible. There were insuffient samples to produce a failure envelope for siltstone, but the Mohr's circle and failure envelopes for sandstone, mudstone and coal were drawn (Figures 6.1, 6.2 and 6.3). It should be noted that some of the height to width ratios tested were below 2, because of sample preparation problems, but the results from these samples appear to be reasonable.

From the results, simplified linear Mohr/Coulomb failure envelopes have been developed, which have the following relationships for confining stresses less than 15 MN/m²:

SANDSTONE: $\tau = 6.9 + \sigma \mathrm{Tan}45^\circ$

MUDSTONE: $\tau = 6.9 + \sigma \mathrm{Tan}38^\circ$

COAL: $\tau = 3.0 + \sigma \mathrm{Tan}45^\circ$

τ = Shear stress (MN/m²)

σ = Normal stress (MN/m²)

The low values for coal cohesion can be explained by the presence of cleat planes which results in discontinuous material. The influence of bedding angle was not investigated as all samples were undercored along the original core axis, hence the principal stress direction was approximately 80° to the bedding dip.

6.2.4 Direct Shear

Shear strength along discontinuities was investigated using a direct shear apparatus. Only a small number of tests were carried out, because of a shortage of suitable samples. Two mudstone joints, one mudstone and one coal bedding plane were sheared, all shearing taking place along the dip of the discontinuit There were no significant peak values and the residual values are given below:

MUDSTONE JOINT (50° dip): Friction angle = 19.9°
MUDSTONE JOINT (30° dip): Friction angle = 27.1°
MUDSTONE BEDDING (15° dip): Friction angle = 23.3°
COAL BEDDING (15° dip): Friction angle = 23.8°

The low friction angles in comparison to the internal friction angles are a result of testing discontinuity weakness planes.

6.2.5 Slake Durability

Slake durability tests on the immediate floor strata were undertaken to assess the effect of water on the competence of the rock units. From the standard testing procedure, results of the Slake Durability Index (second cycle) were 16.8%, 78.5% and 95.3% for three footwall mudstone samples. The higher values appeared to be associated with the sand content within the sample and hence the consequent reduction in clay content.

6.2.6 Swelling Index

Two Swelling Strain Index (unconfined) tests were carried out, one floor mudstone and one roof siltstone. The results were 2.9% and 2.5% for the siltstone and mudstone respectively. Partial disintegration of the siltstone and complete disintegration of the mudstone took place, this indicates that the maximum swelling would probably have been greater than that recorded.

6.3 Rock Mass Parameters

The rock mass parameters that are required for analysis purposes are; the relationship between stress and strain (Young's Modulus & Poisson's Ratio), and the strength characteristics. Estimates of these parameters have been made from laboratory testing of intact samples, which tend to be stiffer and stronger than the rock mass itself. Scaling factors need to be applied from the laboratory results to obtain *in situ* estimates. This process is not well understood as the real rock mass is usually non-homogeneous and discontinuous, thus forming a complex structure. There is insufficient information to undertake a detailed analysis, therefore simple scaling factors will be applied.

Based on previous work (Raney et al, 1976) the Young's Modulus for rock and coal was reduced by factors of 3 and 5 respectively. Poisson's ratio estimates from laboratory testing are not regarded as being representative of the rock mass, hence values of 0.19 and 0.3 for rock and coal will be used (Pariseau & Sorensen, 1979 and Kulhawy, 1975). The Shear Modulus will be estimated from the Young's Modulus and Poisson's Ratio (assuming an isotropic elastic material), using the following formula (Plane Strain analysis):

$$G = E/2(1+\nu)$$

G = Shear Modulus

E = Young's Modulus

ν = Poisson's Ratio

The rock mass parameters from the laboratory tests and the previous assumptions are given below:

Material	E (MN/m²)	G (MN/m²)	ROE
ROCK	3.9×10^3	1.6×10^3	0.19
COAL	3.9×10^2	1.5×10^2	0.30

E = Young's Modulus
G = Shear Modulus
ROE = Poisson's Ratio

From triaxial testing the linear Mohr/Coulomb failure envelopes have been estimated. These estimates do not take into account the effect of discontinuities in the rock mass, and hence they have been adjusted to give the following relationships:

Material	C (MN/m²)*	PHI (degrees)**
SANDSTONE	2.3	40.0
MUDSTONE	2.3	33.0
COAL	0.55	40.0

C = Rock Mass Cohesion
PHI = Internal Friction Angle

* The cohesion values were obtained by dividing the rock and coal cohesion values (from testing) by 3 and 5 respectively.

** The internal friction angles were obtained by subtracting 5° from the laboratory results to allow for the low discontinuity friction angles obtained from the direct shear tests.

These adjustments also bring the estimates closer to values used in previous published work (Kidybinski & Babcock, 1973 and Fadeev & Abdyldayev, 1979).

The effects of anisotropy and time dependent behaviour have not been considered as they are difficult to investigate and the required complexity is beyond the scope of this study.

6.4 Proposed Mining Method

The method under consideration will involve multiple access from a surface mine highwall, and headings driven down dip (approximately 1500m to a fault boundary). This concept of punch mining from the highwall would utilize high capacity equipment to extract coal from the portals serving individual mining rooms. As the parallel rooms are extracted, and the portals are advanced along the highwall, the old portals become redundant and will be covered during reclamation.

6.5 Stability Analysis

A number of possible mine geometries have been studied with the assumed rock mass parameters and initial stress conditions held constant. The sensitivity of the mine structure to variation of these parameters has therefore not been considered. The stability of coal pillars and surrounding strata have been considered separately for analytic purposes, but interactions at roof and floor will be present. The geometries analysed represent extraction ratios of 60%, 55% and 50%.

6.5.1 Coal Pillar Strength

The cube strength of coal has been estimated from the uniaxial compressive strength results. Adjustments have been made to allow for sample size and shape using the following formula based on Hustrulid (1975):

$$\sigma_c = \sigma_{ct}.\sqrt{H}/(0.778 + 0.222.W/H)$$

σ_c = Compressive strength of a 1 inch cube
σ_{ct} = Test sample compressive strength
H = Test sample height (inches)
W = Test sample width (inches)

Only one uniaxial compressive test sample result was available and this is not considered to be sufficient for normal design purposes, but with no other data available this result was used. For the test sample of height 2.02 inches and width (diameter) 1.62 inches the uniaxial compressive strength was 15.6 MN/m². The calculated cube compressive strength is 21.0 MN/m² for a 1 inch cube. All mine pillars will have dimensions greater than 3 ft. (0.9m) and hence the pillar cube compressive strength will be 3.5 MN/m² (one sixth of the one inch cube strength). The size factor will therefore be constant and the shape factor will vary according to the following equation (Hustrulid, 1975):

$$\sigma_p = \sigma_c(0.778 + 0.222\ W/H)$$

σ_p = Pillar compressive strength (MN/m^2)
σ_c = Cube compressive strength (MN/m^2)

The height of rooms, and hence that of pillars has been assumed to be 2.5m and this reduces the equation to the form below:

$$\sigma_p = 2.72 + 0.31\ W$$

σ_p = Pillar compressive strength (MN/m^2)
W = Width of square pillar (m)

The width used in the equation assumes that the pillars are square, but the proposed mining method will not utilise square pillars. Pillars will be long and thin, thus an effective width should be used for design purposes. The effect of unequal pillar side lengths on pillar strength has not been previously studied in any great detail. Sheorey & Singh (1974) have concluded that the strength of a rectangular pillar is the same as that of a square pillar whose sides are equal to the average of the two rectangular pillar widths. This result indicates that for a given pillar area a rectangular pillar will have a higher strength than a square one. For wide pillars with confined cores this may be correct, but for thin, long pillars the equivalent square pillar width should not be the average of the two sides. This is understood when a rectangular pillar with one side of zero length is considered. The equivalent square pillar will have a width equal to half of the non-zero length of the rectangular pillar, which is incorrect. It would seem more appropriate to base the design of a rectangular pillar on its equivalence to a square pillar of the same plan area. Using this hypothesis, and the assumption of a pillar length of 30m parallel to the long axis of the rooms, the pillar strength relationship becomes:

$$\sigma_p = 2.72 + 1.7\sqrt{W_t}$$

W_t = Pillar width between rooms (m)
σ_p = Pillar compressive strength (MN/m^2)

This relationship is presented graphically in Figure 6.4. It should be noted that this relationship is only valid for pillars with a height of 2.5m and a long dimension of 30m.

6.5.2 Numerical Analysis

The DDSEAMS program was used to analyse three layouts at a depth of 150m (Runs 21, 22 & 23) with the graphical results presented in Appendix 8. The mine geometries for these runs are shown in Figure 6.5 together with the average vertical stress for each pillar. The rock mass and coal seam parameters were estimated from the geotechnical testing and adjusted for in situ conditions (tabulated previously). The overburden rock density was assumed to be equivalent to 0.025 MN/m^2 per metre of depth. No data for the pre-mining stress field was available so hydrostatic conditions were assumed. This was thought to be reasonable because of the shallow nature of the excavations.

The PSTRESS program was run on the data from the three DDSEAMS program runs, to produce values for the stability of the surrounding strata. In all three runs the roof sandstone was found to be stable, but slight instability in the floor mudstone was observed. The stability criterion results, 0.75m into the floor mudstone, are presented in Figure 6.7 for the present mining room and the previous room.

Pillar safety factors (based on elastic stress comparisons) can be calculated by dividing the pillar strength by the average pillar stress. These results are presented in Figure 6.6, where pillar strengths of 6.12 and 7.53 MN/m^2 have been assumed for the 4m and 6m wide pillars respectively.

6.6 Discussion of Results

In considering the stability of the mine structure it will be assumed that only the room being mined, and the previous room, need to be stable. This requires that the abutment pillar (No.1), and pillars No.2 and No.3 should be stable. This assumption is only valid when failed pillars do not exhibit brittle behaviour, but yield progressively, thus avoiding catastrophic failures.

6.6.1 Pillar Stability

Using the tributary area theory, the expected pillar stresses for extraction ratios of 60%, 55% and 50%, are 9.4, 8.3 and 7.5 MN/m² respectively. For these, pillar widths of 15.4m (60% extraction), 10.8m (55% extraction) and 7.8m (50% extraction) would be required to give a safety factor of 1.

The results from the numerical modelling indicate that the proximity of the abutment to the last two pillars, has the effect of reducing their average stress values below that predicted by the tributary area theory. If a room width of 6m is assumed, then the tributary area theory predicts that a pillar width of 7m is required for a safety factor of 1 (pillars 30m long and extraction ratio of 46%). The pillar safety factors for the three runs (Figure 6.6), predicted by the numerical model, indicate that extraction ratios above 50% should be possible. The results illustrate the undesirable aspects of having non-uniform pillar sizes, due to the relatively low strengths of narrow pillars. As the pillar width is reduced, the strength is reduced, and the pillar stress is increased. This indicates that maximum extraction will be achieved with uniform pillar widths. Design on the basis of a safety factor of 1 is considered to be adequate, as the worst possible case of greatest depth is analysed.

Pillar stabilities are predominantly controlled by the vertical stresses, which can be reasonably predicted using overburden density assumptions. The effect of horizontal stress upon the pillar stability is not expected to be great, as the seam is gently dipping. The assumption that the seam can be analysed as being flat is not expected to affect the results by more than 5%. and the approach is therefore considered to be valid.

6.6.2 Opening Stability

The stability of the roof span is not likely to be controlled by intact rock shear failure, as it consists of a massive sandstone strata unit over 6m thick. From the limited discontinuity data available, steep joint sets (approximately 60° dip) are known to exist, but their spacing and orientation are unknown. Stability of wedges delineated by these steep joint sets and bedding planes will be greatly affected by the horizontal stresses, which are at present unknown. Consequently no complete stability analysis can be undertaken at present, but it should be mentioned that experience has shown roof beds of this type to be very stable with roof bolting support. In order to estimate the support requirements, further information on the dip, orientation, spacing and shear strength of these discontinuities is required.

The orientation of rooms will be a major factor in analysing the roof and rib stability. Slabbing failure of pillar sides into rooms is dependent upon the cleat direction, spacing and continuity, which are unknown. Pillar slabbing is unsafe, causes production delays, and also has the effect of increasing opening spans and reducing effective pillar strengths.

Floor stability problems are often encountered when weak floors are highly stressed, producing failures which migrate into the entry (floor heave). High horizontal stresses may cause buckling failures of thin, weak floor beds, which are further pronounced by highly stressed pillar abutments loading the floor strata beyond its bearing capacity. The effect of water on the floor may be a major factor for the mudstones and siltstones. Swelling Index and Slake Durability tests indicate that the swelling of floor beds, together with their reduced strength when wet, will cause problems for heavy mobile machinery. Floor heave will probably not be a problem as it is a time-dependent phenomenon and the most highly stressed zones will be at the ends of rooms. The stress criterion results for the floor mudstones (Figure 6.7), based on geotechnical testing and stresses from the numerical modelling, indicate that slight instability of floor strata at the centre of openings will be present.

The overall analysis has been based upon limited test results from the more competent portions of the strata, because of sample preparation problems for the weaker units. This means that the average testing results will be biased, towards the higher strength values. Adjustments have been made by applying scaling factors to estimate the rock mass parameters based on previously published results. These factors are not well understood and may not be applicable to the strata under study, thus a degree of uncertainty has been introduced.

This design analysis is sufficient for the initial technical and economic feasibility stages. Better predictions can be made by undertaking _in situ_ testing of full size excavations, at sufficient depth, with monitoring of strata behaviour.

7. CONCLUSIONS

7.1 Modelling Techniques

1. The numerical analysis technique adopted provides improved prediction of stress distributions compared to simpler techniques, such as the tributary area and beam theory. This is especially true in the proximity of abutments, for workings of limited lateral extent in relation to depth, and where multiple seam interactions are present.

2. Layered strata with stiffer mechanical properties cannot be modelled by assigning unmined coal seams in the numerical model presented.

3. Physical modelling techniques provide a simple means of qualitatively simulating complex failure mechanisms in mine structures, by relating their behaviour to the failures observed in real mine situations.

4. The use of a stress criterion to predict zones of overstressed rock is useful for indicating potential failure zones.

5. When pillar safety factors or strata stress criterion values predict that failures will take place, the

resulting stress re-distributions are not accounted for in the numerical analysis.

7.2 Multi-Seam Studies

1. The numerical model predicted zones of potential instability that correspond to observed instability in the 3-D physical model.

2. The pillar failures observed in the 3-D physical model were similar to those observed in the underground phenomenological study.

3. The base friction model predicted a cave angle of approximately 70° for de-pillaring operations in the lower seam.

4. The numerical model only predicts potential failure zones, and should therefore not be used to estimate the stress re-distributions, as it does not model these failures.

7.3 Mine Design Simulation

1. From geotechnical testing of core samples of the proposed mine strata at Coal Valley the following

results were obtained:

(a) Uniaxial Compression Testing:

	Young's Modulus (MN/m²)	Poisson's Ratio	Compressive Strength (MN/m²)
SANDSTONE (3 samples)	1.36 × [illegible]	0.267	73.9
SILTSTONE (2 samples)	1.00×10^4	0.288	66.2
MUDSTONE (1 sample)	8.62×10^3	0.172	70.2
COAL * (1 sample)	1.92×10^3	-	15[illegible]

* Undercored sample (no strain gauges attached)

(b) Brazilian Testing (tensile strength):

SANDSTONE (14 samples) = 2.29 MN/m²

SILTSTONE (6 samples) = 3.47 MN/m²

MUDSTONE (11 samples) = 3.97 MN/m²

COAL (4 samples) = 0.91 MN/m²

(c) Triaxial Compression Testing:

— (confining stresses less than 15 MN/m²)

Linear Mohr/Coulomb failure envelopes:

SANDSTONE: $\tau = 6.9 + \sigma \mathrm{Tan}45^{\circ}$

MUDSTONE: $\tau = 6.9 + \sigma \mathrm{Tan}38^{\circ}$

COAL: $\tau = 3.0 + \sigma \mathrm{Tan}45^{\circ}$

τ = Shear stress (MN/m^2)

σ = Normal stress (MN/m^2)

(d) Direct Shear Testing of Discontinuities:

MUDSTONE JOINT (50° dip): Friction angle = 19.9°

MUDSTONE JOINT (30° dip): Friction angle = 27.1°

MUDSTONE BEDDING (15° dip): Friction angle = 23.3°

COAL BEDDING (15° dip): Friction angle = 23.8°

(e) Slake Durability Testing of Footwall Mudstones:

SDI (average of 3 samples) = 63.5%

SDI = Slake Durability Index (second cycle)

(f) Swelling Index Testing:

SSI (average of 2 samples) = 2.7%

SSI = Swelling Strain Index (unconfined)

2. The estimated rock mass parameters from the empirically adjusted geotechnical results are:

Material	E (MN/m²)	G (MN/m²)	ROE
ROCK	3.9×10^3	1.6×10^3	0.19
COAL	3.9×10^2	1.5×10^2	0.30

E = Young's Modulus

G = Shear Modulus

ROE = Poisson's Ratio

3. The estimated linear Mohr/Coulomb failure envelopes for the rock mass types are:

Material	C (MN/m²)	PHI (degrees)
SANDSTONE	2.3	40.0
MUDSTONE	2.3	33.0
COAL	0.55	40.0

C = Rock Mass Cohesion

PHI = Internal Friction Angle

4. The estimated pillar strength for long pillars (30m parallel to rooms) is given by:

$$\sigma_p = 2.72 + 1.7\sqrt{W_t}$$

W_t = Pillar width between rooms (m)

σ_p = Pillar compressive strength (MN/m^2)

5. This initial analysis indicates that extraction ratios (by area) greater than 50% may be possible at 150m depth.

6. The analysis is based on geotechnical testing of core from shallow seam conditions which may not be representative of the strata conditions at greater depth.

8. RECOMMENDATIONS

8.1 Modelling Techniques

1. Predictions of actual rock mass behaviour and failure mechanisms should be improved. This could be done by comprehensive geotechnical testing of intact rock and discontinuities, definition of structural geology (including joint surveys) and measurement of *in situ* stresses. Monitoring of the defined rock structure should be carried out during excavation, and back analysis techniques used to provide an accurate means of predicting the behaviour of the mine structure from data collected prior to mining.

2. Numerical methods should be developed to simulate the actual rock mass behaviour when failures occur. This could possibly be achieved by combinations of boundary element, finite element and block models. An example of this could be; to define an active caving zone (caved rock) by means of a block model, this could interface with a finite element model from the active caving zone to the caving limits (failed rock), which is then interfaced with a boundary element model for the remainder of the rock mass (pre-failure).

3. Pillar failure mechanisms should be investigated

further, under actual mine conditions, to improve pillar strength prediction capabilities. This should include time dependent analysis as pillar deterioration with time is commonly observed in coal mines.

4. Where significant failures are present in the mining structure, elastic analysis techniques do not provide adequate estimation of the resulting stress re-distributions. Therefore it is recommended that more complex analysis techniques, that model these failure mechanisms, should be employed.

5. The limitations of modelling techniques should be investigated further, as the ability to model actual rock mass behaviour is still in its rudimentary stage. Better techniques are constantly being developed, but their applicability in modelling a complex reality contain many uncertainties.

6. The applicability of two-dimensional analysis techniques should be investigated further, as they are often used because three-dimensional techniques are too complex and expensive to undertake.

8.2 Multi-Seam Studies

1. Where caving phenomena are encountered, analysis techniques that model these complex failures should be employed.

2. The rock mass behaviour and multi-seam interactions during caving should be investigated further to enable realistic modelling of mine structures.

3. Coal pillar strength relationships should be investigated further to improve prediction capabilities for Rocky Mountain conditions.

8.3 Mine Design Simulation

1. Further geotechnical testing of strata conditions at greater depth should be carried out.

2. Monitoring of the rock mass behaviour around actual mine openings, at the depth conditions expected, should be undertaken.

3. Time-dependent behaviour of mine pillars and strata should be investigated, as the proposed mining method will probably involve pillars that exhibit time-dependent yield behaviour.

4. More complex modelling techniques should be employed for prediction of the behaviour of mine structures. The results of strata monitoring for experimental openings would be required for realistic modelling.

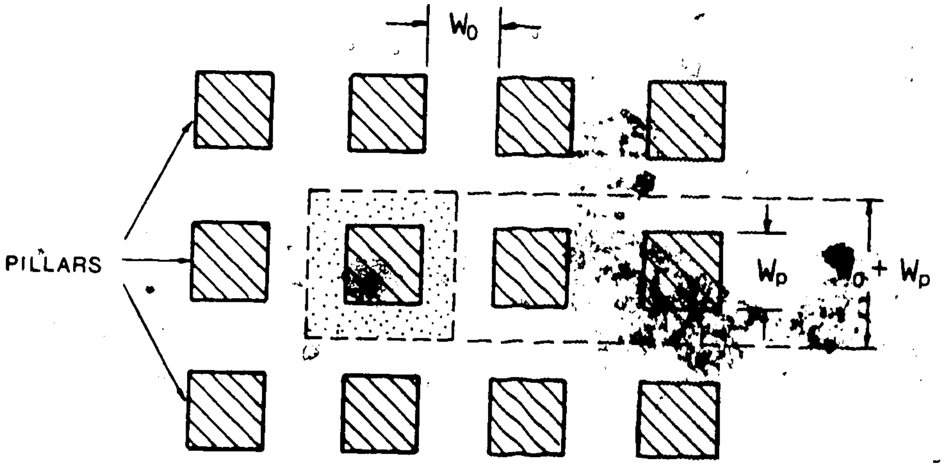
W_o
PILLARS
W_p
$W_o + W_p$

FIGURE 2.1 SQUARE PILLAR LAYOUT PLAN

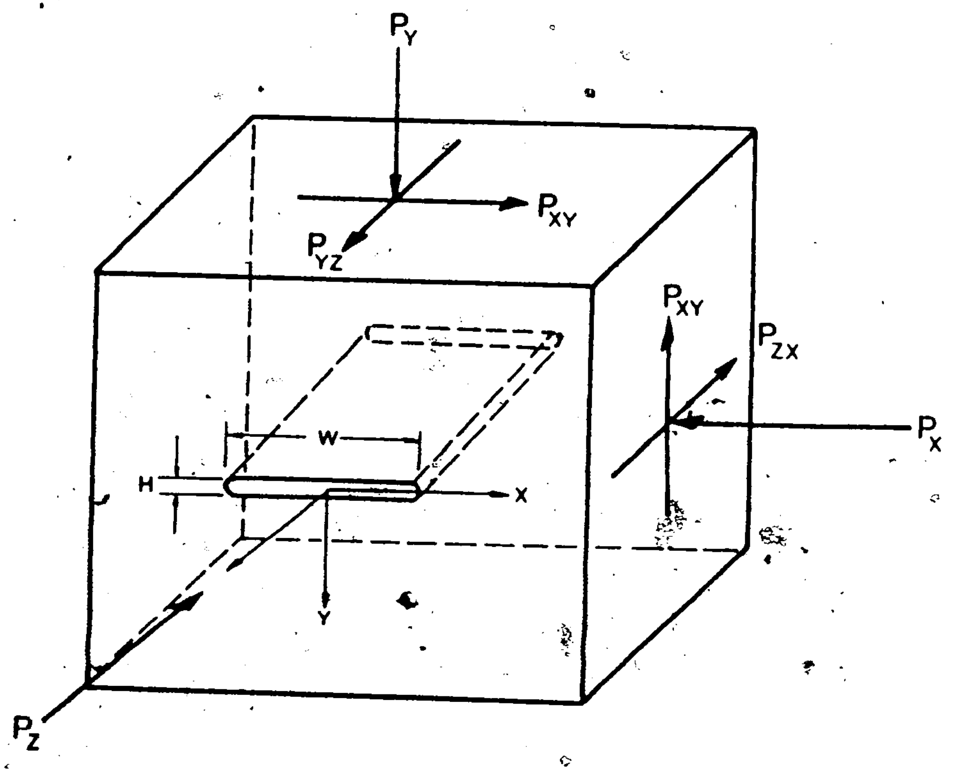
P_Y
P_{XY}
P_{YZ}
P_{XY}
P_{ZX}
P_X
W
H
X
Y
P_Z

FIGURE 3.1 CONFIGURATION OF FLAT ELLIPTICAL CRACK

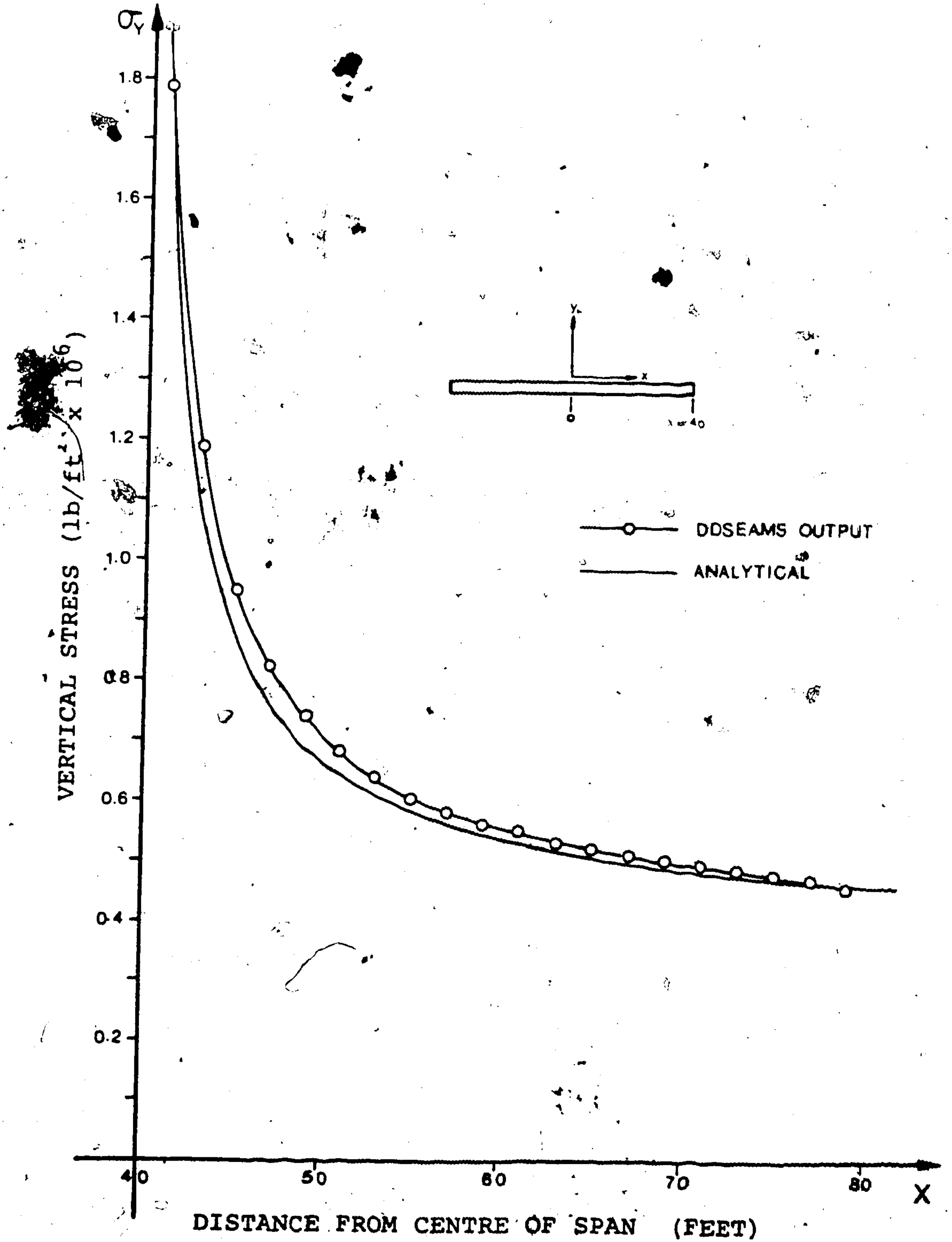

FIGURE 3.2 ANALYTICAL/NUMERICAL VERTICAL STRESS COMPARISON

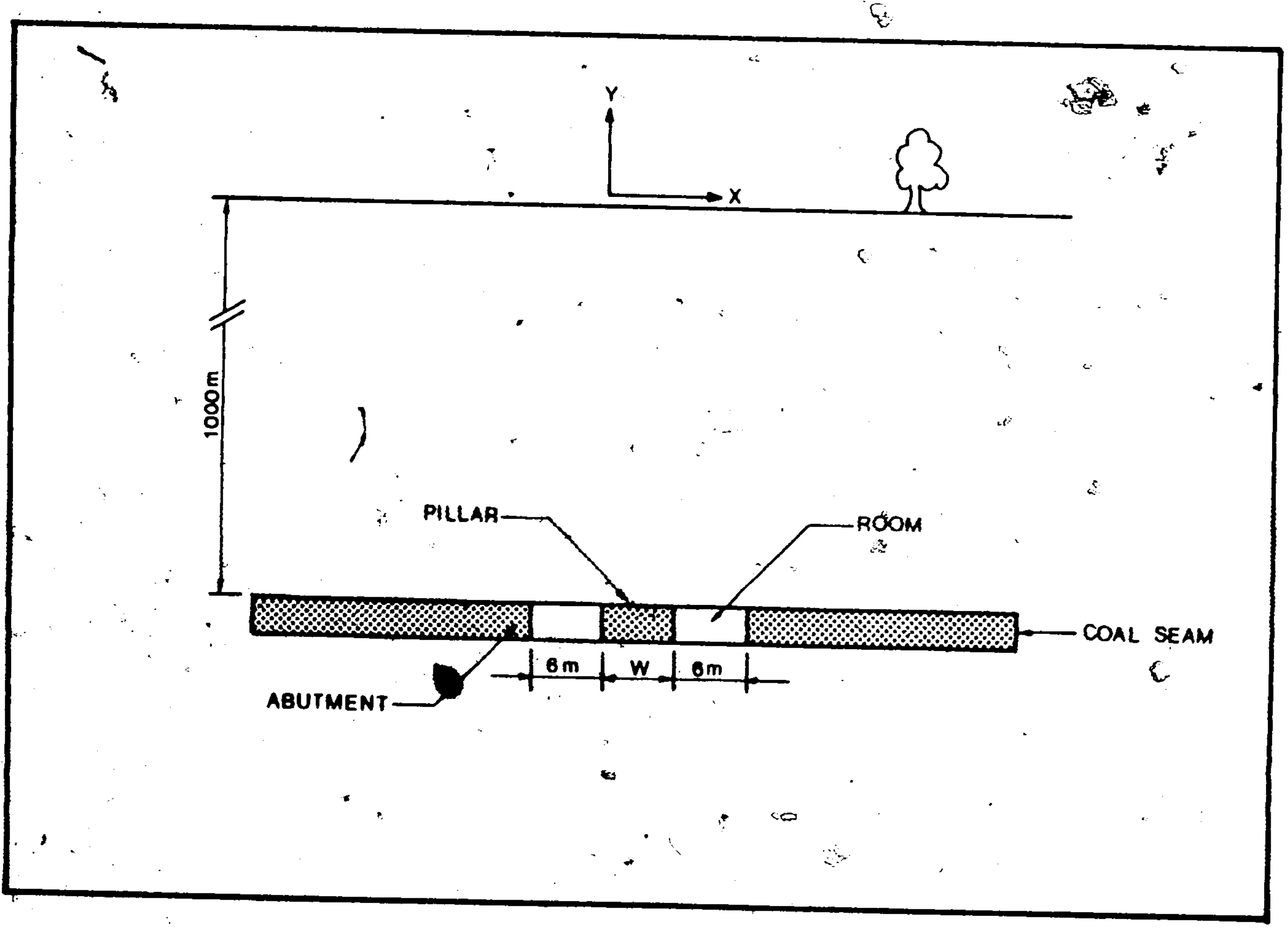
Y
X
1000m
PILLAR
ROOM
COAL SEAM
ABUTMENT
6m
W
6m

FIGURE 3.3 SIMPLIFIED MINE LAYOUT

PARAMETER	RUN NUMBER					
	06	07	08	09	10	11
DEPTH OF SEAM (m)	1000.0	1000.0	1000.0	1000.0	1000.0	1000.0
SEAM THICKNESS (m)	3.0	3.0	3.0	3.0	3.0	3.0
SEAM YOUNG'S MODULUS (MN/m^2)	3.0×10^3	3.0×10^3	3.0×10^3	3.0×10^3	3.0×10^3	1.5×10^3
SEAM SHEAR MODULUS (MN/m^2)	1.2×10^3	1.2×10^3	1.2×10^3	1.2×10^3	1.2×10^3	0.6×10^3
NUMBER OF SEAM ELEMENTS	80	80	80	80	80	80
ELEMENT HALF-WIDTH (m)	0.25	0.25	0.25	0.25	0.25	0.25
UNIT WEIGHT OF ROCK (MN/m^3)	0.025	0.025	0.025	0.025	0.025	0.025
ROCK YOUNG'S MODULUS E_{xx} (MN/m^2)	3.0×10^4	3.0×10^4	3.0×10^4	3.0×10^4	6.0×10^4	3.0×10^4
ROCK YOUNG'S MODULUS E_{YY} (MN/m^2)	3.0×10^4	3.0×10^4	3.0×10^4	3.0×10^4	6.0×10^4	3.0×10^4
ROCK YOUNG'S MODULUS E_{zz} (MN/m^2)	3.0×10^4	3.0×10^4	3.0×10^4	3.0×10^4	6.0×10^4	3.0×10^4
ROCK SHEAR MODULUS G_{xY} (MN/m^2)	1.1×10^4	1.1×10^4	1.1×10^4	1.1×10^4	2.3×10^4	1.1×10^4
POISSON'S RATIO Y DUE TO X, ν_{xY}	0.025	0.025	0.025	0.025	0.025	0.025
POISSON'S RATIO X DUE TO Z, ν_{zx}	0.025	0.025	0.025	0.025	0.025	0.025
POISSON'S RATIO Z DUE TO Y, ν_{Yz}	0.025	0.025	0.025	0.025	0.025	0.025
PILLAR WIDTH (m)	12.0	6.0	3.0	1.5	3.0	3.0
RATIO OF FIELD STRESS, K $=\sigma_h/\sigma_v$	0.33	0.33	0.33	0.33	0.33	0.33
SPAN OF ROOMS (m)	6.0	6.0	6.0	6.0	6.0	6.0

FIGURE 3.4 TABLE OF MAJOR PARAMETERS FOR RUNS 06 TO 11

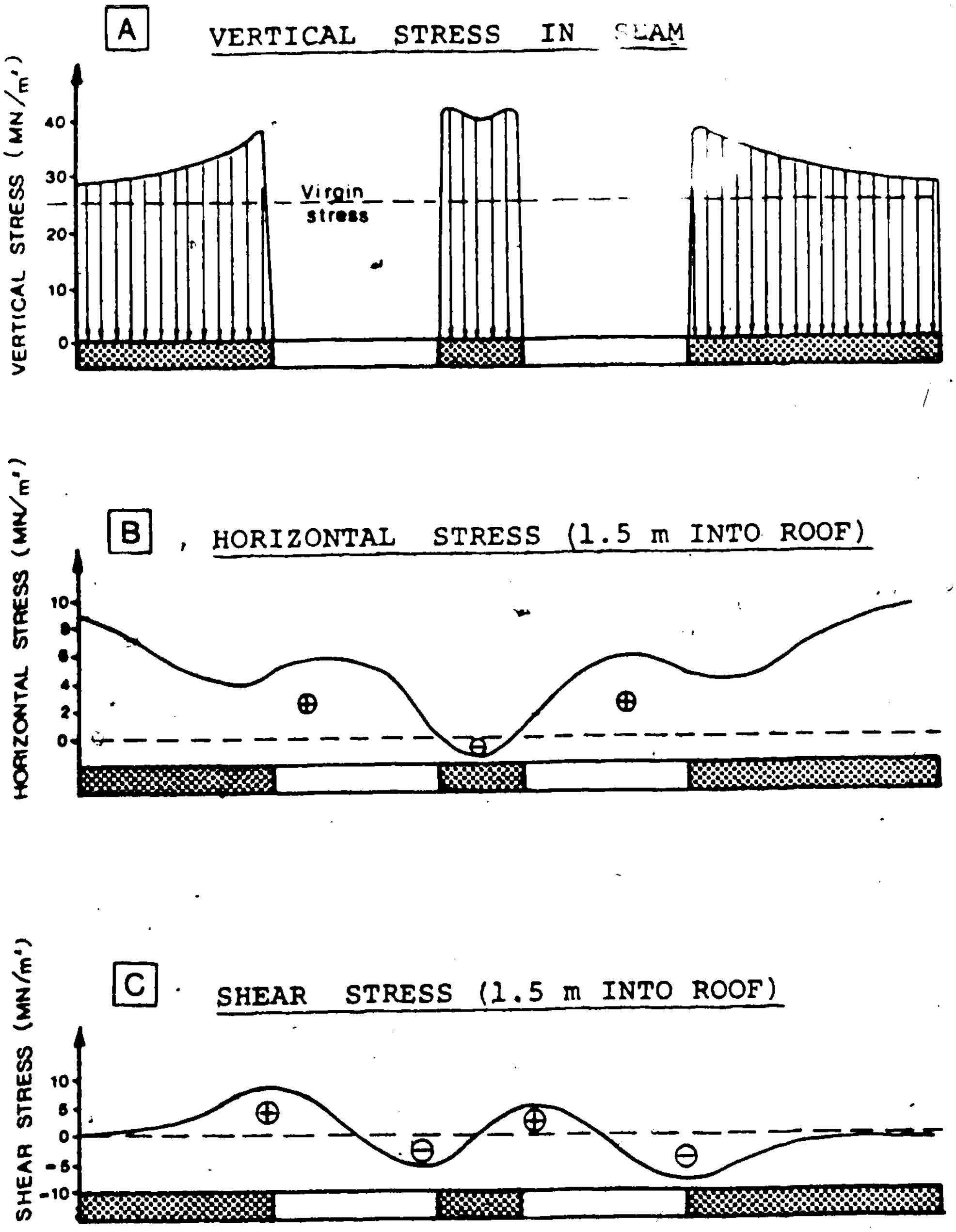

FIGURE 3.5 STRESS RESULTS FOR RUN 08

PARAMETER	RUN NUMBER 06	07	08	09	10	11
PILLAR WIDTH (m)	12.0	6.0	3.0	1.5	3.0	3.0
PILLAR VERTICAL STRESS (AVERAGE) (MN/m^2)	32.2	36.0	40.0	43.7	34.6	34.7
PILLAR VERTICAL STRESS (CENTRE) (MN/m^2)	30.8	34.9	39.4	43.3	34.3	34.4
PILLAR VERTICAL STRESS (MAXIMUM) (MN/m^2)	35.8	38.1	40.9	43.9	34.9	35.0
DISPLACEMENT OF ROOF (CENTRE OF SPAN) mm	8.5	9.5	10.5	11.4	5.9	12.1
DISPLACEMENT OF PILLAR (CENTRE TOP) mm	2.8	4.9	7.4	9.1	4.6	9.2
HORIZ. STRESS IN ROOF ABOVE PILLAR CENTRE (MN/m^2)	6.3	1.4	-1.3	-1.3	-2.0	-1.9
SHEAR STRESS IN ROOF 0.25m INTO ABUTMENT (MN/m^2)	7.6	7.8	8.2	8.7	8.0	7.9
SHEAR STRESS IN ROOF 0.25m INTO PILLAR (MN/m^2)	7.8	7.4	4.8	1.6	4.1	4.1

FIGURE 3.6 TABULATED COMPARISON OF SIMPLIFIED LAYOUT

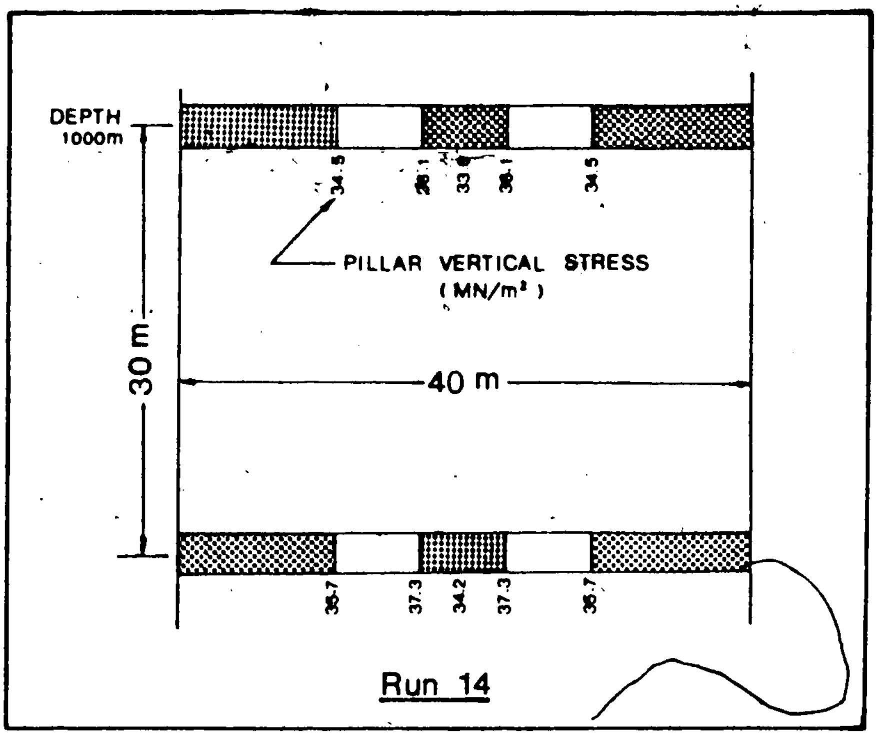
DEPTH
1000m
34.5
36.1
33.8
36.1
34.5
PILLAR VERTICAL STRESS
(MN/m²)
30 m
40 m
35.7
37.3
34.2
37.3
35.7

Run 14

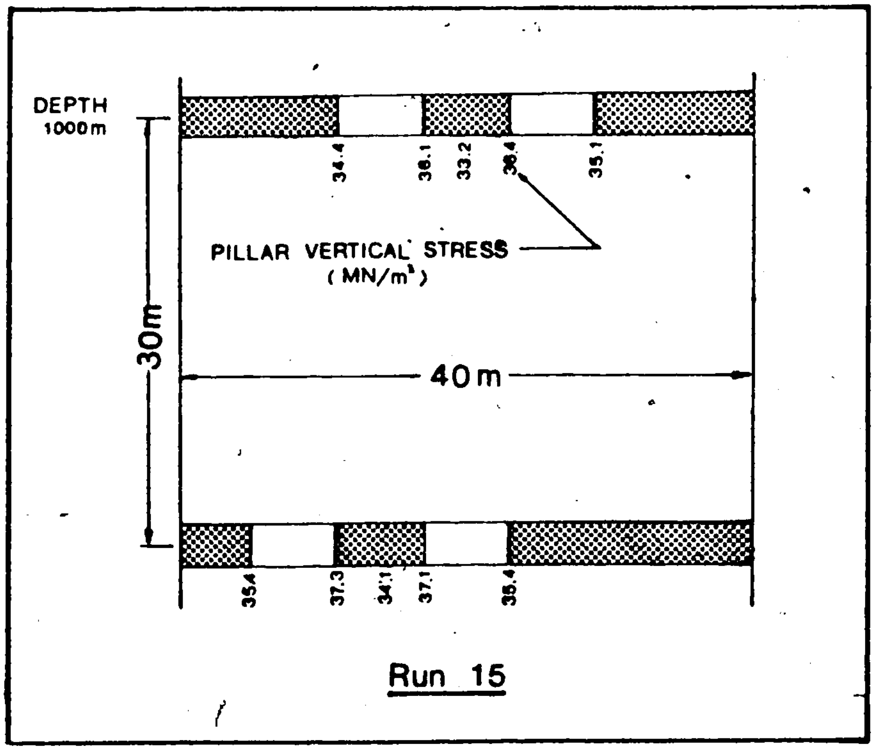
DEPTH
1000m
34.4
36.1
33.2
36.4
35.1
PILLAR VERTICAL STRESS
(MN/m²)
30m
40 m
35.4
37.3
34.1
37.1
35.4

Run 15

FIGURE 3.7 PILLAR VERTICAL STRESSES - RUNS 14 & 15

Run 17

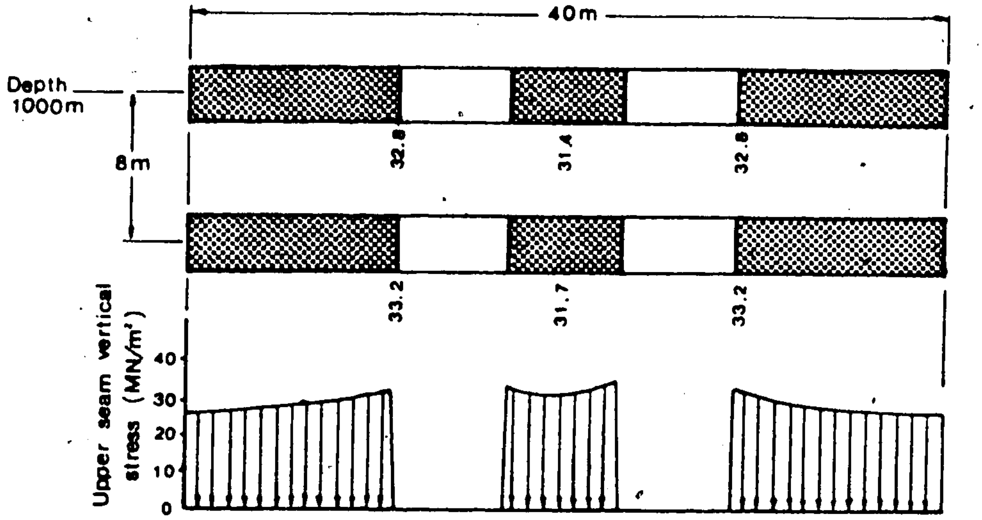
40m
Depth
1000m
8m
32.8
31.4
32.8
33.2
31.7
33.2
Upper seam vertical stress (MN/m²)
40
30
20
10
0

Run 18

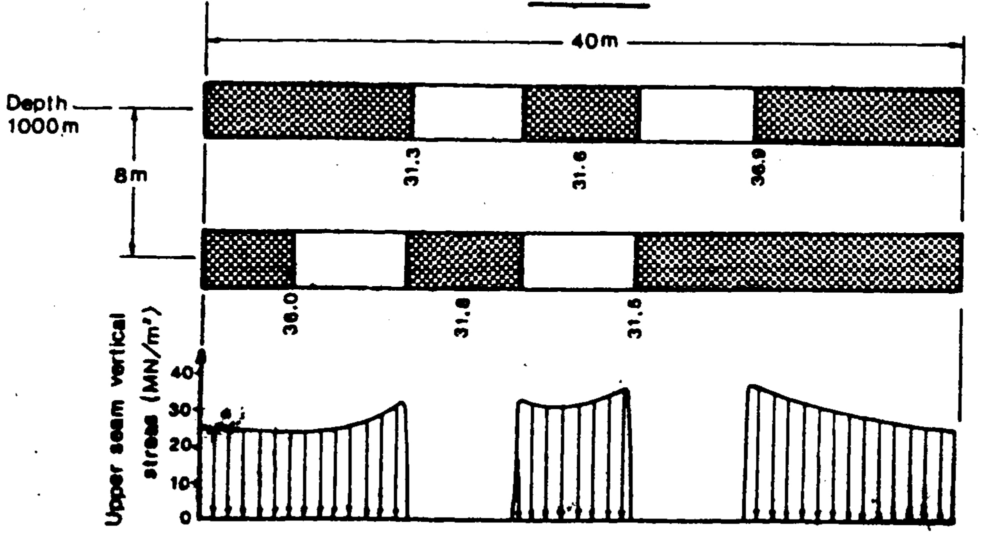
40m
Depth
1000m
8m
31.3
31.6
36.9
36.0
31.8
31.5
Upper seam vertical stress (MN/m²)
40
30
20
10
0

FIGURE 3.8 PILLAR VERTICAL STRESSES - RUNS 17 & 18

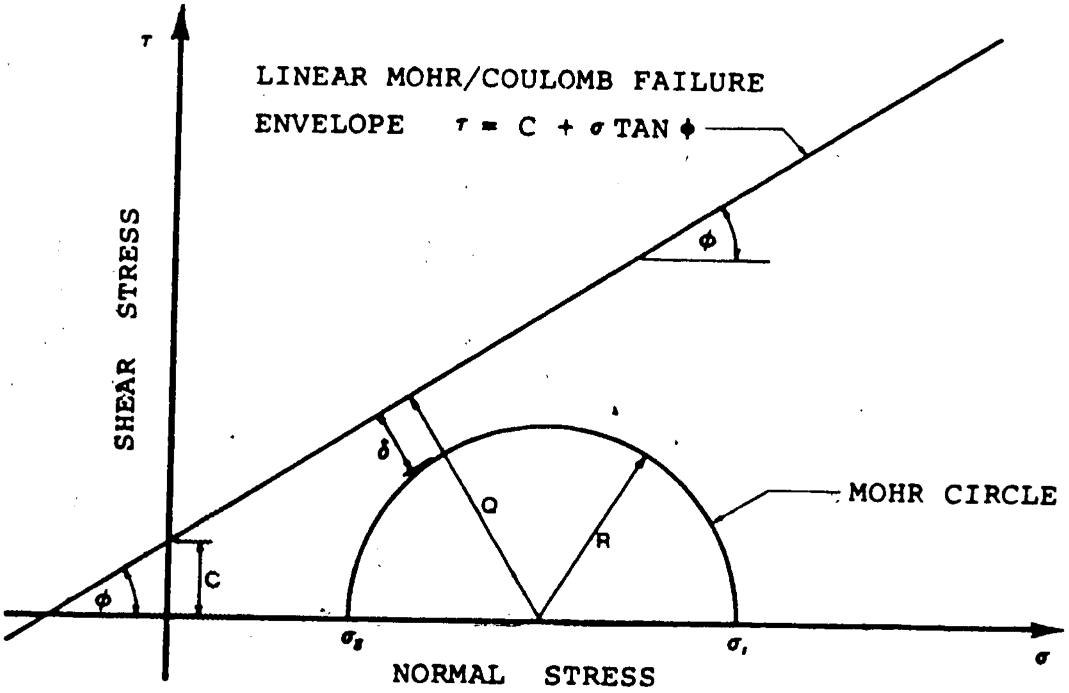
τ
LINEAR MOHR/COULOMB FAILURE
ENVELOPE τ = C + σ TAN ϕ
ϕ
SHEAR STRESS
δ
Q
R
MOHR CIRCLE
C
ϕ
σ₃
σ₁
σ
NORMAL STRESS

FIGURE 4.1 MOHR/COULOMB FAILURE CRITERION

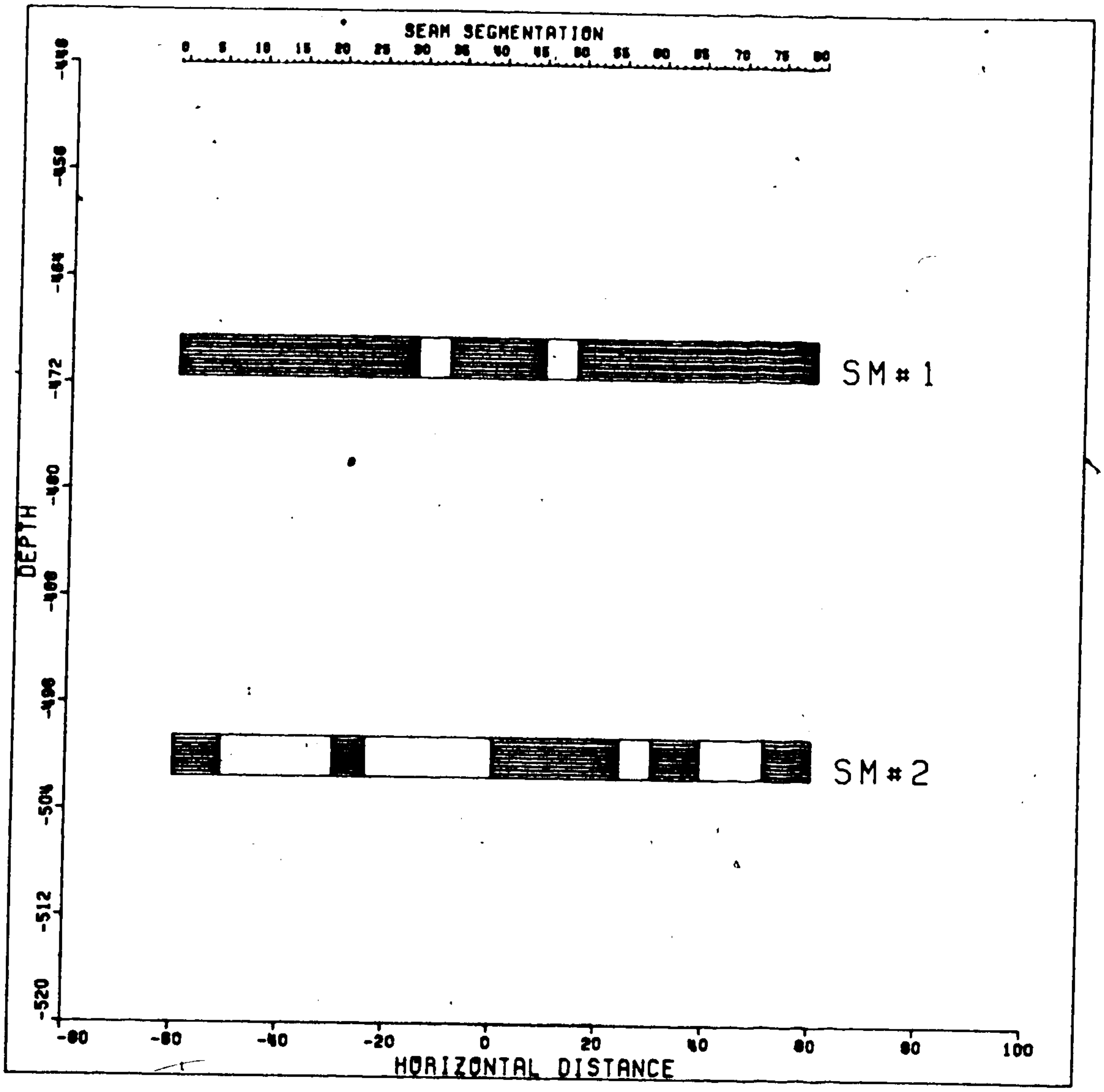
SEAM SEGMENTATION
0
5
10
15
20
25
30
35
40
45
50
55
60
65
70
75
80
SM#1
SM#2
DEPTH
-448
-456
-464
-472
-480
-488
-496
-504
-512
-520
HORIZONTAL DISTANCE
-80
-60
-40
-20
0
20
40
60
80
100

Figure 5.1 Mine Layout for Run 19

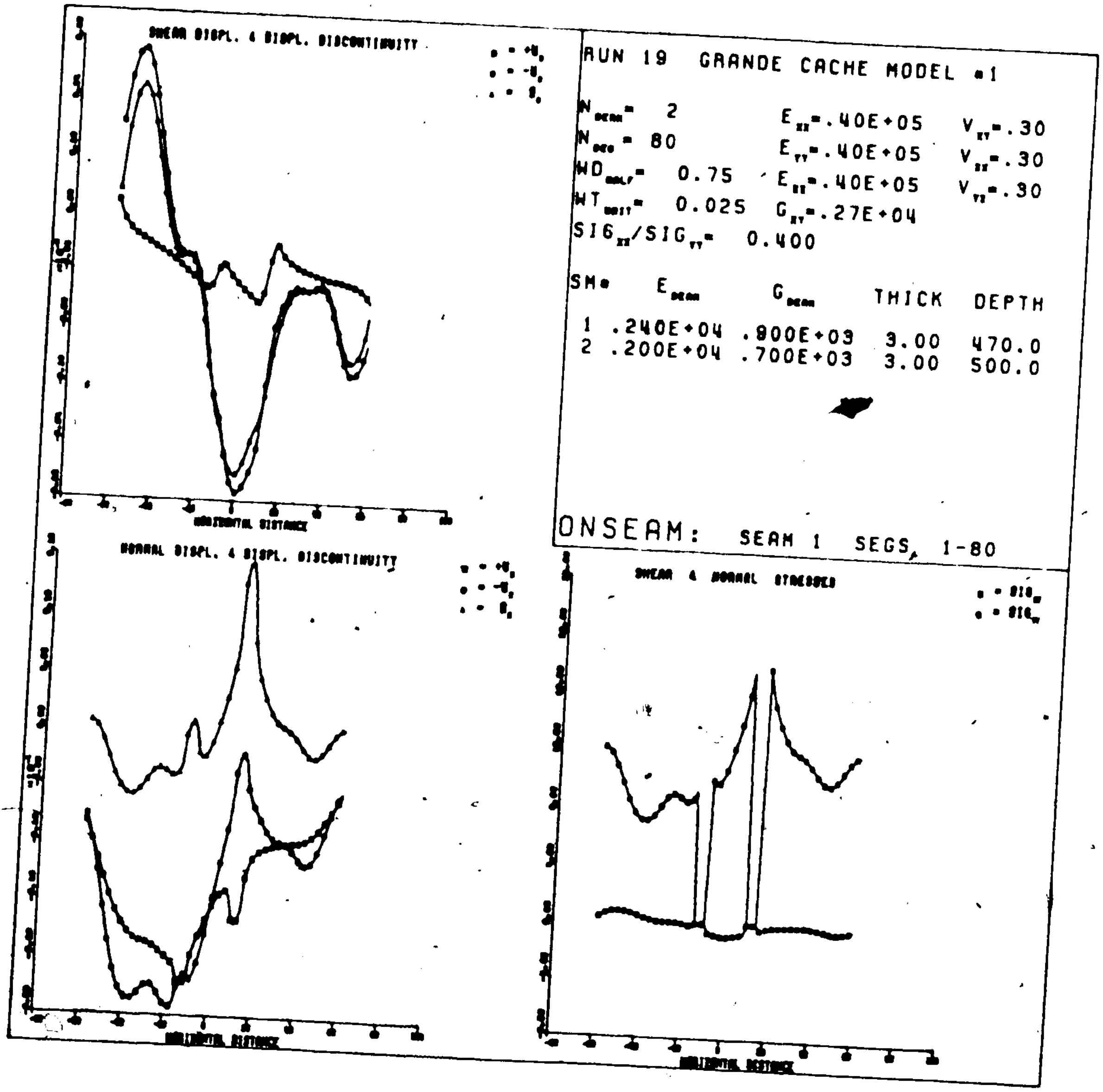

```
RUN 19  GRANDE CACHE MODEL #1

N SEAM=  2              E XX=.40E+05   V XY=.30
N SEG = 80              E YY=.40E+05   V XZ=.30
WD=    0.75             E ZZ=.40E+05   V YZ=.30
WT=    0.025            G XY=.27E+04
SIG XX/SIG YY=  0.400

SM#    E SEAM      G SEAM      THICK   DEPTH
 1  .240E+04   .800E+03    3.00    470.0
 2  .200E+04   .700E+03    3.00    500.0

ONSEAM:  SEAM 1  SEGS, 1-80
```

Figure 5.2 Numerical Results for Upper Seam (Run 19)

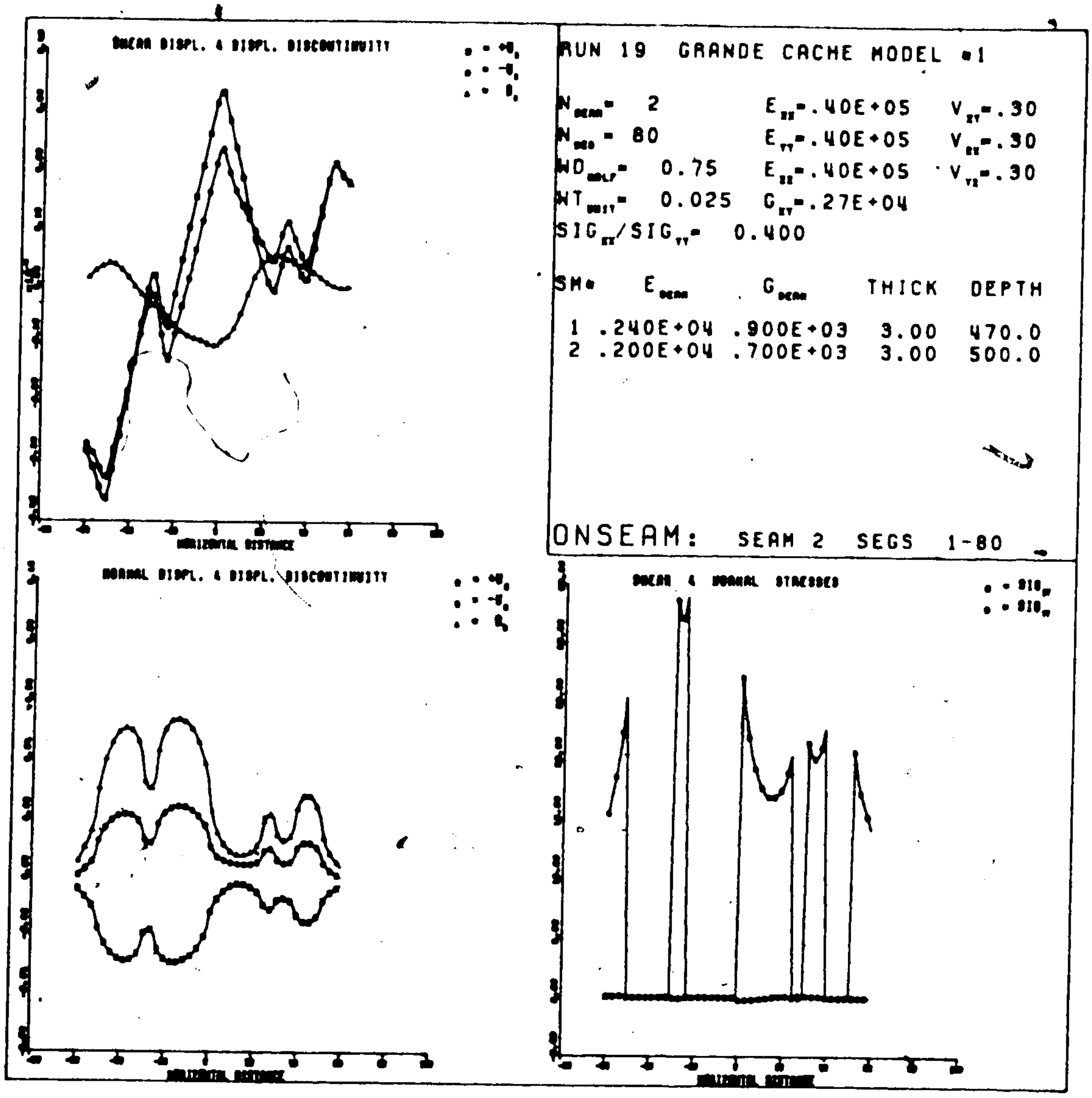

RUN 19 GRANDE CACHE MODEL #1

N_{SEAM}= 2 E_{XX}=.40E+05 V_{XY}=.30
N_{SEG} = 80 E_{YY}=.40E+05 V_{ZX}=.30
WD_{HALF}= 0.75 E_{ZZ}=.40E+05 V_{YZ}=.30
WT_{UNIT}= 0.025 G_{XY}=.27E+04
SIG_{XX}/SIG_{YY}= 0.400

SM#	E_{SEAM}	G_{SEAM}	THICK	DEPTH
1	.240E+04	.900E+03	3.00	470.0
2	.200E+04	.700E+03	3.00	500.0

ONSEAM: SEAM 2 SEGS 1-80

Figure 5.3 Numerical Results for Lower Seam (Run 19)

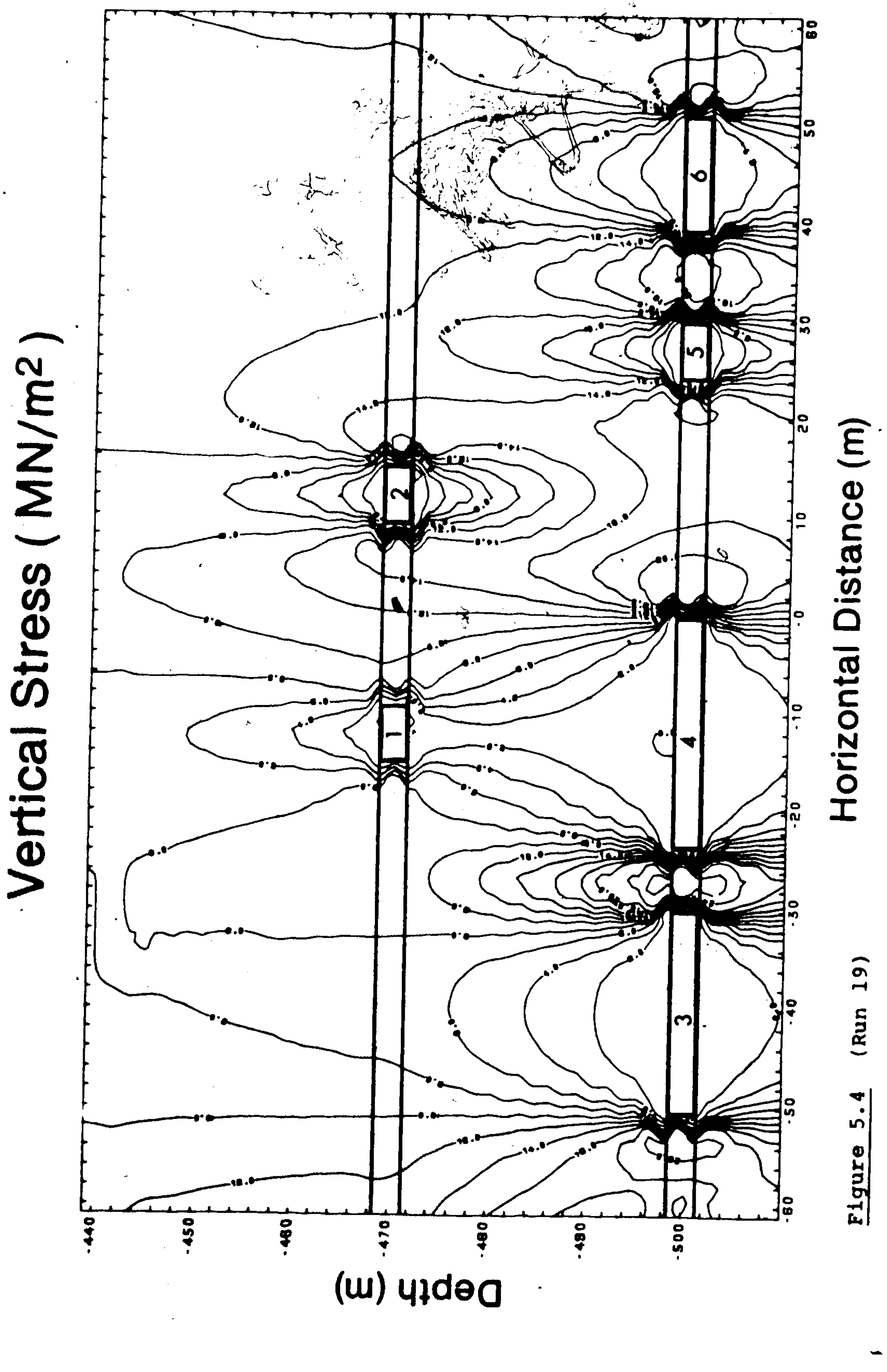

Figure 5.4 (Run 19)

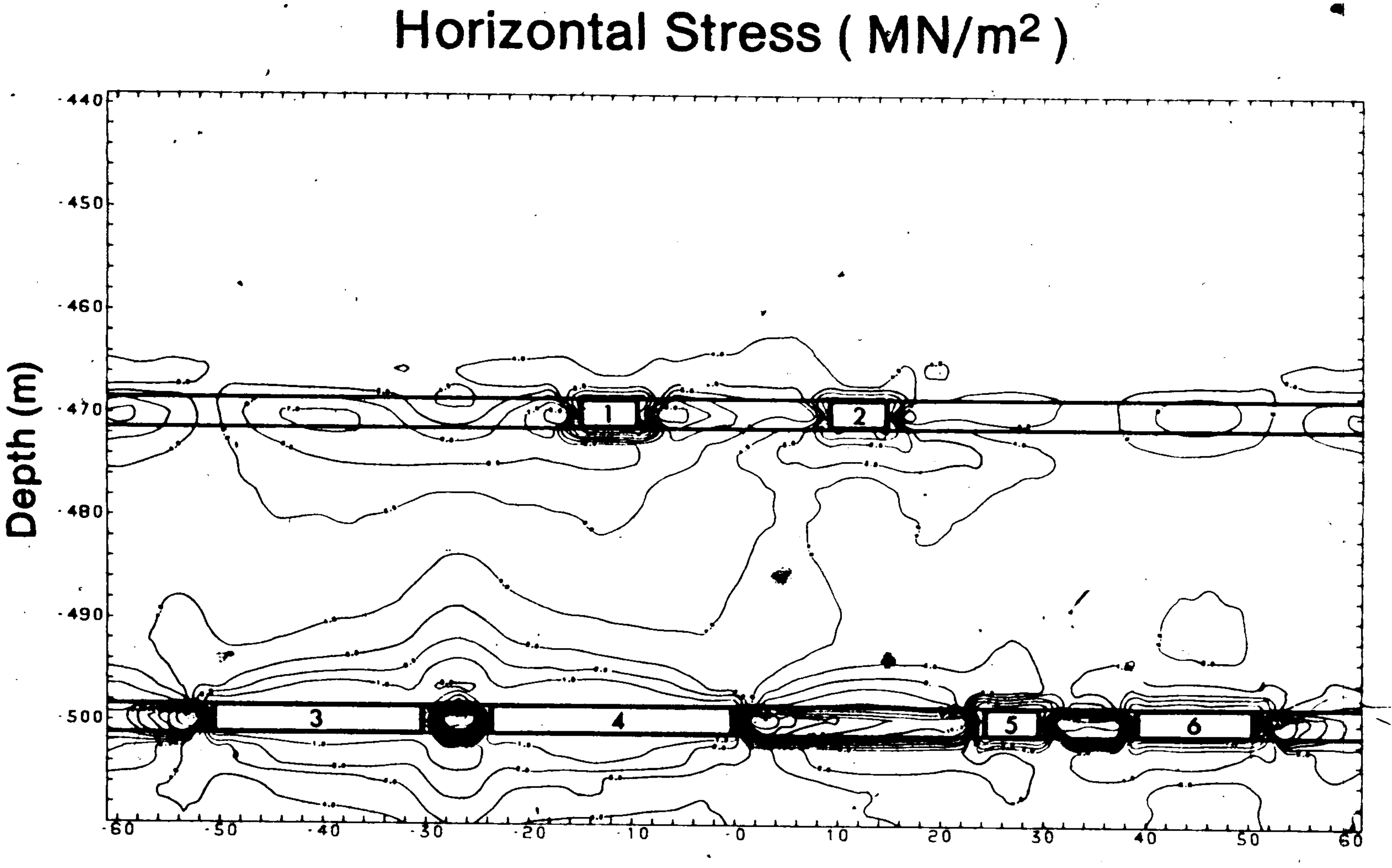

Figure 5.5 (Run 19)

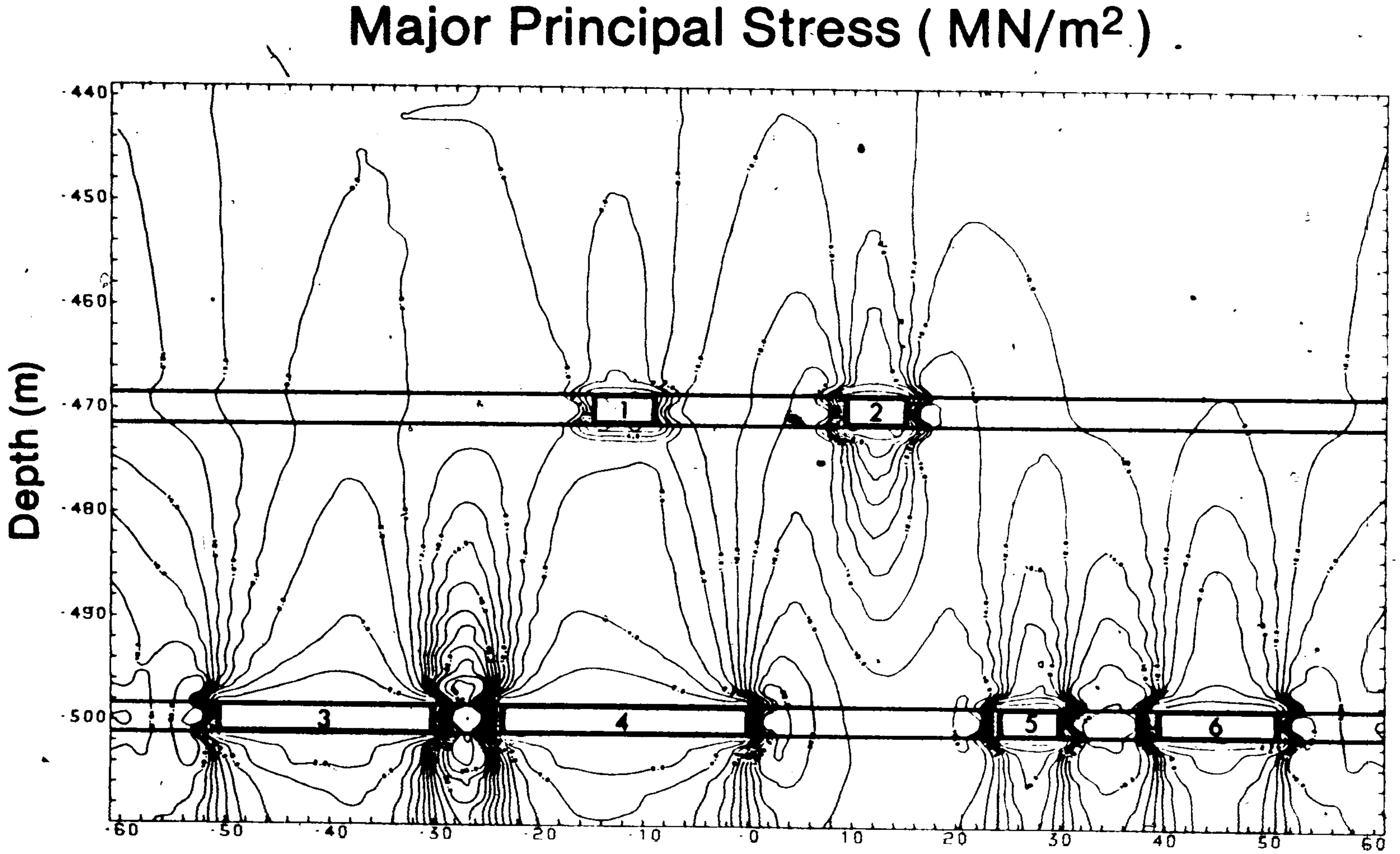

Figure 5.6 (Run 19)

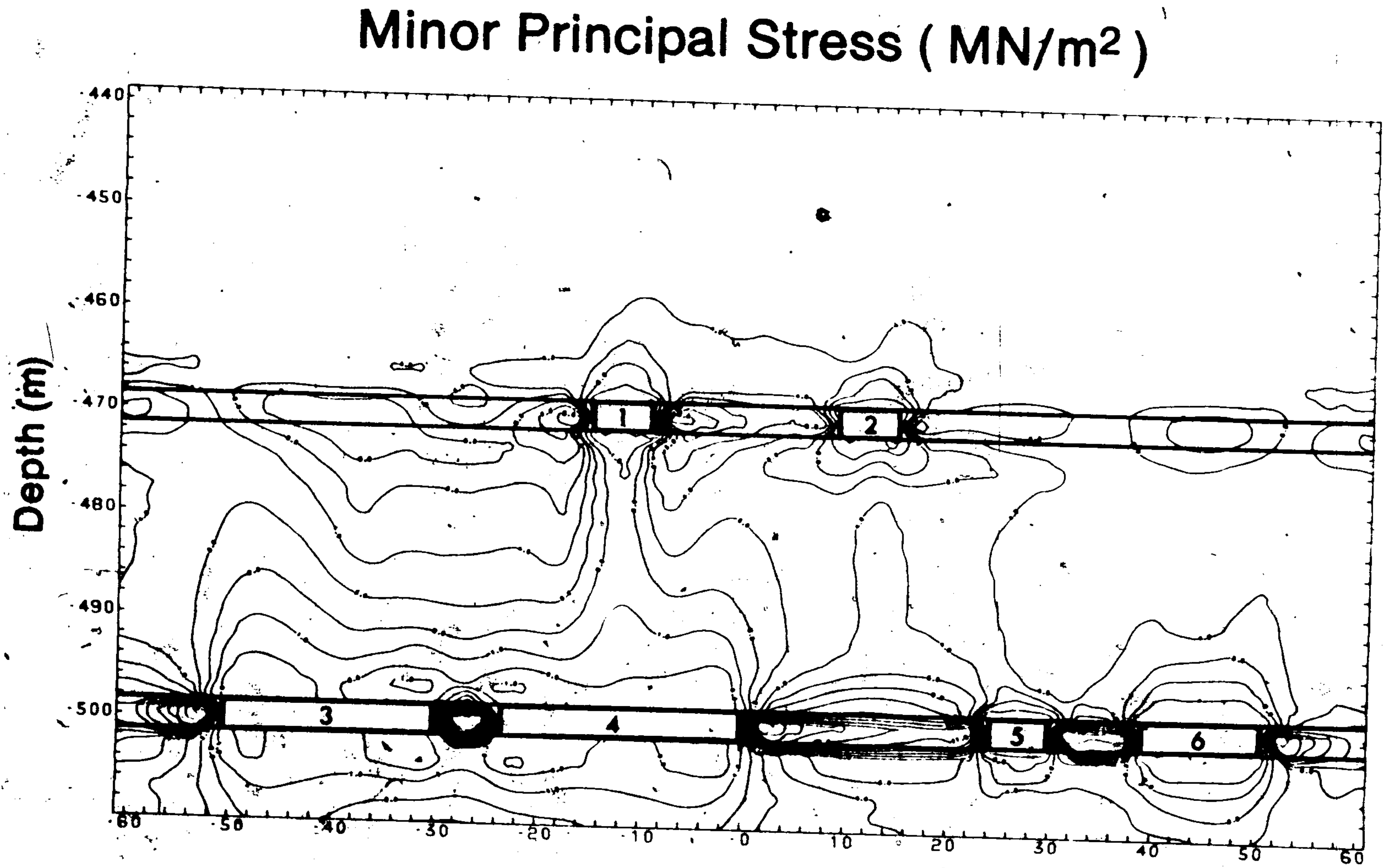

Figure 5.7 (Run 19)

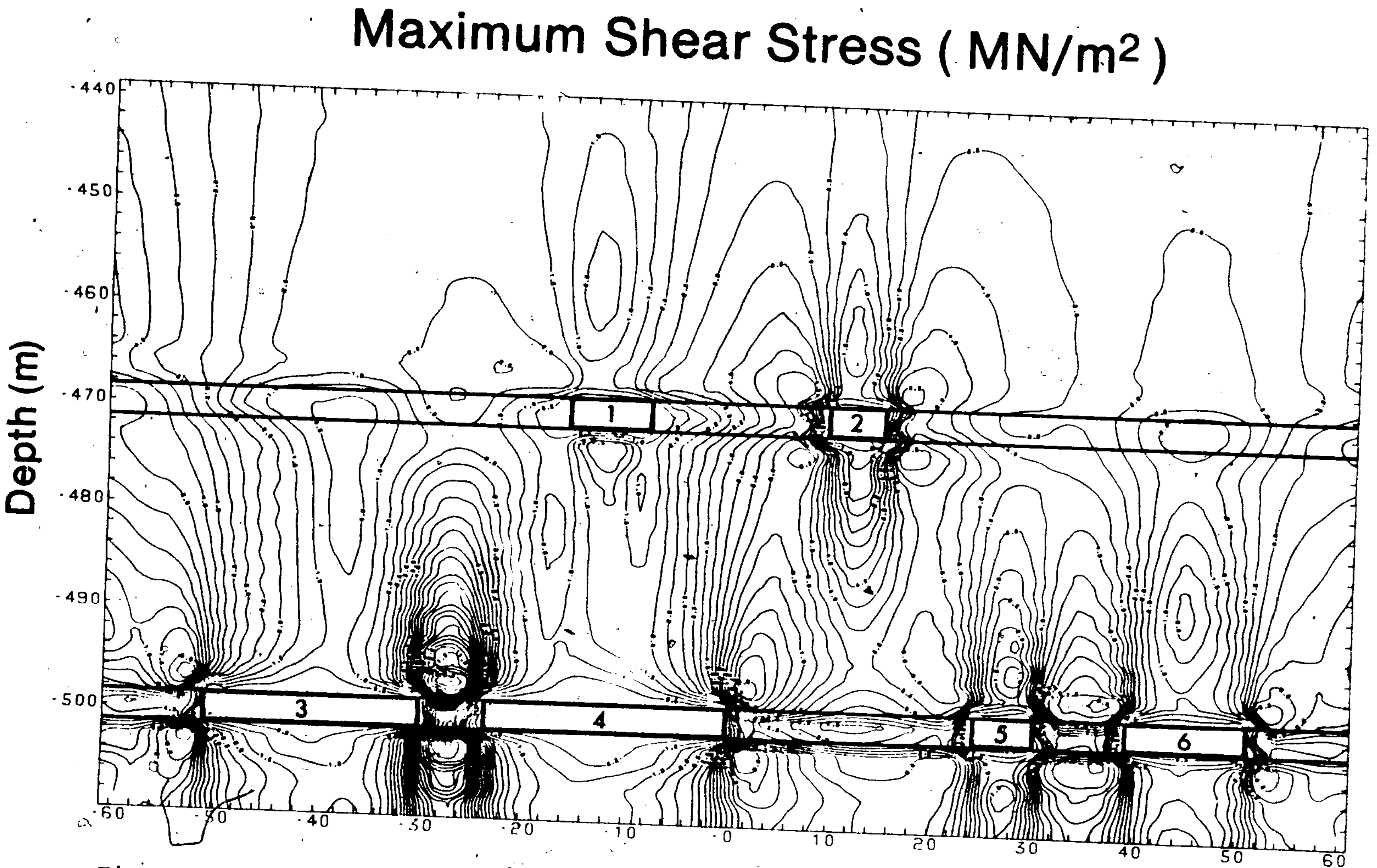

Figure 5.8 (Run 19)

STRESS CRITERION (Negative Areas Shaded)

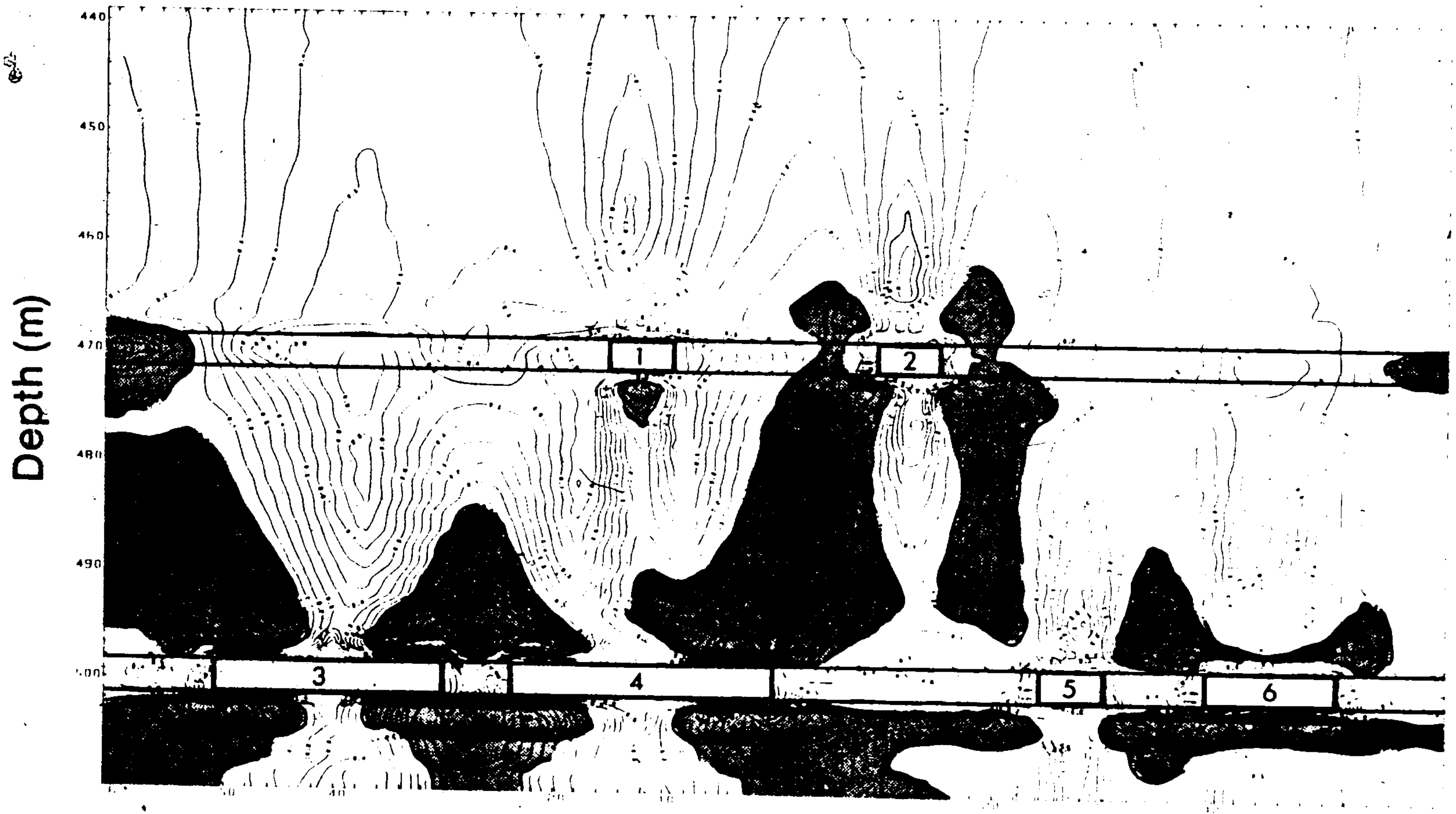

Figure 5.9 (Run 19)

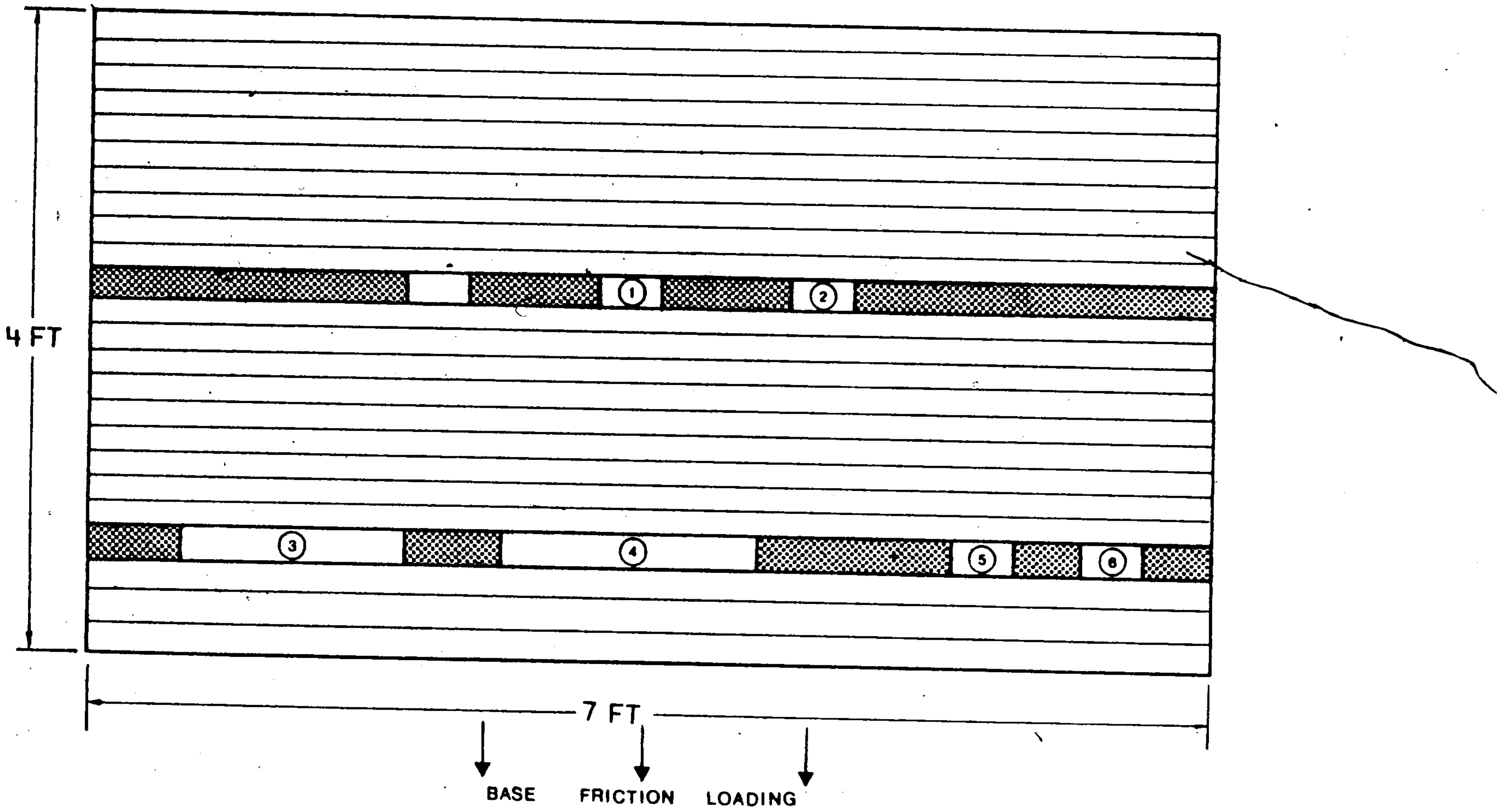
4 FT
7 FT
1
2
3
4
5
6
BASE FRICTION LOADING

FIGURE 5.10 BASE FRICTION MODEL LAYOUT

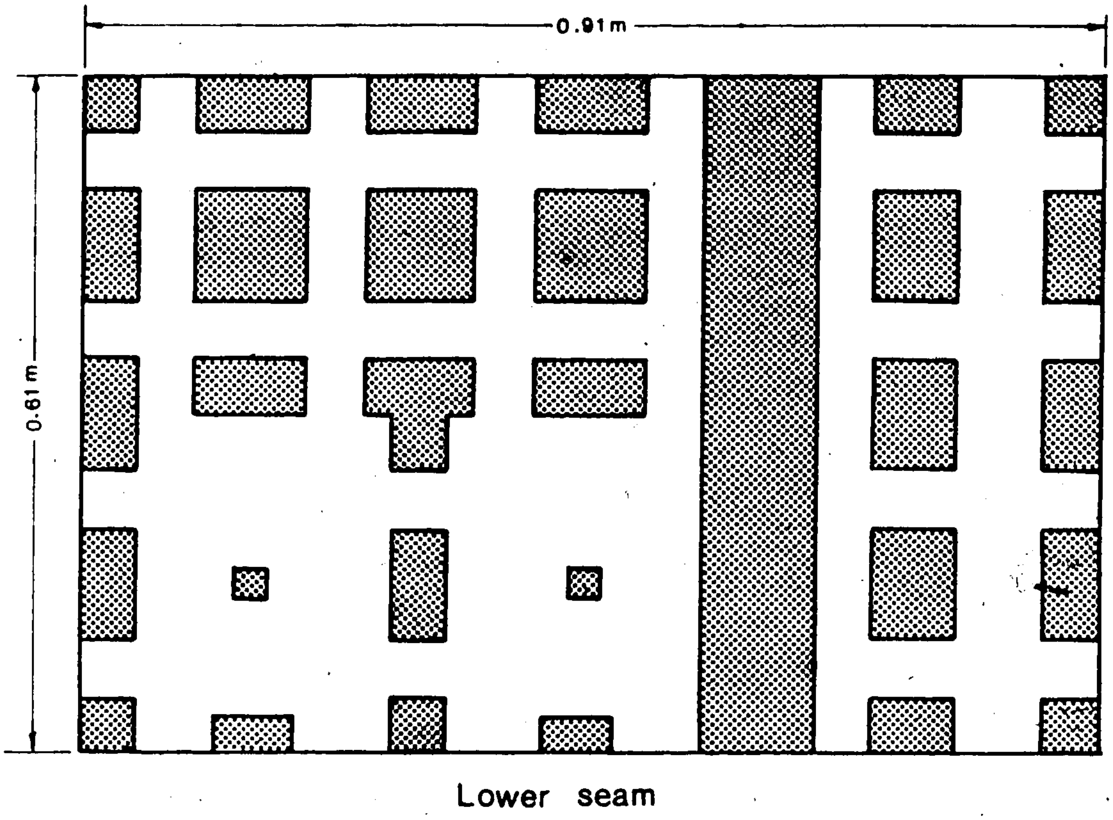
0.91m
0.61 m
Lower seam

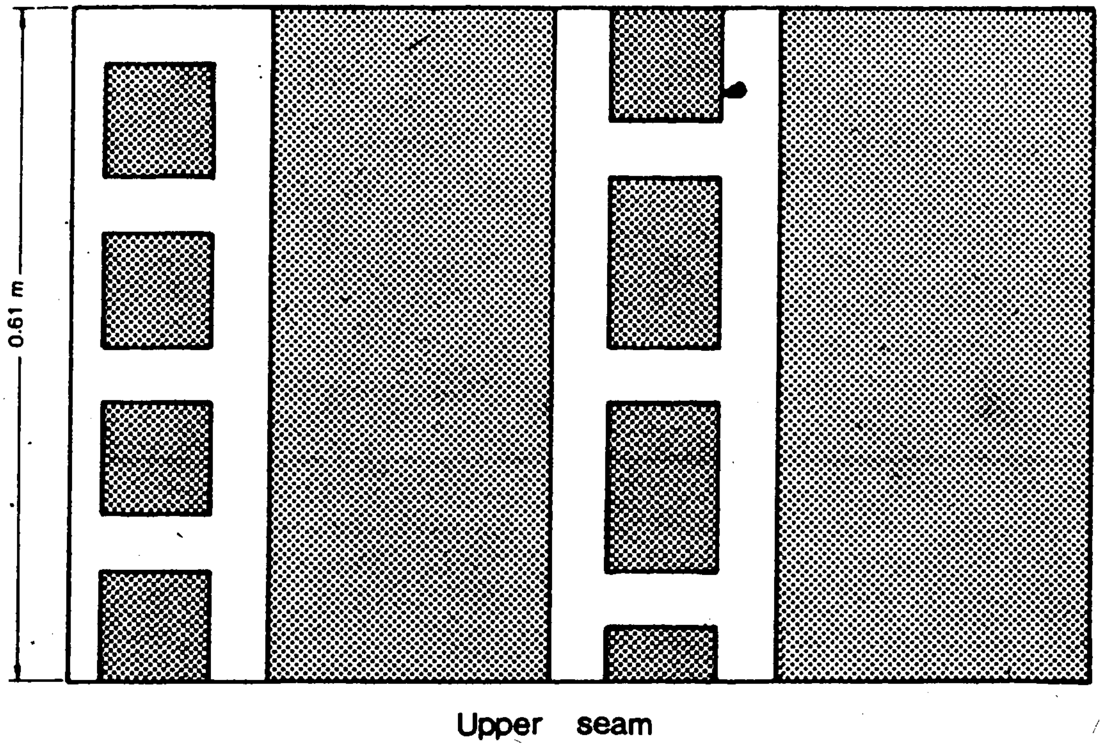
0.61 m
Upper seam

FIGURE 5.11 3-D PHYSICAL MODEL LAYOUT PLAN

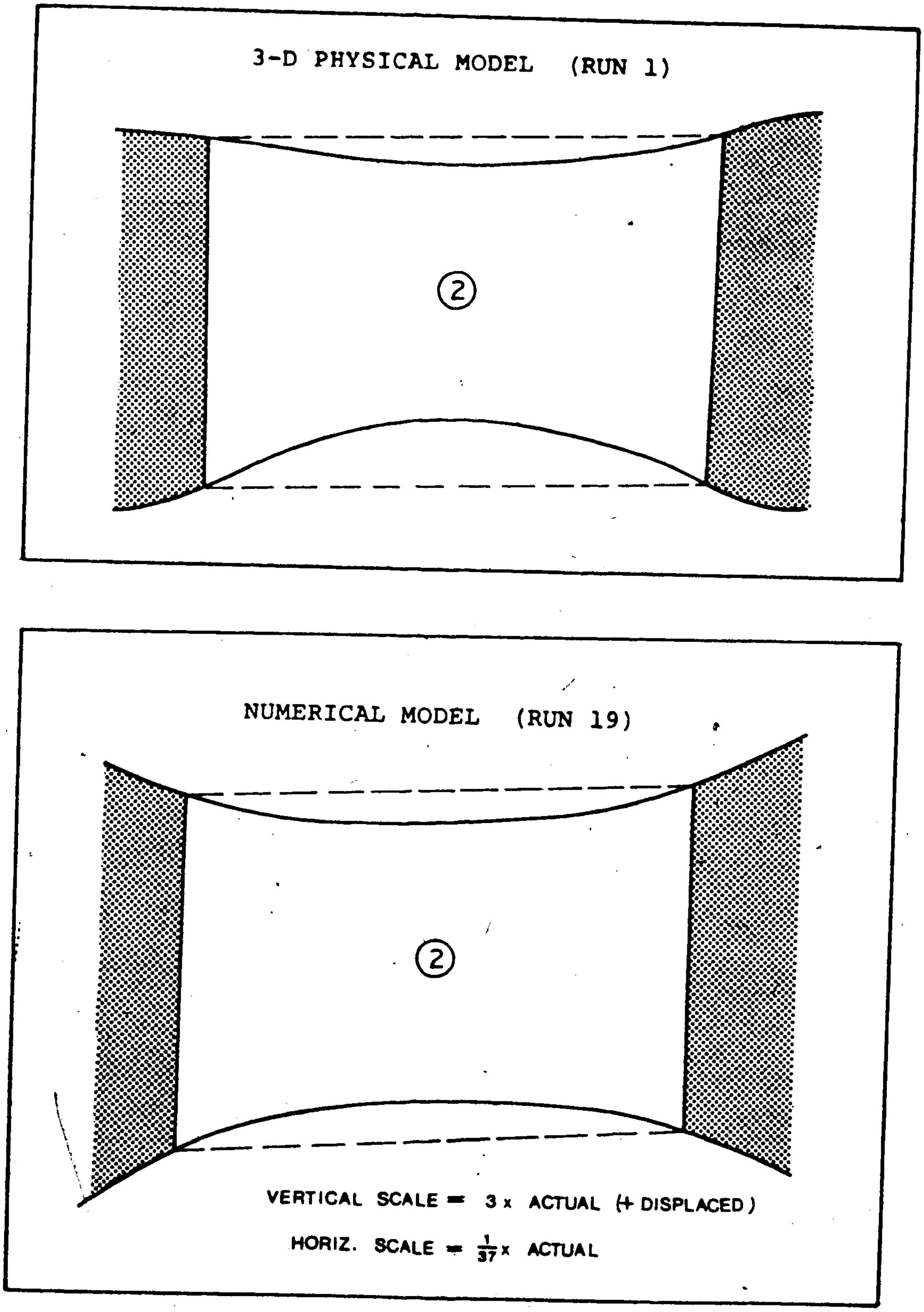
3-D PHYSICAL MODEL (RUN 1)
②
NUMERICAL MODEL (RUN 19)
②
VERTICAL SCALE = 3 x ACTUAL (+ DISPLACED)
HORIZ. SCALE = $\frac{1}{37}$x ACTUAL

FIGURE 5.12 NUMERICAL / 3-D PHYSICAL MODEL COMPARISON (OPENING 2)

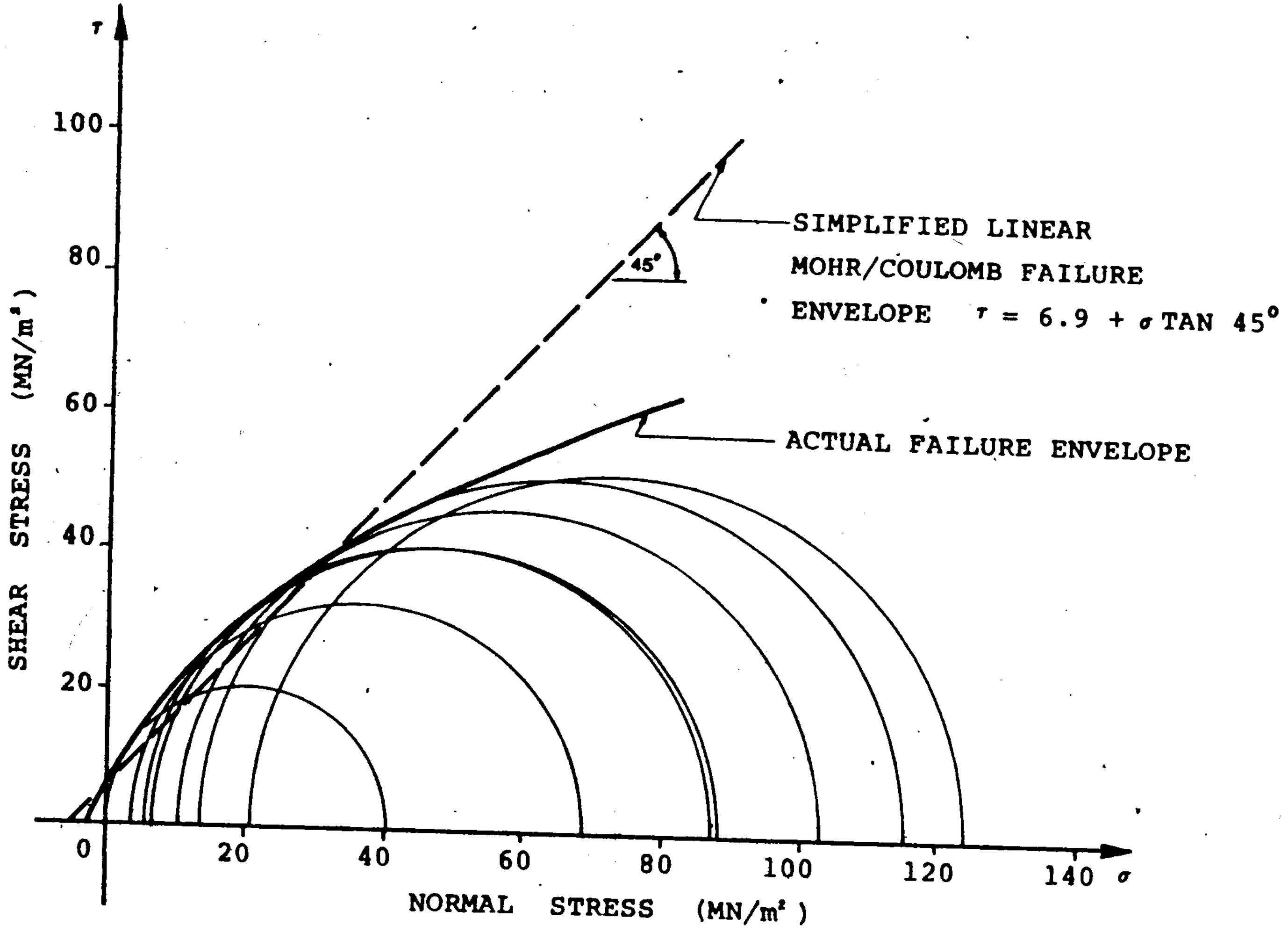

FIGURE 6.1 TRIAXIAL TEST RESULTS - SANDSTONE

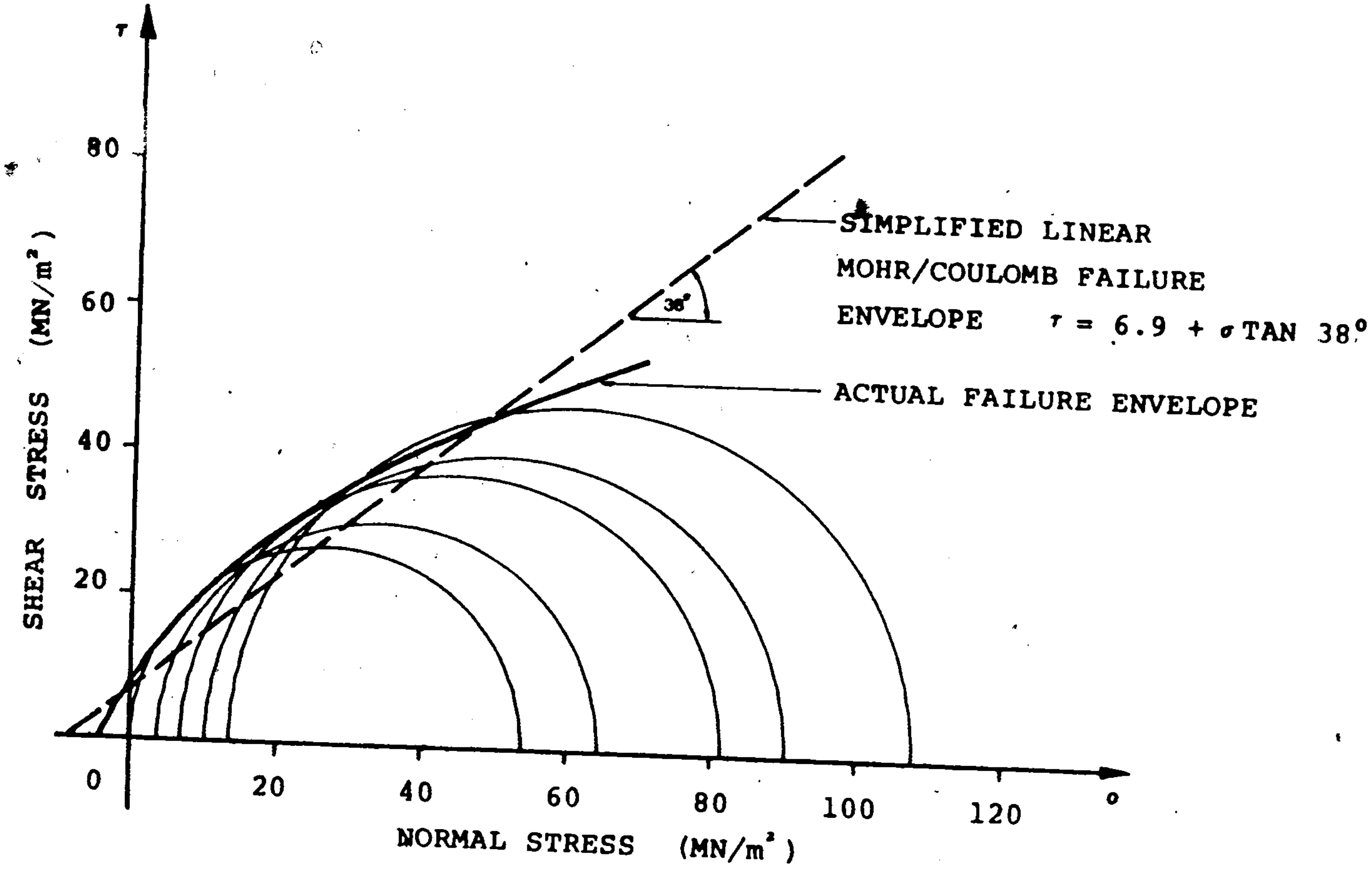

FIGURE 6.2 TRIAXIAL TEST RESULTS - MUDSTONE

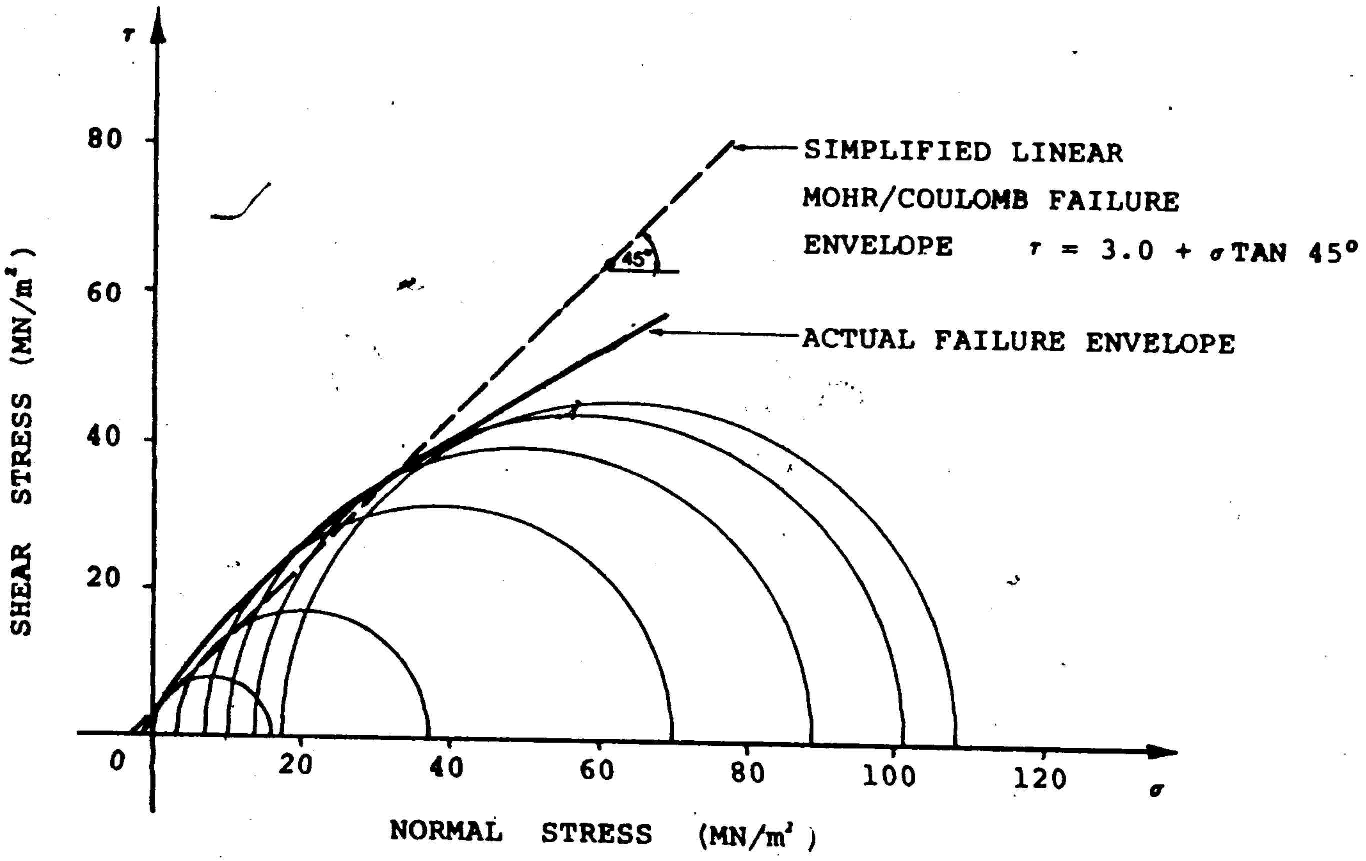

FIGURE 6.3 TRIAXIAL TEST RESULTS - COAL

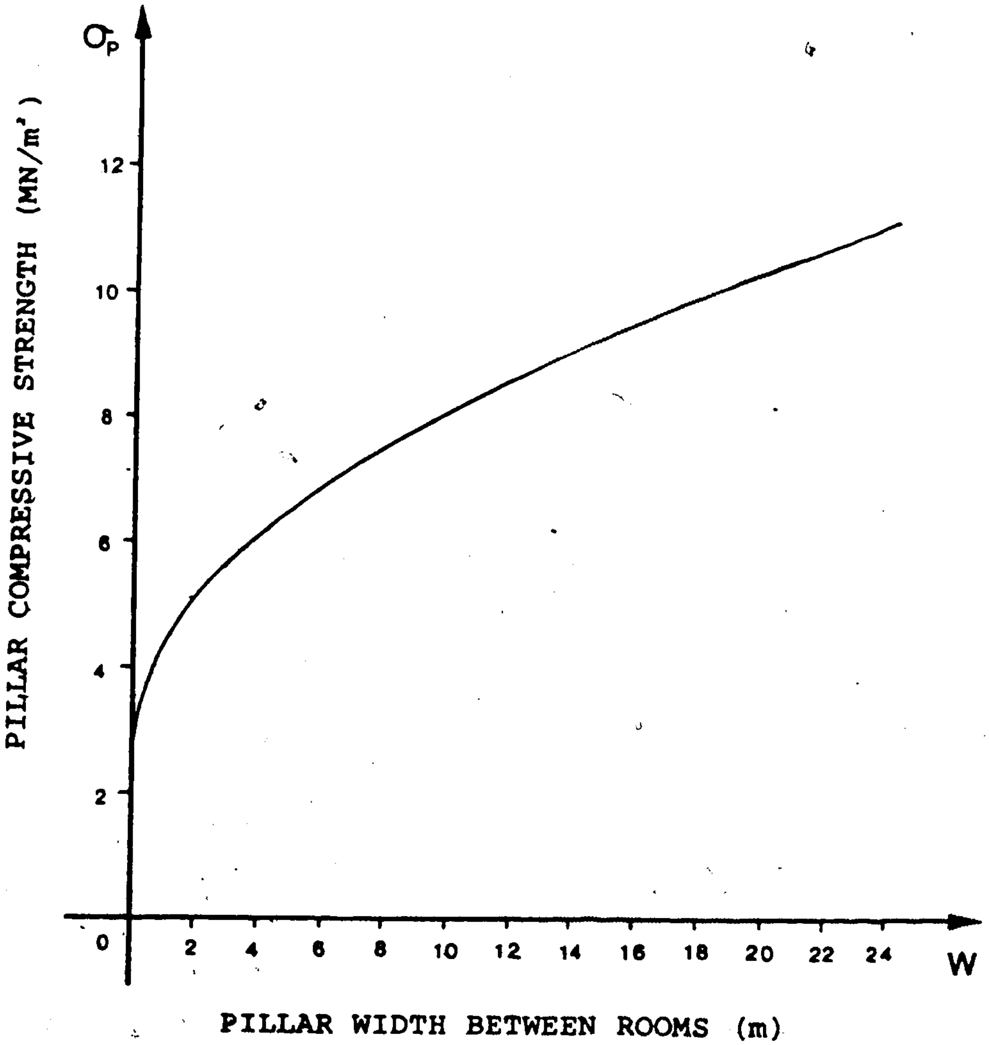

FIGURE 6.4 PILLAR STRENGTH AS A FUNCTION OF WIDTH

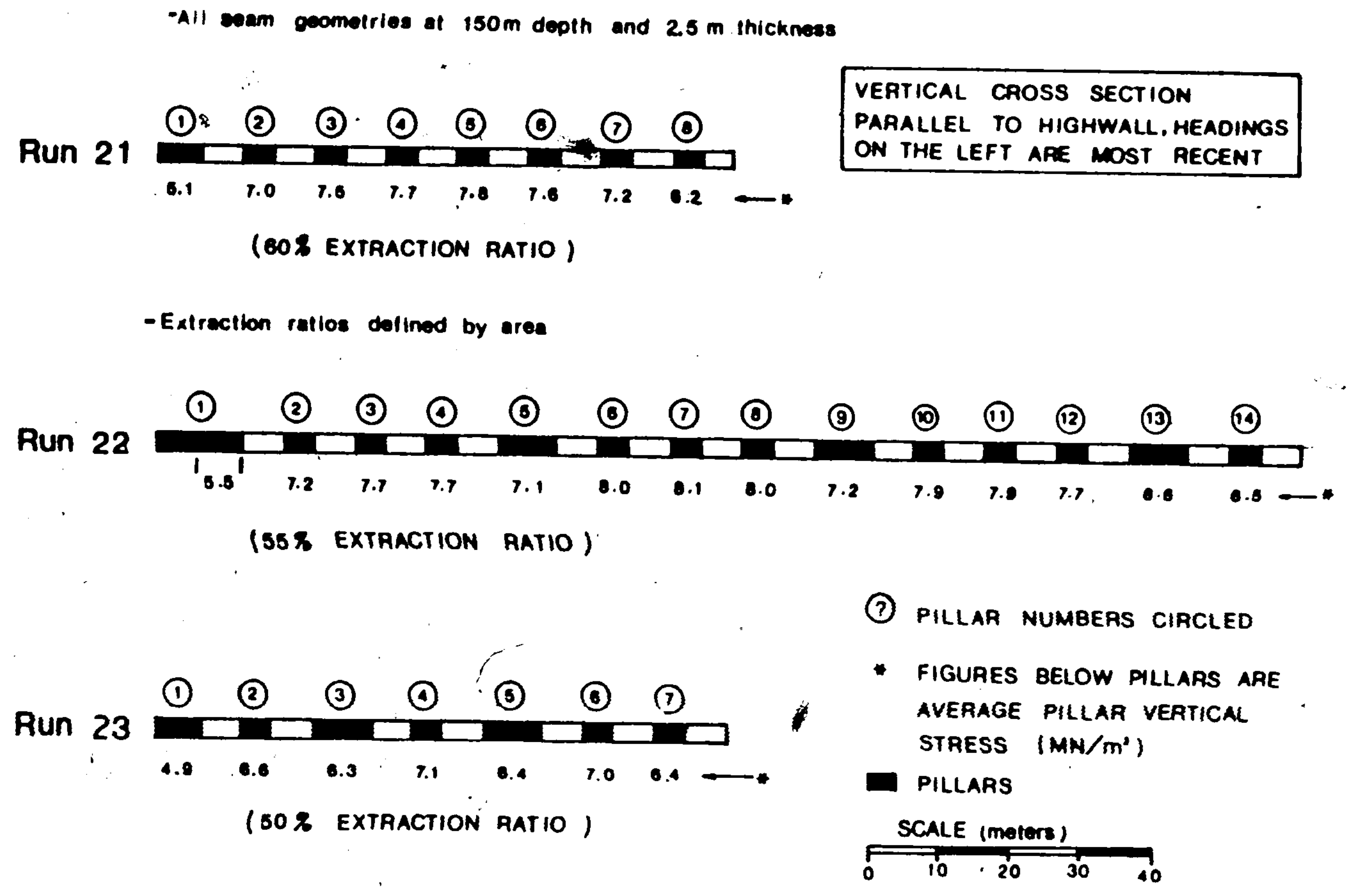
-All seam geometries at 150m depth and 2.5 m thickness
VERTICAL CROSS SECTION PARALLEL TO HIGHWALL, HEADINGS ON THE LEFT ARE MOST RECENT
Run 21
① ② ③ ④ ⑤ ⑥ ⑦ ⑧
6.1 7.0 7.6 7.7 7.8 7.6 7.2 6.2 ←*
(60% EXTRACTION RATIO)
-Extraction ratios defined by area
Run 22
① ② ③ ④ ⑤ ⑥ ⑦ ⑧ ⑨ ⑩ ⑪ ⑫ ⑬ ⑭
5.5 7.2 7.7 7.7 7.1 8.0 8.1 8.0 7.2 7.9 7.9 7.7 6.6 6.5 ←*
(55% EXTRACTION RATIO)
Run 23
① ② ③ ④ ⑤ ⑥ ⑦
4.9 6.6 6.3 7.1 6.4 7.0 6.4 ←*
(50% EXTRACTION RATIO)
⑦ PILLAR NUMBERS CIRCLED
* FIGURES BELOW PILLARS ARE AVERAGE PILLAR VERTICAL STRESS (MN/m²)
■ PILLARS
SCALE (meters)
0 10 20 30 40

FIGURE 6.5 MINE SIMULATION LAYOUTS AND PILLAR VERTICAL STRESSES

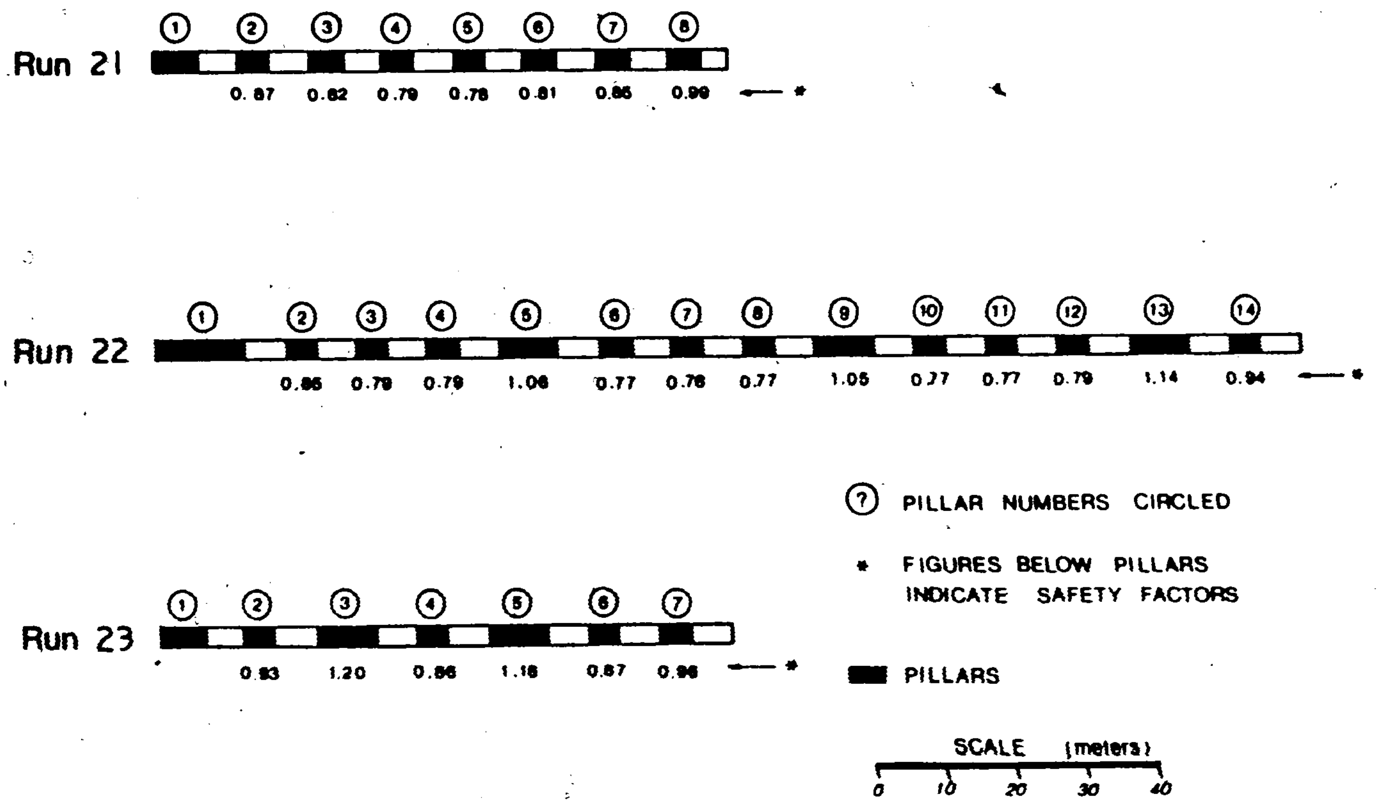

Run 21
①
②
③
④
⑤
⑥
⑦
⑧
0.87
0.82
0.79
0.78
0.81
0.86
0.99
*
Run 22
①
②
③
④
⑤
⑥
⑦
⑧
⑨
⑩
⑪
⑫
⑬
⑭
0.86
0.79
0.79
1.06
0.77
0.78
0.77
1.05
0.77
0.77
0.79
1.14
0.94
*
Run 23
①
②
③
④
⑤
⑥
⑦
0.93
1.20
0.86
1.18
0.87
0.96
*
⑦ PILLAR NUMBERS CIRCLED
* FIGURES BELOW PILLARS INDICATE SAFETY FACTORS
PILLARS
SCALE (meters)
0
10
20
30
40

FIGURE 6.6 MINE SIMULATION LAYOUTS AND PILLAR SAFETY FACTORS

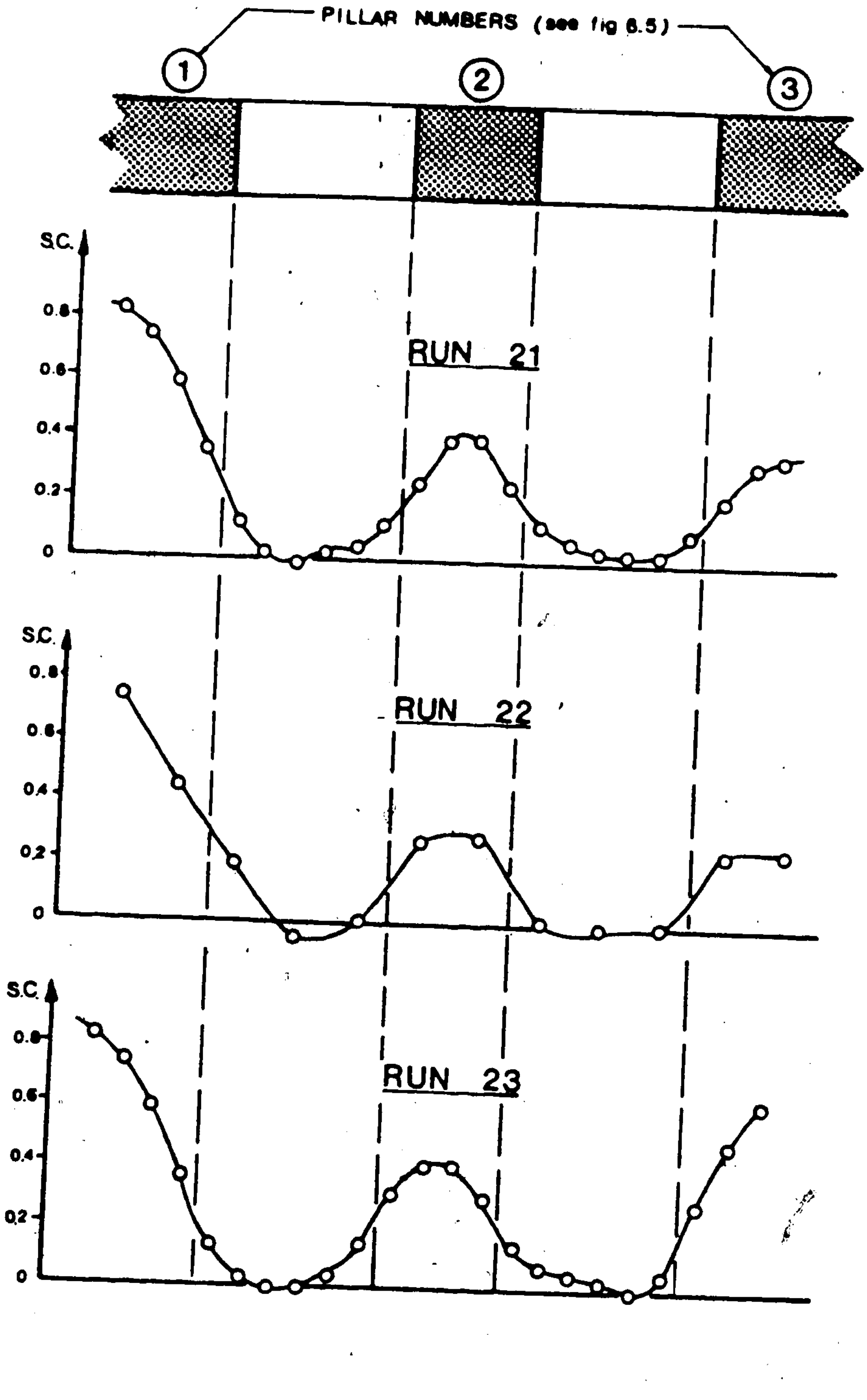

FIGURE 6.7 STRESS CRITERION

(0.75m INTO FLOOR)

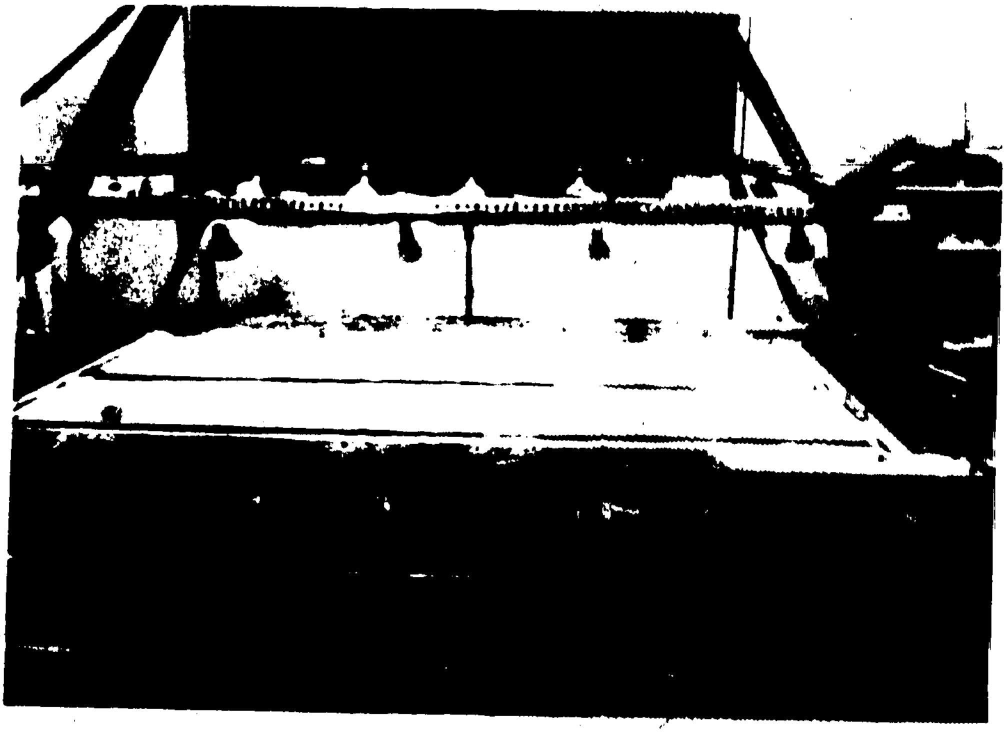

Plate 1. BASE FRICTION APPARATUS

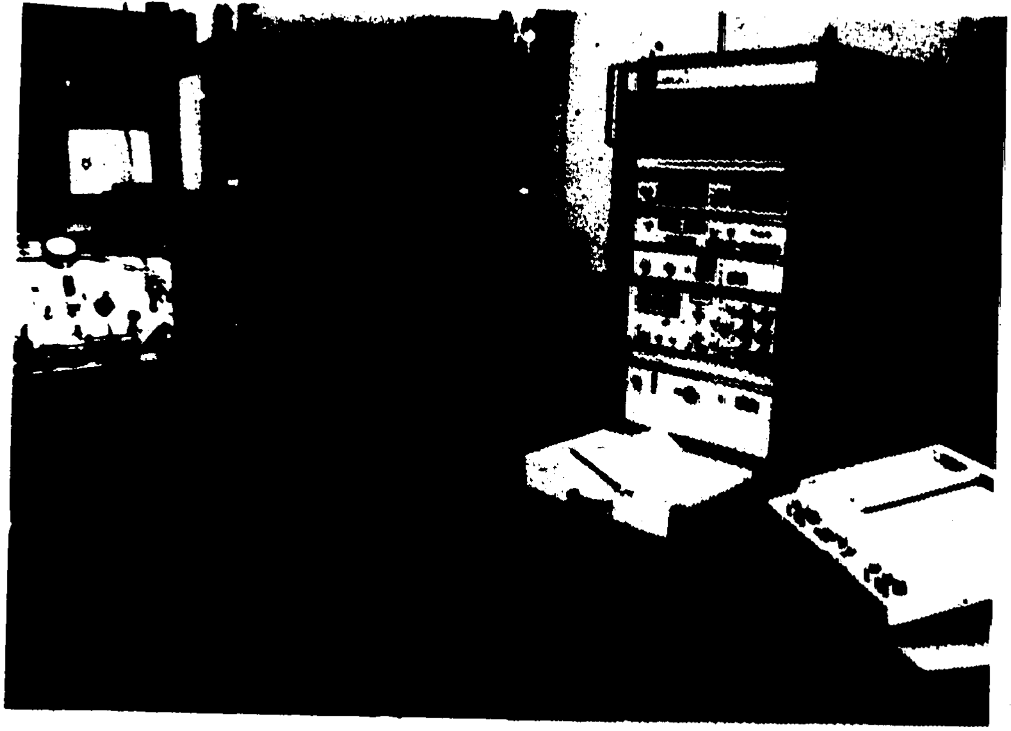

Plate 2. MTS SERVO CONTROLLED STIFF TESTING MACHINE

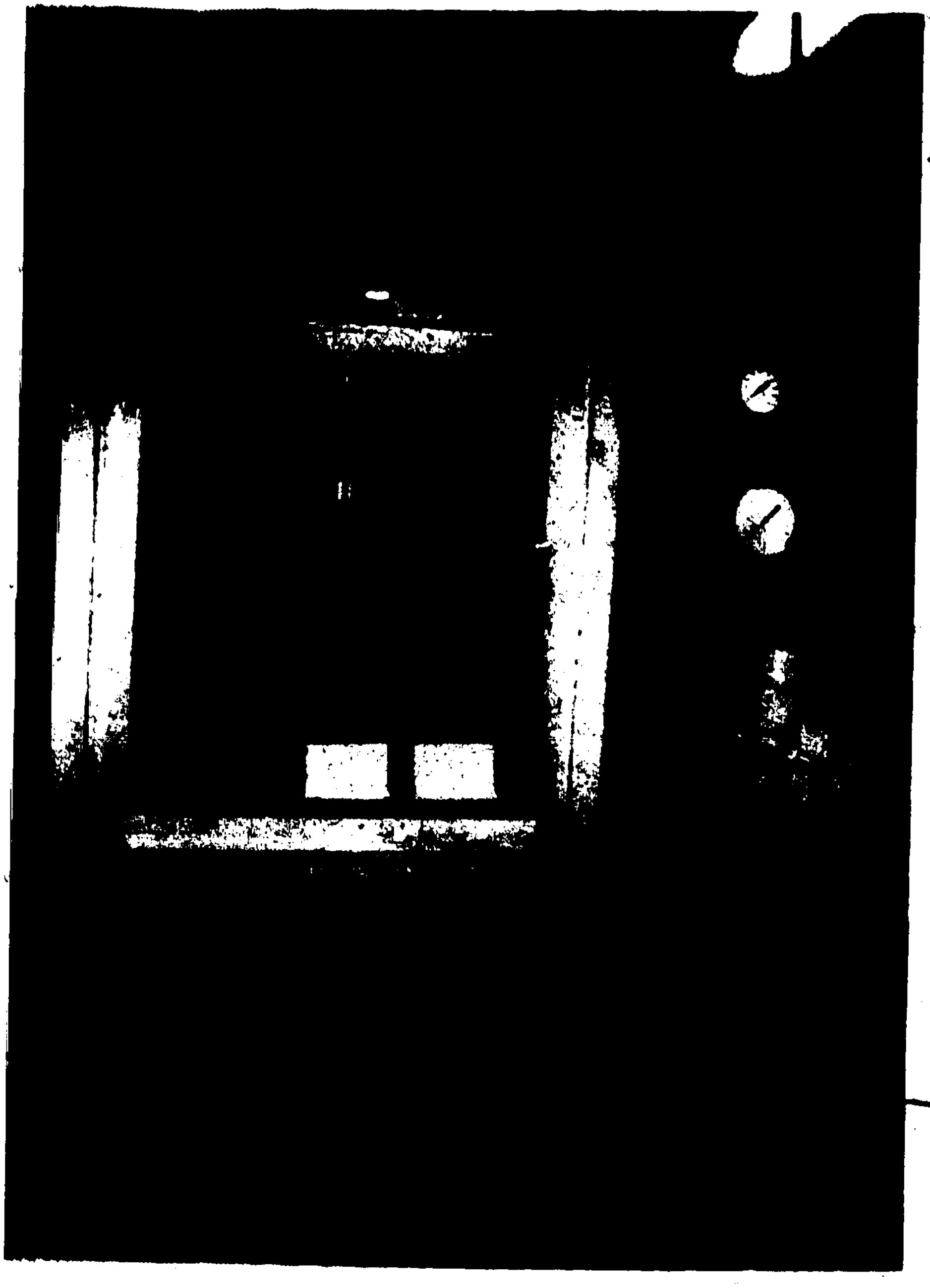

Plate 3. 3-D MODEL IN COMPRESSION FRAME

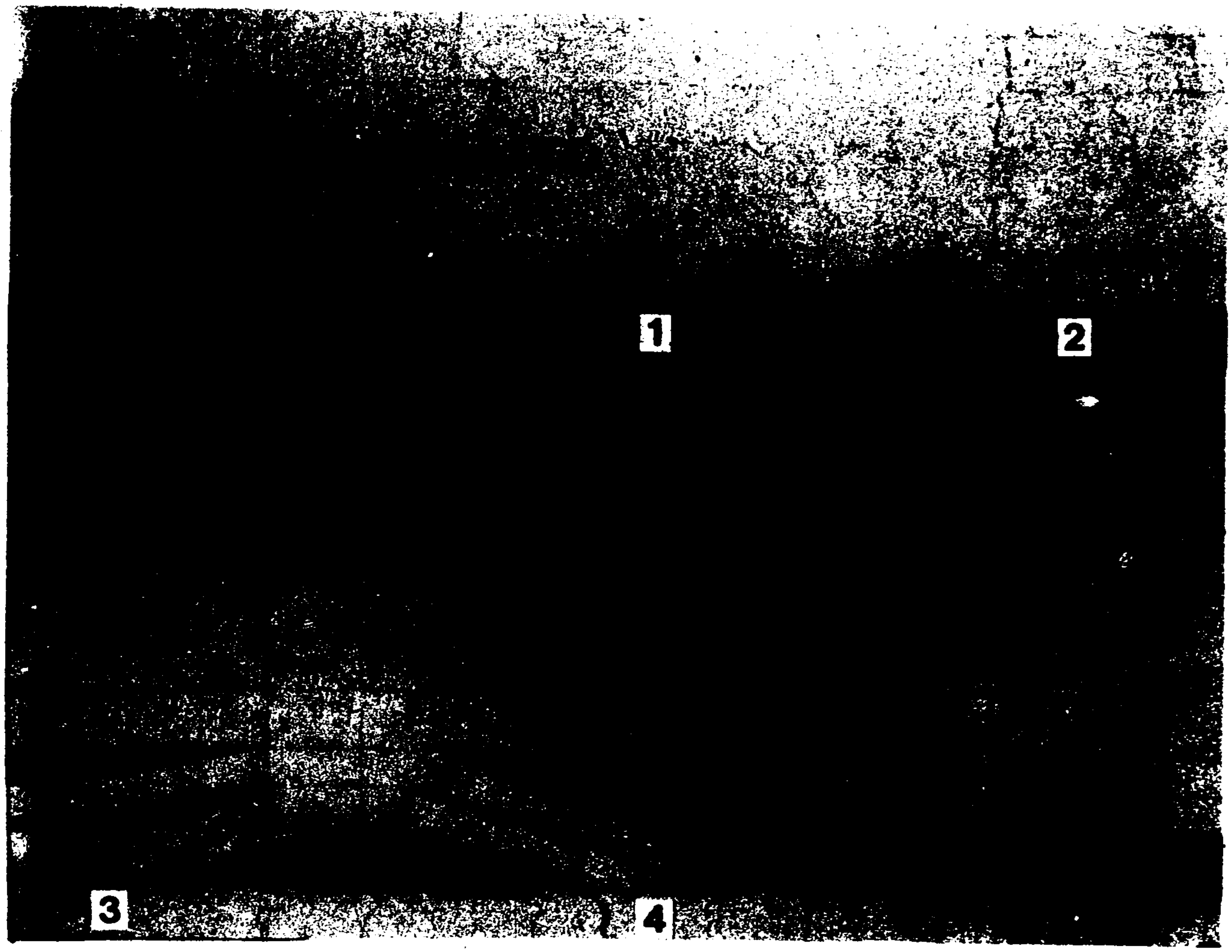

Plate 4. BASE FRICTION MODEL - CAVING INITIATED

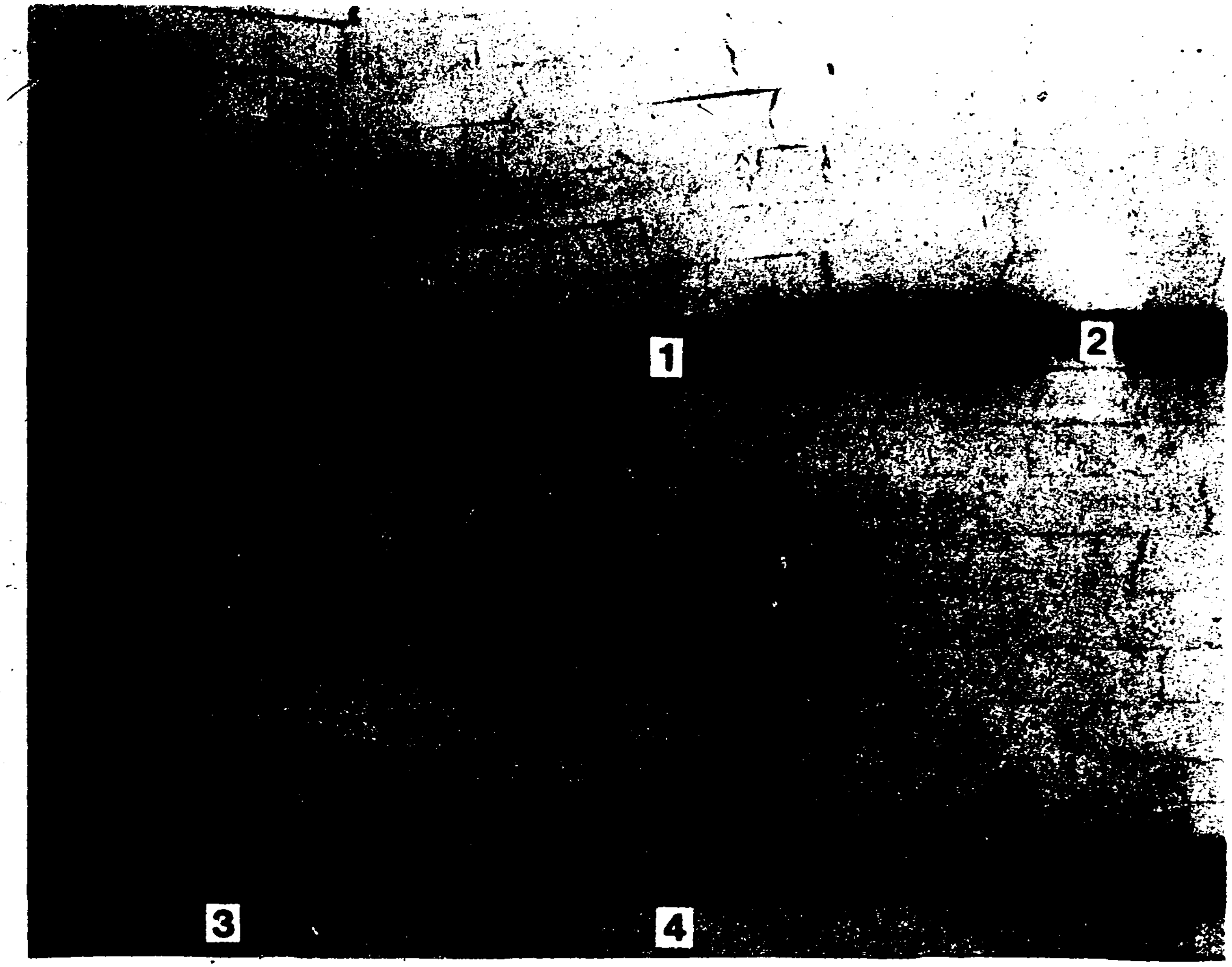

Plate 5. BASE FRICTION MODEL -FINAL CAVE

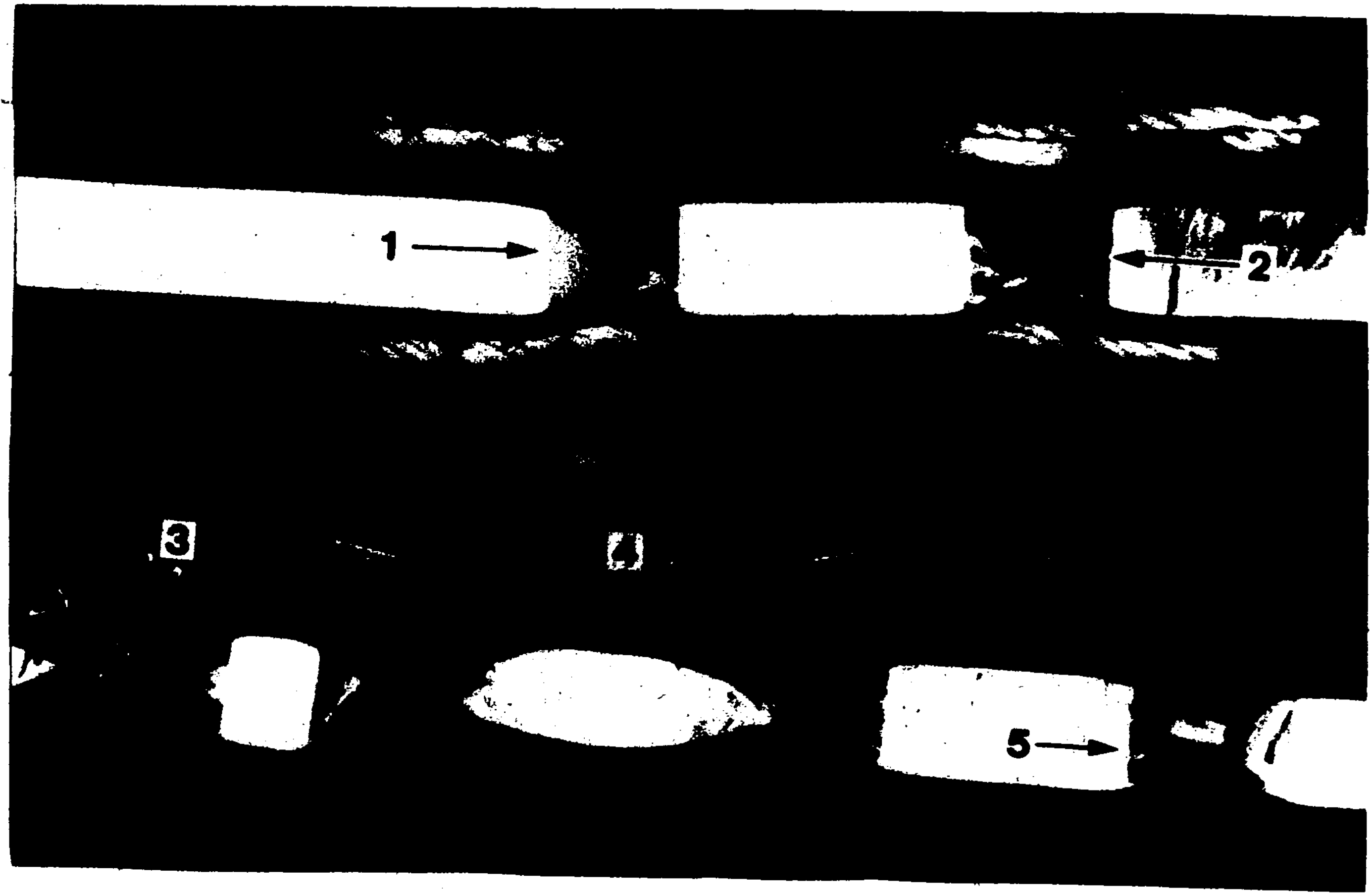

Plate 6. 3-D MODEL (RUN 1) - YIELD STATE

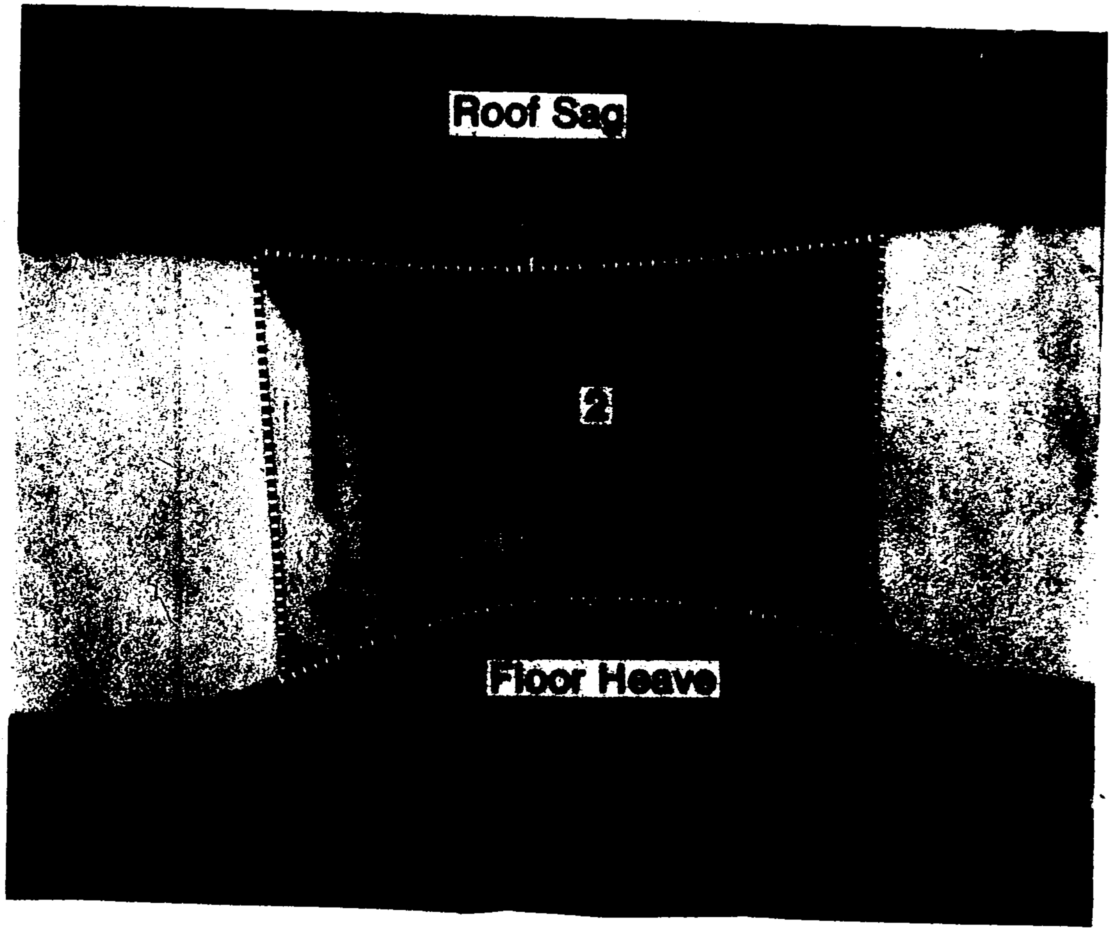
Roof Sag
2
Floor Heave

Plate 7. 3-D MODEL (RUN 1, OPENING No.2) - YIELD STATE

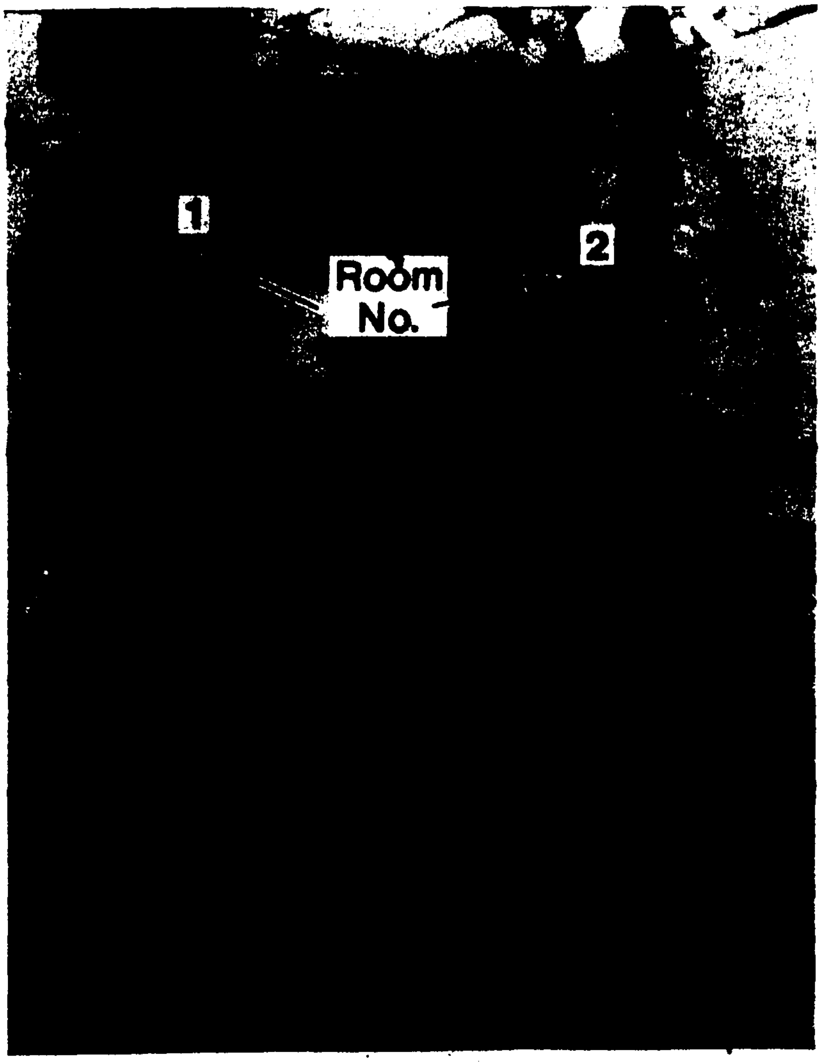

Plate 8. 3-D MODEL - AFTER TEST

(RUN 1, PLAN VIEW, UPPER SEAM)

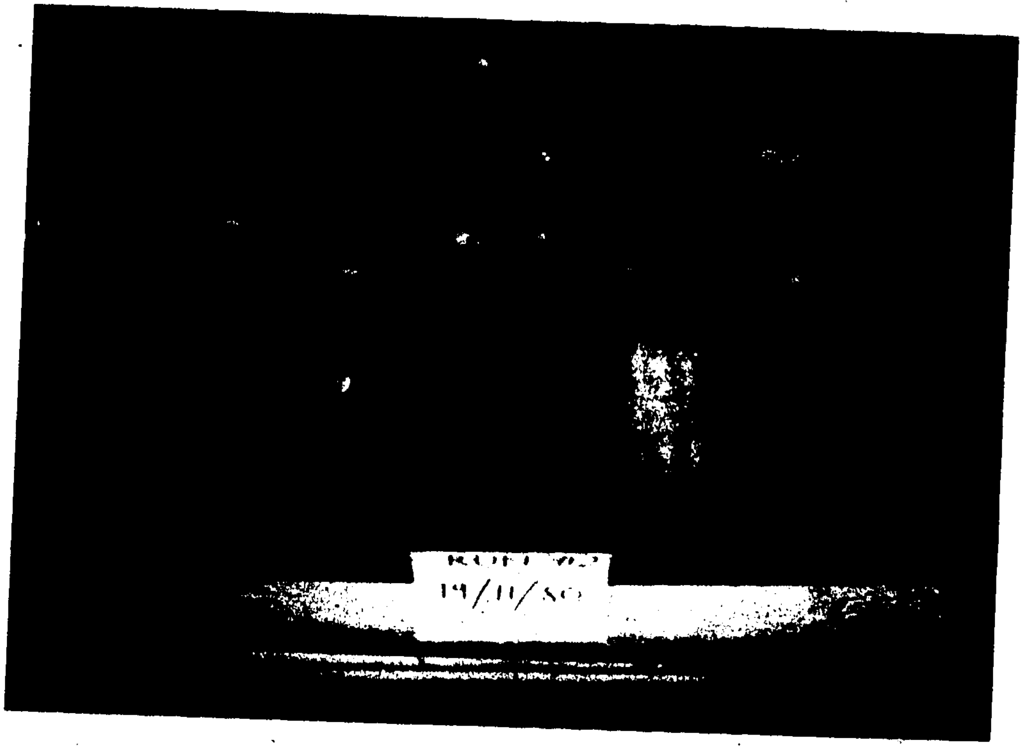

Plate 9. 3-D MODEL (RUN 2, LOWER SEAM) - BEFORE TEST

Plate 10. 3-D MODEL (RUN 2, UPPER SEAM) - BEFORE TEST

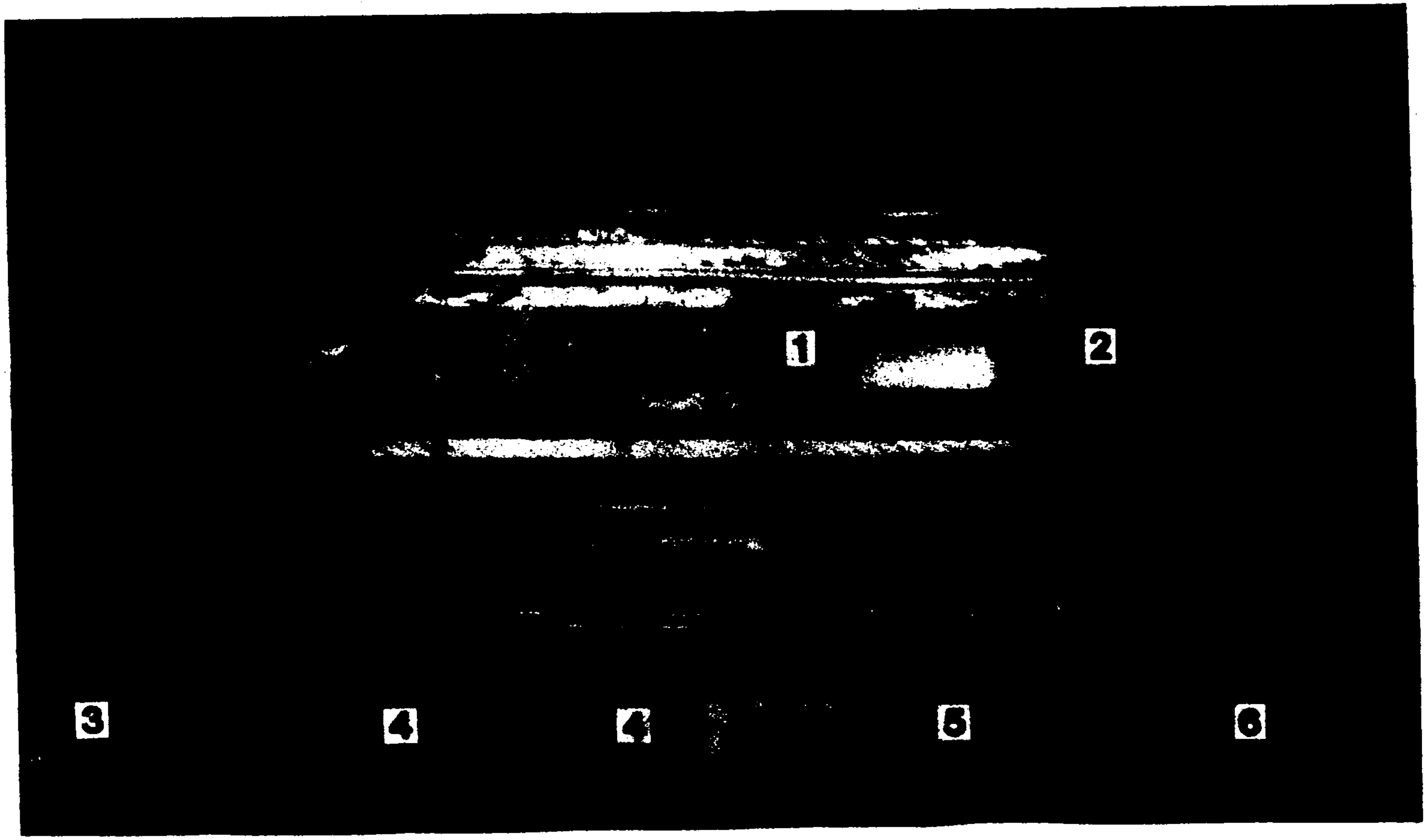

Plate 11. 3-D MODEL (RUN 2, SIDE VIEW) - BEFORE TEST

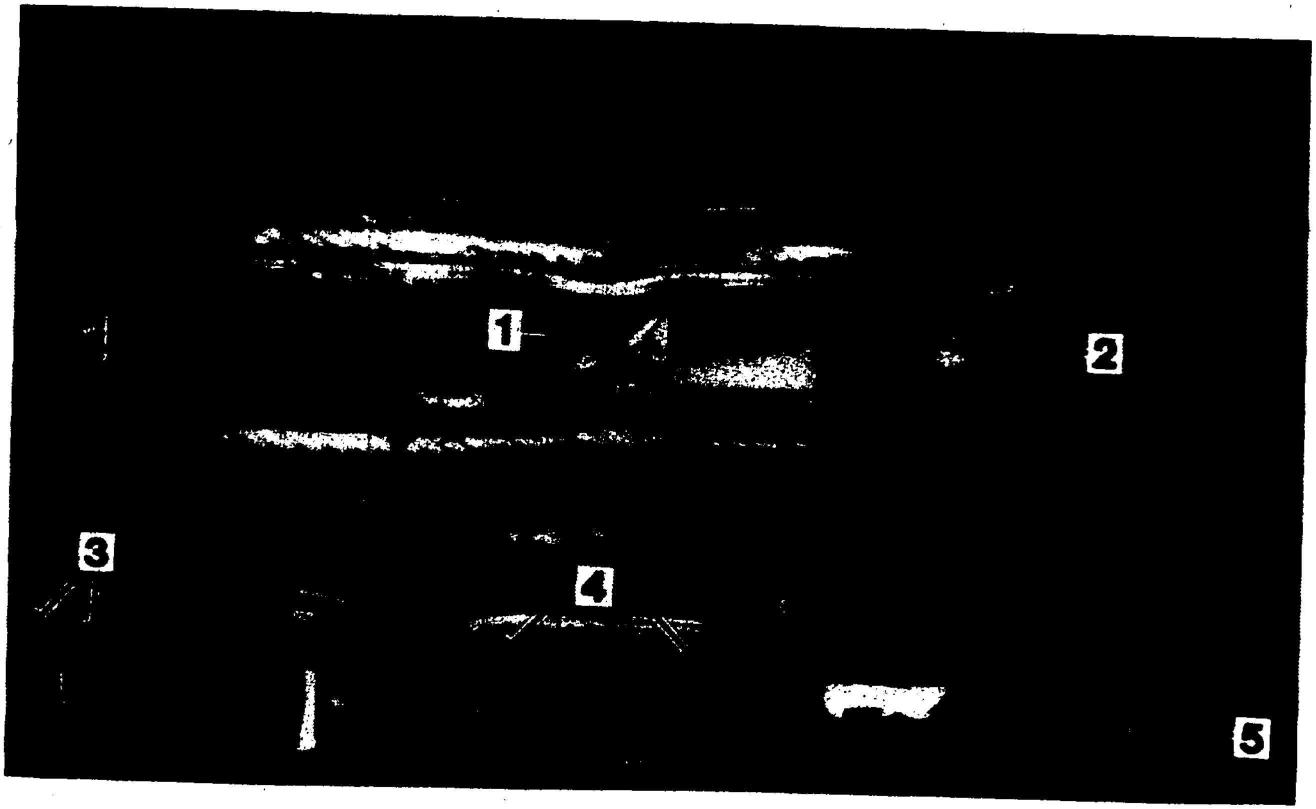

Plate 12. 3-D MODEL (RUN 2, SIDE VIEW) - 0.78 MN/m^2

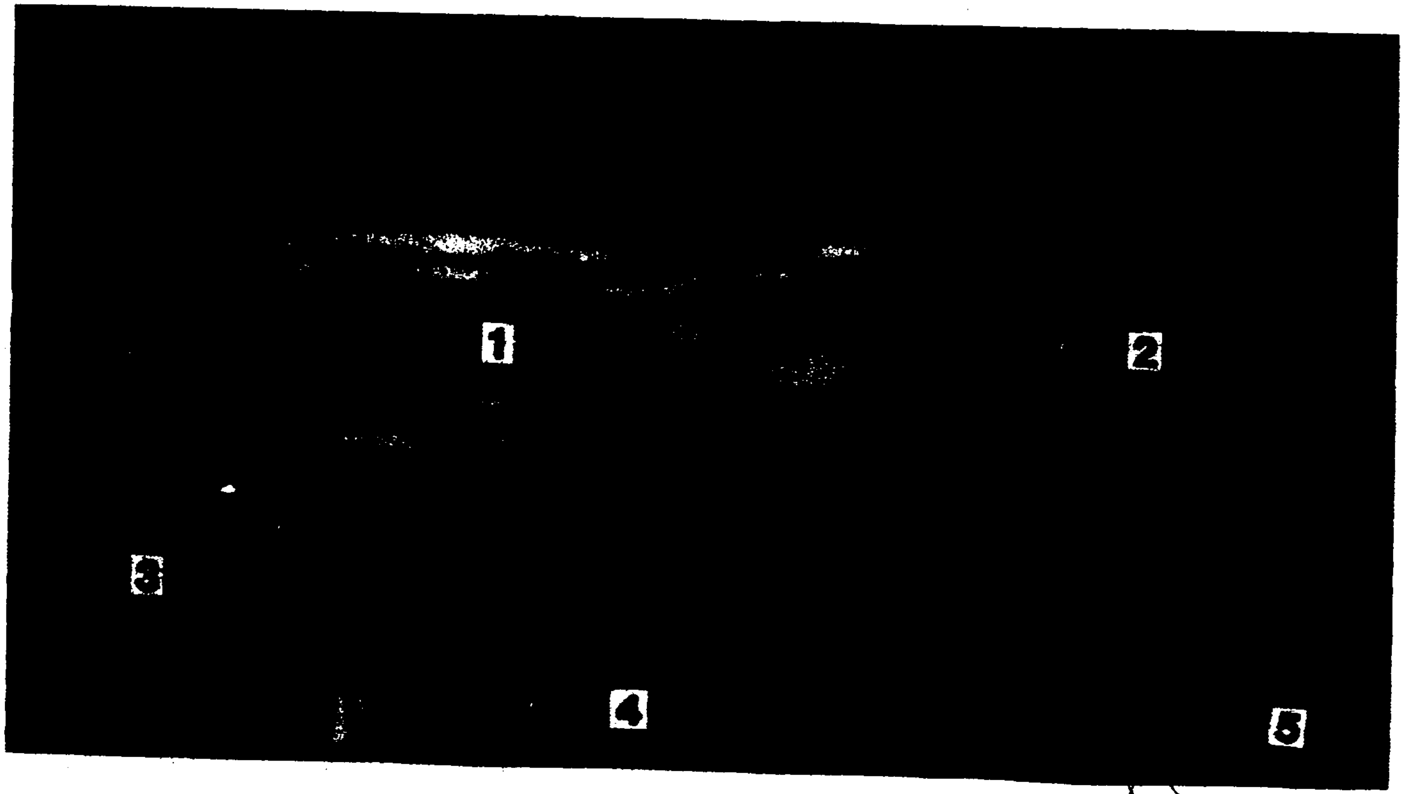

Plate 13. 3-D MODEL (RUN 2, SIDE VIEW) - YIELD STATE

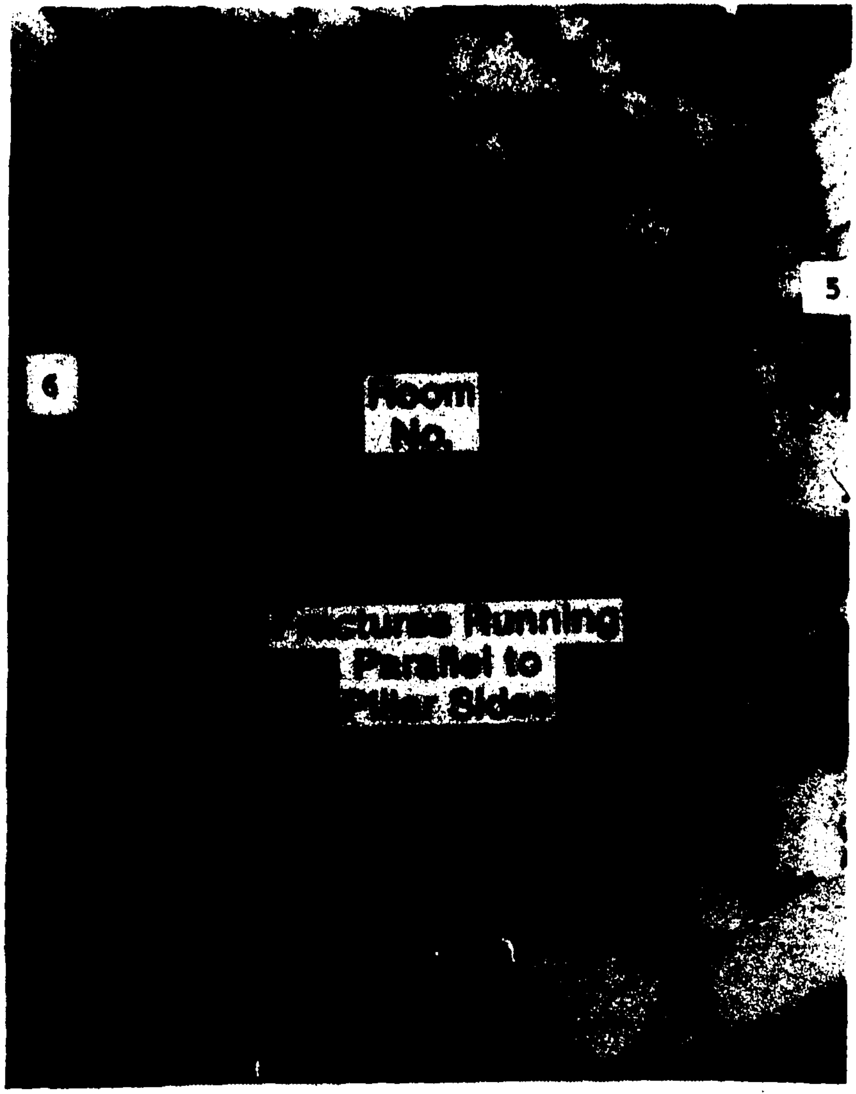
5
6
Room No.
Fractures Running Parallel to Pillar Sides

Plate 14. 3-D MODEL - AFTER TEST

(RUN 2, PLAN VIEW, LOWER SEAM)

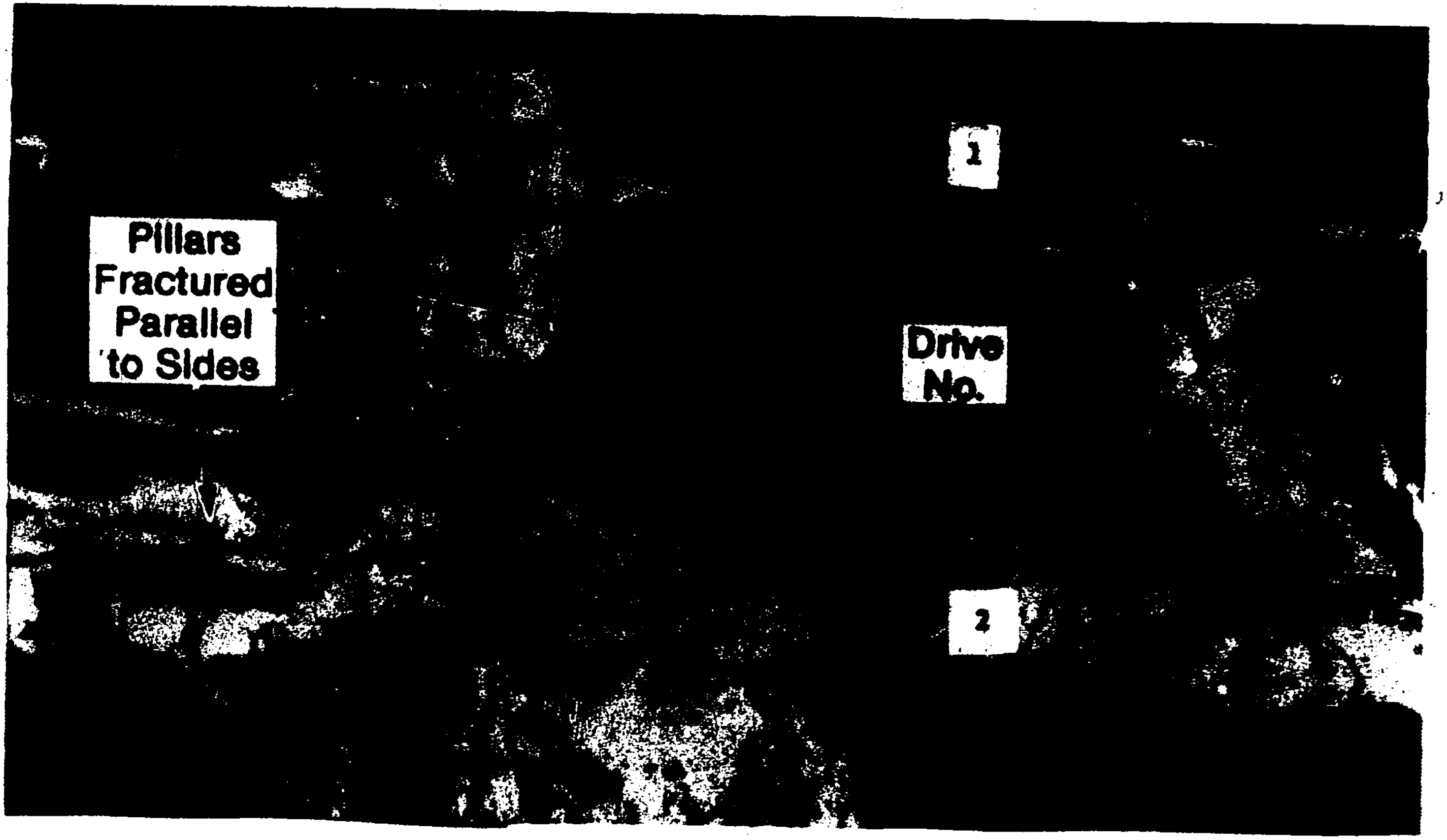
Pillars Fractured Parallel to Sides
1
Drive No.
2

Plate 15. 3-D MODEL (RUN 2, PLAN VIEW, UPPER SEAM) - AFTER TEST

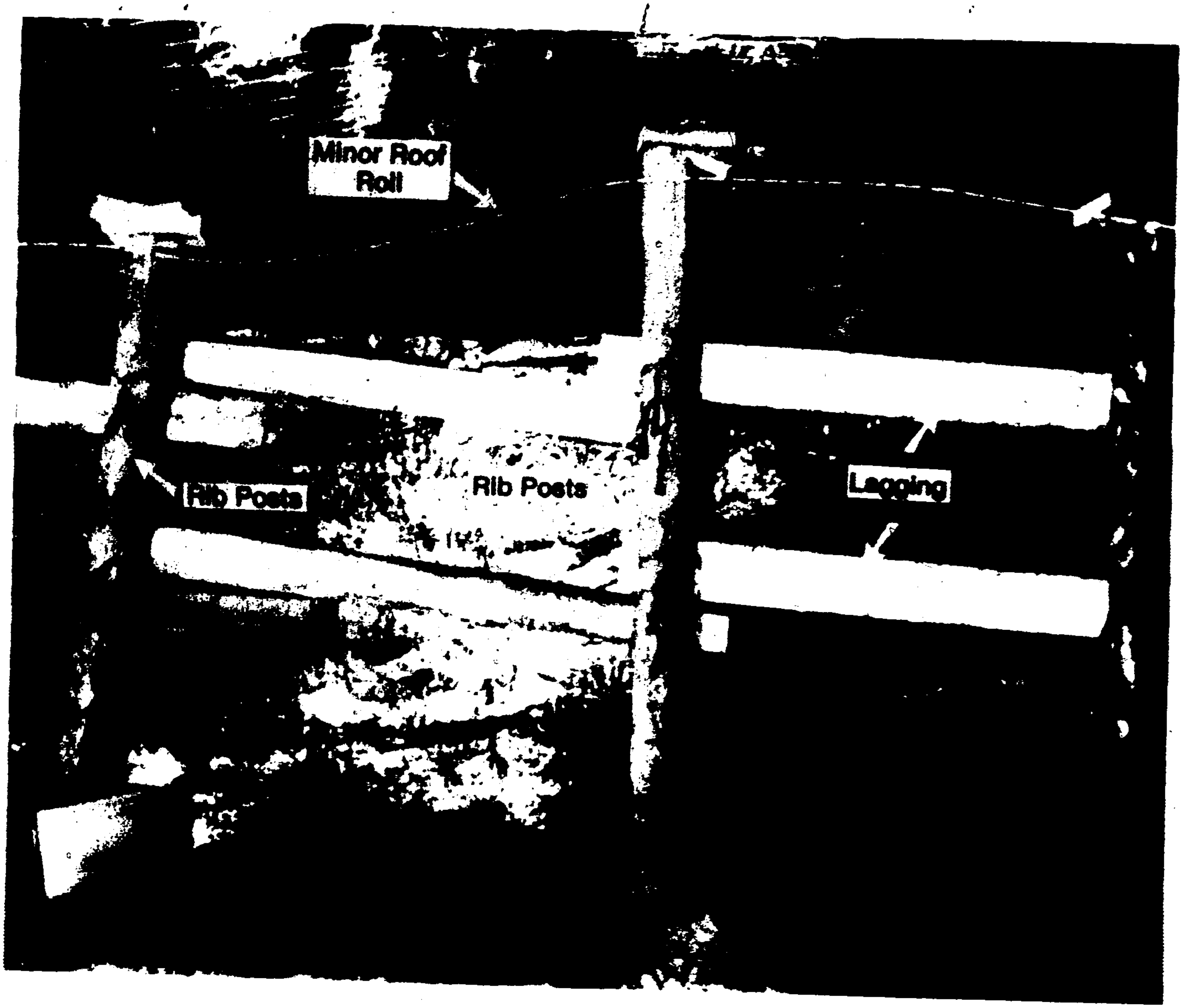
Minor Roof Roll
Rib Posts
Rib Posts
Lagging

Plate 16. NEWLY EXPOSED PILLAR SIDE AND SUPPORTS

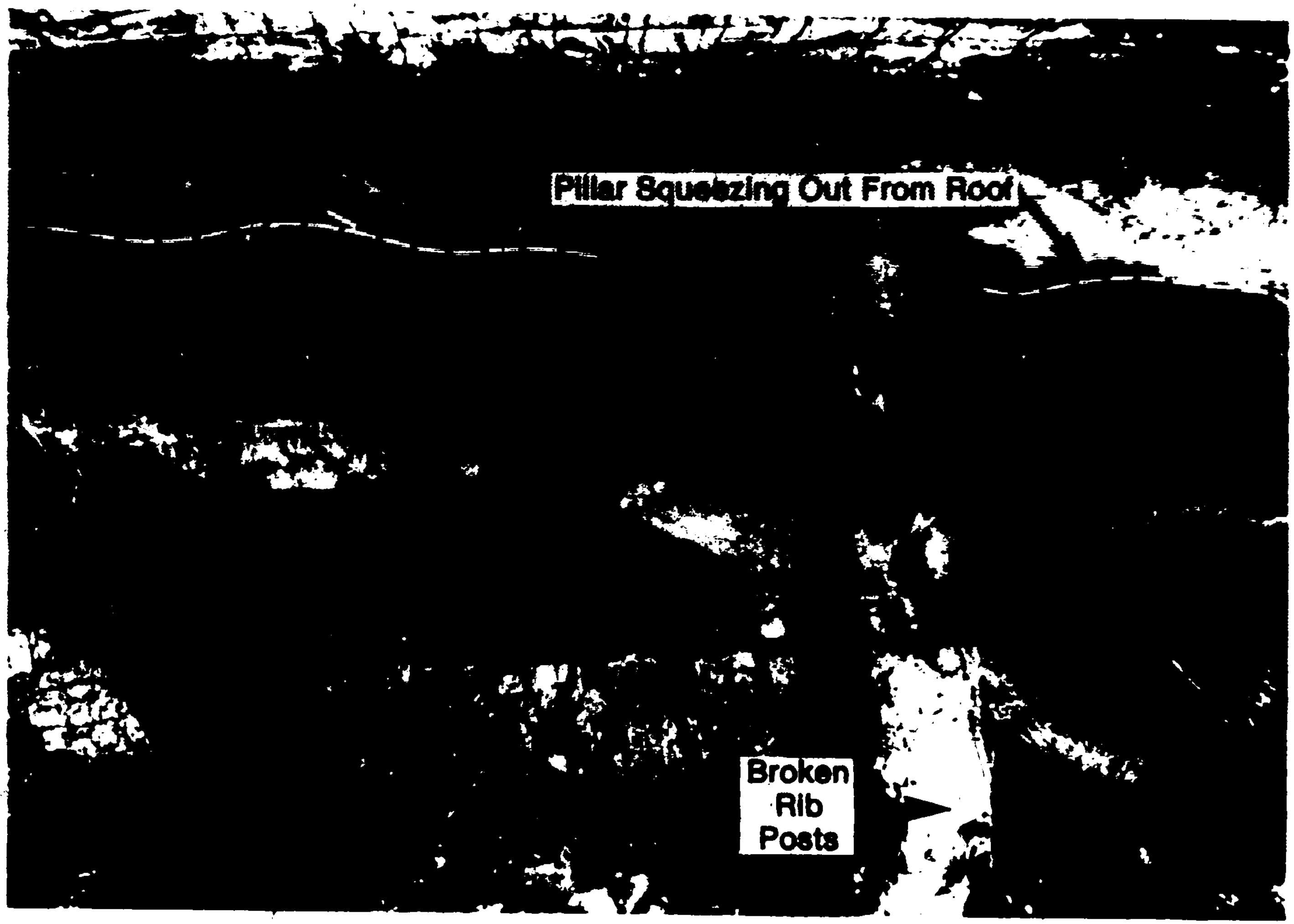
Pillar Squeezing Out From Roof
Broken Rib Posts

Plate 17. PILLAR EXPANSION NEAR ROOF

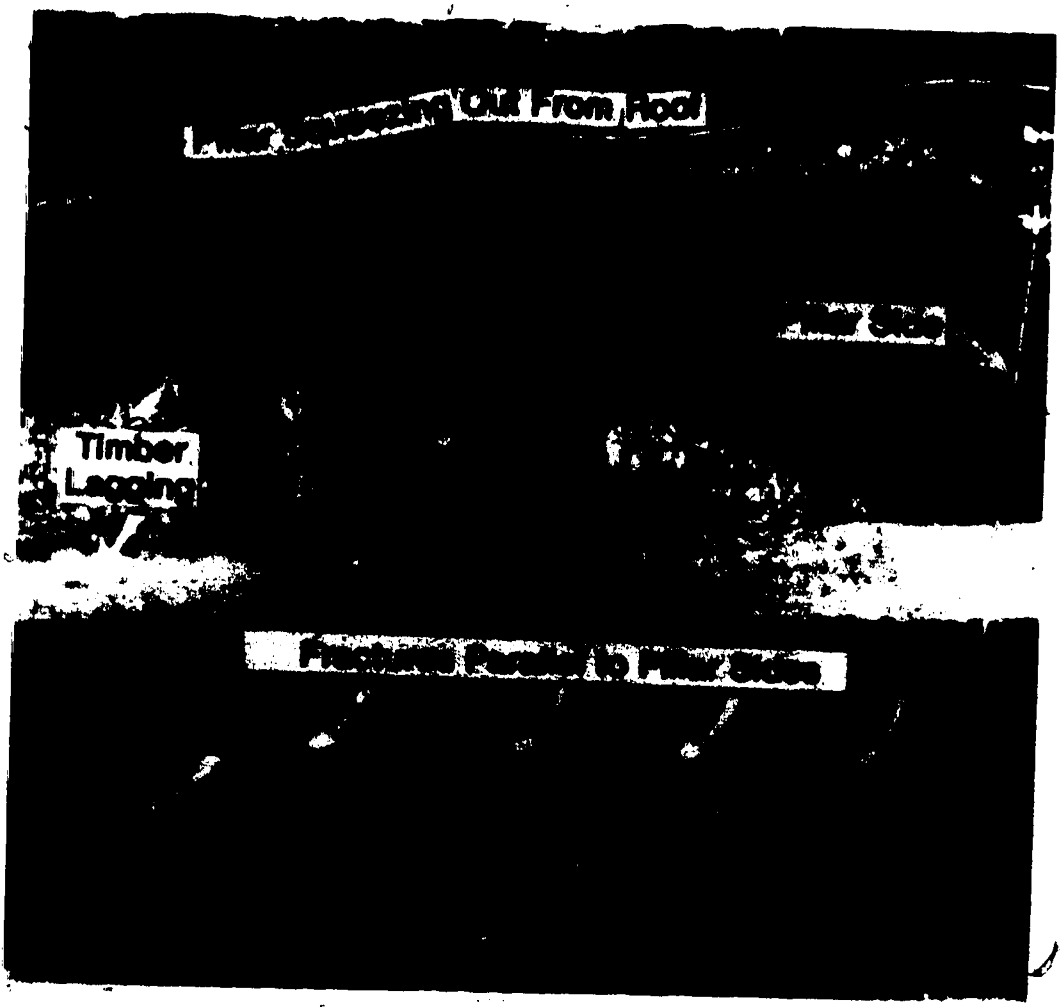
Out From Roof
Timber
Lagging

Plate 18. PILLAR FRACTURING

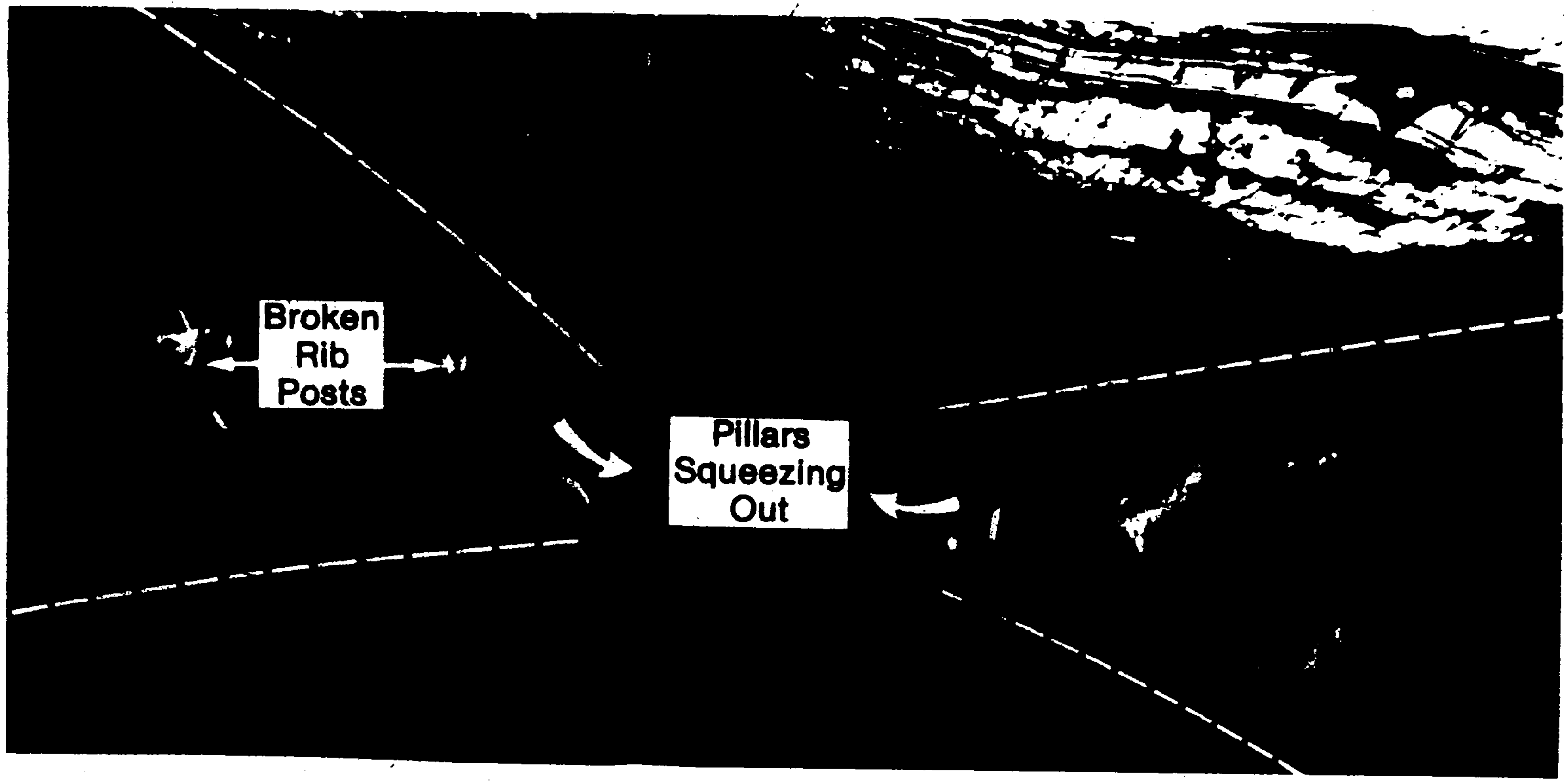
Broken
Rib
Posts
Pillars
Squeezing
Out

Plate 19. PILLAR EXPANSION AND FAILURE OF SUPPORTS

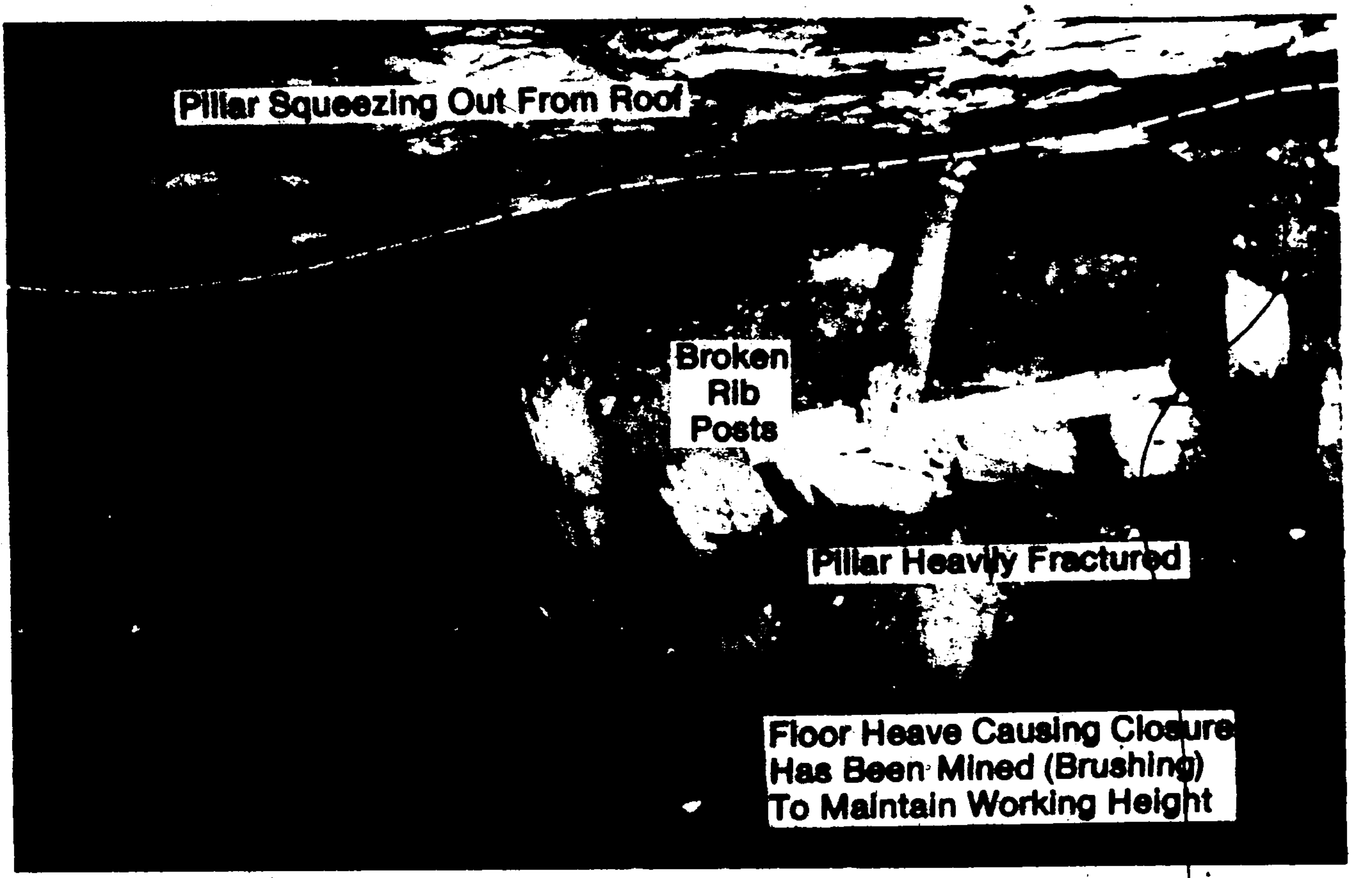
Pillar Squeezing Out From Roof
Broken Rib Posts
Pillar Heavily Fractured
Floor Heave Causing Closure Has Been Mined (Brushing) To Maintain Working Height

Plate 20. PILLAR EXPANSION, FLOOR HEAVE AND SUPPORT FAILURE

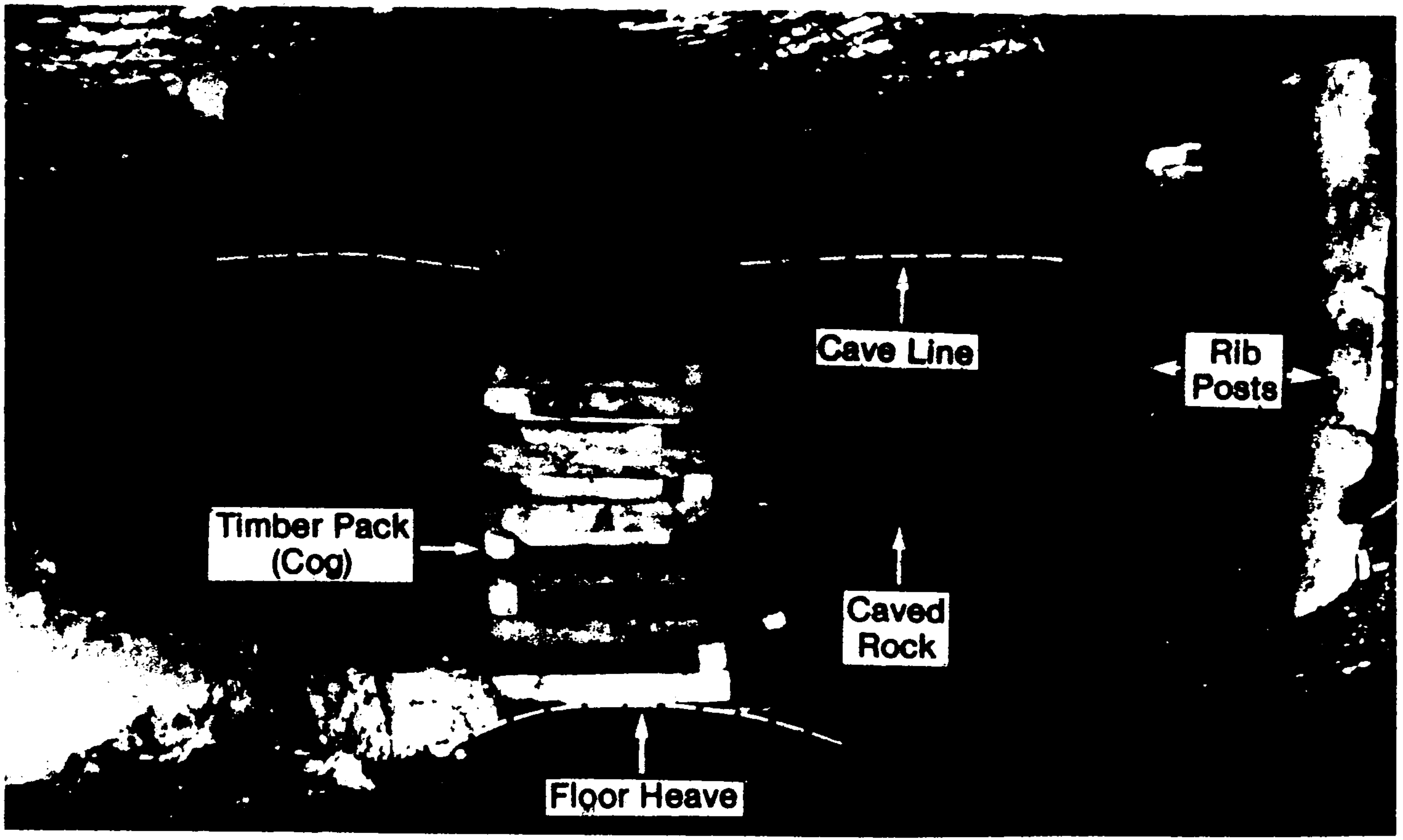
Cave Line
Rib Posts
Timber Pack (Cog)
Caved Rock
Floor Heave

Plate 21. CAVED AREA AND FLOOR HEAVE

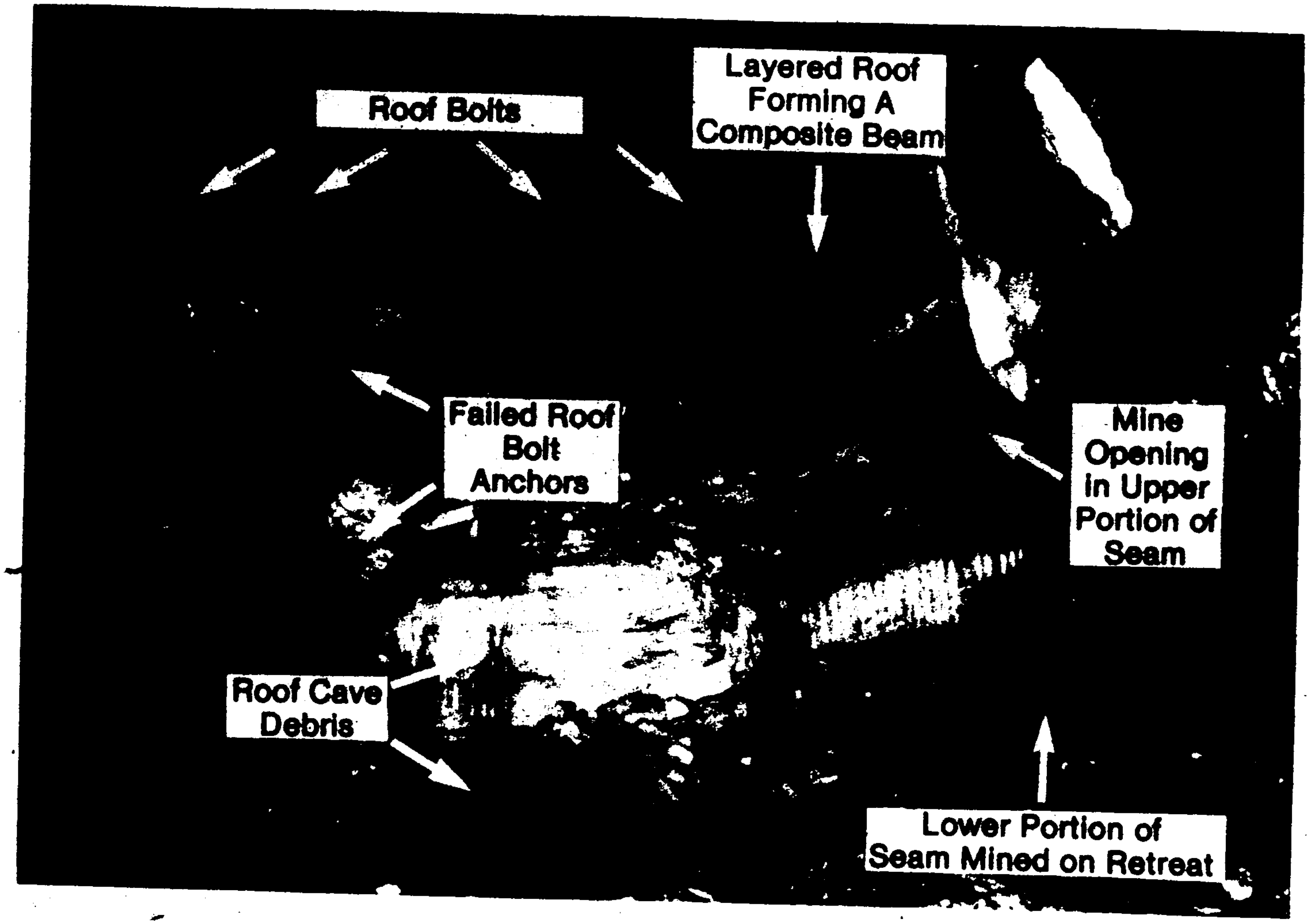
Roof Bolts
Layered Roof Forming A Composite Beam
Failed Roof Bolt Anchors
Mine Opening in Upper Portion of Seam
Roof Cave Debris
Lower Portion of Seam Mined on Retreat

Plate 22. CAVE OF IMMEDIATE ROOF BEDS

Bibliography

Agapito, J.F.T; Bennett, J.W. & Hunter, J.P. *ROCK MECHANICS FOR TWO SEAM MINING AT THE BIG ISLAND TRONA MINE, STAUFFER CHEMICAL COMPANY OF WYOMING* 19th US Symposium on Rock Mechanics, 1978, pp 57-64.

Aggson, J.R. *HOW TO PLAN GROUND CONTROL* Coal Mining and Processing, Dec. 1979, pp 70-73.

Archibald, J.F., Singh, K.N., Calder, P.N. & Nantel, J. *INVESTIGATION OF THE POST PILLAR CUT AND FILL MINING METHOD* 10th Canadian Rock Mechanics Symposium, 1975, pp 119-160.

Banerjee, P.K. *AN INTEGRAL EQUATION METHOD FOR THE ANALYSIS OF PIECE-WISE NON-HOMOGENEOUS ELASTIC SOLIDS OF ARBITRARY SHAPE* International Journal of Mechanical Sciences, V18 1976, pp 293-303.

Barron, K. *AN AIR INJECTION TECHNIQUE FOR INVESTIGATING THE INTEGRITY OF PILLARS AND RIBS IN COAL MINES* International Journal of Rock Mechanics and Mining Science, V15 1978, pp 69-76.

Bielenstein, H.U.; Wright, P.L. & Mikalson, D. *MULTI-SEAM MINING AT SMOKY RIVER* Sixth International St[illegible]ta Control Conference, Banff, 1977, 40 pages.

Bieniawski, Z.T. *NOTE ON IN SITU TESTING OF THE STRENGTH OF COAL PILLARS* Journal of the South African Institute of Mining & Metallurgy, May 1968, pp 455-465.

Brady, B.H.G. *AN ANALYSIS OF ROCK BEHAVIOUR IN AN EXPERIMENTAL STOPING BLOCK AT THE MOUNT ISA MINE, QUEENSLAND, AUSTRALIA* International Journal of Rock Mechanics & Mining Science, V14 1977, pp 59-66.

Brady, B.H.G. & Bray, J.W. *THE BOUNDARY ELEMENT METHOD FOR DETERMINING STRESSES AND DISPLACEMENTS AROUND LONG OPENINGS IN A TRIAXIAL STRESS FIELD* International Journal of Rock Mechanics & Mining Science, V15 1978, pp 21-28.

Brady,B.H.G. & Bray,J.W. *THE BOUNDARY ELEMENT METHOD FOR ELASTIC ANALYSIS OF TABULAR OREBODY EXTRACTION, ASSUMING COMPLETE PLANE STRAIN* International Journal of Rock Mechanics & Mining Science, V15 1978, pp 29-37.

Brady,B.H.G. *A BOUNDARY ELEMENT METHOD FOR THREE-DIMENSIONAL ELASTIC ANALYSIS OF TABULAR OREBODY EXTRACTION* 19th US Symposium on Rock Mechanics, V1 1978, pp 431-438.

Brady,B.H.G. *A DIRECT FORMULATION OF THE BOUNDARY ELEMENT METHOD OF STRESS ANALYSIS FOR COMPLETE PLANE STRAIN* International Journal of Rock Mechanics & Mining Science, V16 1979, pp 325-344.

Chan,S.S.M. & Beus,M.J. *INTERPRETATION OF IN SITU DEFORMATIONAL BEHAVIOUR OF A RECTANGULAR TEST SHAFT USING FINITE ELEMENT METHOD* Interntional Symposium on Field Measurements in Rock Mechanics, Zurich 1977, pp 889-903.

Christov,T. & Iliev,S. *CONSIDERATION OF NATURAL STRESSES IN THE ROCK MASSIF AND THE TECHNOLOGY OF CONSTRUCTION WITH RESPECT TO THE CALCULATION OF UNDERGROUND OPENING BY MEANS OF THE FINITE ELEMENT METHOD* International Symposium on Field Measurements in Rock Mechanics, Zurich 1977, pp 905-918.

Coates,D.F. *PROBABILITY OF PILLAR FAILURE AT ELLIOTT LAKE* Advances in Rock Mechanics (Proc. of 3rd ISRM Congress), 1974, pp 990-996.

Coates,D.F. *ROCK MECHANICS PRINCIPLES* Mines Branch Monograph 874, Ottawa, 1967.

Cogan,J. *AN APPROACH TO CREEP BEHAVIOUR IN FAILED ROCKS* 19th US Symposium on Rock Mechanics, 1978, pp 400-407.

Crouch S.L. & Fairhurst,C. *ANALYSIS OF ROCK MASS DEFORMATIONS DUE TO EXCAVATIONS* Rock Mechanics Symposium A.S.M.E., 1973, pp 25-40.

Crouch,S.L. *ANALYSIS OF STRESSES AND DISPLACEMENTS AROUND UNDERGROUND EXCAVATIONS: AN APPLICATION OF THE DISPLACEMENT DISCONTINUITY METHOD* Dept. of Civil & Mineral Engineering, University of Minnesota, Minneapolis, 1976.

Crouch, S.L. *COMPUTER SIMULATION OF MINING IN FAULTED GROUND* Journal of the South African Institute of Mining & Metallurgy, Jan. 1979, pp 159-173.

Crouch, S.L. *SOLUTION OF PLANE ELASTICITY PROBLEMS BY THE DISPLACEMENT DISCONTINUITY METHOD - 1. INFINITE BODY SOLUTION* International Journal for Numerical Methods in Engineering, V10 1976, pp 301-343.

Cummins, A.B. & Given, I.A. (editors) *SME MINING ENGINEERING HANDBOOK* A.I.M.E., New York 1973, V1.

Cundall, P.A. *A COMPUTER MODEL FOR SIMULATING PROGRESSIVE LARGE SCALE MOVEMENT IN BLOCK ROCK SYSTEMS* Proc. of Symposium of the International Society of Rock Mechanics, 1971 Nancy 2, No.8.

Dunham, R.K. & Stace, R.L. *INTERACTION PROBLEMS IN MULTI-SEAM MINING* 19th US Symposium on Rock Mechanics, 1978, pp 174-179.

Duvall, W.I. *GENERAL PRINCIPLES OF UNDERGROUND OPENING DESIGN IN COMPETENT ROCK* 17th US Symposium on Rock Mechanics, 1976, pp 3A1-1 to 3A1-11.

Ealy, D.L.; Mazurak, R.E. & Langrand, E.L. *A GEOLOGICAL APPROACH FOR PREDICTING UNSTABLE ROOF AND FLOOR CONDITIONS IN ADVANCE OF MINING* Mining Congress Journal, March 1979, pp 17-22.

Fadeev, A.B. & Abdyldayev, E.K. *ELASTOPLASTIC ANALYSIS OF STRESSES IN COAL PILLARS BY FINITE ELEMENT METHOD* Rock Mechanics 11, 1979, pp 243-251.

Faustov, G.T. & Abashin, P.A. *CALCULATION OF PILLARS IN THE ELASTICO-PLASTIC STATE* Soviet Mining Science, V10 1974, pp 277-285.

Goodman, R.E. *METHODS OF GEOLOGICAL ENGINEERING* West Publishing Co., 1976, 472 pages.

Gowd,T.N. & Rummel,F. *EFFECT OF FLUID INJECTION ON THE FRACTURE BEHAVIOUR OF POROUS ROCK* International Journal of Rock Mechanics & Mining Science, V14 1977, pp 203-208.

Grant,F. *A REVIEW OF HISTORICAL UNDERGROUND COAL MINE STRATA CONTROL PARAMETERS IN WESTERN CANADA IN RELATION TO THE REQUIREMENTS FOR PRESENT AND FUTURE COAL MINES* CANMET report ERP/MRL 77-101(TR), 1977.

Grobbelaar,C. *THE THEORETICAL STRENGTH OF MINE PILLARS - PART I THE CUBE STRENGTH OF PILLAR MATERIAL* Journal of the South African Institute of Mining & Metallurgy, Nov. 1968, pp 173-183.

Gyenge,M. & Ladanyi,B. *PIT SLOPE MANUAL* CANMET report 77-29, 1977.

Hardy,M.P. & Agapito,J.F.T. *PILLAR DESIGN IN UNDERGROUND OIL SHALE MINES* 16th US Symposium on Rock Mechanics, 1975, pp 257-266.

Hobbs,D.W. *SCALE MODEL STUDIES OF STRATA MOVEMENT AROUND MINE ROADWAYS. APPARATUS, TECHNIQUE AND SOME PRELIMINARY RESULTS* International Journal of Rock Mechanics & Mining Science, V3 1966, pp 101-127.

Hoek,E. & Brown,E.T. *UNDERGROUND EXCAVATION ENGINEERING* Institute of Mining & Metallurgy, 1980.

Hoek,E. *ROCK MECHANICS LABORATORY TESTING IN THE CONTEXT OF A CONSULTING ENGINEERING ORGANISATION* International Journal of Rock Mechanics & Mining Science, V14 1977, pp 93-101.

Hustrulid,W.A. & Gangerico,R. *THE SPLIT-PLATEN TECHNIQUE FOR DETERMINING LOAD-DEFORMATION BEHAVIOUR OF MODEL COAL MINE PILLARS* 19th US Symposium on Rock Mechanics, V1 1978, pp 130-136.

Hustrulid,W.A. *A REVIEW OF COAL PILLAR STRENGTH FORMULAS* Rock Mechanics 8, Springer-Verlag, 1975, pp 115-145.

International Society for Rock Mechanics, Commission on

Standardisation of Laboratory and Field Tests *SUGGESTED METHODS FOR:- DETERMINING TENSILE STRENGTH OF ROCK MATERIALS*(V15 1978, pp 99-103); *DETERMINING THE STRENGTH OF ROCK MATERIALS IN TRIAXIAL COMPRESSION* (V15 1978, pp 47-51); *DETERMINING THE UNIAXIAL COMPRESSIVE STRENGTH AND DEFORMABILITY OF ROCK MATERIALS* (V16 1979, pp 135-140);*THE QUANTITATIVE DESCRIPTION OF DISCONTINUITIES IN ROCK MASSES*(V15 1978, pp 319-368) International Journal of Rock Mechanics & Mining Science.

Jaeger,J.C. & Cook,N.G.W. *FUNDAMENTALS OF ROCK MECHANICS* Chapman & Hall, London 1977, 585 pages.

Jeremic,M.L. *CHARACTERISTICS OF WESTERN CANADIAN COAL SEAMS AND THEIR EFFECT ON MINE DESIGN* Mining Magazine, Dec. 1980, pp. 557-564.

Jeremic,M.L. *COAL BEHAVIOUR IN THE ROCKY MOUNTAIN BELT OF CANADA* International Congress on Rock Mechanics, Montreux, 1979, pp 189-195.

Jeremic,M.L. *COAL STRENGTHS IN THE ROCKY MOUNTAINS* World Coal, V6 N9, Sept. 1980,pp 40-43.

Jeremic, M.L. *EFFECT OF COAL SEAM STABILITY ON HYDRAULIC MINE DESIGN* Journal of Mines, Metals and Fuels, May 1980, pp 93-99.

Jeremic,M.L. *INFLUENCE OF SHEAR DEFORMATION STRUCTURES IN COAL ON SELECTING METHODS OF MINING* Rock Mechanics 13, 1980, pp 23-38.

Jeremic,M.L. *RUPTURING CRITERIA OF COAL BEARING STRATA, W. CANADA* Modern Geology, V7 1980,pp 191-199.

Jeremic,M.L. *STRENGTH OF COAL FROM THE STAR-KEY MINE NEAR EDMONTON, ALBERTA* CIM Bulletin, Feb. 1979.

Kalia,H. *SUPPORT CONSIDERATIONS FOR THE LONGWALL MINING OF COAL* Mining Congress Journal, Sept. 1974, pp 126-128.

Karwoski,W.J. & Van Dillen,D.E. *APPLICATIONS OF BUMINES THREE-DIMENSIONAL FINITE ELEMENT COMPUTER CODE TO LARGE*

MINE STRUCTURAL PROBLEMS 19th US Symposium on Rock Mechanics, V2 1978, pp 114-120.

Kidybinski,A. & Babcock,C.O. *STRESS DISTRIBUTION AND ROCK FRACTURE ZONES IN THE ROOF OF LONGWALL FACE IN A COAL MINE* Rock Mechanics 5, 1973, pp 1-19.

King,H.J.; Whittaker,B.N. & Batchelor,A.S. *THE EFFECTS OF INTERACTION IN MINE LAYOUTS* 5th International Strata Control Conference, 1972.

Kulhawy,F.H. *STRESS DEFORMATION PROPERTIES OF ROCK AND ROCK DISCONTINUITIES* Engineering Geology,V9 N4, Dec. 1975, pp 327-350.

Langland,R.T. *EXPERIMENTAL INVESTIGATION OF ROOM AND PILLAR COAL MINING IN THE EASTERN UNITED STATES* International Symposium on Field Measurements in Rock Mechanics.

Mendes,F.M. & Da Gamma,C.D. *LABORATORY SIMULATION OF MINE PILLAR BEHAVIOUR* 14th US Symposium on Rock Mechanics, 1973, pp 107-119.

Millard,D.J.; Newman,P.C. & Phillips,J.W. *THE APPARENT STRENGTH OF EXTENSIVELY CRACKED MATERIALS* Proc. of the Physical Society, B. V68, 1955, pp 723-728.

Ortlepp,W.D. & Nicoll,A. *THE ELASTIC ANALYSIS OF OBSERVED STRATA MOVEMENT BY MEANS OF AN ELECTRICAL ANALOG* Journal of the South African Institute of Mining & Metallurgy, V65 N4, Nov. 1964, pp 214-235.

Ortlepp,W.D. & Cook,N.G.W. *THE MEASUREMENT AND ANALYSIS OF THE DEFORMATION AROUND DEEP, HARD ROCK EXCAVATIONS* 4th International Conference on Strata Control & Rock Mechanics, 1964, pp 140-150.

Oravecz,K.I. *ANALOGUE MODELLING OF STRESSES AND DISPLACEMENTS IN BORD AND PILLAR WORKINGS OF COAL MINES* International Journal of Rock Mechanics & Mining Science, V14 1977, pp 7-23.

Pariseau,W.G. *LIMIT DESIGN OF MINE PILLARS UNDER UNCERTAINTY* 16th US Symposium on Rock Mechanics, 1975, pp 287-301.

Pariseau,W.G. & Sorensen,W.K. *3D MINE PILLAR DESIGN INFORMATION FROM 2D FEM ANALYSIS* International Journal of Rock Mechanics & Mining Science, V3 1979, pp 145-157.

Parker,J. *HOW TO DESIGN BETTER MINE OPENINGS* Engineering & Mining Journal, Dec. 1973, pp 76-80.

Raney,E.M.; Van Dillen,D.; Chuang,K.P. & Balachandra *THREE DIMENSIONAL FINITE ELEMENT ANALYSIS OF A COAL MINE CROSSCUT AND ENTRY INTERSECTION* 17th US Symposium on Rock Mechanics, 1976, pp 1A6-1 to 1A6-5.

Salamon,M.D.G. *ELALSTIC ANALYSIS OF DISPLACEMENTS AND STRESSES INDUCED BY THE MINING OF SEAM OR REEF DEPOSITS (FOUR PARTS)* Journal of the South African Institute of Mining & Metallurgy, Nov. 1963, pp 128-149; Jan. 1964, pp 197-218; May 1964, pp 468-500; Dec. 1964, pp 319-338.

Salamon,M.D.G. & Oravez,K.I. *THE ELECTRICAL RESISTANCE ANALOG AS AN AID TO THE DESIGN OF PILLAR WORKINGS* Proc. of 2nd Congress of the International Society of Rock Mechanics, 1970, Paper 4-18.

Salamon,M.D.G. *A METHOD OF DESIGNING BORD AND PILLAR WORKINGS* Journal of the South African Institute of Mining & Metallurgy, Sept. 1967, pp 68-78.

Salamon,M.D.G. & Munro,A.H. *A STUDY OF THE STRENGTH OF COAL PILLARS* Journal of the South African Institute of Mining & Metallurgy, Sept. 1967, pp 55-67.

Sheorey,P.R. & Singh,B. *ESTIMATION OF PILLAR LOADS IN SINGLE AND CONTIGUOUS SEAM WORKINGS* International Journal of Rock Mechanics & Mining Science, V11 1974, pp 97-102.

Sheorey,P.R. & Singh,B. *STRENGTH OF RECTANGULAR PILLARS IN PARTIAL EXTRACTION* International Journal of Rock Mechanics & Mining Science, V11 1974, pp 41-44.

Sorensen,W.K. & Pariseau *STATISTICAL ANALYSIS OF LABORATORY COMPRESSIVE STRENGTH AND YOUNG'S MODULUS DATA FOR THE DESIGN OF PRODUCTION PILLARS IN COAL MINES* 19th US Symposium on Rock Mechanics, 1978, pp 30-37.

Starfield,A.M. & Crouch,S.L. *ELASTIC ANALYSIS OF SINGLE SEAM EXTRACTION* 14th US Symposium on Rock Mechanics, 1973, pp 421-439.

Starfield,A.M. & Fairhurst,C. *HOW HIGH SPEED COMPUTERS ADVANCE DESIGN OF PRACTICAL MINE PILLAR SYSTEMS* Engineering & Mining Journal, May 1968, pp 78-84.

Starfield,A.M. & Wawersik,W.R. *PILLARS AS STRUCTURAL COMPONENTS IN ROOM AND PILLAR MINE DESIGN* 10th US Symposium on Rock Mechanics, 1968, pp 793-809.

Starfield,A.M. & McClain,W.C. *PROJECT SALT VAULT: A CASE STUDY IN ROCK MECHANICS* International Journal of Rock Mechanics & Mining Science, 1973.

Stimpson,B. *MODELLING MATERIALS FOR ENGINEERING ROCK MECHANICS* International Journal for Rock Mechanics & Mining Science, V7 1970, p.77.

Szwilski,A.B. & Whittaker,B.N. *CONTROL OF STRATA MOVEMENT AROUND FACE ENDS* The Mining Engineer, July 1975, pp 515-525.

Timoshenko,S.P. & Goodier,J.N. *THEORY OF ELASTICITY* McGraw-Hill Kogakusha, 3rd Edition, 1970.

Wagner,H. *DETERMINATION OF THE COMPLETE LOAD-DEFORMATION CHARACTERISTICS OF COAL PILLARS* Advances in Rock Mechanics (Proc. of 3rd ISRM Congress), 1974, pp 1076-1081.

Whittaker,B.N. & Singh,R.N. *DESIGN AND STABILITY OF PILLARS IN LONGWALL MINING* The Mining Engineer, July 1979, pp 59-70.

Whittaker,B.N. & Pye,J.H. *GROUND MOVEMENTS ASSOCIATED WITH THE NEAR SURFACE CONSTRUCTION OPERATIONS OF A MINE IN COAL MEASURES STRATA* International Journal of Rock Mechanics & Mining Science, V14 1977, pp 67-75.

Whittaker,B.N. & Hodgkinson,D.R. *REINFORCEMENT OF WEAK STRATA* The Mining Engineer, June 1971, pp 595-609.

Wijk,G. *SOME NEW THEORETICAL ASPECTS OF INDIRECT MEASUREMENTS OF THE TENSILE STRENGTH OF ROCKS* International Journal of Rock Mechanics & Mining Science, V15 1978, pp 149-160.

Wilson,A.H. *CONCLUSIONS FROM RECENT STRATA CONTROL MEASUREMENTS MADE BY THE MINING RESEARCH ESTABLISHMENT* The Mining Engineer, April 1964, pp 367-375.

Wilson,A.H. & Ashwin,D.P. *RESEARCH INTO THE DETERMINAION OF PILLAR SIZE* The Mining Engineer N141, June 1972, pp 409-427.

Wright,F.D. & Ahmed,B. *LOAD DEFORMATION CHARACTERISTICS OF MODEL MINE PILLARS BEFORE AND AFTER CRUSHING* 10th US Symposium on Rock Mechanics, 1968, pp 785-792.

Wright,P.L. *LAYOUT OF CONTIUOUS MINER OPERATIONS IN THE SMOKY RIVER MINES* CIM Bulletin, March 1973, PP 167-171.

Zhitkov,E.F. *CALCULATION OF THE WIDTHS OF ROOMS AND PILLARS WITH ROOF CONTROL BY CONVERGENCE ON YIELDING PILLARS* Soviet Mining Science, V11 1975, pp 17-22.

Zienkiewicz,O.C. *THE FINITE ELEMENT METHOD* McGraw Hill, 3rd ed. 1977, 787 pages.

APPENDIX 1

DDSEAMS PROGRAM DESCRIPTION

PROGRAM DDSEAMS DESCRIPTION

Section 2. INTRODUCTION
Section 3. MATHEMATICAL THEORY
Section 4. NUMERICAL PROCEDURE
Section 5. PROGRAM OPERATION

R.Wright

December 12th. 1979

Mineral Engineering Dept.,
University of Alberta

Chapter 2

INTRODUCTION

The design of underground mining structures for tabular orebodies, such as coal seams, is primarily controlled by stability analyses. In order to make an assessment of the stability of an excavation it is necessary to estimate the total stresses and displacements after excavation has taken place (the total stresses are the sum of the initial stresses and those induced by the excavation, whereas the displacements are only those induced by the excavation i.e. the initial displacements are zero). These stresses and displacements are then compared with a set of stability or failure criteria to assess the stability of the proposed design.

The total stresses and displacements after excavation has taken place are functions of: (i) the initial stress state prior to excavation, (ii) the geometry of the excavation, (iii) the rock mass characteristics, and (iv) the excavation sequence.

(i) The initial stress state is usually unknown and must be measured or estimated from knowledge of similar strata conditions elsewhere.

(ii) The excavation geometry is a three dimensional surface which is usually complex in reality and thus is normally simplified to permit analysis to be undertaken on a reasonable scale.

(iii). The rock mass characteristics define the relation between the stress changes and the displacements that they induce, the nearer this relation is to reality, the greater the complexity of analysis required for solution. The relation may be elastic (linear or non-linear), plastic (rigid/ideally plastic, elastic/ideally plastic or elasto-plastic), or creep (visco-elastic or visco-plastic). The material properties may be the same in all directions (isotropic), equal in two directions (transversely isotropic) or different in all three directions (orthotropic). Geologically the rock strata usually has discontinuities (joints and faults) and the analysis may take this non-homogeneous rock mass into account.

(iv) The excavation sequence is only important where the rock mass characteristics have irrecoverable displacements as in plasticity (yield functions), creep (time dependent yield) and slip surfaces (joints, faults). These relationships exhibit path dependent effect upon the final results and require that the excavation sequence be examined as well.

Historically the types of analyses that were possible, were simple and very restrictive in their applications. Usually the geological structure had to be ignored, and the excavation geometry and material behaviour greatly simplified in order to provide closed form solutions. With the advent of computers, numerical methods have become available which enable complex geometries in three dimensions, with complex material behaviour and the modelling of geological reality to be undertaken. However, these complex formulations are both difficult to set up, and expensive to run, which usually precludes them from use in practical mine design.

The errors involved in quantifying the rock mass characteristics by measurement or estimation from intact material properties and geological structure are significant enough to question the use of complex rock behaviour assumptions in the analysis. It has been shown that for relatively deep excavations the zone of inelastic behaviour (region of yielding and failure) is usually only confined to the immediate vicinity of the excavation and that the remainder of the rock mass may be assumed to behave elastically.

There exists the need for a method of analysis of mine excavations which is based on relatively simple assumptions of rock mass characteristics, is able to simulate sufficiently complex excavation geometries, and is both simple and cheap to run, thus enabling many layouts to be analysed. This usually requires that plane strain formulations are used which reduce the problem to a two dimensional one, and the assumption of linear elastic behaviour of the rock mass to simplify the analysis. These simplifications are adequate when the main requirement is for an analysis technique which is used to examine the sensitivity of the overall design with respect to variation of each of the major parameters in turn.

Finite element and finite difference computer programs divide the whole area of influence of the excavation into discrete elements and approximations are made to each element.

This makes them relatively powerful for modelling complex geometries and material properties, but time consuming to prepare and costly to run. Boundary element programs only divide the boundary surfaces into discrete elements, from which the stresses and displcements at any point in the rock mass can be calculated. Because of the reduced number of elements with boundary element programs in comparison to finite element programs, they are usually much easier to set up and cheaper to run.

The DDSEAMS program described in this report is a boundary element program which utilises the Displacement Discontinuity Method as developed by S.L.Crouch. This program is a two-dimensional formulation (plane strain) for analysis of multiple seam extraction of linearly elastic coal seams in an orthotropic linear elastic half-space. The seams are assumed to have negligible width in comparison to their length and lie parallel and not too close to the surface. The program, as developed within the department, can handle up to five seams with up to eighty elements per seam, and is suitable for both interactive and batch operating modes. A special feature of the program is that it can produce graphical output of stresses and displacements within the area of interest whilst in interactive mode.

Chapter 3

MATHEMATICAL THEORY

This section will only summarise the major stages in the solution process and all detailed equations and some intermediate steps are shown in ref. 1. The numerical solution procedure is described in the next section, and this section will only deal with the derivation of the influence functions for the fundamental displacement discontinuity line segment that is used in the solution.

The theory of elasticity is used to calculate the effect of a constant displacement discontinuity over a finite line segment parallel to the surface of a semi-infinite, homogeneous, orthotropic linear elastic body $y>0$ (see Fig. 3.1).

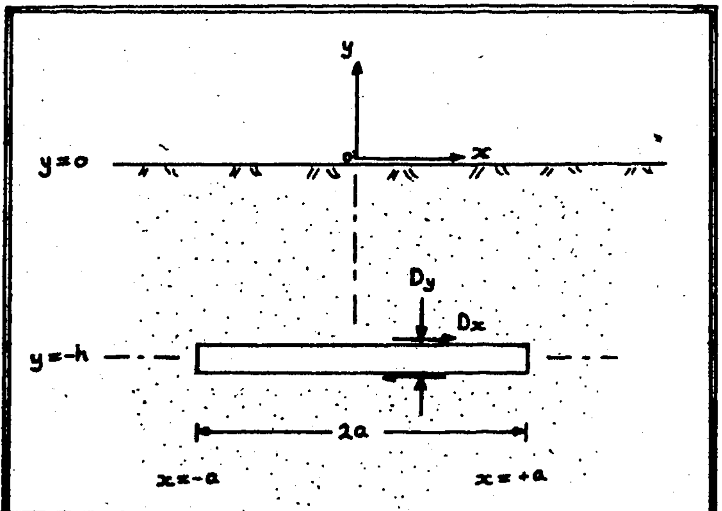

Fig. 3.1

The special case in which the directions of elastic symmetry of the material are parallèl to the x and y axes will be analysed, and plane strain conditions will reduce the problem to a two-dimensional one. The following boundary conditions are assumed :

(i) The displacements are continuous everywhere in the body, except over the line segment in question.

(ii) The normal and shear stresses are zero all along the surface of the half-space (ground surface).

(iii) All stresses and displacements are zero at infinity.

The problem considered will be the solution for the line segment shown in Fig. 3.1 where :

$$|x| < a \quad , \quad y = -h \quad (h > 0)$$

These conditions can be expressed as :-

$$\lim_{-y \to h_-} U_x(x,y) - \lim_{-y \to h_+} U_x(x,y) = \begin{cases} D_x \, , & |x| < a \\ 0 \, , & |x| > a \end{cases}$$

$$\lim_{-y \to h_-} U_y(x,y) - \lim_{-y \to h_+} U_y(x,y) = \begin{cases} D_y \, , & |x| < a \\ 0 \, , & |x| > a \end{cases}$$

Where:-

$$\sigma_{xy} = \sigma_{yy} = 0 \, , \quad (-\infty < x < \infty \, , \; y = 0)$$

The subscripts on (h_-andh_+) denote the negative and positive sides of the line y = -h (i.e. h_+denotes the top of the crack)
D_x and $D_y$are the relative shear and normal displacements between the two surfaces of the crack.

U_x and U_y are the actual displacements of the crack surfaces in the x and y directions respectively.

The solution to this problem is found using the method of images (Ref. 1), giving the results in the form:

$$U_i = \overset{A}{U}_i + \overset{I}{U}_i + \overset{S}{U}_i \qquad (i = 1,2)$$

$$\sigma_{ij} = \overset{A}{\sigma}_{ij} + \overset{I}{\sigma}_{ij} + \overset{S}{\sigma}_{ij} \qquad (j,i = 1,2)$$

Where the superscripts denote the solution types:

A = Actual displacement discontinuity

I = Image displacement discontinuity

S = Supplemental displacement discontinuity solution

The index notation refers to the usual tensorial notation, where the direction of the x and y axes are replaced by x_1 and x_2 respectively, thereafter the subscripts 1 and 2 refer to the direction in which the function they define acts.

The solution is obtained from the solution of a constant displacement discontinuity over a finite line segment in an infinite body and superimposing an image solution to create a shear stress free surface (ground surface), and a supplemental solution to reduce the normal stresses to zero along the same surface.

3.1 Actual Displacement Discontinuity

The solution for the actual constant displacement discontinuity over the line segment in an infinite body

$$D_i = (D_x, D_y), \quad |x| < a, \quad y = -h$$

can be written as follows for $\hat{U}_x$ and $\hat{\sigma}_{xx}$:-

$$\hat{U}_x = -D_x\left[\frac{1}{(1+g_1)}\cdot\frac{\partial f(x,y_1+h_1)}{\partial y_1} - \frac{1}{(1+g_2)}\cdot\frac{\partial f(x,y_2+h_2)}{\partial y_2}\right] + D_y\left[\frac{\gamma_1}{(1-g_1)}\cdot\frac{\partial f(x,y_1+h_1)}{\partial x} - \frac{\gamma_2}{(1-g_2)}\cdot\frac{\partial f(x,y_2+h_2)}{\partial x}\right]$$

$$\hat{\sigma}_{xx} = C_{66}D_x\left[\frac{1}{\gamma_1^2}\cdot\frac{\partial^2 f(x,y_1+h_1)}{\partial x\,\partial y_1} - \frac{1}{\gamma_2^2}\cdot\frac{\partial^2 f(x,y_2+h_2)}{\partial x\,\partial y_2}\right] + C_{66}D_y\left[\frac{1}{\gamma_1}\cdot\frac{\partial^2 f(x,y_1+h_1)}{\partial y_1^2} - \frac{1}{\gamma_2}\cdot\frac{\partial^2 f(x,y_2+h_2)}{\partial y_2^2}\right]$$

Where :-

$$f(x,y_i+h_i) = -\frac{(1+g_1)(1+g_2)}{2\pi(g_1-g_2)}\Bigg[(y_i+h_i)\arctan\left(\frac{y_i+h_i}{x-a}\right) - (y_i+h_i)\arctan\left(\frac{y_i+h_i}{x+a}\right)$$

$$- (x-a)\ell_n\sqrt{(x-a)^2+(y_i+h_i)^2} + (x+a)\ell_n\sqrt{(x+a)^2+(y_i+h_i)^2}\Bigg],$$

y = scaled y co-ordinates

$$h_i = h/\gamma_1$$

$$y_i+h_i = (y+h)/\gamma_i \qquad (i = 1,2)$$

γ_i = solution constant

$$g_i = (C_{11}\gamma_i^2 - C_{66})/(C_{12} + C_{66}) \qquad (i = 1,2)$$

C_{11}, C_{66}, C_{12} etc. are the material constants for relating stresses to strains.

The full equations can be seen in ref.1.

3.2 Image Displacement Discontinuity

Expressions for the displacements $\overset{I}{U}_x$ and stresses $\overset{I}{\sigma}_{xx}$ due to the image displacement discontinuity in an infinite body (shown in Fig. 3.2) may be written in a similar way. e.g. for $\overset{I}{U}_x$ and $\overset{I}{\sigma}_{xx}$:-

$$\overset{I}{U}_x = D_x\left[\frac{1}{(1+g_1)}\cdot\frac{\partial f(x,y_1-h_1)}{\partial y_1} - \frac{1}{(1+g_2)}\cdot\frac{\partial f(x,y_2-h_2)}{\partial y_2}\right] + D_y\left[\frac{\gamma_1}{(1+g_1)}\cdot\frac{\partial f(x,y_1-h_1)}{\partial x} - \frac{\gamma_2}{(1+g_2)}\cdot\frac{\partial f(x,y_2-h_2)}{\partial x}\right]$$

$$\overset{I}{\sigma}_{xx} = -G_{66}D_x\left[\frac{1}{\gamma_1^2}\cdot\frac{\partial^2 f(x,y_1-h_1)}{\partial x\,\partial y_1} - \frac{1}{\gamma_2^2}\cdot\frac{\partial^2 f(x,y_2-h_2)}{\partial x\,\partial y_2}\right] + C_{66}D_y\left[\frac{1}{\gamma_1}\cdot\frac{\partial^2 f(x,y_1-h_1)}{\partial y_1^2} - \frac{1}{\gamma_2}\cdot\frac{\partial^2 f(x,y_2-h_2)}{\partial y_2^2}\right]$$

Where :
$$f(x,y_i-h_i) = -\frac{(1+g_1)(1+g_2)}{2\pi(g_1-g_2)}\left[(y_i-h_i)\arctan\left(\frac{y_i-h_i}{x-a}\right) - (y_i-h_i)\arctan\left(\frac{y_i-h_i}{x+a}\right) - (x-a)\,\ell_n\sqrt{(x-a)^2+(y_i-h_i)^2} + (x+a)\,\ell_n\sqrt{(x+a)^2+(y_i-h_i)^2}\right]$$

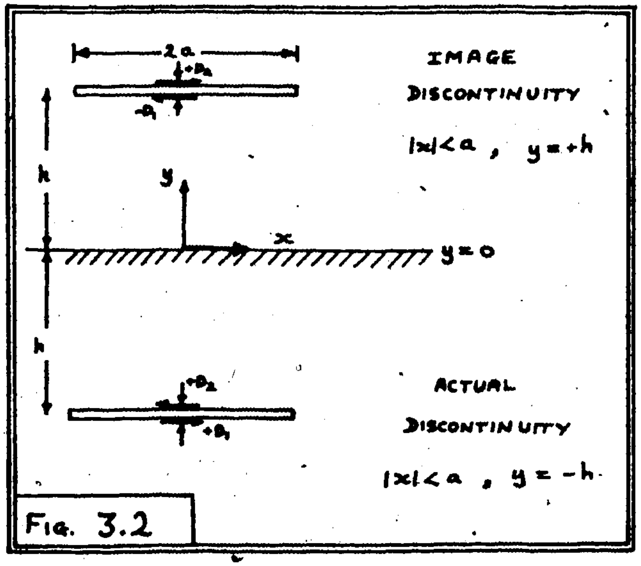

Fig. 3.2

3.3 Supplemental Displacement Discontinuity

[illegible] superposition of the actual and image stresses on the [illegible] = 0 , the normal stresses are :

$$\overset{A+I}{\sigma}_{yy} = \overset{A}{\sigma}_{yy} + \overset{I}{\sigma}_{yy} \quad , \quad \overset{A}{\sigma}_{yy} = \overset{I}{\sigma}_{yy}$$

and the shear stresses are zero :

$$\overset{A}{\sigma}_{xy} + \overset{I}{\sigma}_{xy} = 0 \quad , \quad \overset{A}{\sigma}_{xy} = -\overset{I}{\sigma}_{xy}$$

The normal stresses are eliminated by superimposing a supplemental displacement discontinuity for the half space y<0, that has appropriate stress boundary values on y = 0 :

$$\begin{aligned} \overset{S}{\sigma}_{xy} &= 0 \\ \overset{S}{\sigma}_{yy} &= -2\,\overset{I}{\sigma}_{yy} \end{aligned} \qquad -\infty < x < +\infty \;,\; y = 0$$

The boundary value of $\overset{S}{\sigma}_{yy}$ is defined in terms of the image displacement discontinuity because this solution does not introduce additional discontinuities in the half space y≤0.

The supplemental solution may be written in terms of a single potential $\overset{S}{\Phi}(x,y)$ and the stresses $\overset{S}{\sigma}_{xy}$ and $\overset{S}{\sigma}_{yy}$ are found :

$$\sigma_{xy} = -C_{66}\left[\frac{\partial^2 \overset{S}{\Phi}(x,y_1)}{\partial x\,\partial y_1} - \frac{\partial^2 \overset{S}{\Phi}(x,y_2)}{\partial x\,\partial y_2}\right]$$

$$\sigma_{yy} = -C_{66}\left[\gamma_1\frac{\partial^2 \overset{S}{\Phi}(x,y_1)}{\partial y_1^2} - \gamma_2\frac{\partial^2 \overset{S}{\Phi}(x,y_2)}{\partial y_2^2}\right]$$

Where :

$$\nabla^2 \overset{s}{\Phi}(x,y) = \frac{\partial^2 \overset{s}{\Phi}(x,y)}{\partial x^2} + \frac{\partial^2 \overset{s}{\Phi}(x,y)}{\partial y^2} = 0$$

so that $\overset{s}{\sigma}_{xy}$ is automatically zero when $y = 0$.
This can be reduced to the following for $\overset{s}{U}_x$ and $\overset{s}{\sigma}_{xx}$:

$$\overset{s}{U}_x = -\left[\frac{2D_x}{\gamma_1-\gamma_2}\left[\frac{1}{\gamma_1}\left\{\frac{\partial f(x,y_1-h_1)}{\partial y_1} - \frac{\partial f(x,y_1-h_2)}{\partial y_1}\right\} - \frac{\gamma_2}{1+\gamma_2}\left\{\frac{\partial f(x,y_2-h_1)}{\partial y_2} - \frac{\partial f(x,y_2-h_2)}{\partial y_2}\right\}\right]\right.$$
$$\left. + \frac{2D_y}{\gamma_1-\gamma_2}\left[\frac{\gamma_1}{1+\gamma_2}\left\{\gamma_1\frac{\partial f(x,y_1-h_1)}{\partial x} - \gamma_2\frac{\partial f(x,y_1-h_2)}{\partial x}\right\} - \frac{\gamma_2}{1+\gamma_2}\left\{\gamma_1\frac{\partial f(x,y_2-h_1)}{\partial x} - \gamma_2\frac{\partial f(x,y_2-h_2)}{\partial x}\right\}\right]\right]$$

$$\overset{s}{\sigma}_{xx} = \left[\frac{2C_{66}D_x}{\gamma_1-\gamma_2}\left[\frac{1}{\gamma_1}\left\{\frac{\partial^2 f(x,y_1-h_1)}{\partial x\,\partial y_1} - \frac{\partial^2 f(x,y_1-h_2)}{\partial x\,\partial y_1}\right\} - \frac{1}{\gamma_2}\left\{\frac{\partial^2 f(x,y_2-h_1)}{\partial x\,\partial y_2} - \frac{\partial^2 f(x,y_2-h_2)}{\partial x\,\partial y_2}\right\}\right]\right.$$
$$\left. - \frac{2C_{66}D_y}{\gamma_1-\gamma_2}\left[\frac{1}{\gamma_1}\left\{\frac{\partial^2 f(x,y_1-h_1)}{\partial y_1^2} - \gamma_2\frac{\partial^2 f(x,y_1-h_2)}{\partial y_1^2}\right\} - \frac{1}{\gamma_2}\left\{\gamma_1\frac{\partial^2 f(x,y_2-h_1)}{\partial y_2^2} - \gamma_2\frac{\partial^2 f(x,y_2-h_2)}{\partial y_2^2}\right\}\right]\right]$$

Where $f(x,y_i-h_i)$ has the same meaning as for the image displacement discontinuity solution.

3.4 Complete Solution

The complete solution to the problem is given by the sum of the three separate components, using the principle of superposition. (The full equations can be seen in ref. 1.) The equations are elaborated by substitution of the appropriate derivatives of the function f(x,y). The results can be presented in the following manner :

$$\sigma_{xx} = \left[G_1(x+a,y) - G_1(x-a,y) \right] D_x + \left[G_2(x+a,y) - G_2(x-a,y) \right] D_y$$

$$\sigma_{yy} = \left[G_3(x+a,y) - G_3(x-a,y) \right] D_x + \left[G_4(x+a,y) - G_4(x-a,y) \right] D_y$$

$$\sigma_{xy} = \left[G_5(x+a,y) - G_5(x-a,y) \right] D_x + \left[G_6(x+a,y) - G_6(x-a,y) \right] D_y$$

$$U_x = \left[G_7(x+a,y) - G_7(x-a,y) \right] D_x + \left[G_8(x+a,y) - G_8(x-a,y) \right] D_y$$

$$U_y = \left[G_9(x+a,y) - G_9(x-a,y) \right] D_x + \left[G_{10}(x+a,y) - G_{10}(x-a,y) \right] D_y$$

Chapter 4

NUMERICAL PROCEDURE

The mathematical theory in section 3. has only discussed a constant displacement discontinuity over a finity line segment. The distribution of stresses and displacements within the structure has been calculated as a function of the closure (roof to floor convergence) and ride (shear displacement between roof and floor) components. In reality the closure and ride components of an excavation within a seam are not constant over the whole span, but are functions of the position along the opening.

4.1 Single Seam

This variation of displacement discontinuities can be numerically modelled by treating the excavation as a series of finite line segments joined end to end as in Fig. 4.1

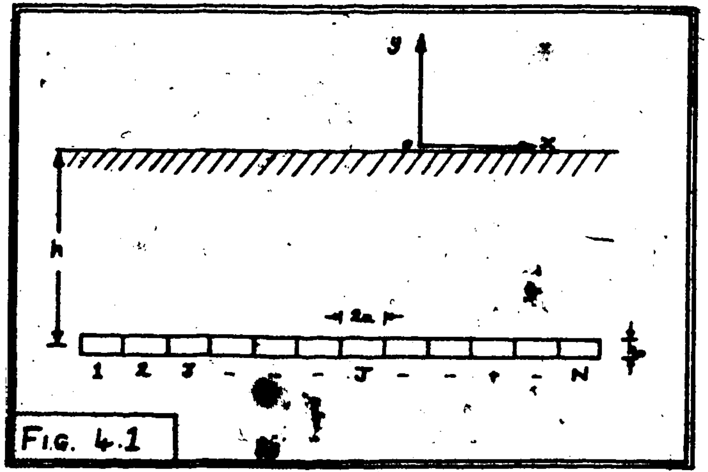

FIG. 4.1

Using the principle of superposition the total induced stresses and displacements at any point are found by summation of the effect of each displacement discontinuity element (seam element). The only problems that remain are the treatment of mined and unmined seam elements, the calculation of the closure and ride components (D_n and D_s) to be applied to each seam element, and the treatment when complete closure between roof and floor takes place. The seam is defined by assuming that each element which has not been mined has a normal stiffness K_n and a shear stiffness K_s .

The induced stresses at the centre of the i th. seam element may be expressed in terms of the displacement discontinuities (closure D_n^i and ride D_s^i , i=1,N) at all N elements as follows :

$$\left.\begin{aligned} \sigma_s^i &= \sum_{j=1}^{N} A_{ss}^{ij} D_s^j + \sum_{j=1}^{N} A_{sn}^{ij} D_n^j \\ \sigma_n^i &= \sum_{j=1}^{N} A_{ns}^{ij} D_s^j + \sum_{j=1}^{N} A_{nn}^{ij} D_n^j \qquad (i = 1,N) \end{aligned}\right\} \text{EQ. 4.1}$$

where A_{ss}^{ij}, A_{sn}^{ij}, A_{ns}^{ij} AND A_{nn}^{ij} are the influence coefficients relating induced stresses due to each seam element :

$$\left.\begin{aligned}
\overset{ij}{\underset{ss}{A}} &= \underset{5}{G}(\overset{i}{x}-\overset{j}{x}+a,-h) - \underset{5}{G}(\overset{i}{x}-\overset{j}{x}-a,-h)\\
\overset{ij}{\underset{sn}{A}} &= \underset{6}{G}(\overset{i}{x}-\overset{j}{x}+a,-h) - \underset{6}{G}(\overset{i}{x}-\overset{j}{x}-a,-h)\\
\overset{ij}{\underset{ns}{A}} &= \underset{3}{G}(\overset{i}{x}-\overset{j}{x}+a,-h) - \underset{3}{G}(\overset{i}{x}-\overset{j}{x}-a,-h)\\
\overset{ij}{\underset{nn}{A}} &= \underset{4}{G}(\overset{i}{x}-\overset{j}{x}+a,-h) - \underset{4}{G}(\overset{i}{x}-\overset{j}{x}-a,-h)
\end{aligned}\right\}\text{EQ. 4.2}$$

where the G functions are obtained from ref..1.

It is assumed that the initial stress state if such that the principal stresses are in the direction of the x and y axes and that the magnitude of the vertical stress is proportional to the rock density and the depth.

i e.

$$\left.\begin{aligned}
\left(\overset{i}{\underset{s}{\sigma}}\right)_{TOTAL} &= 0\\
\left(\overset{i}{\underset{n}{\sigma}}\right)_{TOTAL} &= \overset{i}{\underset{n}{\sigma}} + h\gamma_r
\end{aligned}\right\}\text{EQ. 4.3}$$

$$(i = 1,N)$$

A system of 2N simultaneous linear equations is formed for the required solution of 2N displacement discontinuities acting on N seam elements by equating EQ 4.1 and EQ 4.3. This solution will only be valid if all the elements are mined, and there is no total closure between roof and floor.

To simulate an unmined element, that element is assigned induced stress values which are proportional to the displacement discontinuity values :

$$\sigma_s^i = K_s D_s^i \quad , \quad \sigma_n^i = K_n D_n^i \qquad (i=1,N) \qquad \text{EQ. 4.4}$$

The final equations are :

EQ. 4.5		MINED	UNMINED
$\sum_{j=1}^{N} A_{ss}^{ij} D_s^j + \sum_{j=1}^{N} A_{sn}^{ij} D_n^j$	$=$	0	$K_s D_s^j$
$\sum_{j=1}^{N} A_{ns}^{ij} D_s^j + \sum_{j=1}^{N} A_{nn}^{ij} D_n^j$	$=$	$-h\gamma_r$	$K_n D_n^j$

where each element is defined as mined or unmined and the relevant equation is associated with it.

4.1.1 Complete Closure

So far no account has been taken of the possibility of complete closure taking place (a common phenomenon in coal mining methods) and this situation is accounted for during the iterative solution of the series of equations in EQ 4.5 by the following steps :

(1) At each stage of iteration, the displacement of the elements approaches more closely the final solution (the iterative procedure is described later). These values may be denoted as $D_n^i(k)$ and $D_s^i(k)$ for the i th. element after the k th. iteration

cycle.

(2) If the i th. element is mined, the closure $\overset{i}{D}_{n}$ (k) is tested to see whether it is greater than or equal to the seam thickness. If this is the case, we assume that the solution for this element is given by :

$$\overset{i}{D}_{s} = 0 \quad , \quad \overset{i}{D}_{n} = h.$$

i.e. no shear stress is transferred between the roof and floor and the closure is held equal to the seam thickness h.

(3) After the next cycle of iteration, the stresses acting across all elements that were assumed to undergo complete closure during the previous cycle are computed. If the normal stress (σ_{n}) is tensile (negative) at any such element, then the complete closure restraint is removed and the normal displacement discontinuity is allowed to change.

Because the roof and floor are allowed to slide freely over each other (zero shear stress) then the solution is path independent (i.e. independent of the mining sequence) and a unique solution is obtained. Once the solution is found, the stresses (hence strains) and displacements at any point may be found by calculting the influence coefficients of each element and using these combined with the displacement discontinuity solutions.

4.1.2 Iteration Process

The 2N simultaneous linear equations can be written in the form :

$$\left.\begin{aligned} \sum_{j=1}^{N} A_{ss}^{ij} D_s^{j} + \sum_{j=1}^{N} A_{sn}^{ij} D_n^{j} - B_s^{i} &= 0 \\ \sum_{j=1}^{N} A_{ns}^{ij} D_s^{j} + \sum_{j=1}^{N} A_{nn}^{ij} D_n^{j} - B_n^{i} &= 0 \qquad (i = 1, N) \end{aligned}\right\} \text{EQ. } 4.6$$

where (no closure) :

		MINED	UNMINED
B_s^i	=	0	$k_s D_s^i$
B_n^i	=	$-h\gamma_r$	$k_n D_n^i$

If the i th. equation has experienced complete closure, then the i th. seam element conditions are defined and the i th. equations are eliminated from the system provided the next cycle does not provide tensile stresses in that element, thus causing it to be freed again.

The system of equations is solved by Gauss-Seidel iteration with over-relaxation. The Gauss-Seidel iterative procedure is a method where an assumption is first made for the solution values of D_n^i and D_s^i and during each iteration cycle a better approximation for the value of each unknown is calculated. The method is made more efficient by using values which have been calculated in the present cycle for the calculation of the remainder of unknowns in that cycle. A further optimisation is achieved by using over-relaxation, where convergence of the solution is accelerated by calculating the convergence (difference in solution value since the previous cycle) of each unknown and applying a weighting factor (over-relaxation factor) to give a better approximation :

$$\left.\begin{aligned} \left(\overset{i}{D}_s\right)^{(n+1)} &= \left(\overset{i}{D}_s\right)^{(n)} + \omega\left(\Delta \overset{i}{D}_s\right)^{(n+1)} \\ \left(\overset{i}{D}_n\right)^{(n+1)} &= \left(\overset{i}{D}_n\right)^{(n)} + \omega\left(\Delta \overset{i}{D}_n\right)^{(n+1)} \end{aligned}\right\} \text{EQ. 4.7}$$

where :

ω = OVER RELAXATION FACTOR $(1 \leq \omega \leq 2)$

$\left(\overset{i}{D}_s\right)^{(n+1)}$ = $(n+1)$ TH APPROXIMATION OF $\overset{i}{D}_s$

$\left(\overset{i}{D}_s\right)^{(n)}$ = n TH APPROXIMATION OF $\overset{i}{D}_s$

$$\left(\Delta \overset{i}{D}_n\right)^{(n+1)} = \left(\overset{i}{D}_n\right)^{(n+1)}_{*} - \left(\overset{i}{D}_n\right)^{(n)}$$

* denotes the n+1 th. solution using Gauss-Seidel without over-relaxation.

The iteration process has converged when :

$$\left|\left(\Delta \overset{i}{D}_s\right)^{(n+1)}\right| \leq \varepsilon \text{ AND } \left|\left(\Delta \overset{i}{D}_n\right)^{(n+1)}\right| \leq \varepsilon$$

where ε is the specified error for all seam elements.

4.2 Multiple Seams

The basic, method is the same as for a single seam, except that each individual seam has a specified depth, thickness, material properties and element types (see Fig. 4.2)

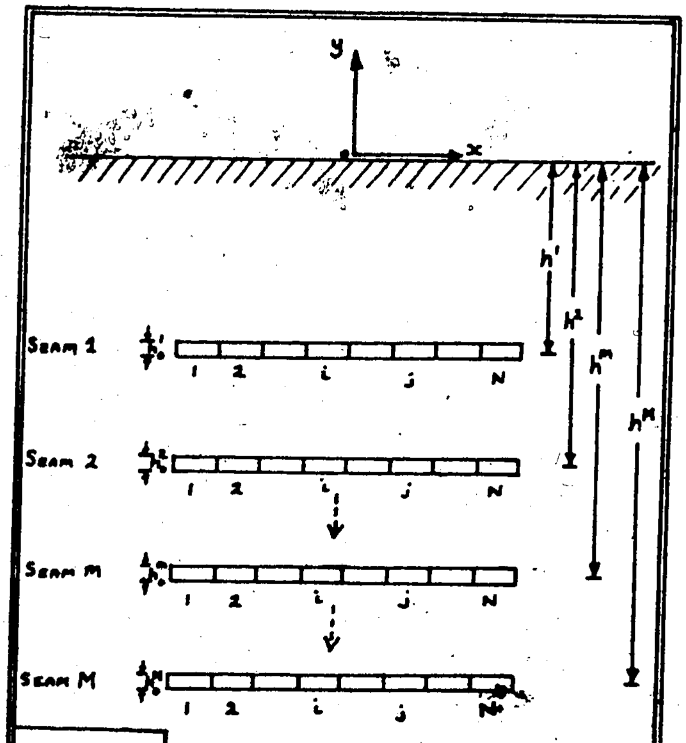

y
x
h^1
h^2
h^m
h^M
Seam 1
t_0^1
1 2 i j N
Seam 2
t_0^2
1 2 i j N
Seam m
t_0^m
1 2 i j N
Seam M
t_0^M
1 2 i j N

Fig. 4.2 (M seams)

For M seams with N elements in each seam, the stresses at any arbitrary point (x,y) in the half-space $y \leqslant 0$ may be written :

$$\sigma_{xy}(x,y) = \sum_{m=1}^{M}\left\{\sum_{j=1}^{N}\left[\overset{m}{\underset{5}{G}}(x-\overset{j}{x}+a,y)-\overset{m}{\underset{5}{G}}(x-\overset{j}{x}-a,y)\right]\left(\overset{j}{\underset{s}{D}}\right)^{m}+\sum\left[\overset{m}{\underset{6}{G}}(x-\overset{j}{x}+a,y)-\overset{m}{\underset{6}{G}}(x-\overset{j}{x}-a,y)\right]\left(\overset{j}{\underset{n}{D}}\right)^{m}\right\}$$

$$\sigma_{yy}(x,y) = \sum_{m=1}^{M}\left\{\sum_{j=1}^{N}\left[\overset{m}{\underset{3}{G}}(x-\overset{j}{x}+a,y)-\overset{j}{\underset{3}{G}}(x-\overset{j}{x}-a,y)\right]\left(\overset{j}{\underset{s}{D}}\right)^{m}+\sum\left[\overset{m}{\underset{4}{G}}(x-\overset{j}{x}+a,y)-\overset{m}{\underset{4}{G}}(x-\overset{j}{x}-a,y)\right]\left(\overset{j}{\underset{n}{D}}\right)^{m}\right\}$$

EQ. 4.8

where :

$\overset{j}{x}$ is the x co-ord. of the mid-point of the j th. element (all j th. elements have the same x co-ord.)

Functions $\overset{m}{\underset{3}{G}}$ to $\overset{m}{\underset{6}{G}}$ refer to functions [illegible] to $\underset{6}{G}$ given in Section 3. and ref. 1. , for the m th. seam, with h replaced by the depth of the seam $\overset{m}{h}$.

The solutions are obtained by solving the following system of equations in the same manner as for a single seam :

	MINED	UNMINED
$\sum_{m=1}^{M}\left\{\sum_{j=1}^{N}\left(\overset{ij}{\underset{ss}{A}}\right)^{\ell m}\left(\overset{j}{\underset{s}{D}}\right)^{m}+\sum\left(\overset{ij}{\underset{sn}{A}}\right)^{\ell m}\left(\overset{j}{\underset{n}{D}}\right)^{m}\right\} =$	0	$\underset{s}{\overset{\ell}{K}}\left(\overset{i}{\underset{s}{D}}\right)^{\ell}$
$\sum_{m=1}^{M}\left\{\sum_{j=1}^{N}\left(\overset{ij}{\underset{ns}{A}}\right)^{\ell m}\left(\overset{j}{\underset{s}{D}}\right)^{m}+\sum\left(\overset{ij}{\underset{nn}{A}}\right)^{\ell m}\left(\overset{j}{\underset{n}{D}}\right)^{m}\right\} =$	$-h\,\gamma_r$	$\underset{n}{\overset{\ell}{K}}\left(\overset{i}{\underset{n}{D}}\right)^{\ell}$

$(i=1,N;\ \ell=1,m)$ EQ. 4.9.

where $\overset{\ell}{K}_s$ and $\overset{\ell}{K}_n$ are the shear and normal stiffness for the ℓ th. seam

i.e.

$$\left.\begin{aligned}\overset{\ell}{K}_s &= (G_{SEAM})^{\ell} / h_o^{\ell} \\ \overset{\ell}{K}_n &= (E_{SEAM})^{\ell} / h_o^{\ell}\end{aligned}\right\} \text{EQ. 4.10}$$

$(\overset{ij}{A})^{\ell m}_{n}$ are the required influence coefficients at the ℓ th. seam, originating from the m th. seam.

$(\overset{j}{D})_s$ and $(\overset{j}{D})_n$ are the shear and normal displacement discontinuities at the j th. element of the m th. seam.

This is a system of 2xNxM linear simultaneous equations.

The program DDSEAMS has been developed for solution of multiple seam mining problems, with up to five seams and 80 elements modelling each seam.

Chapter 5

PROGRAM OPERATION

The computer program DDSEAMS solves the numerical problem in Section 4., and outputs results in tabular or graphical form. The program was developed to be simple and quick to set up a particular mine layout and allows interactive investigation of the stress and displacement distributions formed. If required the program may be run in batch mode, but only tabular results may be printed in this mode as the graphics option must be run from a terminal. A list of the major subroutines and variables, together with a program listing is given in Appendix 1.

The program is written in Fortran IV and is intended to be used in conjunction with the integrated graphics (*IG) and plotting (*PLOTLIB) subroutine packages available in the University of Alberta Computing Centre. Single precision is used throughout, as this gives sufficient accuracy and is more efficient in computing time than the use of double precision storage and calculations. The problem solution may be saved as a binary data file for re-running the program again, avoiding the cost of re-solution.

As many as five seams with up to eighty elements per seam may be modelled with the program in its present form. Each seam has the same start and end x co-ords, and the same number of elements. The equations are solved using Gauss-Seidel iteration with over-relaxation, with the user controlling the solution tolerance, over-relaxation factor and the maximum number of iterations. After the solution has been found, and the output mode has been defined, there are four alternative procedures : saving the solution as a data file, calculating the stresses and displacements at a particular seam, caculating the stresses, strains and displacements at a particular depth, and the termination of the program run.

5.1 Input/Output

INPUT

UNIT 4 ....For a new run the data defining a particular problem is read in from unit 4.

UNIT 5 ....The commands controlling the program run are read in from unit 5 which defaults to *SOURCE* (The Terminal) for interactive operation.

UNIT 7 ....For a re-run the solution for the problem is read in from the data file attached to unit 7.

OUTPUT

UNIT 3 ....The offseam results are written to the file attached to unit 3 in a form that can be readily used in any later analyses (e.g. for contour plotting of principal stress calculations).

UNIT 6 ....The user prompt and error messages, plus graphical output whilst in graphics mode, are output to unit 6 which defaults to *SINK* (The Terminal) for interactive use.

UNIT 7 ....The solution can be saved on unit 7 as a binary data file.

UNIT 8 ..The printed results are output in tabular form to unit 8 which is queued for printing, a typical output is shown in Appendix .

UNIT 9 ....The data for plotting of graphical output is written to unit 9 whilst in interactive graphics mode.

The data file on unit 4 must contain data in the following form :

1. Title Card (20A4)

A title consisting of less than 80 alphanumeric characters (only the first 35 characters will be printed in graphical mode).

2. Dimension Card (2I5,F10.3)

(i) NSEAM = Number of seams

(ii) NSEG = Number of elements

(iii) HW = Half-width of each seam element

3. Elastic Constants Card (4E11.4,3F5.2)

(i) EXX = Modulus of elasticity in x direction

(ii) EYY = Modulus of elasticity in y direction

(iii) EZZ = Modulus of elasticity in z direction

(iv) GXY = Shear Modulus in x,y plane

(v) VXY = Poissons' ratio, y strain due to x strain

(vi) VZX = Poissons' ratio, x strain due to z strain

(vii) VYZ = Poissons' ratio, z strain due to y strain

4. Rock Parameters Card (2F10.3)

(i) DENS = Density of country rock (FORCE/UNIT VOLUME)

(ii) SRATIO = Primitive horizontal to vertical stress ratio.

Seam Cards for each seam :

5. Seam Data Card (F6.2,F8.2,2E11.4)

(i) THICK = Seam thickness

(ii) DEPTH = Seam depth

(iii) ESEAM = Stiffness modulus of seam

(iv) GSEAM = Shear modulus of seam

6. Seam Excavation Card (80I1)

Each character represents a seam element, 1=mined and 2=unmined, NSEG seam elements must be specified.

5.2 Running Program

In interactive mode the program is first compiled to form the object code for the program :

```
$r *fortg scards=ddseam.s spunch=ddseam.o par=d,noload
```

The program can now be run as follows :

```
$r  ddseam.o+*ig+*plotlib 3=(results) 4=(data) 7=(save) 8=(print)
9=(pdf)
```

The program prompts the user for execution commands and prints the alternatives which are available or the formats of the data it requires, making the running of the program relatively simple.

For graphical output, after graphical data has been written onto unit 9 = (pdf), the *calcomp plot program must be run in order to get a hard copy from the calcomp plotter.

Run time depends upon the number of elements and seams, and upon the number of internal points that are calculated. For four seams with 75 elements per seam, about 12 seconds is required, whereas for two such seams only 6 seconds is required.

References:

1. Crouch, Steven l.: "Analysis of Stresses and Displacements Around Underground Excavations: an Application of the Displacement Discontinuity Method"; *Dept. of Civil and Mineral Engineering, University of Minnesota*, Minneapolis, (1976).

APPENDIX 1.

Computer Program DDSEAMS

Internal Subroutines

ONSEAM...Computes the stresses and displacements at the mid-point of all elements in a given range for a given seam.

OFSEAM...Computes the stresses, strains and displacements for a specified depth at x co-ords the same as the centres of each seam element in the given range.

GFUNC...Computes the G functions as given in ref. 1.

GRAPH...Plots up to 5 curves on one graph

GETTY...Sets up the arrays for subroutine GRAPH

STATS...Plots the problem specifications

MINEX...Plots a cross section of the mine layout

IBAR...Hatches the unmined portions of the seam plotted by MINEX

MESSGE...Places a message on the plot

Internal Functions

VAVG...Calculates an average value for a real array

VMIN...Finds a minimum vaue for a real array

VMAX...Finds a maximum value for a real array

ITEM...Places a menu item at (x,y) and returns an integer picture name

External Subroutines

PLOTS...Initialises plotting file

IGCTRL...Device control routine

IGBGNS...Creates a sub-picture within an existing one or empty current one

IGENDS...Ends a sub-picture and returns to the picture started by IGBGNS or IGCTNS

IGVWPT...Viewport transformation for a picture of a specific size and location

IGCTNS...Re-activates a picture to the current one for additions or changes

IGVEC...Multiple line drawing routine

IGTXT...Draws a text string (transformation of picture is applied)

IGFMT...Converts a variable value to a character representation as text

IGMR...Adds a non-intensified line to the end of the current picture (co-ord displacement)

IGTRAN...Linear transformation of the picture when drawn

IGDRON...Translates data to form a picture at the terminal or to the tape unit [illegible] for plot files

IGDELS...Deletes a picture from the data structure

IGMA...Adds a non-intensified line to the end of the current picture/object

IGPIKS...Returns a picture name for the current position of the cursor on the screen

SCALE...Finds the scale parameters for graphs

LINE...Plots data onto graph with scaling applied

AXIS2...Draws a single graph axis with marks and numeration

IGTXTH...Adds a text string to a picture without transformations applied

Main Variables

NSEAMS - total number of seams

NSEG - total number of seam elements

HW - half-width of each seam element

DENSE - density of the country rock

SRATIO - primitive horizontal to vertical stress ratio

DEPTH - array containing the seam depths

THICK - array containing the seam thicknesses

MIN - array of the mined state for each seam (1=mined, 2=unmined)

ESEAM - elastic moduli for each seam

GSEAM - shear moduli for each seam

H - array of offseam levels

EXX,EYY,EZZ - elastic moduli for country rock in x, y and z directions respectively

VYX,VZX,VYZ - Poissons' ratios for the country rock

DS - array of shear displacement discontinuities

DN - array of normal displacement discontinuities

ASS,ASN,ANS,ANN - Stress Influence Coefficients

BSS,BSN,BNS,BNN - Displacement Influence Coefficients

MENU1 - array of 1st. command menu picture names

MENU2 - array of 2nd. command menu picture names

IPLOT - picture name of plotting area overlay

ITEXT - picture name of command area overlay

GRAF - array of picture names of plotted graphs

IMINE - picture name of mine cross section

Program DDSEAMS listing

```
C**********************************************************************C
C                                                                      C
C                                                                      C
C  TITLE: "Analysis of Stresses and Displacements Around Multiple,    C
C          Parallel Seam-type Deposits by the Displacement             C
C          Discontinuity Method"                                       C
C                                                                      C
C  CODE NAME: DDSEAM                                                   C
C                                                                      C
C  AUTHOR: Steven L. Crouch                                            C
C                                                                      C
C  IMPLEMENTED/ADAPTED by: Fred E. Eves                                C
C                                                                      C
C  VERSION: 0                          DATE: FEBRUARY, 1978            C
C                                                                      C
C                                                                      C
C      Program DDSEAM computes the displacements and stresses induced C
C  by the minig of multiple, parallel seam-type deposits using        C
C  Crouch's "Displacement Discontinuity Method".  The program can be  C
C  run either interactively or in batch mode.  The computed results   C
C  may be obtained in the form of printed tables and/or plotted       C
C  graphs.  The *IG and *PLOTLIB library routines are used to imple-  C
C  ment the graphics option.                                           C
C                                                                      C
C     Aside from the changes made to incorporate the plotting         C
C  capability, parts of the rpogram have been rewritten inorder to    C
C  increase efficiency.                                                C
C                                                                      C
C  SUBROUTINES called by DDSEAM:                                       C
C     ONSEAM   - computes the stresses & displacements a[illegible] seam.  C
C     OFSEAM   - computes the stresses & displacements along any      C
C                parallel line in the half-space y<0 not on a seam.   C
C     GFUNC    - computes the G-function values as indicated on pages C
C                232-234 of Crouch's report.                           C
C     GRAPH    - plots up to 5 curves on a single labeled graph.      C
C     GETTY    - moves the curve data into columns of a single matrix C
C                for the curve plotting routine, GRAPH.                C
C     STATS    - plots the specifications describing the multiple     C
C                seam mine.                                            C
C     MINEX    - plots a cross-section of the multiple seam mine.     C
C                                                                      C
C**********************************************************************C
      COMMON/CONS/HW,DENSE,SRATIO,NSEAMS,NSEG
      COMMON/CMO/ ICARD(80),EXX,EYY,EZZ,VYX,VZX,VYZ,GXY
      COMMON/CM1/ GAM1,GAM2,Q1,Q2,CN1,CN2,S11,S22,S12,C66,B,BC66,
     *            GM12,GM12$2,GM1$2,GM2$2,GM1$3,GM2$3,Q1P1,Q2P1
      COMMON/CM2/ ASS(80,5,5),ASN(80,5,5),ANS(80,5,5),ANN(80,5,5),
     1            BSS(80,5,5),BSN(80,5,5),BNS(80,5,5),BNN(80,5,5)
      COMMON/CM3/ DEPTH(5),PS(5),PN(5),THICK(5),ESEAM(5),
     *            GSEAM(5),MIN(80,5)
      COMMON/CM4/ DS(80,5),DN(80,5)
      COMMON/CM5/ UXP(80,5),UXM(80,5),UYP(80,5),UYM(80,5),SIGS(80,5),
     1            SIGN(80,5)
      COMMON/CM6/ UX(80,5),UY(80,5),ESXX(80,5),ESYY(80,5),ESXY(80,5),
     1            SIGXX(80,5),SIGYY(80,5),SIGXY(80,5),H(5)
C
      DIMENSION X(80),XM(82),YY(248)
      COMPLEX*8 YYID(3),CDUMMY
      REAL    K1,K2,KS,KN,XVWPT(5),YVWPT(5)
      INTEGER WINDOW,CALC,DATSET,IDAT(4),MENU1(5),MENU2(5),
     1          GRAF(3),XTITLE(5),YTITLE
      DATA      IDAT/'SAVE','ONSE','OFFS','STOP'/,
     1          ITEXT/'TEXT'/, IPLOT/'DRAW'/, IDENT/'IDEN'/,
     2          IMINE/'MINE'/, ISTAT/'STAT'/, CALC/'CALC'/,
     3          GRAF/'PLT1','PLT2','PLT3'/,
     4          WINDOW/'WIND'/,
     5          XVWPT/-1.,-1.,.5,.5,-1./, YVWPT/-.75,.75,.75,-.75,-.75/,
     6          XTITLE/'HORI','ZONT','AL D','ISTA','NCE'/, YTITLE/' '/
C
C---  initialize
      LVL=0
C
C     Determine whether a new problem is to be solved or whether a
C     previously solved problem is to be read in.
C       IOPT=1 -> pre-defined problem.
C       IOPT=2 -> new problem.
    5 PRINT 2001
      READ1011, IOPT
      GOTO (10,20),IOPT
        PRINT2096, IOPT
        GOTO 5
   10 READ(7) ASS,ANN,ASN,ANS,BSS,BNN,BSN,BNS,DS,DN,PS,PN,X,H,DEPTH,
                THICK,ESEAM,GSEAM,EXX,EYY,EZZ,GXY,VYX,VZX,VYZ,K1,K2,
                GAM1,GAM2,Q1,Q2,CN1,CN2,S11,S22,S12,C66,B,BC66,
                GM12,GM12$2,GM1$2,GM2$2,GM1$3,GM2$3,Q1P1,Q2P1,
     4          DENSE,SRATIO,HW,DMAX,OMEGA,
     5          MIN,ICARD,NSEAMS,NSEG,NITER
C     allow for a change in the pre-existing stress ratio.
      PRINT2003
      READ1002, SRATIO
      GOTO 500
C
C---  Read in parameters defining a new problem.
   20 READ(4,1001) ICARD
      READ(4,1003) NSEAMS,NSEG,HW
      READ(4,1004) EXX,EYY,EZZ,GXY,VYX,VZX,VYZ
      READ(4,1005) DENSE,SRATIO
C
C---  Compute constants GAM1, GAM2, etc.
C
      PI=4.*ATAN(1.)
      S11=1./EXX
      S22=1./EYY
      S33=1./EZZ
      S12=-VYX/EXX
      S13=-VZX/EXX
      S23=-VYZ/EZZ
      CON=S11*S22-S12*S12+(2.*S12*S13*S23-S11*S23*S23-S22*S13*S13)/S33
      C11=(S22-S23*S23/S33)/CON
      C12=-(S12-S13*S23/S33)/CON
      C22=(S11-S13*S13/S33)/CON
      C66=GXY
      DET=C11*C22-C12*C12
      IF (DET.GT.0.) GO TO 50
      PRINT2017
      STOP
   50 K1=SQRT(C22/C11)
      K2=0.5*(C11*C22-C12*(2.*C66+C12))/(C11*C66)
      IF (K2-K1) 55,60,65
   55 PRINT2018
```

```
      STOP
   60 PRINT2019
      STOP
C
C---  Compute constants used in subroutine GFUNC.
   65 SUM=SQRT((K1+K2)/2.)
      DIF=SQRT((K2-K1)/2.)
      GAM1=SUM+DIF
      GAM2=SUM-DIF
      GM12=GAM1*GAM2
      GM12$2=GM12**2
      GM1$2=GAM1**2
      GM2$2=GAM2**2
      GM1$3=GM1$2*GAM1
      GM2$3=GM2$2*GAM2
      Q1=(C11*GM1$2-C66)/(C12+C66)
      Q2=(C11*GM2$2-C66)/(C12+C66)
      Q1P1=1.+Q1
      Q2P1=1.+Q2
C
      B=Q1P1*Q2P1/(2.*PI*(Q1-Q2))
      CN1=(GAM1+GAM2)/(GAM1-GAM2)
      CN2=2.*GM12/(GAM1-GAM2)
      BC66=B*C66
C
C---  Read in specifications for the various seams.
      DO 70 M=1,NSEAMS
        READ(4,1006) THICK(M),DEPTH(M),ESEAM(M),GSEAM(M)
        READ(4,1011) (MIN(N,M),N=1,NSEG)
   70 CONTINUE
C***********************************************************
C***         COMPUTE INFLUENCE COEFFICIENTS.            ***
C***********************************************************
      DO 200 L=1,NSEAMS
        HL=DEPTH(L)
        DO 200 M=1,NSEAMS
          HM=DEPTH(M)
          DO 200 K=1,NSEG
            KK=2*(K-1)
            XP=HW*(KK+1)
            XM=HW*(KK-1)
            CALL GFUNC(XP,HM,-HL,G1P,G2P,G3P,G4P,G5P,G6P,G7P,G8P,G9P,
     *                                                          G10P)
            CALL GFUNC(XM,HM,-HL,G1M,G2M,G3M,G4M,G5M,G6M,G7M,G8M,G9M,
     *                                                          G10M)
            ASS(K,M,L)=BC66*(G5P-G5M)
            ASN(K,M,L)=BC66*(G6P-G6M)
            ANS(K,M,L)=BC66*(G3P-G3M)
            ANN(K,M,L)=BC66*(G4P-G4M)
            BSS(K,M,L)=B*(G7P-G7M)
            BSN(K,M,L)=B*(G8P-G8M)
            BNS(K,M,L)=B*(G9P-G9M)
            BNN(K,M,L)=B*(G10P-G10M)
  200 CONTINUE
C
C     INITIALIZE
C
  210 DO 220 M=1,NSEAMS
        PS(M)=0.
        PN(M)=DENSE*DEPTH(M)
      DO 220 I=1,NSEG
        DS(I,M)=0.
        DN(I,M)=0.
  220 CONTINUE
C
  230 DO 240  I=1,NSEG
        X(I)=HW*(2*I-1-NSEG)
  240 CONTINUE
C*******************************************************************
C***         SOLVE EQUATIONS BY GAUSS-SIEDEL ITERATION          ***
C***         PROCESS - WITH OVER-RELAXATION.                    ***
C*******************************************************************
C      solve for shear & normal displacement dicontinuities.
      NITER=0
      PRINT2035
  250 PRINT2042
      READ1013, N,TOL,OMEGA
  251 PRINT2043
      READ1000, IANS
      GOTO(252,254),IANS
        GOTO 251
  252 PRINT2044
  254 DO 290 ITER=1,N
        DMAX=0.
        DO 280 L=1,NSEAMS
          HO=THICK(L)
          KS=GSEAM(L)/HO
          KN=ESEAM(L)/HO
          PPS=PS(L)
          PPN=PN(L)
          ASSLL=ASS(1,L,L)
          ANNLL=ANN(1,L,L)
          DO 280 IL=1,NSEG
            MINE=MIN(IL,L)
            TMS=0.
            TMN=0.
            DDS=DS(IL,L)
            DDN=DN(IL,L)
            DO 260 M=1,NSEAMS
              DO 260 JM=1,NSEG
                DMS=DS(JM,M)
                DMN=DN(JM,M)
                LD=IL-JM
                K=IABS(LD)+1
                FAC=ISIGN(1,LD)
                TMS=TMS - ASS(K,M,L)*DMS - FAC*ASN(K,M,L)*DMN
                TMN=TMN - FAC*ANS(K,M,L)*DMS - ANN(K,M,L)*DMN
 260        CONTINUE
C
            GO TO (265,270),MINE
 265        TMS=TMS-PPS
            TMN=TMN-PPN
            DELS=TMS/ASSLL
            DELN=TMN/ANNLL
C        check & correct for complete closure boundary condition.
            IF (DDN.LT.HO.OR.TMN.GT.0.) GOTO 275
            DDN=HO
            DELN=0.
            GOTO 275
C
```

```
  270          TMS=TMS + KS*DDS
               TMN=TMN + KN*DDN
               DELS=TMS/(ASSLL - KS)
               DELN=T[illegible]/(ANNLL - KN)
 C
  275          DS(IL,L)=DDS + OMEGA*DELS
               DN(IL,L)=DDN + OMEGA*DELN
 C
               DELS=ABS(DELS)
               DELN=ABS(DELN)
               DMAX=AMAX1(DMAX,DELS,DELN)
  280     CONTINUE
          GOTO (282,284),IANS
  282     PRINT2045, ITER,DMAX
  284     IF (DMAX.LE.TOL)  GOTO 295
  290 CONTINUE
 C
      NITER=NITER+N
      PRINT2039, NITER,DMAX
  292 PRINT2040
      READ1000, IANS
      GOTO(250,500,9899),IANS
        PRINT2096, IANS
        GOTO 292
 C
  295 NITER=NITER+ITER
      PRINT2041, NITER,OMEGA,DMAX
 C
 C*********************************************************************
 C***                                                               ***
 C***              COMPUTATION CONTROL SECTION                      ***
 C***                                                               ***
 C*********************************************************************
 C     Determine mode of output.
 C       MODE=1 -> graphical only.
 C       MODE=2 -> both graphical & printed.
 C       MODE=3 -> printed only.
  500 PRINT2070
      READ1000,MODE
      GOTO (505,505,505), MODE
        PRINT20[illegible], MODE
        GOTO 500
  505 PRINT2071, MODE
      GOTO (515,510,510), MODE
 C
 C***         OUTPUT THE NINE SPECS.          ***
 C
  510 WRITE(8,2002) ICARD
      WRITE(8,2008) NSEAMS,NSEG,HW
      WRITE(8,2009) DENSE,SRATIO
      WRITE(8,2010) EXX,EYY,EZZ,GXY,VYX,VZX,VYZ
      WRITE(8,2021) K1,K2,GAM1,GAM2,Q1,Q2
      DO 511 M=1,NSEAMS
        WRITE(8,2012) M,THICK(M),DEPTH(M),ESEAM(M),GSEAM(M)
        WRITE(8,2013) (MIN(N,M),N=1,NSEG)
  511 CONTINUE
      WRITE(8,2041) NITER,OMEGA,DMAX
      IF (MODE.EQ.3) GOTO 525
 C
 C***        SET-UP GRAPHICAL PICTURES             ***
```

```
C
  515 CALL PLOTS
        CALL IGCTRL(CALC,'PACK','ON')
        CALL IGCTRL('TERM','KEEP',1)
        YTOP=.75
        CALL IGBGNS(ITEXT)
C---  menu no. 1
          MENU1(1)= ITEM('BLOW-UP GRAPH<E>',.55,YTOP-.03)
          MENU1(2)= ITEM('CALCOMP COPY<E>',.55,YTOP-.09)
          MENU1(3)= ITEM('MINE X-SECTION<E>',.55,YTOP-.15)
          MENU1(4)= ITEM('CONTINUE<E>',.55,YTOP-.21)
C---  menu no. 2
          MENU2(1)= ITEM('REDRAW<E>',.05,YTOP-.03)
          MENU2(2)= ITEM('CALCOMP COPY<E>',.05,YTOP-.09)
        CALL IGENDS(ITEXT)
        CALL IGVWPT(ITEXT,.5,1.,-.75,.75)
        CALL IGBGNS(IPLOT)
C---  define mine cross-section.
          CALL MINEX(IMINE)
          CALL IGVWPT(IMINE,-1.,1.,1.,3.)
C---  define statistics display.
          CALL STATS(IS[illegible])
          CALL IGCTNS([illegible]T)
            [illegible]LL IGBGNS([illegible]ENT)
            [illegible] IGENDS([illegible]T)
          [illegible]LL [illegible]GENDS(ISTAT)
          [illegible]GVWPT(ISTAT,0.0,1.0,0.0,1.0)
C---  define viewports for each of the graphs.
          CALL IGBGNS(GRAF(1))
          CALL IGENDS(GRAF(1))
          CALL IGVWPT(GRAF(1),-1.,0.0,0.0,1.0)
          CALL IGBGNS(GRAF(2))
          CALL IGENDS(GRAF(2))
          CALL IGVWPT(GRAF(2),-1.,0.0,-1.0,0.0)
          CALL IGBGNS(GRAF(3))
          CALL IGENDS(GRAF(3))
          CALL IGVWPT(GRAF(3),0.0,1.0,-1.0,0.0)
        CALL IGENDS(IPLOT)
C
C---  place drawing area in largest left square of screen.
C---  also box this region.
        CALL IGVWPT(IPLOT,-1.0,0.5,-.75,.75)
        CALL IGVEC(5,XVWPT,YVWPT)
  525 PRINT2030
      READ1008, DATSET
      DO 550  I=1,4
        IF  (DATSET.EQ.IDAT(I))  GOTO 575
  550 CONTINUE
      PRINT 2000, DATSET
      GOTO 525
  575 GOTO (600,700,800,9999),I
C***
C***  SAVE the computations of influence coefficients, displacement
C***  discontinuity, and other variables for another run.
C***
  600 WRITE(7) ASS,ANN,ASN,ANS,BSS,BNN,BSN,BNS,DS,DN,PS,PN,X,H,DEPTH,
     1        THICK,ESEAM,GSEAM,EXX,EYY,EZZ,GXY,VYX,VZX,VYZ,K1,K2,
     2        GAM1,GAM2,Q1,Q2,CN1,CN2,S11,S22,S12,C66,B,B066,
     3        GM12,GM12$2,GM1$2,GM2$2,GM1$3,GM2$3,Q1P1,Q2P1,
     4        DENSE,SRATIO,HW,DMAX,OMEGA,
     5        MIN,ICARD,NSEAMS,NSEG,NITER
      GOTO 525
C***
C***  COMPUTE stresses and displacements at seam level(s).
C***
  700 PRINT 2080, NSEAMS,NSEG
      READ1009, ISM,IB,IE
      IF (ISM.GE.1.AND.ISM.LE.NSEAMS) GOTO 710
        PRINT2081, ISM
      GOTO 700
  710 IF (IB.GE.1 .AND. IE.GE.1 .AND. IB.LE.NSEG .AND. IE.LE.NSEG
     1                           .AND. IB.LE.IE)  GOTO 720
        PRINT2095, IB,IE
      GOTO 700
C
  720 CALL ONSEAM(ISM,IB,IE)
      GOTO (775,725,725), MODE
  725   WRITE(8,2050) ISM
        DO 750  J=IB,IE
          WRITE(8,2051) J,UXP(J,[illegible]M),UXM(J,ISM),DS(J,ISM),UYP(J,ISM),
     1                 UYM(J,[illegible]),DN(J,ISM),SIGS(J,ISM),SIGN(J,ISM)
  750   CONTINUE
C
  775 GOTO ([illegible],776,525), MODE
C
C       GRAPHICAL OUTPUT
C
  776 CALL IGCTRL('TERM','ERASE')
        CALL IGBGNS(IDENT)
          CALL IGMR(.015,.02)
          CALL IGTXT('<RSCL>',1.5,'ONSEAM:<E>')
          CALL IGTXT('<RSCL>',.6667,'  SEAM <E>')
          CALL IGFMT(ISM,'I',1)
          CALL IGTXT('  SEGS <E>')
          CALL IGFMT(IB,'I',2)
          CALL IGTXT('-<E>')
          CALL IGFMT(IE,'I',2)
        CALL IGENDS(IDENT)
        N=0
        DO 780  J=IB,IE
          N=N+1
          XX(N)=X(J)
  780   CONTINUE
        N2=N+2
C
C   plot shear displacements and displacement discontinuity values.
         CALL GETYY(3,UXP(IB,ISM),'+U<BSUB>S<E>',UXM(IB,ISM),
     1         '-U<BSUB>S<E>',DS(IB,ISM),' D<BSUB>S<E>',N2,YY,YYID)
          CALL GRAPH(XX,YY,N2,3,YYID,XTITLE,19,YTITLE,1,
     1              'SHEAR DISPL. & DISPL. DISCONTINUITY<E>',GRAF(1))
C
C   plot normal displacements and displacement discontinuity values.
         CALL GETYY(3,UYP(IB,ISM),'+U<BSUB>N<E>',UYM(IB,ISM),
     1         '-U<BSUB>N<E>',DN(IB,ISM),' D<BSUB>N<E>',N2,YY,YYID)
          CALL GRAPH(XX,YY,N2,3,YYID,XTITLE,19,YTITLE,1,
     1              'NORMAL DISPL. & DISPL. DISCONTINUITY<E>',GRAF(2))
C
C   plot shear and normal stresses on each seam element.
          CALL GETYY(2,SIGS(IB,ISM),'SIG<BSUB>XY<E>',SIGN(IB,ISM),
     1         'SIG<BSUB>YY<E>',DUMMY,CDUMMY,N2,YY,YYID)
```

```
       CALL GRAPH(XX,YY,N2,2,YYID,XTITLE,19,YTITLE,1,
     1                 'SHEAR  &  NORMAL  STRESSES<E>',GRAF(3))
      GOTO 9000
C***
C***  COMPUTE stresses and displacements at specified off-seam locat[illegible]
C***
  800 PRINT 2090, NSEG
      LVL=LVL+1
      READ1010, H(LVL),IB,IE
      IF (H(LVL).LE.0.0) GOTO 810
        PRINT2091, H(LVL)
      GOTO 800
  810 IF (IB.GE.1 .AND. IE.GE.1 .AND. IB.LE.NSEG .AND. IE.LE.NSEG
     1                              .AND. IB.LE.IE)  GOTO 820
        PRINT2095, IB,IE
      GOTO 800
C
  820 CALL OFSEAM(LVL,IB,IE)
      GOTO (875,825,825), MODE
  825   WRITE(8,2060) H(LVL)
        DO 850  J=IB,IE
          WRITE(8,2061) J,UX(J,LVL),UY(J,LVL),ESXX(J,LVL),ESYY(J,LVL),
     1                ESXY(J,LVL),SIGXX(J,LVL),SIGYY(J,LVL),SIGXY(J,LVL)
          WRITE(3,3061) J,H(LVL),X(J),UX(J,LVL),UY(J,LVL),ESXX(J,LVL),
     1    ESYY(J,LVL),ESXY(J,LVL),SIGXX(J,LVL),SIGYY(J,LVL),SIGXY(J,LVL)
 3061 FORMAT (I5,2F10.1,5F10[illegible]3F10.1)
  850   CONTINUE
C
  875 GOTO (876,876,525), MODE
C
C       GRAPHICAL OUTPUT
C
  876 CALL IGCTRL('TERM','ERASE')
        CALL IGBGNS(IDENT)
          CALL IGMR(.015,.02)
          CALL IGTXT('<RSCL>',1.5,'OFFSEAM:<E>')
          CALL IGTXT('<RSCL>',.66[illegible],'   Y=<E>')
          CALL IGFMT(H(LVL),'F',7,1)
          CALL IGTXT('  SEGS <E>')
          CALL IGFMT(IB,'I',2)
          CALL IGTXT('-<E>')
          CALL IGFMT(IE,'I',2)
        CALL IGENDS(IDENT)
        N=0
        DO 880  J=IB,IE
          N=N+1
          XX(N)=X(J)
  880,  CONTINUE
        N2=N+2
C
C   plot strain at this level.
          CALL GETYY(3,ESXX(IB,LVL),'E<BSUB>XX<E>',ESYY(IB,LVL),
     1          'E<BSUB>YY<E>',ESXY(IB,LVL),'E<BSUB>XY<E>',N2,YY,YYID)
          CALL GRAPH(XX,YY,N2,3,YYID,XTITLE,19,YTITLE,1,
     1                 'S T R A I N S<E>',GRAF(1))
C
C   plot stresses at this level.
          CALL GETYY(3,SIGXX(IB,LVL),'SIG<BSUB>XX<E>',SIGYY(IB,LVL),
     1      'SIG<BSUB>YY<E>',SIGXY(IB,LVL),'SIG<BSUB>XY<E>',N2,YY,YYID)
          CALL GRAPH(XX,YY,N2,3,YYID,XTITLE,19,YTITLE,1,
     1                   'S T R E S S E S<E>',GRAF(2))
C
C   plot shear and normal displacements at this level.
         CALL GETYY(2,UX(IB,LVL),'U<BSUB>X<E>',UY(IB,LVL),
     1        'U<BSUB>Y<E>',DUMMY,CDUMMY,N2,YY,YYID)
         CALL GRAPH(XX,YY,N2,2,YYID,XTITLE,19,YTITLE,1,
     1                   'SHEAR  &  NORMAL  DISPLACEMENTS<E>',GRAF(3))
      GOTO 9000
C
C
C      *** G R A P H I C S   M O N I T O R ***
C
C
 8000 CALL IGTRAN(ITEXT,'WIND',0.0,0.5,-.75,.75)
      CALL IGCTRL('TERM','ERAS')
 8010 INDEX=IGPIKS(2,MENU2)
      GOTO (8030,8020),INDEX
 8020 CALL IGTRAN('*MP*','WIND',-1.,.5,-.75,.75)
      CALL IGDRON('CALC')
      CALL IGTRAN('*MP*','SCALE',1.)
      GOTO 8010
 8030 CALL IGTRAN(IPLOT,'SCALE',1.0)
      CALL IGCTRL('TERM','ERAS')
C
 9000 CALL IGTRAN(ITEXT,WINDOW,0.5,1.0,-.75,.75)
 9010 INDEX=IGPIKS(4,MENU1)
      GOTO(9100,9200,9300,9400),INDEX
C
C
 9100 CALL MESSGE('>>INDICATE PLOT?<E>',.51,-YTOP)
      INDEX=IGPIKS(3,GRAF)
      CALL IGDELS('MESS')
      GOTO (9110,9120,9130),INDEX
 9110 CALL IGTRAN(IPLOT,WINDOW,-1.0,0.0,0.0,1.0)
      GOTO 8000
 9120 CALL IGTRAN(IPLOT,WINDOW,-1.0,0.0,-1.0,0.0)
      GOTO 8000
 9130 CALL IGTRAN(IPLOT,WINDOW,0.0,1.0,-1.0,0.0)
C
C
 9200 INT=IGBGNS(0)
        CALL IGMA(.51,-.67)
        CALL IGTXT('SELECT OPTION:<E>')
        NPIC1=ITEM('COMPLETE<CRLF>DISPLAY<E>',.51,-.71)
        NPIC2=ITEM('GRAPHS<CRLF>ONLY<E>',.81,-.71)
        INDEX=IGPIKS(NPIC1,NPIC2)
      CALL IGENDS(INT)
      CALL IGDELS(INT)
      CALL IGTRAN('*MP*',WINDOW,-1.,.5,-.75,.75)
      GOTO (9210,9220), INDEX
C
 9210 CALL IGDRON(CALC)
      GOTO 9230
C
 9220 CALL IGTRAN(IPLOT,WINDOW,-1.,0.,0.,1.)
      CALL IGDRON(CALC)
      CALL IGTRAN(IPLOT,WINDOW,-1.,0.,-1.,0.)
      CALL IGDRON(CALC)
      CALL IGTRAN(IPLOT,WINDOW,0.,1.,-1.,0.)
      CALL IGDRON(CALC)
      CALL IGTRAN(IPLOT,'SCAL',1.)
C
 9230 CALL IGTRAN('*MP*','SCAL',1.)
      CALL IGCTRL('TERM','ERASE')
      GOTO 9010
C
C
 9300 CALL IGTRAN(IPLOT,WINDOW,-1.,1.,1.,3.)
      GOTO 8000
C
C
 9400 CALL IGCTRL('TERM','ERASE')
      GOTO 525
C
 9999 IF (MODE.LE.2) CALL IGCTRL(CALC,'ENDPLOT')
      STOP
C
C     FORMAT STATEMENTS.
C
 1000 FORMAT(I1)
 1001 FORMAT (20A4)
 1002 FORMAT (F10.0)
 1003 FORMAT (2I5,F10.3)
 1004 FORMAT (4E11.4,3F5.3)
 1005 FORMAT (2F10.3)
 1006 FORMAT (F6.2,F6.2,2E11.4)
 1007 FORMAT (F8.2,2I4)
 1008 FORMAT(A4)
 1009 FORMAT(3I5)
 1010 FORMAT(F10.1,2I5)
 1011 FORMAT (80I1)
 1013 FORMAT(I3,2F10.0)
C
 2000 FORMAT('-*** BAD DATASET NAME - ',A4//)
 2001 FORMAT(' PROBLEM PREDEFINED? (Y=1,N=2)...(I1)')
 2002 FORMAT(1H1,20A4)
 2003 FORMAT ('0Input new SRATIO, if different.   ...(F10)')
 2008 FORMAT ('0NUMBER OF SEPARATE SEAMS =',I3,/'0NUMBER OF SEGMENTS',
     1'IN EACH SEAM =',I4,/'0HALF-WIDTH OF SEGMENTS =',F6.2)
 2009 FORMAT('0UNIT WEIGHT OF ROCK =',F6.3/,
     1        '0RATIO OF PRE-EXISTING STRESSES SIGXX/SIGYY =',F6.2)
 2010 FORMAT ('0ELASTIC CONSTANTS -',//'   EXX =',E11.4,/'   EYY =',
     1        E11.4,/'   EZZ =',E11.4,/'   GXY =',E11.4,/'   VYX =',
     2        F6.2,/'   VZX =',F6.2,/'   VYZ =',F6.2)
 2012 FORMAT ('-SPECIFICATIONS FOR SEAM NUMBER',I2,/
     1        '0  SEAM THICKNESS =',F8.2/
     2        '               DEPTH =',F8.2/
     3        '    MODULUS OF ELASTICITY =',E10.3/
     4        '           SHEAR MODULUS =',E10.3)
 2013 FORMAT ('0  MINING PATTERN (1 = MINED, 2 = UNMINED)',//5X,133I1)
 2017 FORMAT ('-*** INADMISSIBLE ELASTIC CONSTANTS, C11*C22-C12*C12 LE 0
     1.')
 2018 FORMAT ('-*** COMPLEX GAM1, GAM2 NOT ALLOWED.')
 2019 FORMAT ('-*** GAM1 = GAM2 NOT ALLOWED.')
 2021 FORMAT ('0ELASTIC PARAMETERS - K1 =',F6.2,/
     1        22X,'K2 =',F6.2/,
     2        20X,'GAM1 =',F6.2/,
     3        20X,'GAM2 =',F6.2/,
     4        22X,'Q1 =',F6.2/,
     5        22X,'Q2 =',F6.2)
```

```
2030  FORMAT('OCOMMAND: SAVE,ONSEam,OFFSeam,STOP...(A4)')
2035  FORMAT('- SOLVE for displacement discontinuities.'/)
2039  FORMAT ('O*** ITERATION PROCESS HAS FAILED TO CONVERGE ADEQUATELY'
     1/'      AFTER ',I3,' ITERATIONS.'/'      MAXIMUM DIFFERENCE',
     2' BETWEEN SUCCESSIVE'/'      ITERATES IS',E10.3)
2040  FORMAT('OINDICATE ACTION:'/
     1'      1 - Continue iteration'/
     2'      2 - Accept solution & proceed'/
     3'      3 - Stop'/)
2041  FORMAT('-SOLUTION DATA FOR GAUSS-SIEDEL ITERATION PROCESS'/,
     *       'O  NUMBER OF ITERATIONS:',I10/,
     *       '   RELAXATION FACTOR:',3X,F10.2/,
     *       '   ATTAINED TOLERANCE:',2X,E10.3/)
2042  FORMAT('    # iterations,tolerance,relax. factor: ...(I3,2F10.0)'/
     *        '&?')
2043  FORMAT('OPRINT INTERMEDIATE ITERATION VALUES? (1=Y,2=N)')
2044  FORMAT('-  ITERATION  MAX. RELAXATION'/)
2045  FORMAT(4X,I4,8X,E10.3)
2050  FORMAT ('1    STRESSES, DISPLACEMENTS AND DISPLACEMENT DISCONTINUI
     1TY COMPONENTS AT SEAM #',I1,/
     2'O SEG   UX(POS)   UX(NEG)  DX (=DS)  UY(POS)   UY(NEG)  DY (=DN)
     3     SIGXY      SIGYY',/)
2051  FORMAT (I5,6F10.6,2F10.1)
2060  FORMAT ('1    STRESSES AND DISPLACEMENTS AT OFF-SEAM DEPTH: Y=',
     1   F8.1//'  SEG    X-DISP    Y-DISP XX-STRAIN YY-STRAIN XY-STRAIN
     2   SIGXX      SIGYY      SIGXY'/)
2061  FORMAT (I5,5F10.6,3F10.1)
2070  FORMAT (' INDICATE OUTPUT MODE...(I1)'/
     1          '     1 = graphic only'/
     2          '     2 = graphic & print'/
     3          '     3 = print only')
2071  FORMAT ('   OUTPUT MODE #',I1)
2080  FORMAT ('INPUT: seam#(1-',I1,'), region(1-',I2,')...(3I5)')
2081  FORMAT('    *** SEAM ',I1,' IS NOT DEFINED.'//)
2090  FORMAT ('INPUT: depth(y<=0.0), region(1-',I2,')...(F10.1,2I5)')
2091  FORMAT('    *** DEPTH must be <= 0.0   DEPTH was:',F10.1)
2095  FORMAT('    *** SEGMENT RANGE (',I2,'-',I2,') IS NOT DEFINED.'//)
2096  FORMAT('    *** BAD OPTION:',I2//)
C
C
      END
C-------------------------------------------------   ------------------C
C                                                                      C
      SUBROUTINE OFSEAM(LVL,ISEGB,ISEGE)
C                                                                      C
C--COMPUTE STRESSES AND DISPLACEMENTS AT OFF-SEAM LOCATIONS.           C
C                                                                      C
C----------------------------------------------------------------------C
      COMMON/CONS/HW,DENSE,SRATIO,NSEAMS,NSEG
      COMMON/CM1/ GAM1,GAM2,Q1,Q2,CN1,CN2,S11,S22,S12,C66,B,BC66;
     *            GM12,GM12$2,GM1$2,GM2$2,GM1$3,GM2$3,Q1P1,Q2P1
      COMMON/CM2/ ASS(80,5,5),ASN(80,5,5),ANS(80,5,5),ANN(80,5,5),
     1            BSS(80,5,5),BSN(80,5,5),BNS(80,5,5),BNN(80,5,5)
      COMMON/CM3/ DEPTH(5),PS(5),PN(5),THICK(5),ESEAM(5),
     *            GSEAM(5),MIN(80,5)
      COMMON/CM4/ DS(80,5),DN(80,5)
      COMMON/CM6/ UX(80,5),UY(80,5),ESXX(80,5),ESYY(80,5),ESXY(80,5),
     1            SIGXX(80,5),SIGYY(80,5),SIGXY(80,5),H(5)
C
      Y=H(LVL)
      DO 500 ISEG=ISEGB,ISEGE
        UXX=0.
        UYY=0.
        SGYY=-DENSE*Y
        SGXX=SRATIO*SGYY
        SGXY=0.
        DO 450 M=1,NSEAMS
          HM=DEPTH(M)
          DO 450 IM=1,NSEG
            DDS=DS(IM,M)
            DDN=DN(IM,M)
            LD=2*(ISEG-IM)
            XP=HW*(LD+1)
            XM=HW*(LD-1)
            CALL GFUNC(XP,HM,Y,G1P,G2P,G3P,G4P,G5P,G6P,G7P,G8P,G9P,
     *                                                     G10P)
            CALL GFUNC(XM,HM,Y,G1M,G2M,G3M,G4M,G5M,G6M,G7M,G8M,G9M,
     *                                                     G10M)
            SGXX=SGXX + BC66*((G1P-G1M)*DDS+(G2P-G2M)*DDN)
            SGYY=SGYY + BC66*((G3P-G3M)*DDS+(G4P-G4M)*DDN)
            SGXY=SGXY + BC66*((G5P-G5M)*DDS+(G6P-G6M)*DDN)
            UXX=UXX + B*((G7P-G7M)*DDS+(G8P-G8M)*DDN)
            UYY=UYY + B*((G9P-G9M)*DDS+(G10P-G10M)*DDN)
  450   CONTINUE
        EXX=S11*SGXX + S12*SGYY
        EYY=S22*SGYY + S12*SGXX
        EXY=0.5*SGXY/C66
        ESXX(ISEG,LVL)=EXX
        ESYY(ISEG,LVL)=EYY
        ESXY(ISEG,LVL)=EXY
        UX(ISEG,LVL)=UXX
        UY(ISEG,LVL)=UYY
        SIGXX(ISEG,LVL)=SGXX
        SIGYY(ISEG,LVL)=SGYY
        SIGXY(ISEG,LVL)=SGXY
  500 CONTINUE
      RETURN
C
      END
C----------------------------------------------------------------------C
C                                                                      C
      SUBROUTINE ONSEAM(ISM,ISEGB,ISEGE)
C                                                                      C
C-- COMPUTE STESSES AND DISPLACEMENTS AT SEAM LEVEL INDICATED.          C
C                                                                      C
C----------------------------------------------------------------------C
      COMMON/CONS/HW,DENSE,SRATIO,NSEAMS,NSEG
      COMMON/CM2/ ASS(80,5,5),ASN(80,5,5),ANS(80,5,5),ANN(80,5,5),
     1            BSS(80,5,5),BSN(80,5,5),BNS(80,5,5),BNN(80,5,5)
      COMMON/CM3/ DEPTH(5),PS(5),PN(5),THICK(5),ESEAM(5),
     *            GSEAM(5),MIN(80,5)
      COMMON/CM4/ DS(80,5),DN(80,5)
      COMMON/CM5/ UXP(80,5),UXM(80,5),UYP(80,5),UYM(80,5),SIGS(80,5),
     1            SIGN(80,5)
C
      DO 20 ISEG=ISEGB,ISEGE
        UP = 0.
        UM = 0.
        VP = 0.
        VM = 0.
```

```
       SGS = PS(ISM)
       SGN = PN(ISM)
       DO 10 M = 1,NSEAMS
         DO 10 JM = 1,NSEG
           DDS=DS(JM,M)
           DDN=DN(JM,M)
           LD = ISEG - JM
           K = IABS(LD) + 1
           FAC = ISIGN(1,LD)
           SGS = SGS+     ASS(K,M,ISM)*DDS+FAC*ASN(K,M,ISM)*DDN
           SGN = SGN+FAC*ANS(K,M,ISM)*DDS+     ANN(K,M,ISM)*DDN
           TX =      BSS(K,M,ISM)*DDS+FAC*BSN(K,M,ISM)*DDN
           TY = FAC*BNS(K,M,ISM)*DDS+     BNN(K,M,ISM)*DDN
           UP = UP + TX
           UM = UM + TX
           VP = VP + TY
           VM = VM + TY
           IF (ISM.NE.M) GO TO 10
           IF (ISEG.NE.JM) GO TO 10
           UP = UP - 0.5*DDS
           UM = UM + 0.5*DDS
           VP = VP - 0.5*DDN
           VM = VM + 0.5*DDN
   10  CONTINUE
       UXP(ISEG,ISM)=UP
       UXM(ISEG,ISM)=UM
       UYP(ISEG,ISM)=VP
       UYM(ISEG,ISM)=VM
       SIGS(ISEG,ISM)=SGS
       SIGN(ISEG,ISM)=SGN
   20 CONTINUE
C
C
      RETURN
      END
C----------------------------------------------------------------------C
C                                                                      C
      SUBROUTINE GFUNC(X,H,Y,G1,G2,G3,G4,G5,G6,G7,G8,G9,G10)
C                                                                      C
C-- COMPUTE THE TEN G-FUNCTION VALUES AS GIVEN BY EQ.(37.33)-(37.45)   C
C-- OF CROUCH, STEVEN L.                                               C
C                                                                      C
C----------------------------------------------------------------------C
      COMMON/CM1/ GAM1,GAM2,Q1,Q2,CN1,CN2,S11,S22,S12,C66,B,BC66,
     *            GM12,GM12$2,GM1$2,GM2$2,GM1$3,GM2$3,Q1P1,Q2P1
C
C
      YNH=Y-H
      YPH=Y+H
      YNH$2=YNH**2
      YPH$2=YPH**2
      GM1Y=GAM1*Y
      GM2Y=GAM2*Y
      GM1X=GAM1*X
      GM2X=GAM2*X
      GM12X=GM12*X
      G12X$2=GM12X**2
      GM1X$2=GM1X**2
      GM2X$2=GM2X**2
      GM1H=GAM1*H
      GM2H=GAM2*H
      G1YG2H=GM1Y-GM2H
      G2YG1H=GM2Y-GM1H
C
      U1=1./(GM1X$2+YPH$2)
      U2=1./(GM2X$2+YPH$2)
      GU12=GAM1*U1-GAM2*U2
      V1=1./(GM1X$2+YNH$2)
      V2=1./(GM2X$2+YNH$2)
      W1=1./(G12X$2+G2YG1H**2)
      W2=1./(G12X$2+G1YG2H**2)
      R1=-ALOG(GM1$2*U1)/Q1P1
      R2=-ALOG(GM2$2*U2)/Q2P1
      S1=-ALOG(GM1$2*V1)/Q1P1
      S2=-ALQG(GM2$2*V2)/Q2P1
      T1=-ALOG(GM12$2*W1)/Q1P1
      T2=-ALOG(GM12$2*W2)/Q2P1
      Z1=G1YG2H*W2
      Z2=G2YG1H*W1
      P=GAM2*Z2+GAM1*Z1
      W1PW2=W1+W2
      F=CN1*(GAM1*V1+GAM2*V2)
      FYNH=F*YNH
C
      G1=-YPH*(U1/GAM1-U2/GAM2)-CN1*YNH*(V1/GAM1+V2/GAM2)+CN2/GM12*P
      G2=X*(GU12-F+CN2*(GM2$2*W1+GM1$2*W2))
      G3=YPH*GU12+FYNH-CN2*(GAM1*Z2+GAM2*Z1)
      G4=X*(-(GM1$3*U1-GM2$3*U2)+CN1*(GM1$3*V1+GM2$3*V2)-CN2*
     1      GM12$2*W1PW2)
      G5=X*(GU12+F-GM12*CN2*W1PW2)
      G6=YPH*GU12-FYNH+CN2*P
C
      G8=-0.5*((GAM1*R1-GAM2*R2)-CN1*(GAM1*S1+GAM2*S2)+CN2*(T1+T2))
      G9=-0.5*((Q1*R1/GAM1-Q2*R2/GAM2)+CN1*(Q1*S1/GAM1+Q2*S2/GAM2)-
     1          CN2*(Q1*T1+Q2*T2)/(GM12))
      S1=ATAN(GM1X/YNH)/Q1P1
      S2=ATAN(GM2X/YNH)/Q2P1
      T1=ATAN(GM12X/G2YG1H)/Q1P1
      T2=ATAN(GM12X/G1YG2H)/Q2P1
      R1=0.
      R2=0.
      IF (YPH.EQ.0.) GO TO 15
      R1=ATAN(GM1X/YPH)/Q1P1
      R2=ATAN(GM2X/YPH)/Q2P1
   15 CONTINUE
      G7=(R1-R2)+CN1*(S1+S2)-CN2*(GAM1*T1+GAM2*T2)/(GM12)
      G10=-(Q1*R1-Q2*R2)+CN1*(Q1*S1+Q2*S2)-CN2*(GAM2*Q1*T1+GAM1*Q2*T2)/
     1    (GM12)
C
      RETURN
      END
C**********************************************************************C
C                                                                      C
      SUBROUTINE GRAPH(XX,YY,N2,M,YYID,XTITLE,NX,YTITLE,NY,GTITLE,IPICT)
C                                                                      C
C---  Routine to draw up to 5 curves on one graph.  The scale          C
C---  parameters of the most deviate curve are used for all            C
C---  curves. Each curve must have the same number of points.          C
C         M       no. of curves                                        C
C         N2      no. of data points + 2                               C
```

```
C        XX      vector of absisca values                             C
C        YY(1,j) vector of j'th ordinate values                       C
C        YYID    vector of 16 char. words describing YY(1,j)          C
C        XTITLE  vector of characters to label x-axis.                C
C        NX      no. of chars. in XTITLE  (see AXIS-*PLOTLIB)         C
C        YTITLE  vector of characters to label y-axis.                C
C        NY      no. of chars. in YTITLE  (see AXIS-*PLOTLIB)         C
C        GTITLE  vector of characters used to label the graph.        C
C                This string of characters is terminated by           C
C                the characters "<E>".                                C
C                                                                     C
C*********************************************************************C
      COMPLEX*16 YYID(1)
      DIMENSION XX(1),YY(N2,1),ISYMBL(5)
      INTEGER XTITLE(1),YTITLE(1),GTITLE(1)
      DATA ISYMBL/'a<E>','b<E>','c<E>','d<E>','e<E>'/
C
      N=N2-2
      CALL IGBGNS(IPICT,'WIND',-0.5,11.5,-0.5,8.5)
        CALL SCALE(XX,9.0,N,1)
C
C     find common scaling parameters for all curves
        MN2=M*N2
        CALL SCALE(YY(1,1),8.0,MN2,1)
        AMIN=YY(1,M+1)
        ADELT=YY(2,M+1)
C
C       set scale parameters for each curve
        DO 50  J=1,M
          YY(N+1,J)=AMIN
          YY(N+2,J)=ADELT
   50   CONTINUE
C
C     draw the curves.
        ICHAR=0
        DO 150  J=1,M
          CALL LINE(XX,YY(1,J),N,1,2,ICHAR)
          ICHAR=ICHAR+1
  150   CONTINUE
C
C     plot first the X-axis followed by the Y-axis.
        CALL AXIS2(0.,0.,XTITLE,-NX,9.,0.,XX(N+1),XX(N+2),1.)
        CALL AXIS(0.,0.,YTITLE,NY,8.,90.,AMIN,ADELT)
C
C     describe the curves.
        CALL IGMA(9.5,8.0)
        DO 200  J=1,M
          CALL IGTXT('<ASCL>',.18,'<FONT>','PLOT',ISYMBL(J))
          CALL IGTXT('<FONT>','7ASC',' = <E>',YYID(J),'<CRLF><CRLF><E>')
  200   CONTINUE
C
C     label the graph.
        CALL IGMA(1.5,8.0)
        CALL IGTXT('<ASCL>',.18,GTITLE)
      CALL IGENDS(IPICT)
C
      RETURN
      END
C****************************************************************C
C                                                                C
```

```
      SUBROUTINE GETYY(M,Y1,IDY1,Y2,IDY2,Y3,IDY3,N2,YY,YYID)
C                                                                  C
C---  Routine to move the curve data into columns of a single      C
C---  matrix for the graph plotting routine, GRAPH.  Curve label-  C
C---  ling text is also assembled for each curve.                  C
C        M        number of curves to be assembled.                C
C        Yi       vector containing i'th curve ordinate values     C
C        IDYi     16 char. word describing i'th curve              C
C        N2       no. of data points + 2                           C
C        YY(i,j) vector of j'th ordinate values (output)           C
C        YYID     vector of 16 char. words defining curves(output) C
C                                                                  C
C******************************************************************C
      COMPLEX*16 IDY1,IDY2,IDY3,YYID(1)
      DIMENSION Y1(1),Y2(1),Y3(1),YY(N2,1)
C
      N=N2-2
      YYID(1)=IDY1
      DO 10 , I=1,N
        YY(I,1)=Y1(I)
   10 CONTINUE
C
      IF  (M.LT.2)  GOTO 40
      YYID(2)=IDY2
      DO 20  I=1,N
        YY(I,2)=Y2(I)
   20 CONTINUE
C
      IF  (M.LT.3)  GOTO 40
      YYID(3)=IDY3
      DO 30  I=1,N
        YY(I,3)=Y3(I)
   30 CONTINUE
C
   40 DO 50  J=1,M
        YY(N+1,J)=YY(N,J)
        YY(N+2,J)=YY(N,J)
   50 CONTINUE
C
      RETURN
      END
C===========================================================C
      SUBROUTINE MESSGE(ISTRNG,X,Y)
C                                                           C
C-- to place a message "ISTRNG", starting at ABS(X,Y)       C
C                                                           C
C===========================================================C
      DIMENSION ISTRNG(1)
      CALL I[illegible]GNS('MESSAGE')
        CALL IGMA(X,Y)
        CALL IGTXTH(ISTRNG)
      CALL IGENDS('MESSAGE')
      RETURN
      END
C===========================================================C
C                                                           C
      INTEGER FUNCTION ITEM(ICMD,X,Y)
C                                                           C
C---  Function to place menu item at position X,Y and       C
C---  return a picture name for the item.                   C
```

```
C                                                            C
C============================================================C
      DIMENSION ICMD(1)
      ITEM=IGBGNS(0)
        CALL IGMA(X,Y)
        CALL IGTXT(ICMD)
      CALL IGENDS(ITEM)
      RETURN
      END
C============================================================C
C                                                            C
      SUBROUTINE STATS(IPICT)
C                                                            C
C---  Routine to plot the statistics describing the          C
C---  multiple seam mine.                                    C
C                                                            C
C============================================================C
      COMMON/CONS/HW,DENSE,SRATIO,NSEAMS,NSEG
      COMMON/CMO/ ICARD(20),EXX,EYY,EZZ,VYX,VZX,VYZ,GXY
      COMMON/CM3/ DEPTH(5),PS(5),PN(5),THICK(5),ESEAM(5),
     *            GSEAM(5),MIN(80,5)
C
      CALL IGBGNS(IPICT,'WIND',0.,1.,0.,1.)
        CALL IGMA(1.0,0.0)
        CALL IGDR(-.998,0.0)
        CALL IGDR(0.0,1.0)
C
        CALL IGMA(0.01,.94)
        CALL IGFMT(ICARD,'A',35)
        CALL IGMA(0.01,.84)
        CALL IGTXT('N<BSUB>SEAM<ESUB>=<E>')
        CALL IGFMT(NSEAMS,'I',3)
        CALL IGMA(0.01,.78)
        CALL IGTXT('N<BSUB>SEG <ESUB>=<E>')
        CALL IGFMT(NSEG,'I',3)
        CALL IGMA(0.01,.72)
        CALL IGTXT('WD<BSUB>HALF<ESUB>=<E>')
        CALL IGFMT(HW,'F',6,2)
        CALL IGMA(0.01,.66)
        CALL IGTXT('WT<BSUB>UNIT<ESUB>=<E>')
        CALL IGFMT(DENSE,'F',7,3)
        CALL IGMA(0.01,.6)
        CALL IGTXT('SIG<BSUB>XX<ESUB>/SIG<BSUB>YY<ESUB>=<E>')
        CALL IGFMT(SRATIO,'F',7,3)
C
        CALL IGMA(.4,.84)
        CALL IGTXT('E<BSUB>XX<ESUB>=<E>')
        CALL IGFMT(EXX,'E',7,2)
        CALL IGMA(.4,.78)
        CALL IGTXT('E<BSUB>YY<ESUB>=<E>')
        CALL IGFMT(EYY,'E',7,2)
        CALL IGMA(.4,.72)
        CALL IGTXT('E<BSUB>ZZ<ESUB>=<E>')
        CALL IGFMT(EZZ,'E',7,2)
        CALL IGMA(.4,.66)
        CALL IGTXT('G<BSUB>XY<ESUB>=<E>')
        CALL IGFMT(GXY,'E',7,2)
C
        CALL IGMA(.75,.84)
        CALL IGTXT('V<BSUB>XY<ESUB>=<E>')
```

```
         CALL IGFMT(VYX,'F',3,2)
         CALL IGMA(.75,.78)
         CALL IGTXT('V<BSUB>ZX<ESUB>=<E>')
         CALL IGFMT(VZX,'F',3,2)
         CALL IGMA(.75,.72)
         CALL IGTXT('V<BSUB>YZ<ESUB>=<E>')
         CALL IGFMT(VYZ,'F',3,2)
C
C
         CALL IGMA(0.01,.5)
         CALL IGTXT('SM#   E<BSUB>SEAM<ESUB><E>')
         CALL IGTXT('     G<BSUB>SEAM<ESUB>    THICK  DEPTH<E>')
         CALL IGMA(0.01,.46)
         DO 20 J=1,NSEAMS
           CALL IGTXT('<CRLF><E>')
           CALL IGFMT(J,'I',2)
           CALL IGTXT(' <E>')
           CALL IGFMT(ESEAM(J),'E',8,3)
           CALL IGTXT(' <E>')
           CALL IGFMT(GSEAM(J),'E',8,3)
           CALL IGTXT(' <E>')
           CALL IGFMT(THICK(J),'F',5)
           CALL IGTXT(' <E>')
           CALL IGFMT(DEPTH(J),'F',6,1)
   20   CONTINUE
      CALL IGENDS(IPICT)
C
C
   99 RETURN
      END
C**********************************************************************C
C                                                                      C
      SUBROUTINE MINEX(IMINE)
C                                                                      C
C---  Routine to plot a cross-section of the multiple seam mine        C
C---  that is under investigation.  The same x-axis as used for        C
C---  the graphs is used here to ease interpretation.  Also the        C
C---  seam segmentation is drawn as an additional aid.                 C
C                                                                      C
C**********************************************************************C
      COMMON/CONS/HW,DENSE,SRATIO,NSEAMS,NSEG
      COMMON/CM3/ DEPTH(5),PS(5),PN(5),THICK(5),ESEAM(5),
     *            GSEAM(5),MIN(80,5)
      DIMENSION X(4),Y(4)
C
      IMINE=IGBGNS(0,'WIND',-.5,9.5,-.5,9.5)
        Y(1)=-VMIN(DEPTH,NSEAMS)
        Y(2)=-VMAX(DEPTH,NSEAMS)
C
C---  verify that the scaling in the y-direction is such that the
C---  seams appear about 1/20'th of the vertical scale.
        AVHO=VAVG(THICK,NSEAMS)
        RANGE=ABS(Y(1)-Y(2))
        IF  (AVHO.LE.RANGE/20.)  GOTO 10
          HRNGE=(Y(1)+Y(2))*.5
          Y(1)=HRNGE+10.*AVHO
          Y(2)=HRNGE-10.*AVHO
   10   CALL SCALE(Y,9.0,2,1)
        YMIN=Y(3)
        YDELT=Y(4)
```

```
C
C---  use the same scaling in the x-direction as used for the graphs.
        X(1)=HW*NSEG
        X(2)=-X(1)
        CALL SCALE(X,9.0,2,1)
        XMIN=X(3)
        XDELT=X(4)
C
C---  draw a segmentation axis, annotating every 5'th segment along seam
        W=2.*HW
        NSEG1=NSEG+1
        DTIC=5.*W/XDELT
        AX=(X(2)-HW-XMIN)/XDELT
        AXLEN=(W*NSEG1)/XDELT
        AXDELT=NSEG1/AXLEN
        CALL AX2EP(DTIC,2,0,4)
        CALL AXIS2(AX,9.,'SEAM SEGMENTATION',17,AXLEN,0.,0.,AXDELT,DTIC)
C---  draw X and Y axes.
        CALL AX2EP(1.,2,0,0,D,D,D,D,D,D,D,D)
        CALL AXIS2(0.,0.,'HORIZONTAL DISTANCE',-19,9.0,0.,XMIN,XDELT,1.)
        CALL AXIS2(0.,0.,'DEPTH',5,9.0,90.,YMIN,YDELT,1.)
C
C     draw each seam.
        DO 195  J=1,NSEAMS
          DELY=THICK(J)
          HEIGHT=DELY/YDELT
          AX=X(2)
          VY=-(DEPTH(J)+DELY*.5+YMIN)/YDELT
          IMIN=MIN(1,J)
          ICNT=2
          DO 175  I=2,NSEG
            IF(MIN(I,J).EQ.IMIN)  GOTO 150
            DELX=ICNT*HW
 130        CALL IBAR((AX-XMIN)/XDELT,VY,DELX/XDELT,HEIGHT,IMIN,10)
            AX=AX+DELX
            IMIN=MIN(I,J)
            ICNT=2
            GOTO 175
 150        ICNT=ICNT+2
 175      CONTINUE
          DELX=ICNT*HW
          CALL IBAR((AX-XMIN)/XDELT,VY,DELX/XDELT,HEIGHT,IMIN,10)
C     label the seam by number.
          CALL IGMA((AX+DELX-XMIN)/XDELT,VY)
          CALL IGTXT('<ASCL>',HEIGHT*.65,' SM#<E>')
          CALL IGFMT(J,'I')
 195    CONTINUE
      CALL IGENDS(IMINE)
C
C
      RETURN
      END
C*******************************************************************C
C                                                                   C
      SUBROUTINE IBAR(VX,VY,DELX,DELY,ITYPE,LPB)                    C
C
C---  Routine to draw a seam element as a mined panel or as an      C
C---  unmined pillar at point (VX,VY).                              C
C         VX,VY      lower left corner of element                   C
C         DELX,DELY element width and height                        C
                                                                    C
```

```
C         ITYPE=1   mined element, no hatching
C         ITYPE=2   unmined element, hatching is performed          C
C         LPB       no. of hatch lines per box                      C
C                                                                   C
C*******************************************************************C
C                                                                   C
      CALL IGMA(VX,VY)
      CALL IGDR(0.0,DELY)
      CALL IGDR(DELX,0.0)
      CALL IGDR(0.0,-DELY)
      CALL IGDR(-DELX,0.0)
      IF  (ITYPE.EQ.1)  RETURN
      DH=DELY/LPB
      DX=DELX
      DY=0.0
      DO 10  J=2,LPB
        CALL IGMR(0.0,DH)
        CALL IGDR(DX,0.0)
        DX=-DX
   10 CONTINUE
C
      RETURN
      END
      REAL FUNCTION VAVG(VEC,N)
      DIMENSION VEC(1)
      VAVG=VEC(1)
      IF  (N.LE.1)  RETURN
        DO 10  J=2,N
          VAVG=VAVG+VEC(J)
   10   CONTINUE
        VAVG=VAVG/N
      RETURN
      END
      REAL FUNCTION VMIN(VEC,N)
      DIMENSION VEC(1)
      VMIN=VEC(1)
      IF  (N.LE.1)  RETURN
        DO 10  J=2,N
          IF  (VEC(J).LT.VMIN)  VMIN=VEC(J)
   10   CONTINUE
      RETURN
      END
      REAL FUNCTION VMAX(VEC,N)
      DIMENSION VEC(1)
      VMAX=VEC(1)
      IF  (N.LE.1)  RETURN
        DO 10  J=2,N
          IF  (VEC(J).GT.VMAX)  VMAX=VEC(J)
   10   CONTINUE
      RETURN
      END
```

Program DDSEAMS sample output

```
RUN 02 TEST CRACK NSEQ=40

NUMBER OF SEPARATE SEAMS =  1

NUMBER OF SEGMENTSIN EACH SEAM =  40

HALF-WIDTH OF SEGMENTS =  2.00

UNIT WEIGHT OF ROCK =200.00

RATIO OF PRE-EXISTING STRESSES SIGXX/SIGYY =  0.0

ELASTIC CONSTANTS -

  EXX = 0.7000E+08
  EYY = 0.7000E+08
  EZZ = 0.7000E+08
  GXY = 0.3900E+07
  VYX =  0.25
  VZX =  0.25
  VYZ =  0.25

ELASTIC PARAMETERS - K1 =  1.00
                     K2 =  9.24
                   GAM1 =  4.29
                   GAM2 =  0.23
                     Q1 = 48.39
                     Q2 =  0.02


SPECIFICATIONS FOR SEAM NUMBER 1

  SEAM THICKNESS =     10.00
           DEPTH =   2000.00
  MODULUS OF ELASTICITY = 0.700E+08
          SHEAR MODULUS = 0.390E+07

  MINING PATTERN (1 = MINED, 2 = UNMINED)

    2222222222111111111111111111112222222222


SOLUTION DATA FOR GAUSS-SIEDEL ITERATION PROCESS

  NUMBER OF ITERATIONS:          31
  RELAXATION FACTOR:           1.60
  ATTAINED TOLERANCE:   0.659E-05
```

STRESSES, DISPLACEMENTS AND DISPLACEMENT DISCONTINUITY COMPONENTS AT SEAM #1

SEG	UX(POS)	UX(NEG)	DX (=DS)	UY(POS)	UY(NEG)	DY (=DN)	SIGXY	SIGYY
1	-0.045493	-0.045479	0.000014	-0.030753	-0.021101	0.009652	5.6	467559.4
2	-0.048205	-0.048186	0.000019	-0.031940	-0.019951	0.011990	7.4	483926.9
3	-0.051444	-0.051423	0.000021	-0.033070	-0.018857	0.014213	8.2	499491.2
4	-0.055286	-0.055264	0.000022	-0.034440	-0.017520	0.016919	8.6	518435.3
5	-0.059895	-0.059872	0.000022	-0.036239	-0.015751	0.020488	8.7	543415.4
6	-0.065546	-0.065524	0.000022	-0.038753	-0.013267	0.025486	8.7	578400.9
7	-0.072705	-0.072683	0.000022	-0.042531	-0.009517	0.033014	8.6	631094.1
8	-0.082235	-0.082213	0.000022	-0.048858	-0.003215	0.045643	8.4	719498.0
9	-0.096016	-0.095995	0.000021	-0.061634	0.009538	0.071172	8.3	898202.5
10	-0.119327	-0.119306	0.000022	-0.099748	0.047631	0.147380	8.4	1431619.0
11	-0.128999	-0.128975	0.000024	-0.454025	0.401887	0.855914	0.0	3.8
12	-0.117224	-0.117200	0.000024	-0.622599	0.570444	1.193045	0.0	3.3
13	-0.104092	-0.104069	0.000022	-0.739309	0.687137	1.426448	0.0	-2.8
14	-0.090531	-0.090511	0.000020	-0.827352	0.775166	1.602520	0.0	1.1
15	-0.076774	-0.076756	0.000018	-0.895629	0.843431	1.739061	0.0	0.7
16	-0.062909	-0.062894	0.000015	-0.948613	0.896404	1.845018	0.0	-0.7
17	-0.048979	-0.048967	0.000012	-0.988871	0.936655	1.925528	-0.0	-0.5
18	-0.035009	-0.035000	0.000009	-1.017967	0.965756	1.983736	-0.0	0.8
19	-0.021014	-0.021009	0.000005	-1.036902	0.984686	2.021599	0.0	-0.6
20	-0.007006	-0.007004	0.000002	-1.046237	0.994013	2.040263	0.0	-0.3
21	0.007006	0.007004	-0.000002	-1.046236	0.994014	2.040263	-0.0	-0.2
22	0.021014	0.021009	-0.000005	-1.036901	0.984686	2.021599	0.0	-1.1
23	0.035009	0.035000	-0.000009	-1.017970	0.965757	1.983736	-0.0	1.2
24	0.048979	0.048967	-0.000012	-0.988871	0.936655	1.925528	-0.0	-0.6
25	0.062908	0.062893	-0.000015	-0.948613	0.896405	1.845018	-0.0	-0.8
26	0.076774	0.076756	-0.000018	-0.895629	0.843431	1.739061	0.0	0.5
27	0.090531	0.090511	-0.000020	-0.827353	0.775167	1.602520	-0.0	-0.0
28	0.104092	0.104070	-0.000022	-0.739309	0.687137	1.426447	-0.0	0.6
29	0.117224	0.117201	-0.000024	-0.622601	0.570445	1.193047	-0.0	-2.1
30	0.128999	0.128975	-0.000024	-0.454026	0.401888	0.855915	0.0	-3.3
31	0.119328	0.119306	-0.000022	-0.099747	0.047630	0.147377	-8.4	1431636.0
32	0.096017	0.095995	-0.000021	-0.061634	0.009538	0.071172	-8.3	898201.4
33	0.082235	0.082213	-0.000022	-0.048858	-0.003215	0.045643	-8.4	719497.5
34	0.072706	0.072684	-0.000022	-0.042531	-0.009517	0.033014	-8.6	631094.0
35	0.065546	0.065524	-0.000022	-0.038753	-0.013267	0.025486	-8.7	578400.8
36	0.059895	0.059872	-0.000022	-0.036239	-0.015751	0.020488	-8.7	543415.3
37	0.055286	0.055264	-0.000022	-0.034440	-0.017520	0.016919	-8.6	518435.1
38	0.051444	0.051423	-0.000021	-0.033070	-0.018857	0.014213	-8.2	499491.1
39	0.048205	0.048186	-0.000019	-0.031940	-0.019951	0.011990	-7.4	483926.9
40	0.045493	0.045479	-0.000014	-0.030753	-0.021101	0.009651	-5.6	467559.5

```
STRESSES AND DISPLACEMENTS AT OFF-SEAM DEPTH: Y= -1990.0

SEG    X-DISP      Y-DISP  XX-STRAIN  YY-STRAIN  XY-STRAIN     SIGXX      SIGYY      SIGXY

  1 -0.022921 -0.038119 -0.001470  0.006710 -0.000970   15525.2   473595.2    -7566.6
  2 -0.022243 -0.041114 -0.001546  0.006891 -0.001175   13165.7   485629.4    -9164.3
  3 -0.021166 -0.044185 -0.001649  0.007124 -0.001271    9857.0   501128.1    -9915.0
  4 -0.019575 -0.047977 -0.001782  0.007416 -0.001311    5411.8   520476.1   -10226.5
  5 -0.017314 -0.053028 -0.001956  0.007799 -0.001275    -455.8   545813.1    -9947.2
  6 -0.014165 -0.060162 -0.002189  0.008323 -0.001099   -8087.5   580604.6    -8574.7
  7 -0.009803 -0.070949 -0.002510  0.009079 -0.000631  -17929.3   631063.1    -4922.9
  8 -0.003723 -0.088927 -0.002971  0.010242  0.000543  -30666.8   708248.8     4234.3
  9  0.004921 -0.123921 -0.003665  0.012122  0.003869  -47391.3   836700.2    30181.8
 10  0.017056 -0.211853 -0.004365  0.013973  0.015850  -65097.0   961818.6   123630.7
 11  0.023696 -0.416781 -0.001489  0.003877  0.020789  -38794.0   261724.8   162157.0
 12  0.021691 -0.577373 -0.000923  0.001462  0.013760  -41631.0    91937.7   107326.3
 13  0.018332 -0.693349 -0.000892  0.000831  0.009766  -51047.7    45441.5    76172.9
 14  0.014931 -0.781721 -0.000970  0.000594  0.007199  -61371.0    26242.6    56154.2
 15  0.011810 -0.850501 -0.001076  0.000490  0.005374  -71220.6    16506.4    41918.0
 16  0.009046 -0.903957 -0.001182  0.000443  0.003986  -79977.4    10993.4    31080.0
 17  0.006630 -0.944604 -0.001274  0.000422  0.002874  -87280.4     7691.2    22420.6
 18  0.004511 -0.974001 -0.001348  0.000413  0.001943  -92906.4     5688.8    15151.8
 19  0.002615 -0.993125 -0.001398  0.000410  0.001124  -96719.1     4534.7     8765.9
 20  0.000856 -1.002545 -0.001423  0.000410  0.000368  -98642.3     4006.3     2869.7
 21 -0.000856 -1.002546 -0.001423  0.000410 -0.000368  -98642.3     4005.5    -2869.5
 22 -0.002615 -0.993125 -0.001398  0.000410 -0.001124  -96719.1     4534.3    -8765.8
 23 -0.004511 -0.974001 -0.001348  0.000413 -0.001943  -92906.3     5687.9   -15151.6
 24 -0.006620 -0.944604 -0.001274  0.000422 -0.002874  -87280.7     7690.8   -22420.5
 25 -0.009046 -0.903957 -0.001182  0.000443 -0.003986  -79977.4    10992.8   -31089.9
 26 -0.011810 -0.850501 -0.001076  0.000490 -0.005374  -71220.6    16504.3   -41917.9
 27 -0.014931 -0.781721 -0.000970  0.000594 -0.007199  -61371.0    26242.1   -56154.2
 28 -0.018332 -0.693349 -0.000892  0.000831 -0.009766  -51047.7    45441.5   -76172.9
 29 -0.021691 -0.577374 -0.000923  0.001462 -0.013760  -41630.9    91934.9  -107326.3
 30 -0.023696 -0.416781 -0.001489  0.003877 -0.020789  -38793.9   261722.1  -162157.9
 31 -0.017056 -0.211853 -0.004365  0.013973 -0.015850  -65097.5   961821.6  -123631.4
 32 -0.004921 -0.123921 -0.003665  0.012122 -0.003869  -47391.3   836700.4   -30181.6
 33  0.003722 -0.088927 -0.002971  0.010242 -0.000543  -30666.8   708248.8    -4234.2
 34  0.009803 -0.070949 -0.002510  0.009079  0.000631  -17929.4   631063.1     4922.9
 35  0.014165 -0.060162 -0.002189  0.008323  0.001099   -8087.6   580604.4     8574.7
 36  0.017314 -0.053028 -0.001956  0.007799  0.001275    -455.9   545813.2     9947.2
 37  0.019575 -0.047977 -0.001782  0.007416  0.001311    5411.8   520476.0    10226.5
 38  0.021166 -0.044185 -0.001649  0.007124  0.001271    9856.9   501128.1     9915.0
 39  0.022243 -0.041114 -0.001546  0.006891  0.001175   13165.7   485629.5     9164.3
 40  0.022821 -0.038119 -0.001470  0.006710  0.000970   15525.2   473595.3     7566.6
```

APPENDIX 2

CRACK PROGRAM

Program CRACK listing

```
    READ (4,100) W,ROE,PZ,PY,PX
100 FORMAT (5F10.0)
    WRITE (7,201) W,ROE,PX,PY,PZ
201 FORMAT (//////1X,'CRACK SOLUTION     PROGRAM CRACK.S OUTPUT'//
   +10X,'WIDTH  =  ',F10.1/
   +10X,'POISSONS RATIO = ',F10.4/
   +5X,'PX =',E10.3,5X,'PY = ',E10.3,'PZ = ',E10.3///
   +5X,'X',12X,'SIGX',11X,'SIGY',11X,'SIGZ'/)
  1 READ (4,101) X
101 FORMAT (F10.0)
    IF (X.EQ.999.0) GO TO 998
    XLAM = 1.0/SQRT(1.0-W*W/(4.0*X*X))
    SIGX = (XLAM-1.0)*PZ +PX
    SIGY = PY + 2.0*ROE*(XLAM-1.0)*PZ
    SIGZ = XLAM*PZ
    WRITE (7,202) X,SIGX,SIGY,SIGZ
202 FORMAT (4(E10.3,5X)/)
    GO TO 1
998 WRITE (7,203)
203 FORMAT (/////
   +5X,'Z',12X,'SIGX',11X,'SIGY',11X,'SIGZ'/)
  2 READ (4,102) Z
102 FORMAT (F10.0)
    IF (Z.EQ.999.0) GO TO 999
    ZLAM = 1.0/SQRT(1.0+W*W/(4.0*Z*Z))
    SIGX = (2.0*ZLAM-ZLAM*ZLAM*ZLAM-1.0)*PZ+PX
    SIGY = PY+2.0*ROE*(ZLAM-1.0)*PZ
    SIGZ = ZLAM*ZLAM*ZLAM*PZ
    WRITE (7,202) Z,SIGX,SIGY,SIGZ
    GO TO 2
999 STOP
    END
```

Program CRACK sample output

```
CRACK SOLUTION      PROGRAM CRACK.S OUTPUT

          WIDTH  =           80.0
          POISSONS RATIO =       0.2500
     PX = 0.0             PY =  0.0       PZ =  0.400E+06

        X              SIGX             SIGY             SIGZ

  0.410E+02        0.142E+07        0.711E+06        0.182E+07

  0.430E+02        0.690E+06        0.345E+06        0.109E+07

  0.450E+02        0.473E+06        0.237E+06        0.873E+06

  0.470E+02        0.362E+06        0.181E+06        0.762E+06

  0.490E+02        0.293E+06        0.146E+06        0.693E+06

  0.510E+02        0.245E+06        0.122E+06        0.645E+06

  0.530E+02        0.210E+06        0.105E+06        0.610E+06

  0.550E+02        0.183E+06        0.914E+05        0.583E+06

  0.570E+02        0.161E+06        0.807E+05        0.561E+06

  0.590E+02        0.144E+06        0.721E+05        0.544E+06

  0.610E+02        0.130E+06        0.649E+05        0.530E+06

  0.630E+02        0.118E+06        0.589E+05        0.518E+06

  0.650E+02        0.107E+06        0.537E+05        0.507E+06

  0.670E+02        0.986E+05        0.493E+05        0.499E+06

  0.690E+02        0.909E+05        0.455E+05        0.491E+06

  0.710E+02        0.841E+05        0.421E+05        0.484E+06

  0.730E+02        0.782E+05        0.391E+05        0.478E+06

  0.750E+02        0.729E+05        0.364E+05        0.473E+06

  0.770E+02        0.681E+05        0.341E+05        0.468E+06

  0.790E+02        0.639E+05        0.319E+05        0.464E+06

        Z              SIGX             SIGY             SIGZ

  0.200E+01       -0.360E+06       -0.190E+06        0.498E+02

  0.500E+01       -0.302E+06       -0.175E+06        0.763E+03

  0.100E+02       -0.212E+06       -0.151E+06        0.571E+04

  0.250E+02       -0.356E+05       -0.940E+05        0.596E+05

  0.350E+02        0.126E+05       -0.683E+05        0.114E+06

  0.450E+02        0.309E+05       -0.505E+05        0.167E+06

  0.650E+02        0.342E+05       -0.297E+05        0.247E+06

  0.950E+02        0.242E+05       -0.157E+05        0.313E+06
```

APPENDIX 3

PSTRESS PROGRAM

Program PSTRESS listing

```
      DIMENSION C(5),PHI(5),RPHI(5)
      C(1) = 2.3
      PHI(1)= 40.0
      C(2) = 0.55
      PHI(2) = 40.0
      C(3) = 2.3
      PHI(3) = 33.0
      C(4) = 0.0
      PHI(4) = 0.0
      C(5) = 0.0
      PHI(5) = 0.0
      BOT1 = -148.75
      BOT2 = -151.25
      BOT3 = -1000.0
      BOT4 = -9999.0
      IPAGE = 0
      READ (4,1001) N
      WRITE (7,2001)
      DO 50 J=1,5
   50 RPHI(J) = PHI(J)*3.141593/180.0
      DO 100 I=1,N
      READ(4,1000) NUMEL,GRIDY,GRIDX,DX,DY,EX,EY,EXY,X,Y,XY
      CALL STRESS(X,Y,XY,PM1,PM2,TV3,THETA,IFLAG)
      IF (GRIDY.GE.BOT1) MAT=1
      IF (GRIDY.LE.BOT1.AND.GRIDY.GE.BOT2) MAT=2
      IF (GRIDY.LE.BOT2.AND.GRIDY.GE.BOT3) MAT=3
      IF (GRIDY.LE.BOT3.AND.GRIDY.GE.BOT4) MAT=4
      IF (GRIDY.LE.BOT4) MAT=5
      IF (IFLAG.EQ.0) GO TO 20
      SC = 1.0
      GO TO 19
   20 CALL STABIL(PM1,PM2,RPHI(MAT),C(MAT),SC)
   19 WRITE (8,2000) GRIDY,GRIDX,DX,DY,X,Y,XY,PM1,PM2,THETA,TV3,SC,
     + C(MAT),PHI(MAT)
      IPAGE = IPAGE + 1
      IF (IPAGE.NE.58) GOTO 3
      IPAGE = 1
      WRITE (7,2001)
    3 WRITE (7,2002) GRIDY,GRIDX,DX,DY,X,Y,XY,PM1,PM2,THETA,TV3,SC,
     + MAT
  100 CONTINUE
 1000 FORMAT (I5,10F10.0)
 1001 FORMAT (I5)
 2000 FORMAT (2F10.1,12(1PE10.3))
 2001 FORMAT (1H1/7X,1HY,9X,1HX,4X,6HX-DISP,4X,6HY-DISP,4X,6HSIG XX,4X,
     + 6HSIG YY,4X,6HTAU XY,5X,4HSIG1,6X,4HSIG2,6X,5HTHETA,4X,
     + 6HTAUMAX,4X,7HSTABLTY,3X,3HMAT/)
 2002 FORMAT (2F10.1,10(1PE10.2),I5)
      STOP
      END
      SUBROUTINE STRESS(X,Y,XY,PM1,PM2,TV3,THETA,IFLAG)
C
C
CCCCCCCCCCCCCCCCCCCCCCCCCCCCCCCCCCCCCCCCCCCCCCCCCCCCCCCCCCCCCCCC
C                                                               C
C     SUBROUTINE STRESS - DETERMINES THE PRINCIPAL STRESSES AND C
C                      THEIR DIRECTIONS                         C
C                                                               C
C     INPUT                                                     C
C                                                               C
```

```
C     X   = SIGMA-X STRESS                                             C
C     Y   = SIGMA-Y STRESS                                             C
C     XY  = SHEAR STRESS                                               C
C                                                                      C
C     OUTPUT                                                           C
C                                                                      C
C     PM1    = MAJOR PRINCIPAL STRESS                                  C
C     PM2    = MINOR PRINCIPAL STRESS                                  C
C     TV3    = MAXIMUM SHEAR STRESS                                    C
C     THETA  = DIRECTION OF MAJOR PRINCIPAL STRESS                     C
C                                                                      C
CCCCCCCCCCCCCCCCCCCCCCCCCCCCCCCCCCCCCCCCCCCCCCCCCCCCCCCCCCCCCCCCCCCCCCCC
C
C
C-----CALCULATE PRINCIPAL STRESSES
C
      IFLAG = 0
      IF (X.NE.0.0.OR.Y.NE.0.0.OR.XY.NE.0.0) GO TO 10
      PM1 = 0.0
      PM2 = 0.0
      THETA = 0.0
      TV3 = 0.0
      IFLAG = 1
      GO TO 9
   10 TV1=0.5*(X+Y)
      TV2=0.5*(X-Y)
      TV3=SQRT(TV2**2+XY**2)
      PM1=TV1+TV3
      PM2=TV1-TV3
C
C-----CALCULATE DIRECTION OF PRINCIPAL STRESSES
C
      IF(TV3) 1,2,1
2     THETA=0.785398
      GO TO 3
1     TV1=TV2/TV3
      IF((1.0-ABS(TV1)).GT.0.0001)GOTO 6
      IF(TV1.GT.0.0) THETA=0.0
      IF(TV1.LT.0.0) THETA=1.570796
      GO TO 3
6     THETA=ARCOS(TV1)*0.5
3     IF(XY.LT.0.0) THETA=-THETA
      TV1=PM1
      IF(ABS(PM1).GE.ABS(PM2))GOTO 5
      PM1=PM2
      PM2=TV1
      THETA=THETA+1.570796
5     THETA=THETA*(180./3.141593)
    9 CONTINUE
      RETURN
      END
      SUBROUTINE STABIL (PM1,PM2,PHI,C,SC)
      PTOT = PM1+PM2
      PDIFF = PM1-PM2
      SC = 1.0-PDIFF/(SIN(PHI)*(PTOT+2.0*TAN(PHI)))
      RETURN
      END
      Y       X   X-DISP      Y-DISP     SIG XX     SIG YY     TAU XY     SIG1       SIG2       THETA      TAUMAX     STABLTY   MAT
   -148.0   28.5 [illegible] -1.70E-02  3.10E+00   5.00E-01   3.00E-01  3.13E+00   4.66E-01   6.50E+00   1.33E+00   2.14E-01   1
   -148.0   29.5 [illegible] -1.67E-02  3.10E+00   5.00E-01  -2.00E-01  3.12E+00   4.85E-01  -4.37E+00   1.32E+00   2.25E-01   1
   -148.0   30.5 [illegible] -1.58E-02  3.20E+00   9.00E-01  -9.00E-01  3.51E+00   5.90E-01  -1.90E+01   1.46E+00   2.14E-01   1
   -148.0   31.5  3.62E-03  -1.45E-02  3.20E+00   2.10E+00  -1.50E+00  4.25E+00   1.05E+00  -3.49E+01   1.60E+00   2.88E-01   1
   -148.0   32.5  3.77E-03  -1.29E-02  2.80E+00   4.00E+00  -1.40E+00  4.92E+00   1.88E+00  -5.66E+01   1.52E+00   4.41E-01   1
[illegible] 33.5  4.08E-03  -1.17E-02  2.80E+00   5.00E+00  -5.00E-01  5.11E+00   2.69E+00  -7.78E+01   1.21E+00   6.03E-01   1
   -148.0   34.5  4.35E-03  -1.10E-02  2.90E+00   5.00E+00   3.00E-01  5.04E+00   2.86E+00   8.20E+01   1.09E+00   6.45E-01   1
   -148.0   35.5  4.56E-03  -1.06E-02  3.20E+00   3.90E+00   1.10E+00  4.70E+00 2.[illegible]E+00 5.38E+01 1.15E+00   5.91E-01   1
   -148.0   36.5  4.57E-03  -1.08E-02  3.80E+00   2.20E+00   1.00E+00  4.28E+00 1.[illegible]E+00 2.57E+01 1.28E+00   4.81E-01   1
   -148.0   37.5  4.36E-03  -1.04E-02  4.20E+00   1.30E+00   0.0       4.20E+00   1.30E+00   0.0        1.45E+00   3.71E-01   1
   -148.0   38.5  4.07E-03  -9.31E-03  4.40E+00   1.60E+00  -1.10E+00  4.78E+00   1.22E+00  -1.91E+01   1.78E+00   2.79E-01   1
   -148.0   39.5  3.84E-03  -7.55E-03  4.20E+00   3.60E+00  -2.10E+00  6.02E+00   1.78E+00  -4.09E+01   2.12E+00   3.04E-01   1
   -152.0  -39.5 -4.14E-03  -5.61E-04  4.40E+00   5.30E+00  -5.00E-01  5.52E+00   4.18E+00  -6.60E+01   6.73E-01   7.75E-01   3
   -152.0  -38.5 -4.22E-03   3.48E-04  4.40E+00   5.00E+00  -3.00E-01  5.12E+00   4.28E+00  -6.75E+01   4.24E-01   8.54E-01   3
   -152.0  -37.5 -4.27E-03   1.29E-03  4.10E+00   4.90E+00  -3.00E-01  5.00E+00   4.00E+00  -7.16E+01   5.00E-01   8.22E-01   3
   -152.0  -36.5 -4.25E-03   2.33E-03  3.80E+00   5.00E+00  -4.00E-01  5.12E+00   3.68E+00  -7.32E+01   7.21E-01   7.38E-01   3
   -152.0  -35.5 -4.14E-03   3.59E-03  3.40E+00   4.80E+00  -8.00E-01  5.16E+00   3.04E+00  -6.56E+01   1.06E+00   5.89E-01   3
   -152.0  -34.5 -3.98E-03   5.18E-03  3.20E+00   3.80E+00  -1.40E+00  4.93E+00   2.07E+00  -5.10E+01   1.43E+00   3.66E-01   3
   -152.0  -33.5 -3.91E-03   6.96E-03  3.40E+00   2.10E+00  -1.50E+00  4.38E+00   1.12E+00  -3.33E+01   1.63E+00   1.17E-01   3
   -152.0  -32.5 -3.96E-03   8.45E-03  3.40E+00   8.00E-01  -8.00E-01  3.63E+00   6.66E-01  -1.63E+01   1.48E+00   2.66E-02   3
   -152.0  -31.5 -4.02E-03   9.43E-03  3.20E+00   5.00E-01  -2.00E-01  3.21E+00   4.85E-01  -4.21E+00   1.36E+00  -2.54E-03   3
   -152.0  -30.5 -4.07E-03   9.91E-03  3.20E+00   6.00E-01   3.00E-01  3.23E+00   5.66E-01   6.50E+00   1.33E+00   3.91E-02   3
   -152.0  -29.5 -4.12E-03   9.89E-03  3.30E+00   1.00E+00   9.00E-01  3.61E+00   6.90E-01   1.90E+01   1.46E+00   4.22E-02   3
   -152.0  -28.5 -4.13E-03   9.36E-03  3.30E+00   2.40E+00   1.60E+00  4.51E+00   1.19E+00   3.71E+01   1.66E+00   1.28E-01   3
   -152.0  -27.5 -3.97E-03   8.61E-03  2.80E+00   4.50E+00   1.50E+00  5.37E+00   1.93E+00   5.98E+01   1.72E+00   2.64E-01   3
   -152.0  -26.5 -3.62E-03   8.24E-03  2.70E+00   5.70E+00   5.00E-01  5.78E+00   2.62E+00   8.08E+01   1.58E+00   4.01E-01   3
   -152.0  -25.5 -3.23E-03   8.54E-03  2.70E+00   5.70E+00  -5.00E-01  5.78E+00   2.62E+00  -8.08E+01   1.58E+00   4.01E-01   3
   -152.0  -24.5 -2.87E-03   9.52E-03  2.80E+00   4.60E+00  -1.50E+00  5.45E+00   1.95E+00  -6.05E+01   1.75E+00   2.62E-01   3
   -152.0  -23.5 -2.70E-03   1.09E-02  3.20E+00   2.40E+00  -1.60E+00  4.45E+00   1.15E+00  -3.80E+01   1.65E+00   1.22E-01   3
   -152.0  -22.5 -2.70E-03   1.21E-02  3.30E+00   1.10E+00  -9.00E-01  3.62E+00   7.79E-01  -1.96E+01   1.42E+00   8.42E-02   3
   -152.0  -21.5 -2.74E-03   1.28E-02  3.20E+00   6.00E-01  -3.00E-01  3.23E+00   5.66E-01  -6.50E+00   1.33E+00   3.91E-02   3
   -152.0  -20.5 -2.78E-03   1.29E-02  3.20E+00   6.00E-01   3.00E-01  3.23E+00   5.66E-01   6.50E+00   1.33E+00   3.91E-02   3
   -152.0  -19.5 -2.82E-03   1.26E-02  3.40E+00   1.10E+00   1.00E+00  3.77E+00   7.26E-01   2.05E+01   1.52E+00   3.49E-02   3
   -152.0  -18.5 -2.84E-03   1.17E-02  3.30E+00   2.50E+00   1.70E+00  4.65E+00   1.15E+00   3.84E+01   1.75E+00   9.66E-02   3
   -152.0  -17.5 -2.67E-03   1.07E-02  2.80E+00   4.80E+00   1.60E+00  5.69E+00   1.91E+00   6.10E+01   1.89E+00   2.21E-01   3
   -152.0  -16.5 -2.30E-03   1.01E-02  2.70E+00   6.10E+00   6.00E-01  6.20E+00   2.60E+00   8.03E+01   1.80E+00   3.44E-01   3
   -152.0  -15.5 -1.89E-03   1.02E-02  2.70E+00   6.10E+00  -5.00E-01  6.17E+00   2.63E+00  -8.18E+01   1.77E+00   3.56E-01   3
   -152.0  -14.5 -1.52E-03   1.10E-02  2.80E+00   4.90E+00  -1.60E+00  5.76E+00   1.94E+00  -6.16E+01   1.91E+00   2.19E-01   3
   -152.0  -13.5 -1.35E-03   1.24E-02  3.30E+00   2.60E+00  -1.70E+00  4.69E+00   1.21E+00  -3.92E+01   1.74E+00   1.15E-01   3
   -152.0  -12.5 -1.37E-03   1.35E-02  3.40E+00   1.10E+00  -1.00E+00  3.77E+00   7.26E-01  -2.05E+01   1.52E+00   3.49E-02   3
   -152.0  -11.5 -1.43E-03   1.41E-02  3.30E+00   6.00E-01  -3.00E-01  3.33E+00   5.67E-01  -6.26E+00   1.38E+00   2.32E-02   3
   -152.0  -10.5 -1.48E-03   1.41E-02  3.30E+00   6.00E-01   3.00E-01  3.33E+00   5.67E-01   6.26E+00   1.38E+00   2.32E-02   3
   -152.0   -9.5 -1.54E-03   1.37E-02  3.40E+00   1.10E+00   1.00E+00  3.77E+00   7.26E-01   2.05E+01   1.52E+00   3.49E-02   3
   -152.0   -8.5 -1.57E-03   1.27E-02  3.40E+00   2.60E+00   1.80E+00  4.84E+00   1.16E+00   3.87E+01   1.84E+00   7.23E-02   3
   -152.0   -7.5 -1.40E-03   1.15E-02  2.90E+00   5.00E+00   1.60E+00  5.86E+00   2.04E+00   6.16E+01   1.91E+00   2.36E-01   3
   -152.0   -6.5 -1.03E-03   1.08E-02  2.70E+00   6.20E+00   6.00E-01  6.30E+00   2.60E+00   8.05E+01   1.85E+00   3.34E-01   3
   -152.0   -5.5 -6.21E-04   1.08E-02  2.70E+00   6.20E+00  -6.00E-01  6.30E+00   2.60E+00  -8.05E+01   1.85E+00   3.34E-01   3
   -152.0   -4.5 -2.55E-04   1.16E-02  2.90E+00   5.00E+00  -1.60E+00  5.86E+00   2.04E+00  -6.16E+01   1.91E+00   2.36E-01   3
   -152.0   -3.5 -8.90E-05   1.29E-02  3.40E+00   2.60E+00  -1.80E+00  4.84E+00   1.16E+00  -3.87E+01   1.84E+00   7.23E-02   3
   -152.0   -2.5 -1.19E-04   1.40E-02  3.40E+00   1.10E+00  -1.00E+00  3.77E+00   7.26E-01  -2.05E+01   1.52E+00   3.49E-02   3
   -152.0   -1.5 -1.83E-04   1.45E-02  3.30E+00   6.00E-01  -3.00E-01  3.33E+00   5.67E-01  -6.26E+00   1.38E+00   2.32E-02   3
   -152.0   -0.5 -2.40E-04   1.45E-02  3.30E+00   6.00E-01   3.00E-01  3.33E+00   5.67E-01   6.26E+00   1.38E+00   2.32E-02   3
   -152.0    0.5 -3.05E-04   1.40E-02  3.40E+00   1.10E+00   1.00E+00  3.77E+00   7.26E-01   2.05E+01   1.52E+00   3.49E-02   3
   -152.0    1.5 -3.36E-04   1.29E-02  3.40E+00   2.60E+00   1.80E+00  4.84E+00   1.16E+00   3.87E+01   1.84E+00   7.23E-02   3
   -152.0    2.5 -1.70E-04   1.17E-02  2.90E+00   5.00E+00   1.60E+00  5.86E+00   2.04E+00   6.16E+01   1.91E+00   2.36E-01   3
   -152.0    3.5  1.96E-04   1.09E-02  2.70E+00   6.30E+00   6.00E-01  6.40E+00   2.60E+00   8.08E+01   1.90E+00   3.23E-01   3
   -152.0    4.5  6.07E-04   1.09E-02  2.70E+00   6.30E+00  -6.00E-01  6.40E+00   2.60E+00  -8.08E+01   1.90E+00   3.23E-01   3
```

Sample of PSTRESS output

APPENDIX 4

DDSEAMS PROGRAM TESTING RESULTS

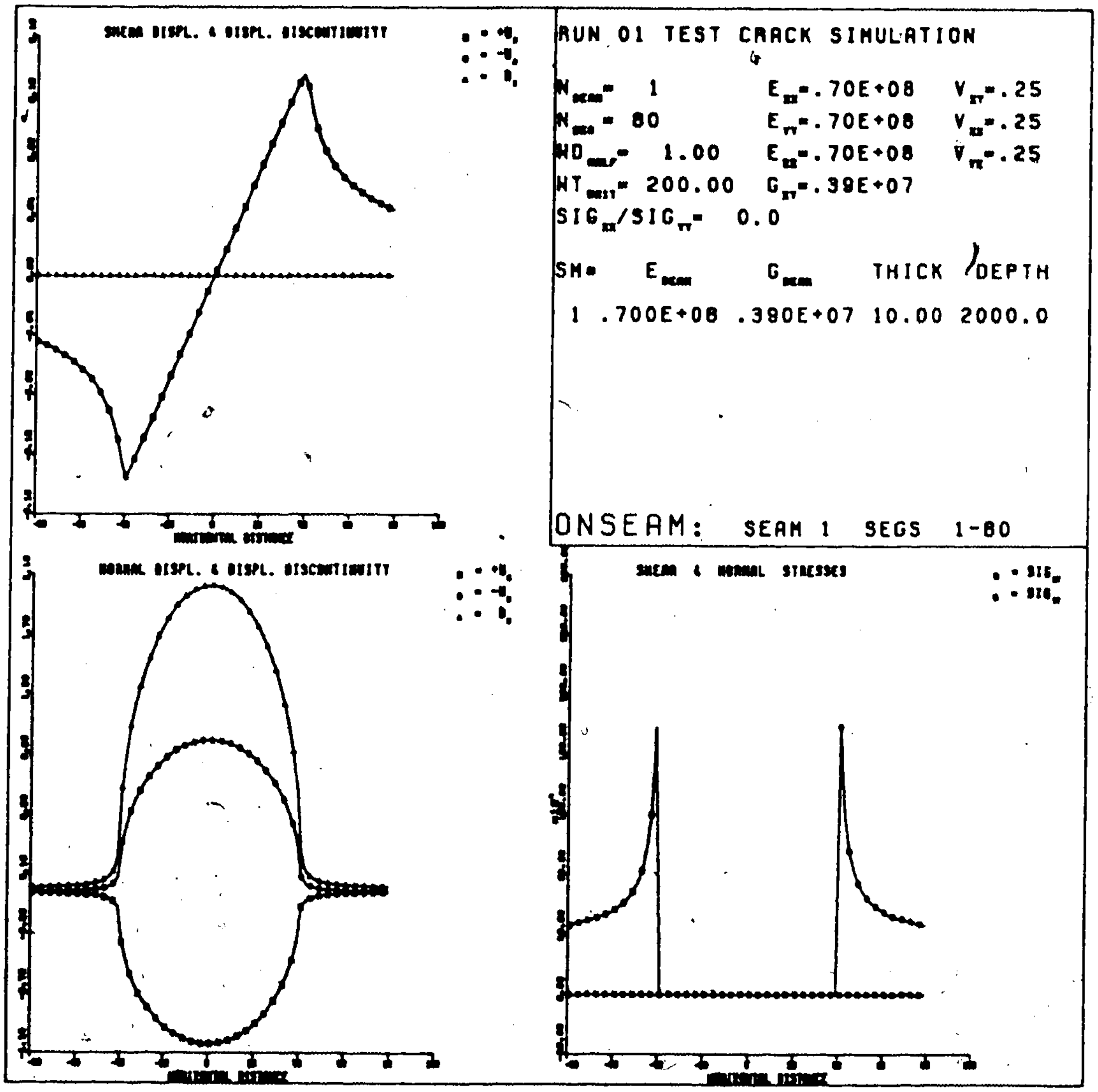

RUN 01 TEST CRACK SIMULATION

N_{SEAM}= 1 E_{XX}=.70E+08 V_{XY}=.25

N_{SEG}= 80 E_{YY}=.70E+08 V_{XZ}=.25

WD_{HALF}= 1.00 E_{ZZ}=.70E+08 V_{YZ}=.25

WT_{UNIT}= 200.00 G_{XY}=.39E+07

SIG_{XX}/SIG_{YY}= 0.0

SM#	E_{SEAM}	G_{SEAM}	THICK	DEPTH
1	.700E+08	.390E+07	10.00	2000.0

ONSEAM: SEAM 1 SEGS 1-80

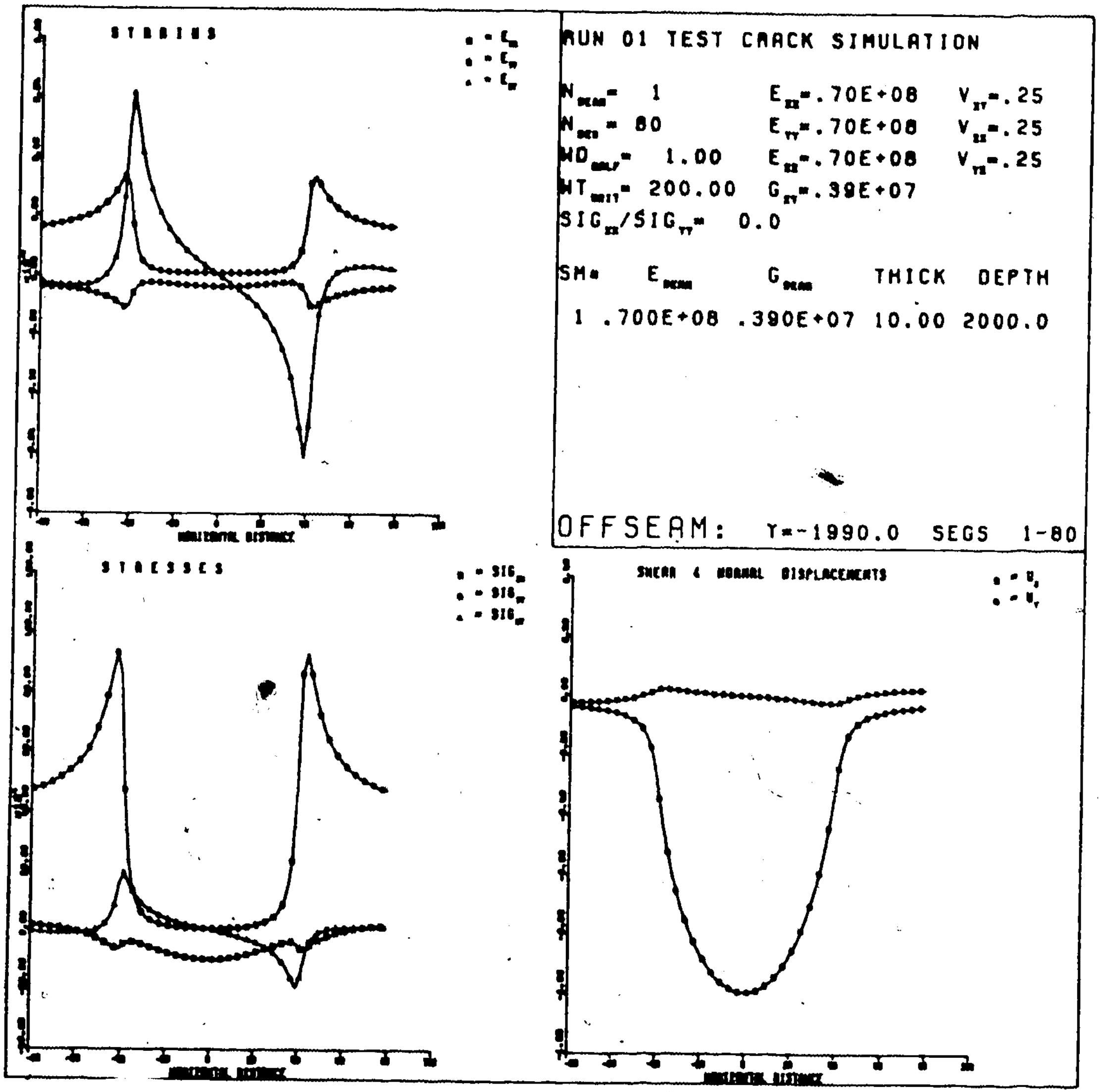

RUN 01 TEST CRACK SIMULATION

N_{SEAM}= 1 E_{XX}=.70E+08 V_{XY}=.25
N_{SEG}= 80 E_{YY}=.70E+08 V_{ZX}=.25
WD_{HALF}= 1.00 E_{ZZ}=.70E+08 V_{YZ}=.25
WT_{UNIT}= 200.00 G_{XY}=.39E+07
SIG_{XX}/SIG_{YY}= 0.0

SM=	E_{SEAM}	G_{SEAM}	THICK	DEPTH
1	.700E+08	.390E+07	10.00	2000.0

OFFSEAM: Y=-1990.0 SEGS 1-80

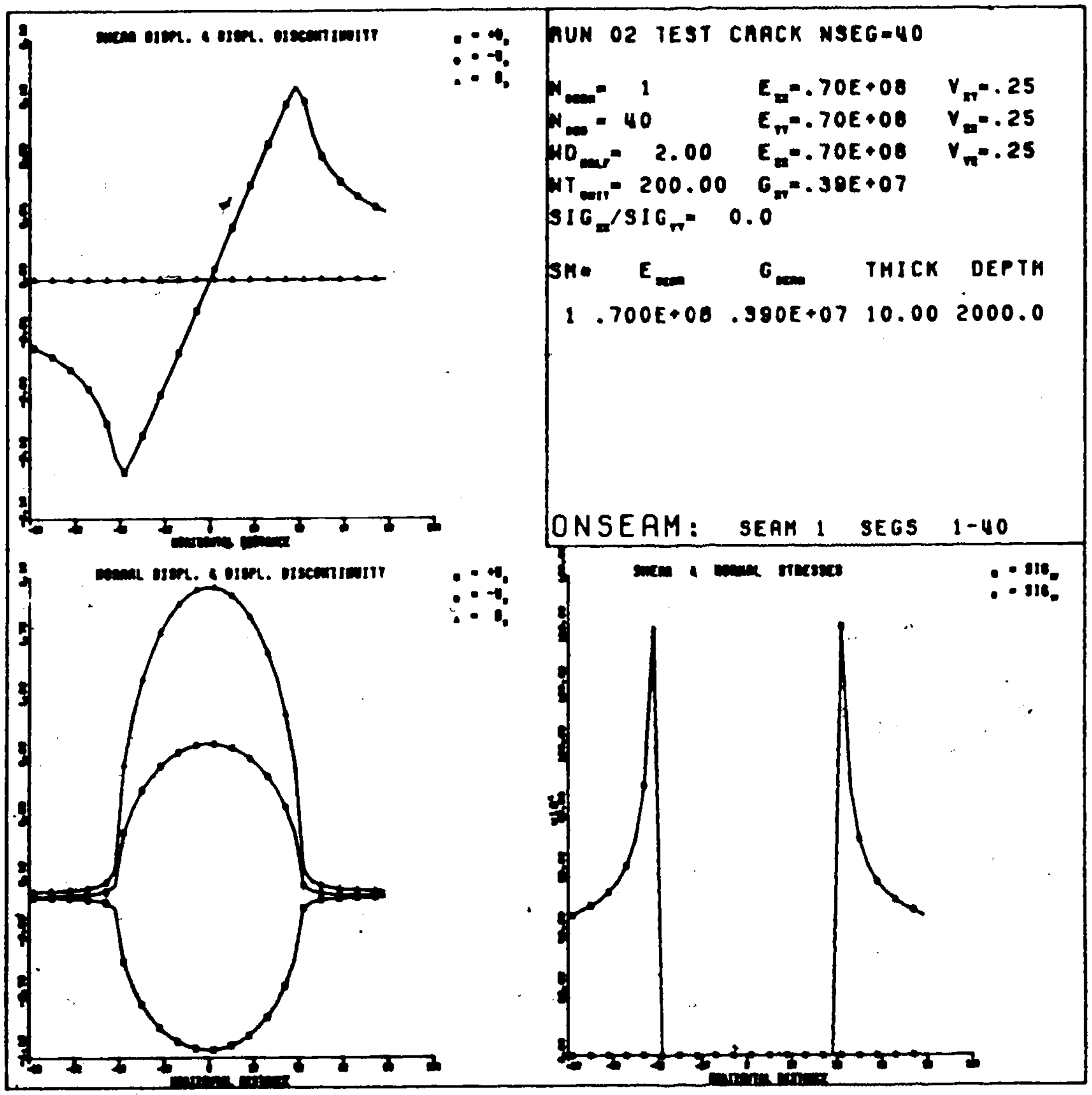

```
RUN 02 TEST CRACK NSEG=40

N_SEAM=  1          E_XX=.70E+08   V_XY=.25
N_SEG = 40          E_YY=.70E+08   V_XZ=.25
WD_HALF=  2.00      E_ZZ=.70E+08   V_YZ=.25
WT_UNIT= 200.00     G_XY=.39E+07
SIG_XX/SIG_YY=  0.0

SM#   E_SEAM     G_SEAM     THICK  DEPTH
 1 .700E+08 .390E+07 10.00 2000.0

ONSEAM:  SEAM 1  SEGS  1-40
```

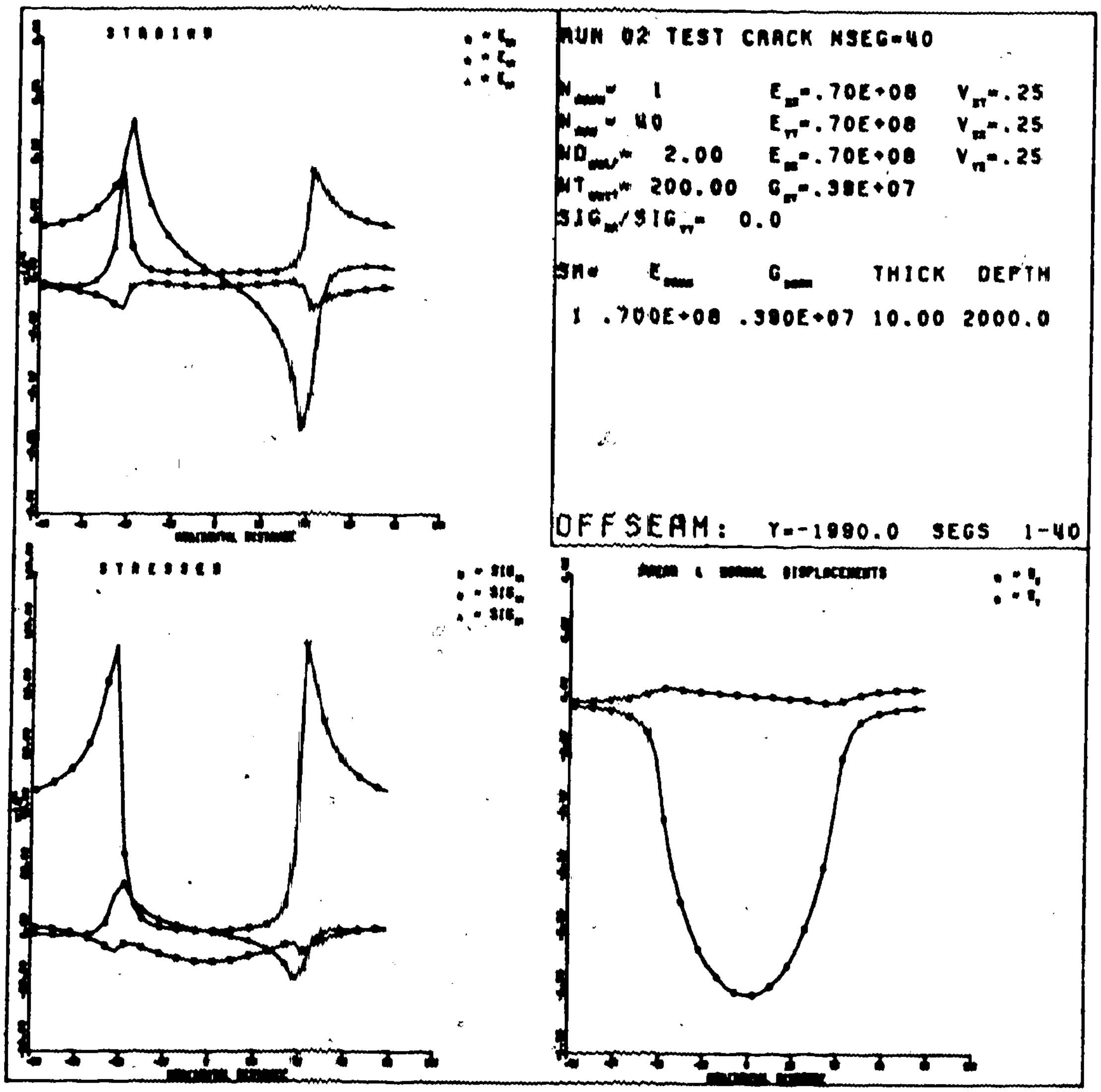

```
RUN 02 TEST CRACK NSEG=40

N  = 1          E  =.70E+08   V  =.25
N  = 40         E  =.70E+08   V  =.25
WD  = 2.00      E  =.70E+08   V  =.25
WT  = 200.00    G  =.38E+07
SIG  /SIG  =  0.0

SM#    E          G          THICK  DEPTH

 1 .700E+08 .380E+07 10.00 2000.0




OFFSEAM:  Y=-1990.0  SEGS  1-40
```

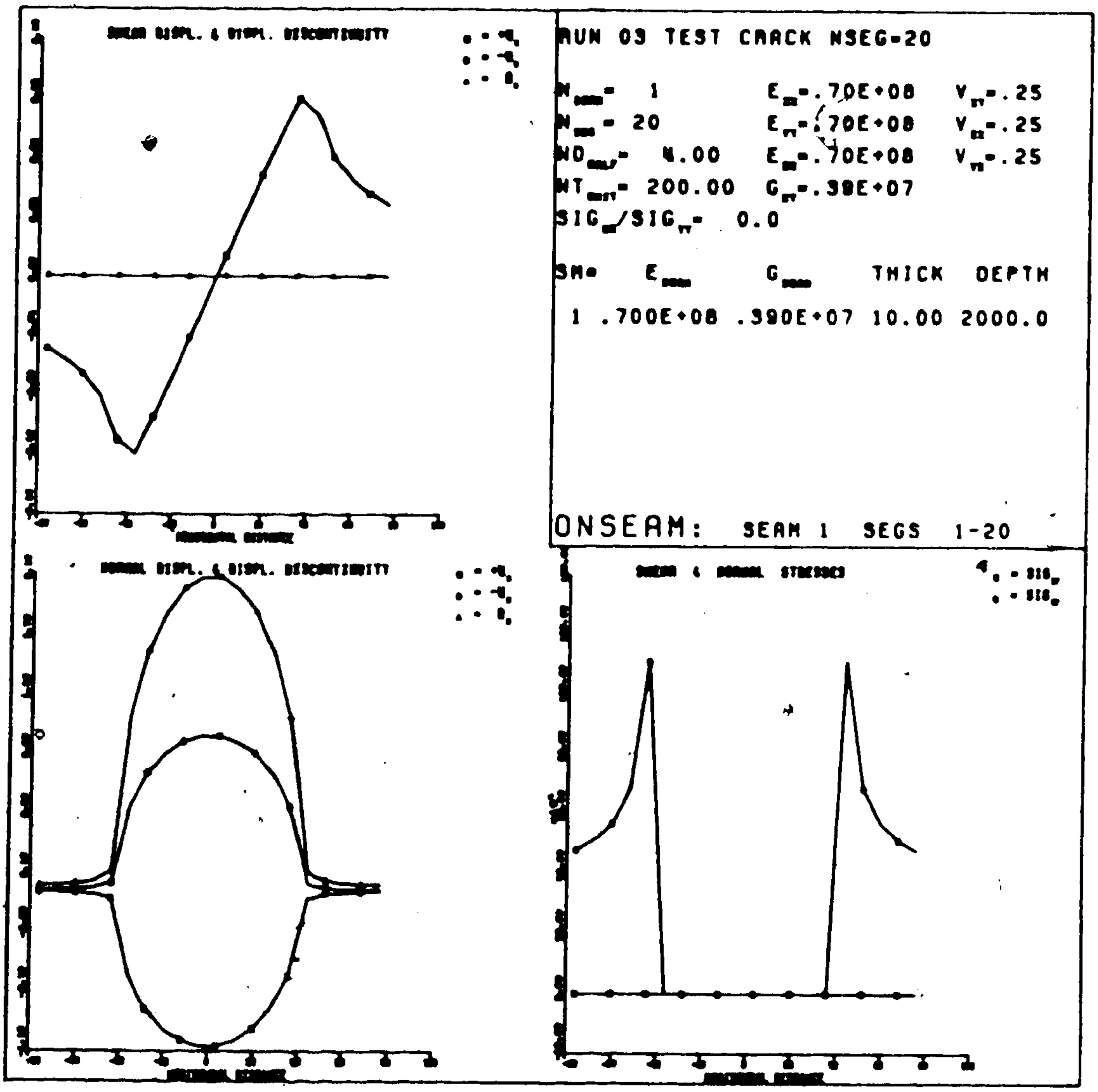

```
RUN 03 TEST CRACK NSEG=20

N[illegible]=  1         E[illegible]=.70E+08   V[illegible]=.25
N[illegible]= 20         E[illegible]=.70E+08   V[illegible]=.25
ND[illegible]=  4.00     E[illegible]=.70E+08   V[illegible]=.25
NT[illegible]= 200.00    G[illegible]=.39E+07
SIG[illegible]/SIG[illegible]=  0.0

SM=    E[illegible]       G[illegible]       THICK   DEPTH

 1  .700E+08  .390E+07  10.00  2000.0




ONSEAM:   SEAM 1   SEGS  1-20
```

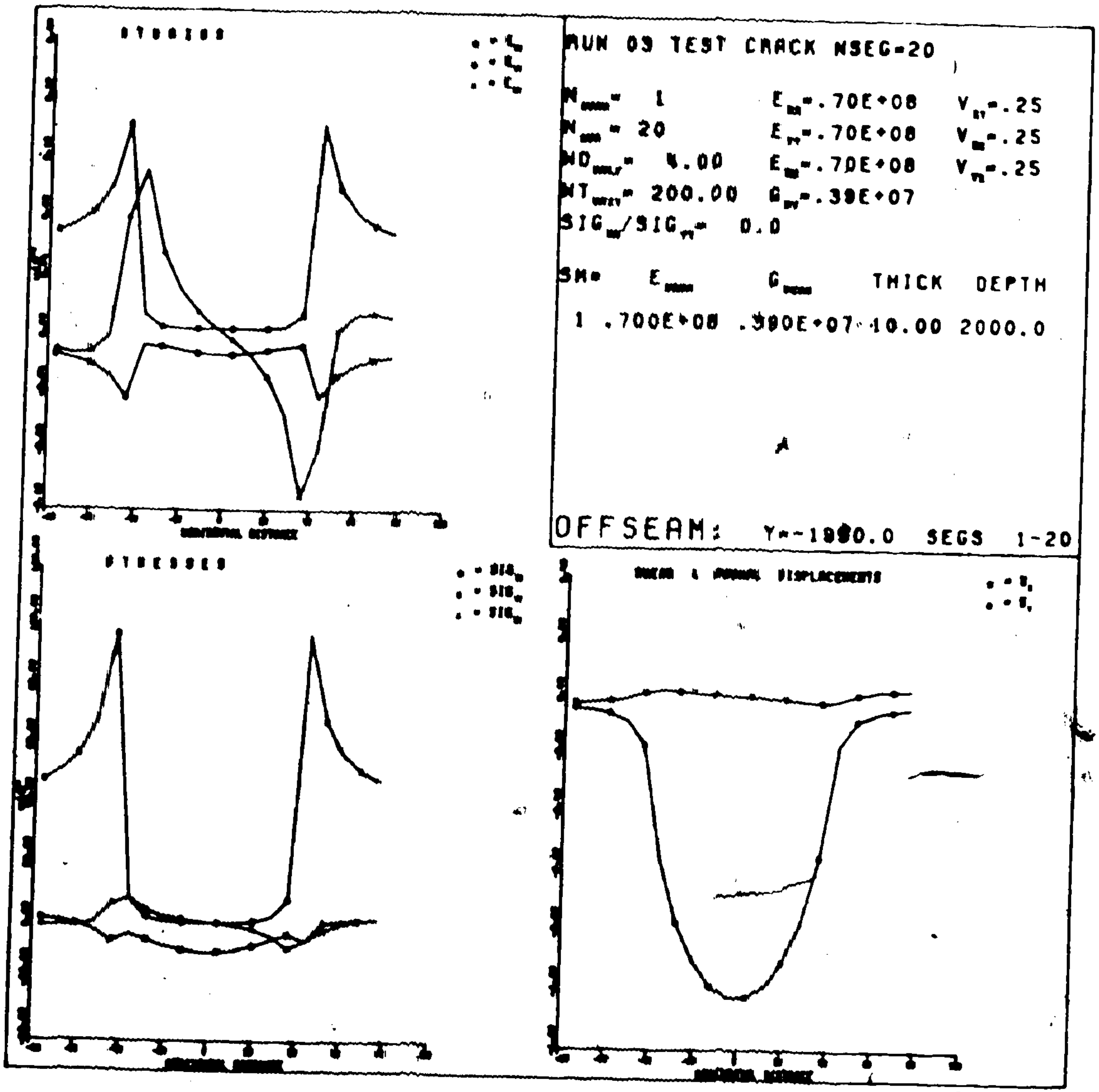

```
RUN 03 TEST CRACK NSEG=20

N    =  1          E  =.70E+08   V  =.25
N   = 20           E  =.70E+08   V  =.25
WD    =  4.00      E  =.70E+08   V  =.25
WT    = 200.00     G  =.39E+07
SIG  /SIG  =  0.0

SM=    E           G          THICK  DEPTH

 1 .700E+08 .390E+07 10.00 2000.0



OFFSEAM:  Y=-1990.0  SEGS  1-20
```

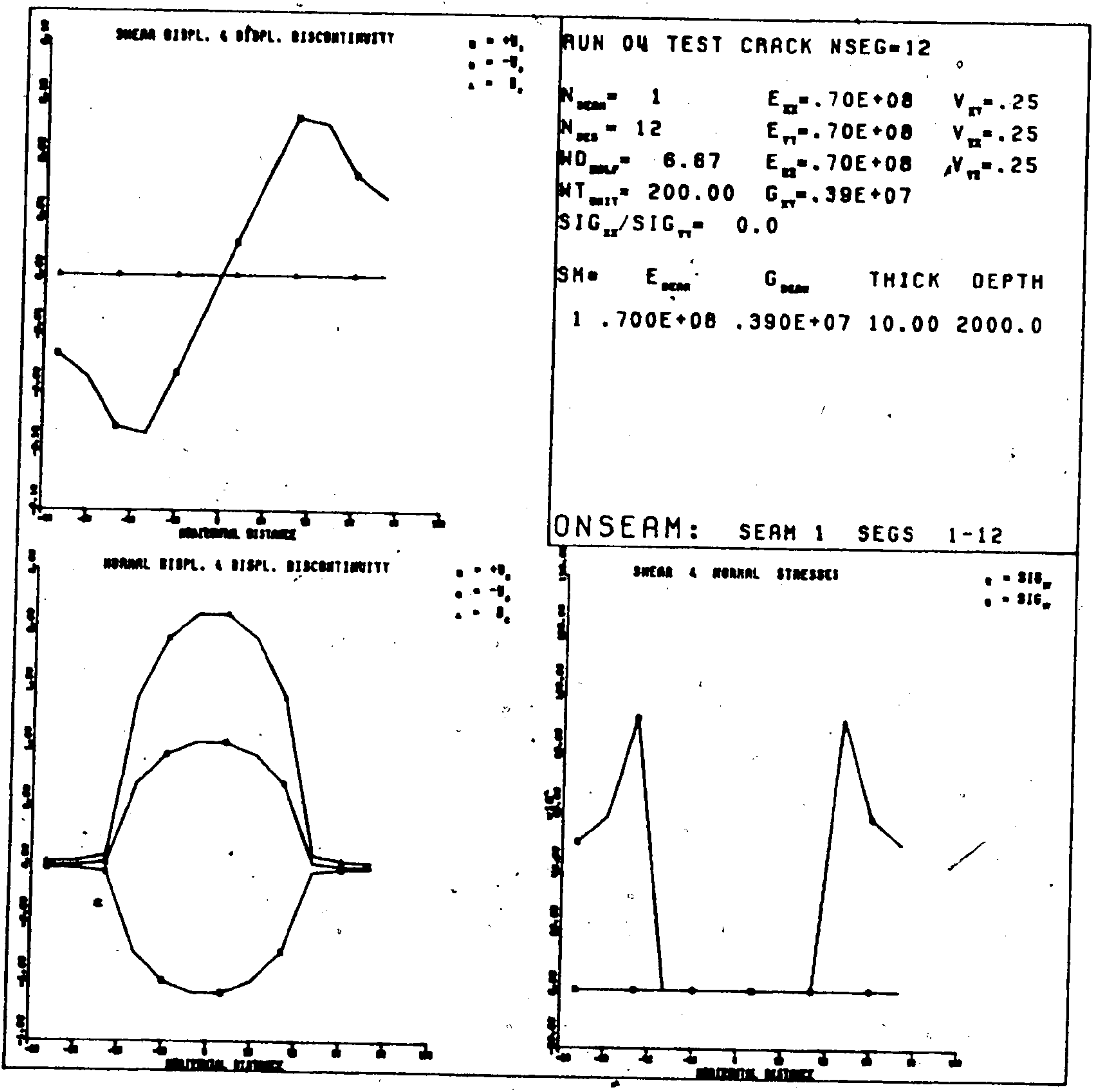

RUN 04 TEST CRACK NSEG=12

N_{SEAM}= 1 E_{XX}=.70E+08 V_{XY}=.25
N_{SEG}= 12 E_{YY}=.70E+08 V_{ZX}=.25
WD_{HALF}= 6.87 E_{ZZ}=.70E+08 V_{YZ}=.25
WT_{UNIT}= 200.00 G_{XY}=.39E+07
SIG_{XX}/SIG_{YY}= 0.0

SM=	E_{SEAM}	G_{SEAM}	THICK	DEPTH
1	.700E+08	.390E+07	10.00	2000.0

ONSEAM: SEAM 1 SEGS 1-12

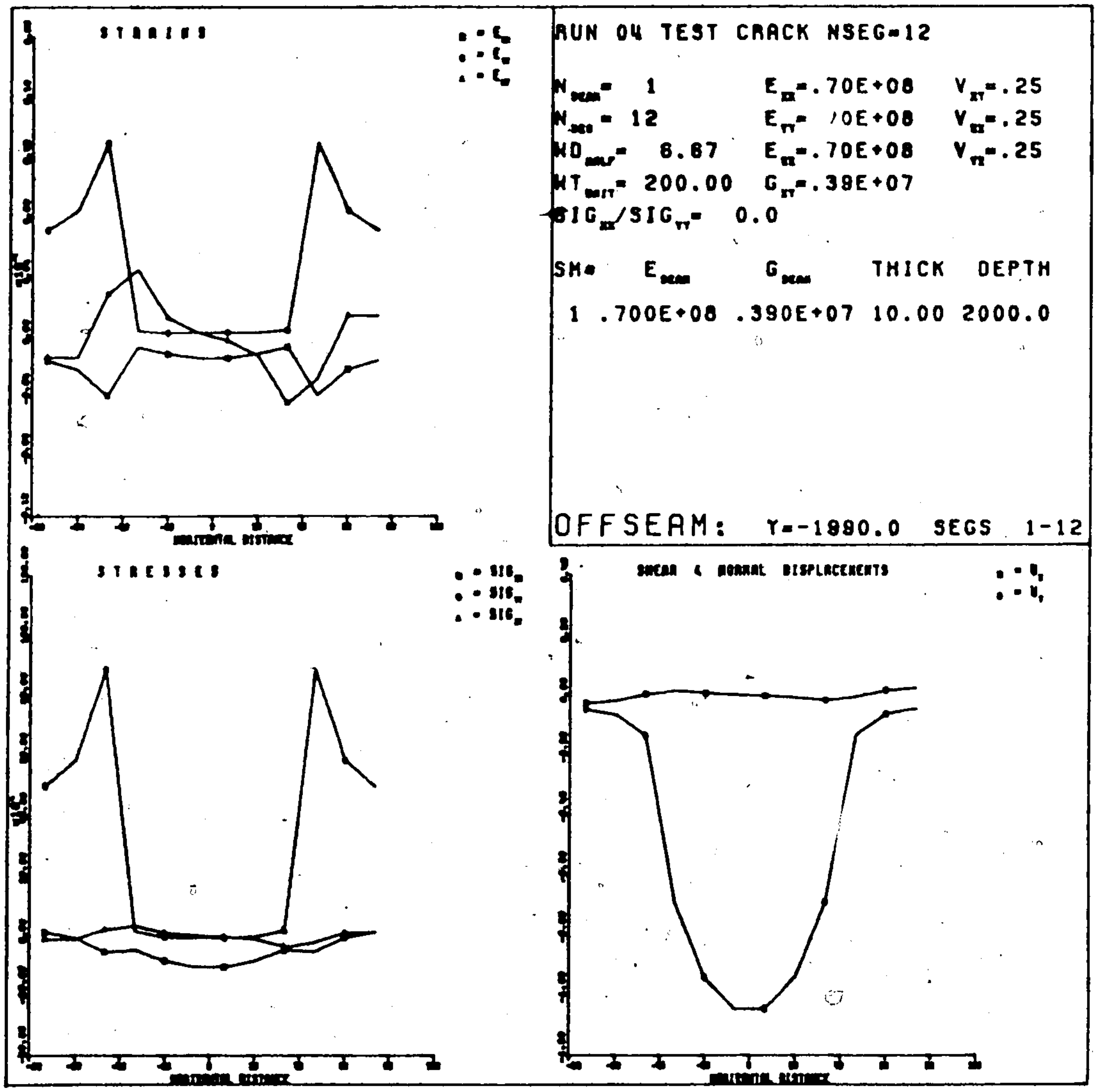

```
RUN 04 TEST CRACK NSEG=12

N_SEAM=   1        E_XX=.70E+08   V_XY=.25
N_SEG = 12         E_YY= /0E+08   V_XZ=.25
WD_HALF=  6.67     E_ZZ=.70E+08   V_YZ=.25
WT_UNIT= 200.00    G_XY=.39E+07
SIG_XX/SIG_YY=  0.0

SM#    E_SEAM      G_SEAM     THICK  DEPTH

 1 .700E+08 .390E+07 10.00 2000.0

OFFSEAM:  Y=-1990.0  SEGS  1-12
```

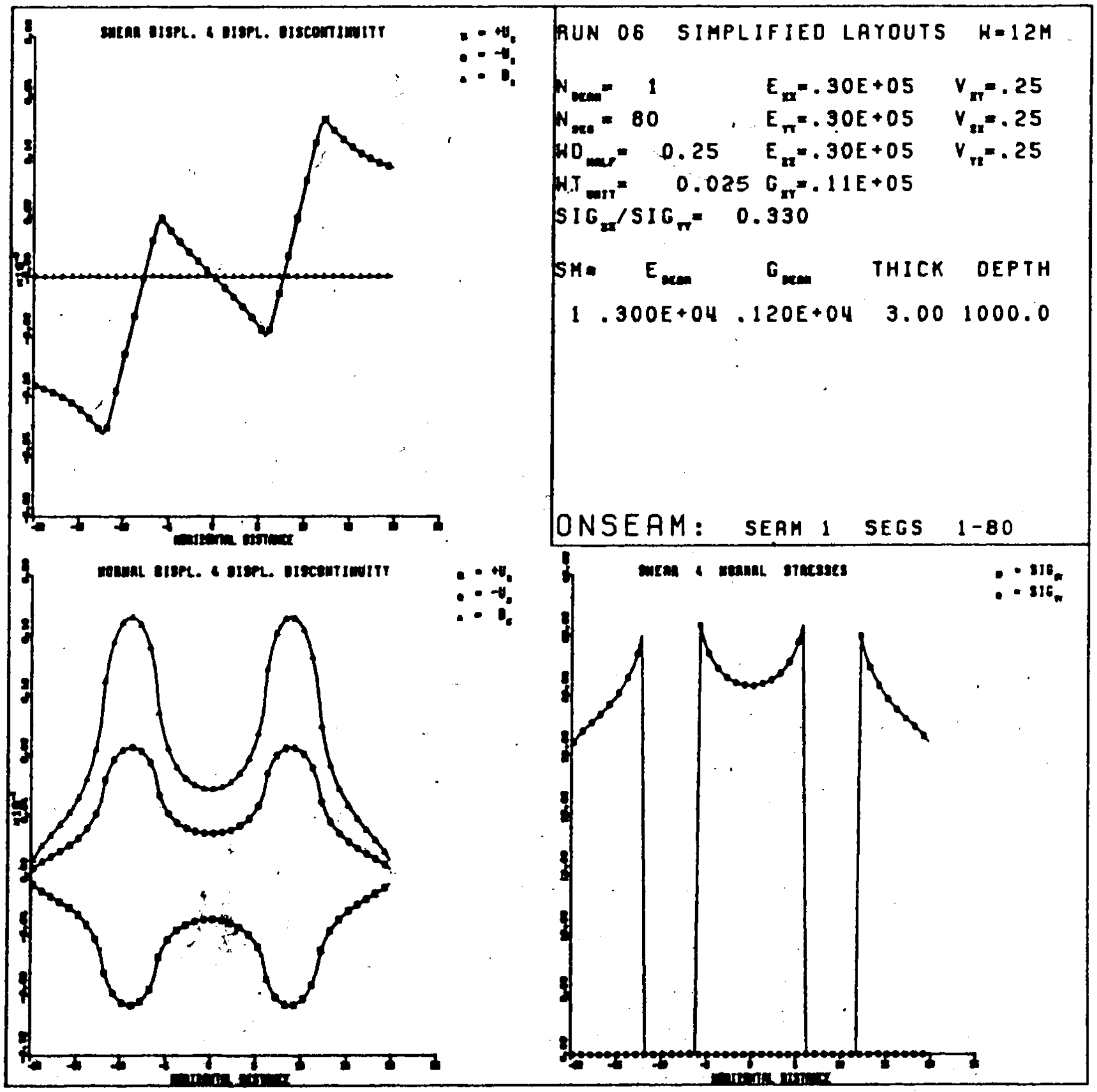

RUN 06 SIMPLIFIED LAYOUTS H=12M

N_{BEAM}= 1 E_{XX}=.30E+05 V_{XY}=.25
N_{SEG}= 80 E_{YY}=.30E+05 V_{ZX}=.25
WD_{HALF}= 0.25 E_{ZZ}=.30E+05 V_{YZ}=.25
WT_{UNIT}= 0.025 G_{XY}=.11E+05
SIG_{XX}/SIG_{YY}= 0.330

SM=	E_{BEAM}	G_{BEAM}	THICK	DEPTH
1	.300E+04	.120E+04	3.00	1000.0

ONSEAM: SEAM 1 SEGS 1-80

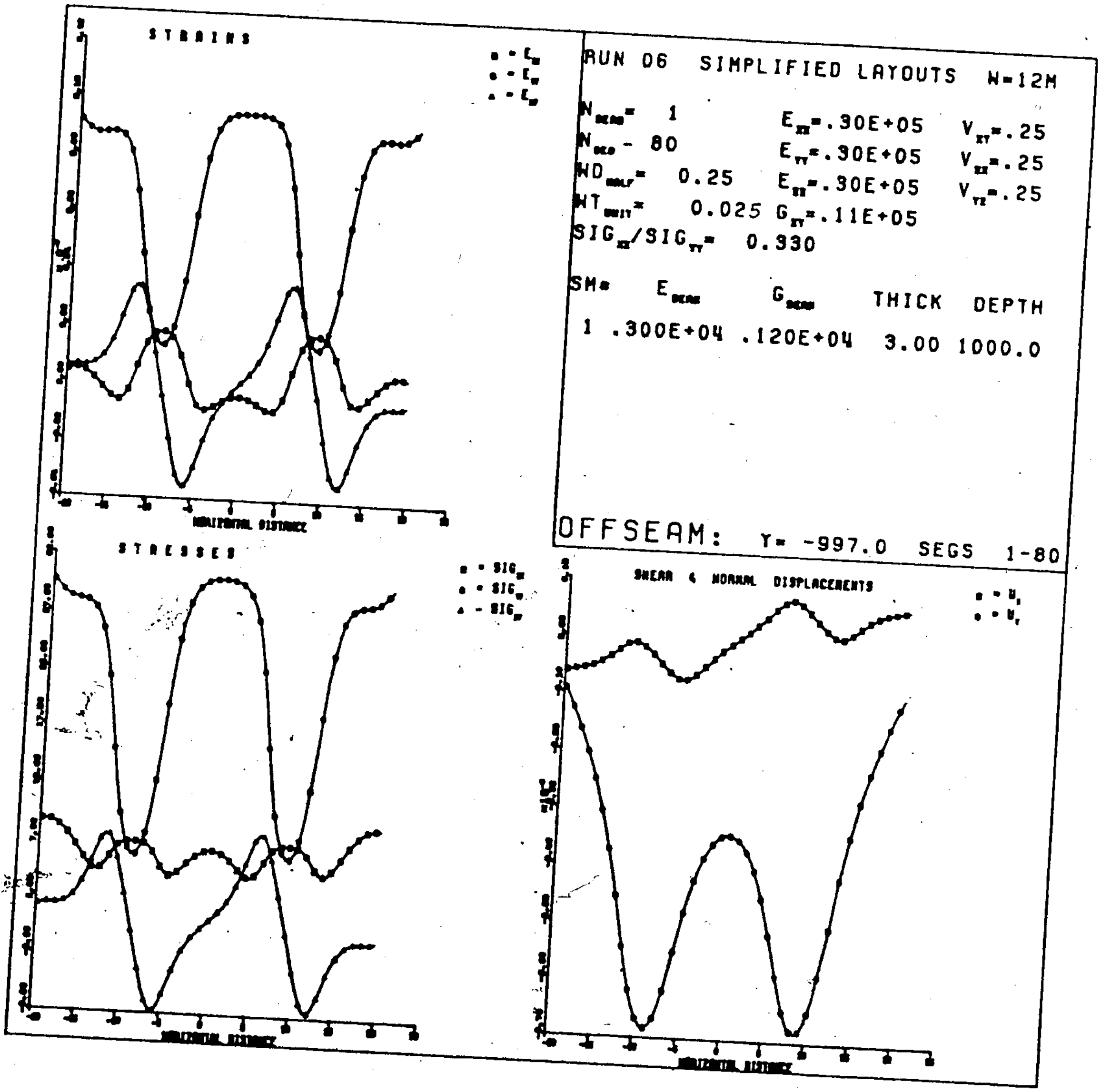

RUN 06 SIMPLIFIED LAYOUTS W=12M

N_{SEAM}= 1 E_{XX}=.30E+05 V_{XY}=.25
N_{SEG}- 80 E_{YY}=.30E+05 V_{ZX}=.25
WD_{HALF}= 0.25 E_{ZZ}=.30E+05 V_{YZ}=.25
WT_{UNIT}= 0.025 G_{XY}=.11E+05
SIG_{XX}/SIG_{YY}= 0.330

SM#	E_{SEAM}	G_{SEAM}	THICK	DEPTH
1	.300E+04	.120E+04	3.00	1000.0

OFFSEAM: Y= -997.0 SEGS 1-80

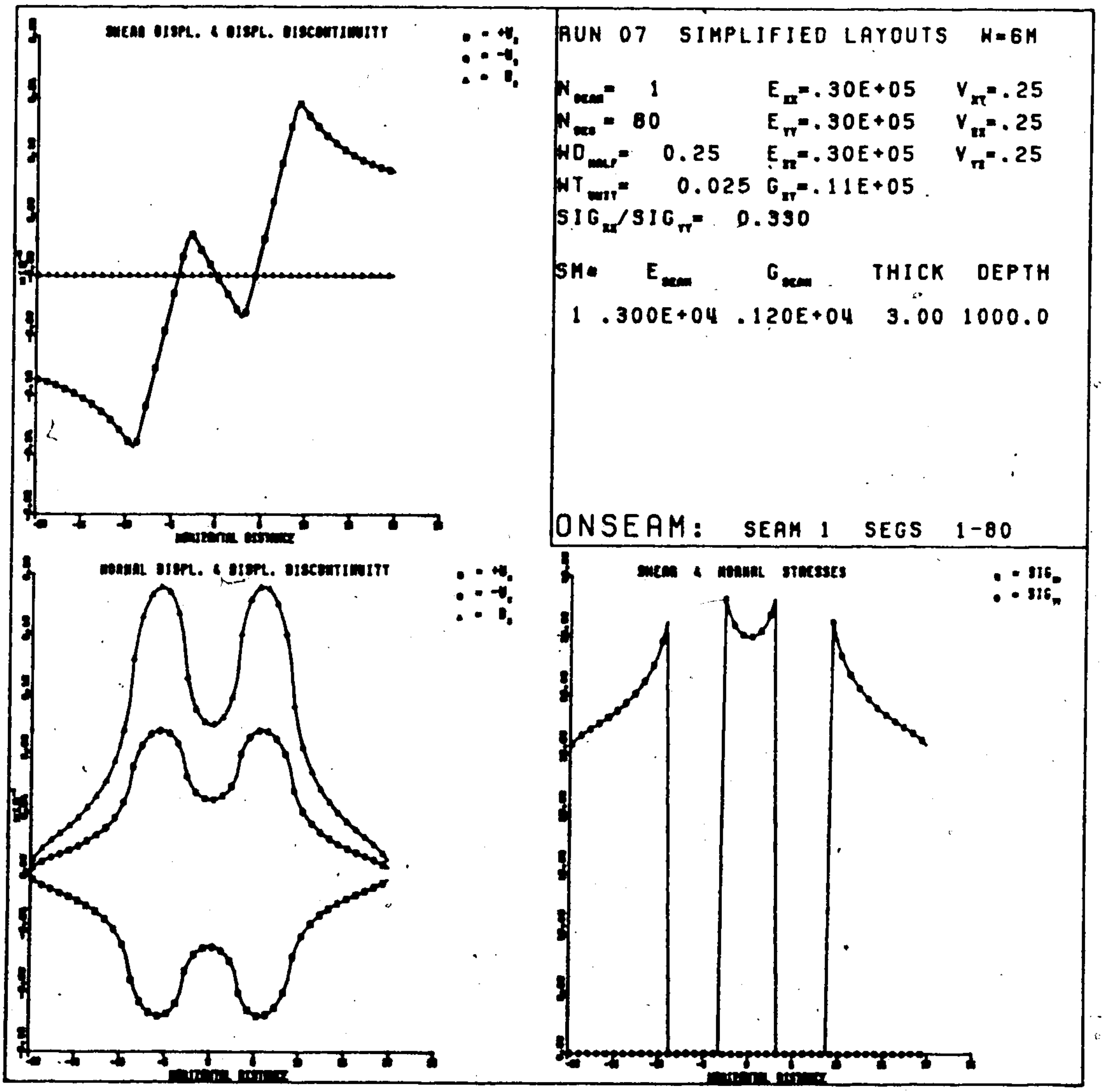

RUN 07 SIMPLIFIED LAYOUTS H=6M

N_{SEAM}= 1 E_{XX}=.30E+05 V_{XY}=.25

N_{SEGS}= 80 E_{YY}=.30E+05 V_{ZX}=.25

WD_{HALF}= 0.25 E_{ZZ}=.30E+05 V_{YZ}=.25

WT_{UNIT}= 0.025 G_{XY}=.11E+05

SIG_{XX}/SIG_{YY}= 0.330

SM#	E_{SEAM}	G_{SEAM}	THICK	DEPTH
1	.300E+04	.120E+04	3.00	1000.0

ONSEAM: SEAM 1 SEGS 1-80

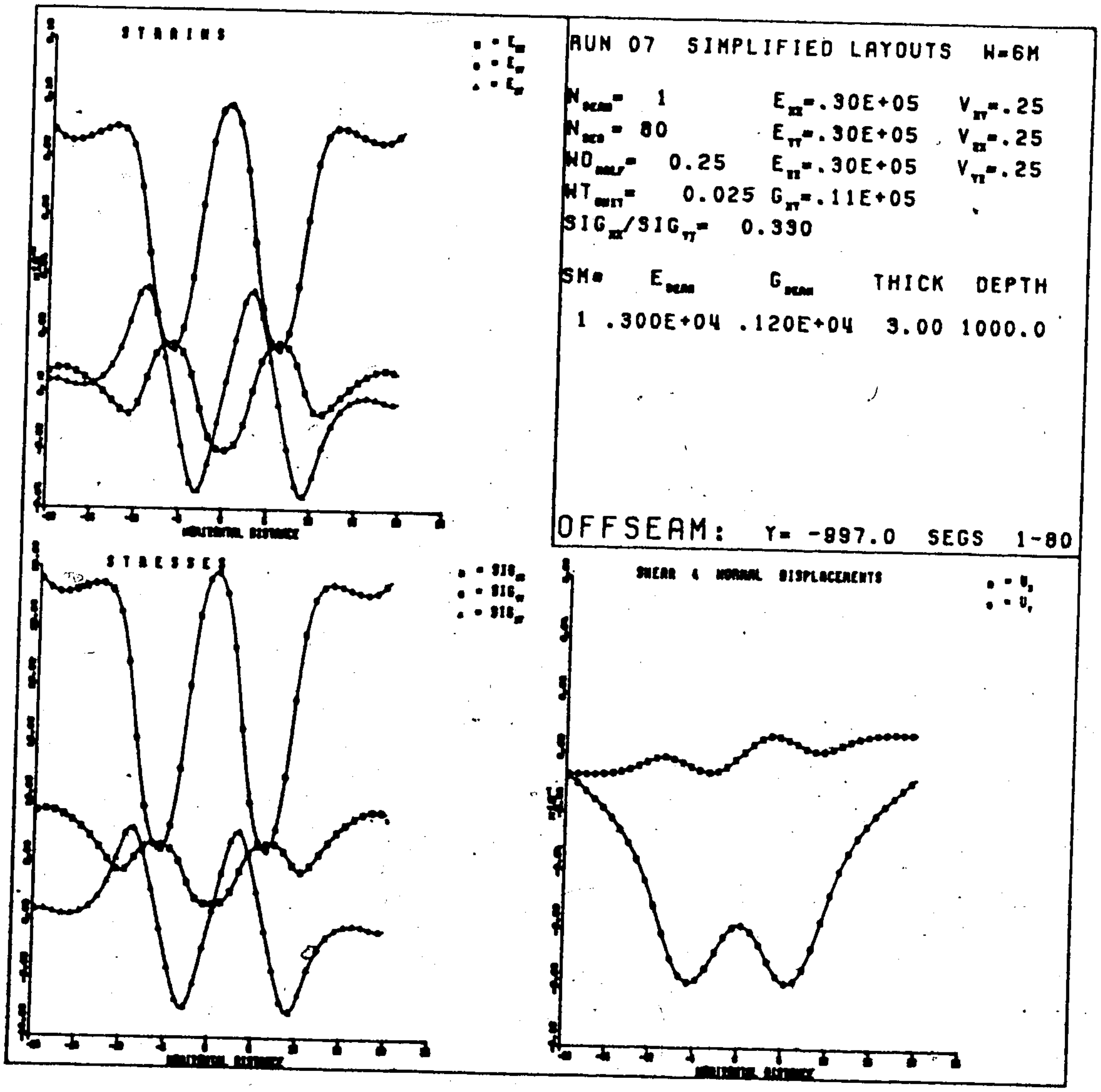

RUN 07 SIMPLIFIED LAYOUTS W=6M

N_{SEAM}= 1 E_{XX}=.30E+05 V_{XY}=.25
N_{SEG}= 80 E_{YY}=.30E+05 V_{ZX}=.25
WD_{HALF}= 0.25 E_{ZZ}=.30E+05 V_{YZ}=.25
WT_{UNIT}= 0.025 G_{XY}=.11E+05
SIG_{XX}/SIG_{YY}= 0.330

SM#	E_{SEAM}	G_{SEAM}	THICK	DEPTH
1	.300E+04	.120E+04	3.00	1000.0

OFFSEAM: Y= -997.0 SEGS 1-80

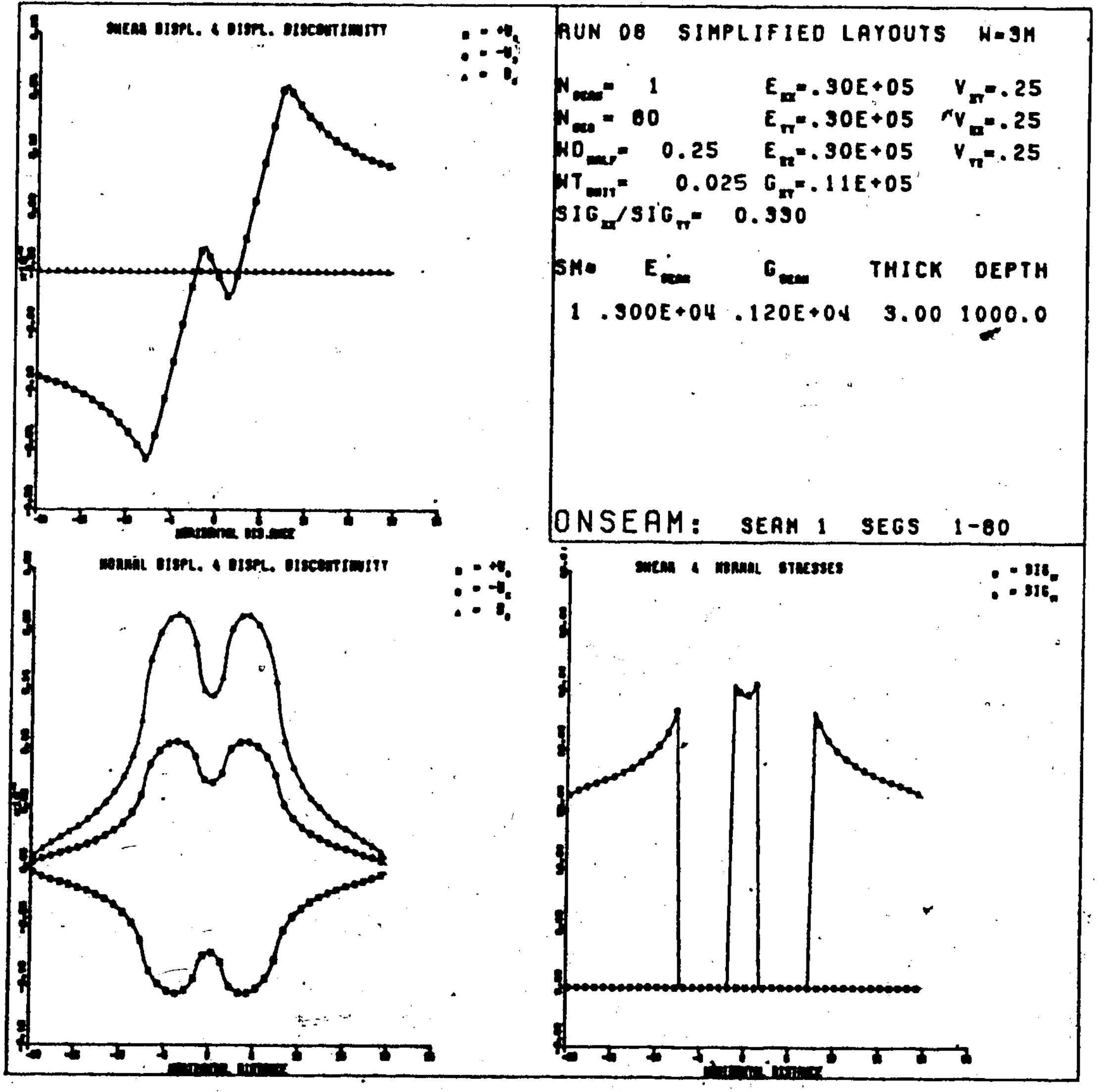

RUN 08 SIMPLIFIED LAYOUTS W=3M

N_{SEAM}= 1 E_{XX}=.30E+05 V_{XY}=.25
N_{SEG} = 80 E_{YY}=.30E+05 V_{XZ}=.25
WD_{HALF}= 0.25 E_{ZZ}=.30E+05 V_{YZ}=.25
WT_{UNIT}= 0.025 G_{XY}=.11E+05
SIG_{XX}/SIG_{YY}= 0.330

SM=	E_{SEAM}	G_{SEAM}	THICK	DEPTH
1	.300E+04	.120E+04	3.00	1000.0

ONSEAM: SEAM 1 SEGS 1-80

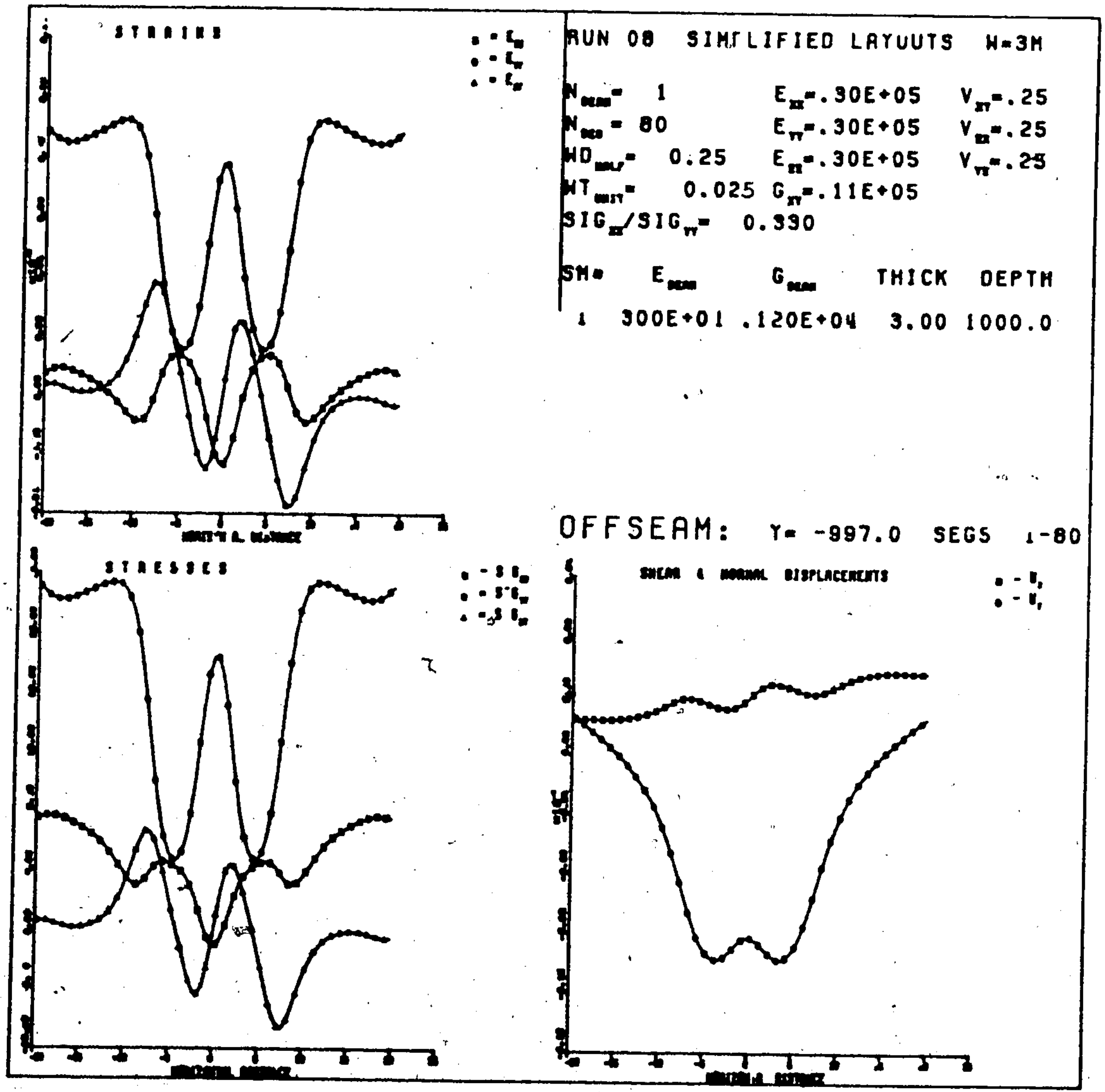

RUN 08 SIMFLIFIED LAYUUTS W=3M

N_{SEAM}= 1 E_{XX}=.30E+05 V_{XY}=.25
N_{SEG}= 80 E_{YY}=.30E+05 V_{ZX}=.25
WD_{HALF}= 0.25 E_{ZZ}=.30E+05 V_{YZ}=.25
WT_{UNIT}= 0.025 G_{XY}=.11E+05
SIG_{XX}/SIG_{YY}= 0.330

SM#	E_{SEAM}	G_{SEAM}	THICK	DEPTH
1	300E+01	.120E+04	3.00	1000.0

OFFSEAM: Y= -997.0 SEGS 1-80

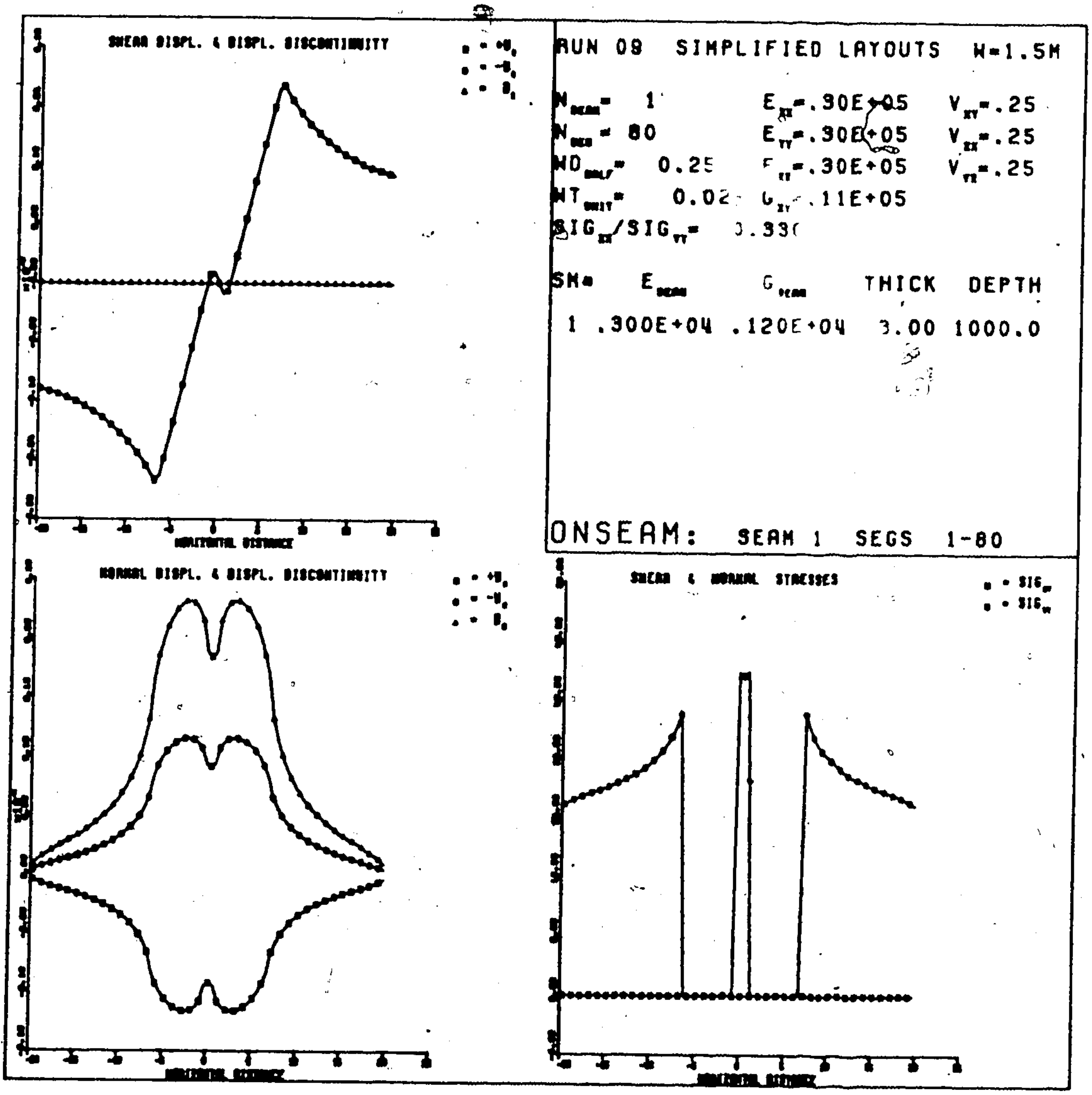

```
RUN 08   SIMPLIFIED LAYOUTS   W=1.5M

N_SEAM=  1          E_XX=.30E+05   V_XY=.25
N_SEG = 80          E_YY=.30E+05   V_XZ=.25
WD_HALF=  0.25      E_ZZ=.30E+05   V_YZ=.25
WT_UNIT=   0.02     G_XY=.11E+05
SIG_XX/SIG_YY=  0.330

SM#    E_SEAM     G_SEAM     THICK  DEPTH
 1 .300E+04 .120E+04   3.00 1000.0

ONSEAM:  SEAM 1  SEGS  1-80
```

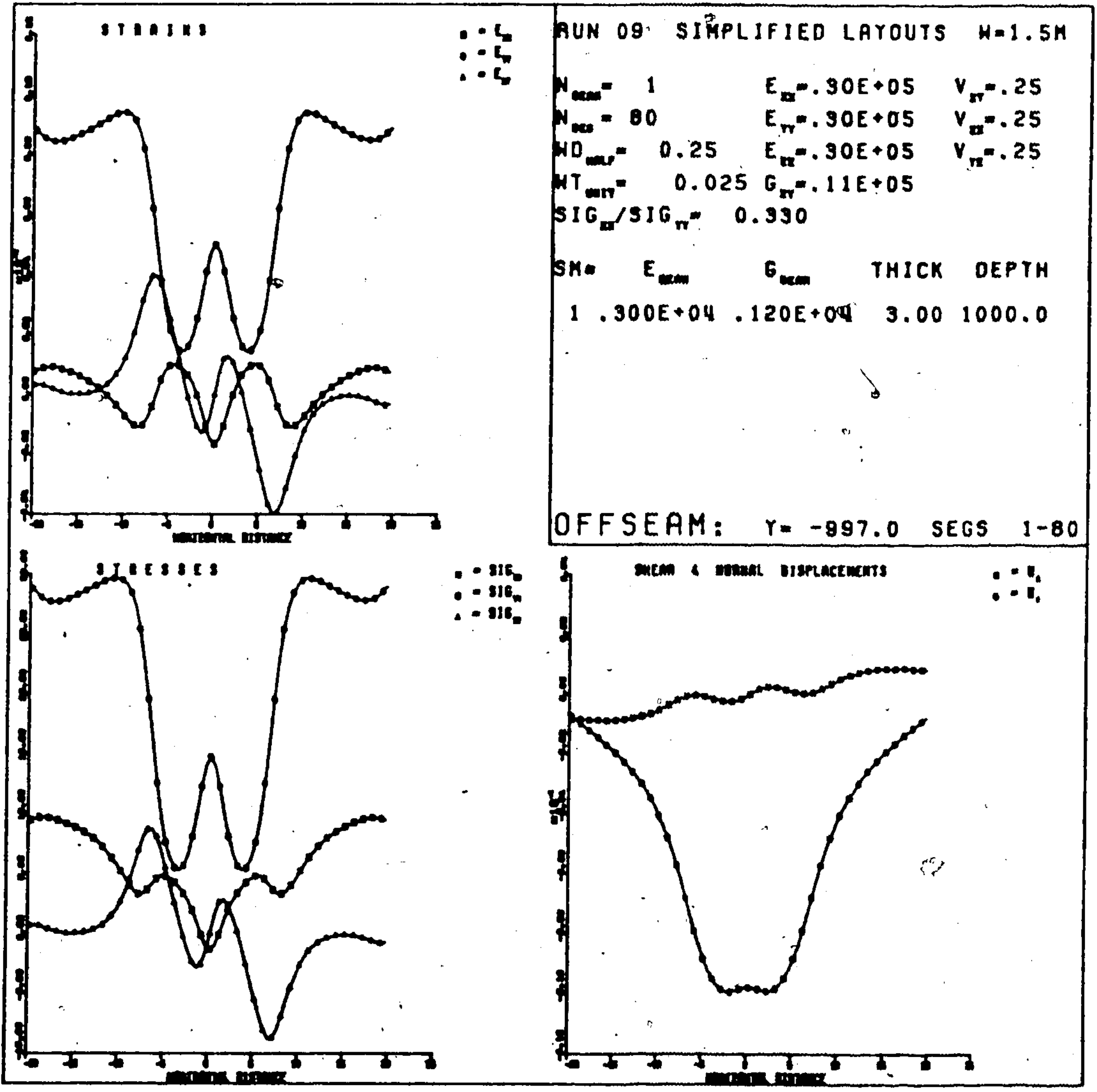

RUN 09 SIMPLIFIED LAYOUTS W=1.5M

N_{SEAM}= 1 E_{XX}=.30E+05 V_{XY}=.25
N_{SEG}= 80 E_{YY}=.30E+05 V_{XZ}=.25
WD_{HALF}= 0.25 E_{ZZ}=.30E+05 V_{YZ}=.25
WT_{UNIT}= 0.025 G_{XY}=.11E+05
SIG_{XX}/SIG_{YY}= 0.330

SM=	E_{SEAM}	G_{SEAM}	THICK	DEPTH
1	.300E+04	.120E+04	3.00	1000.0

OFFSEAM: Y= -997.0 SEGS 1-80

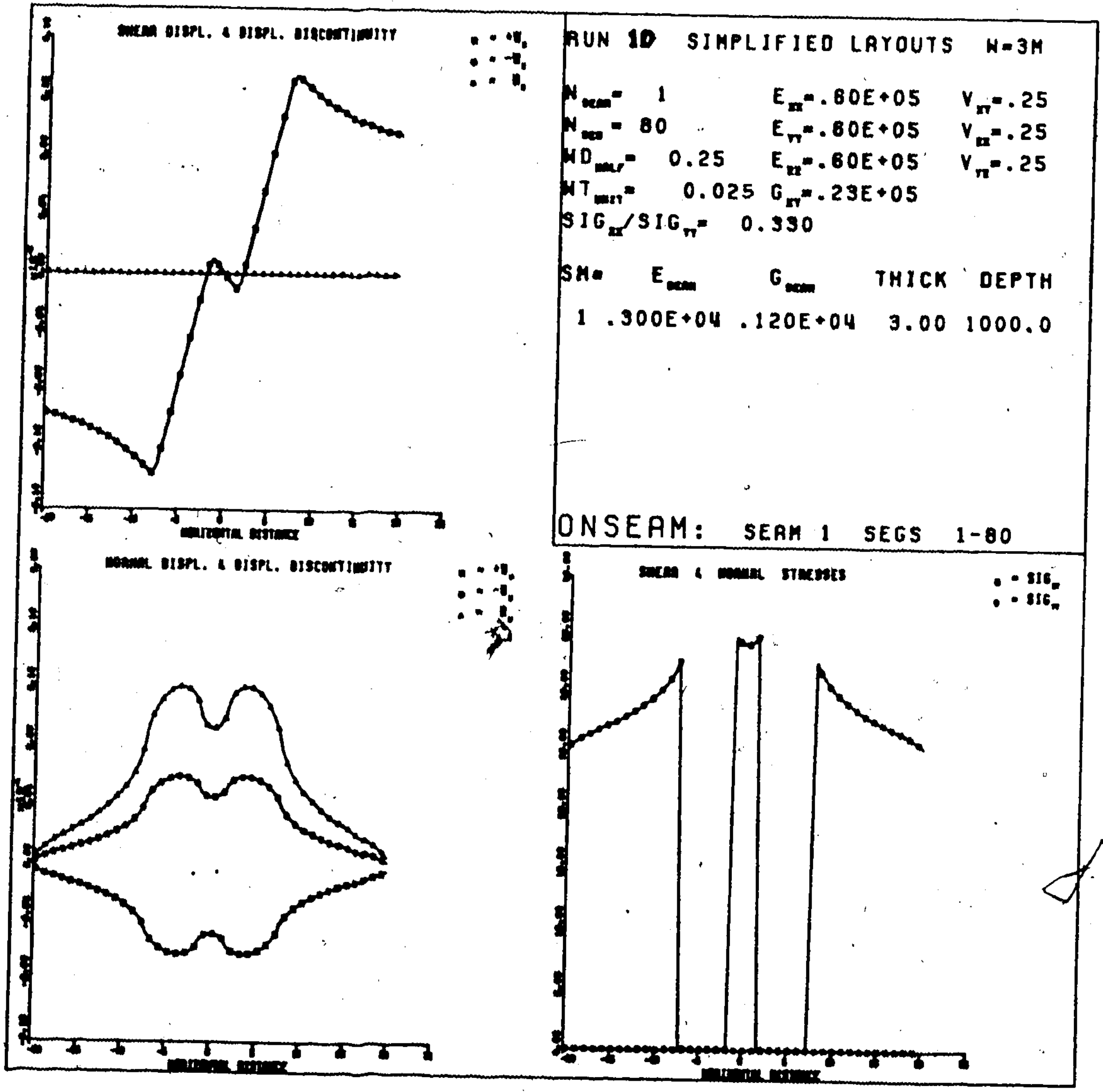

RUN 1D SIMPLIFIED LAYOUTS W=3M

N_{SEAM}= 1 E_{XX}=.80E+05 V_{XY}=.25
N_{SEG}= 80 E_{YY}=.80E+05 V_{XZ}=.25
WD_{HALF}= 0.25 E_{ZZ}=.60E+05 V_{YZ}=.25
WT_{UNIT}= 0.025 G_{XY}=.23E+05
SIG_{XX}/SIG_{YY}= 0.330

SM=	E_{SEAM}	G_{SEAM}	THICK	DEPTH
1	.300E+04	.120E+04	3.00	1000.0

ONSEAM: SEAM 1 SEGS 1-80

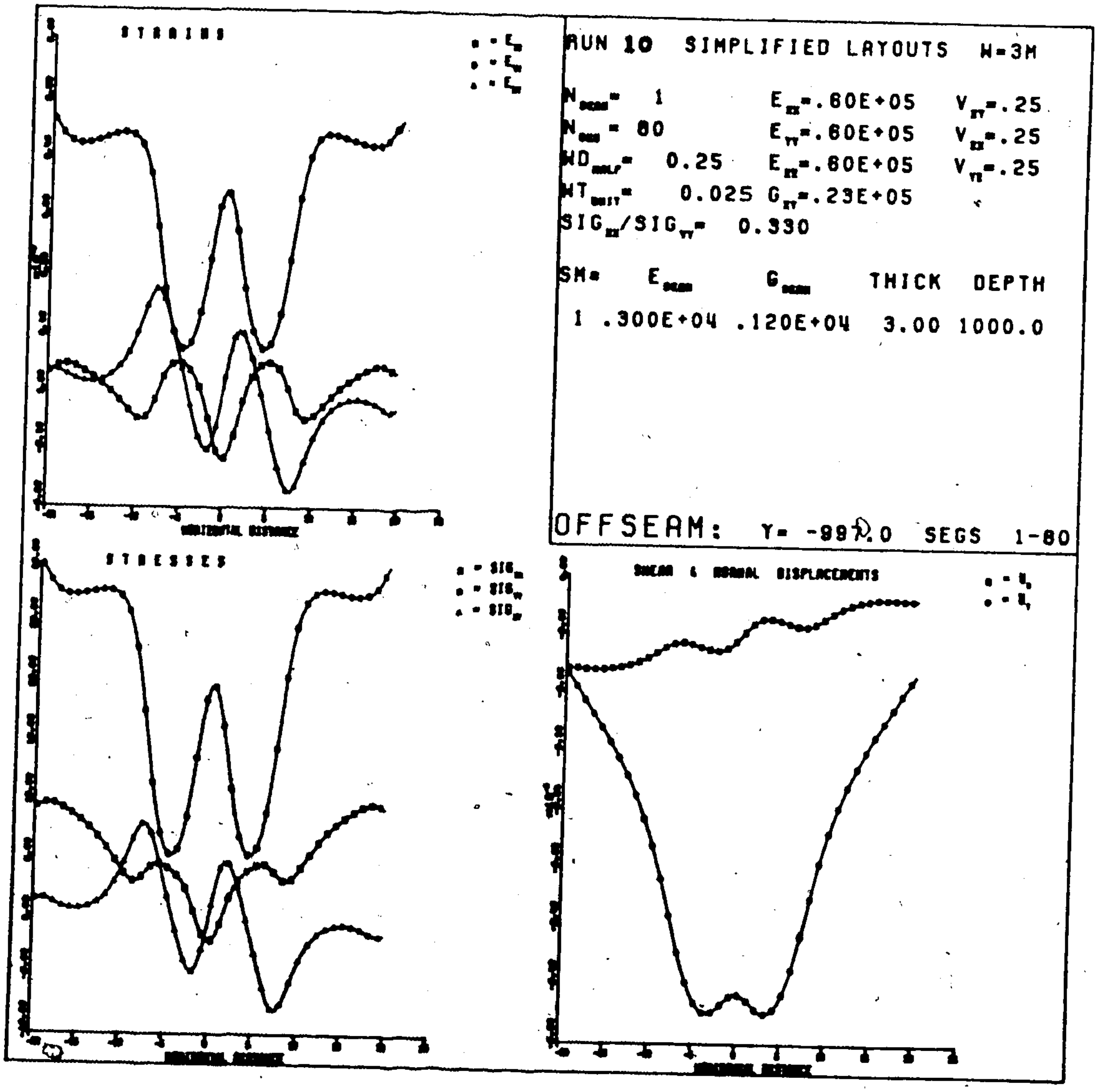

```
RUN 10  SIMPLIFIED LAYOUTS  W=3M

N_SEAM=  1          E_XX=.60E+05  V_XY=.25
N_OWN = 80          E_YY=.60E+05  V_ZX=.25
WD_HALF=  0.25      E_ZZ=.60E+05  V_YZ=.25
WT_UNIT=   0.025 G_XY=.23E+05
SIG_XX/SIG_YY=  0.330

SM=   E_SEAM     G_SEAM     THICK  DEPTH
 1 .300E+04 .120E+04  3.00 1000.0

OFFSEAM:  Y= -997.0  SEGS  1-80
```

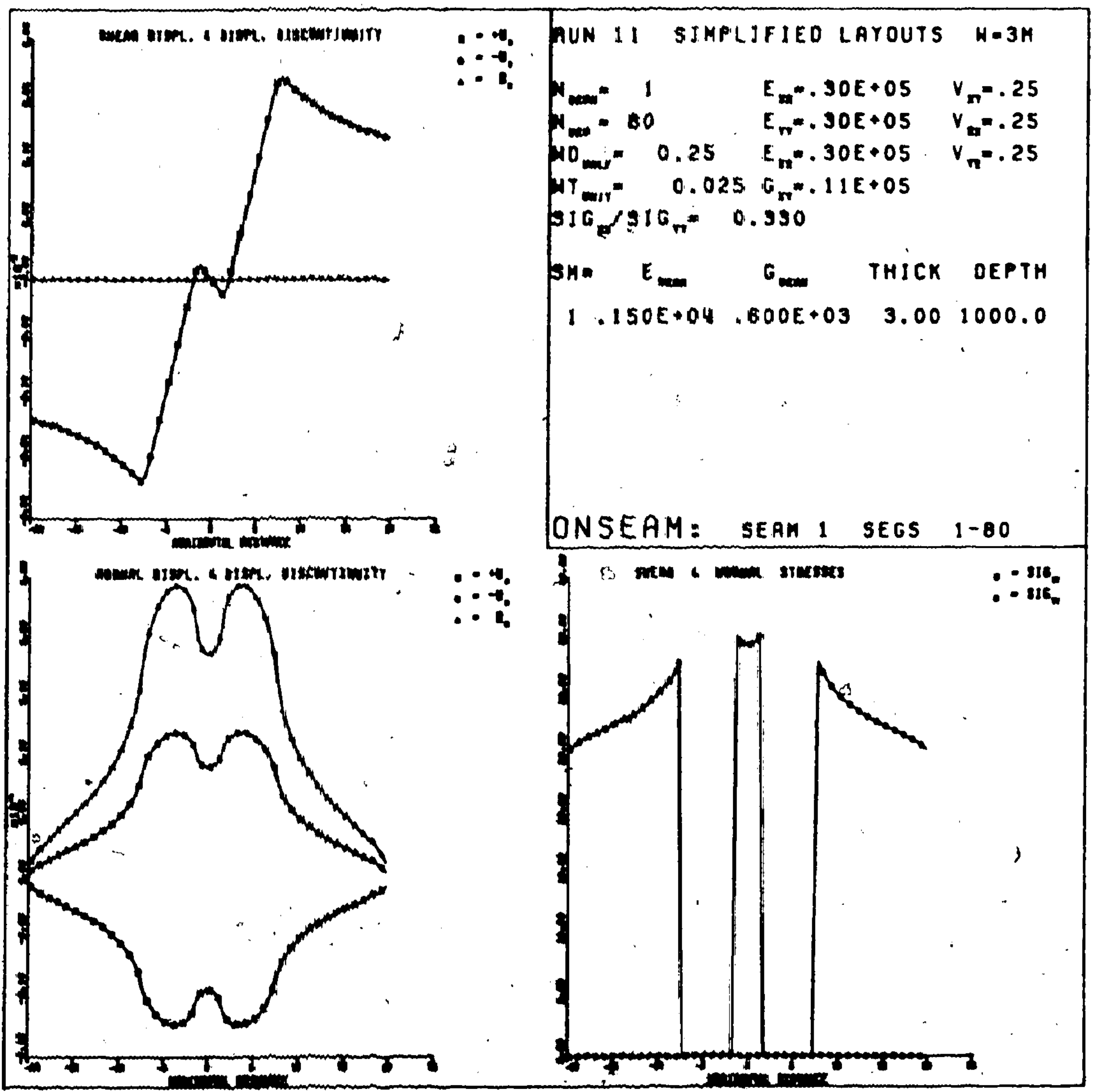

RUN 11 SIMPLIFIED LAYOUTS W=3M

N_{SEAM}= 1 E_{XX}=.30E+05 V_{XY}=.25
N_{SEG}= 80 E_{YY}=.30E+05 V_{XZ}=.25
WD_{UNIT}= 0.25 E_{ZZ}=.30E+05 V_{YZ}=.25
WT_{UNIT}= 0.025 G_{XY}=.11E+05
SIG_{XX}/SIG_{YY}= 0.330

SM=	E_{SEAM}	G_{SEAM}	THICK	DEPTH
1	.150E+04	.600E+03	3.00	1000.0

ONSEAM: SEAM 1 SEGS 1-80

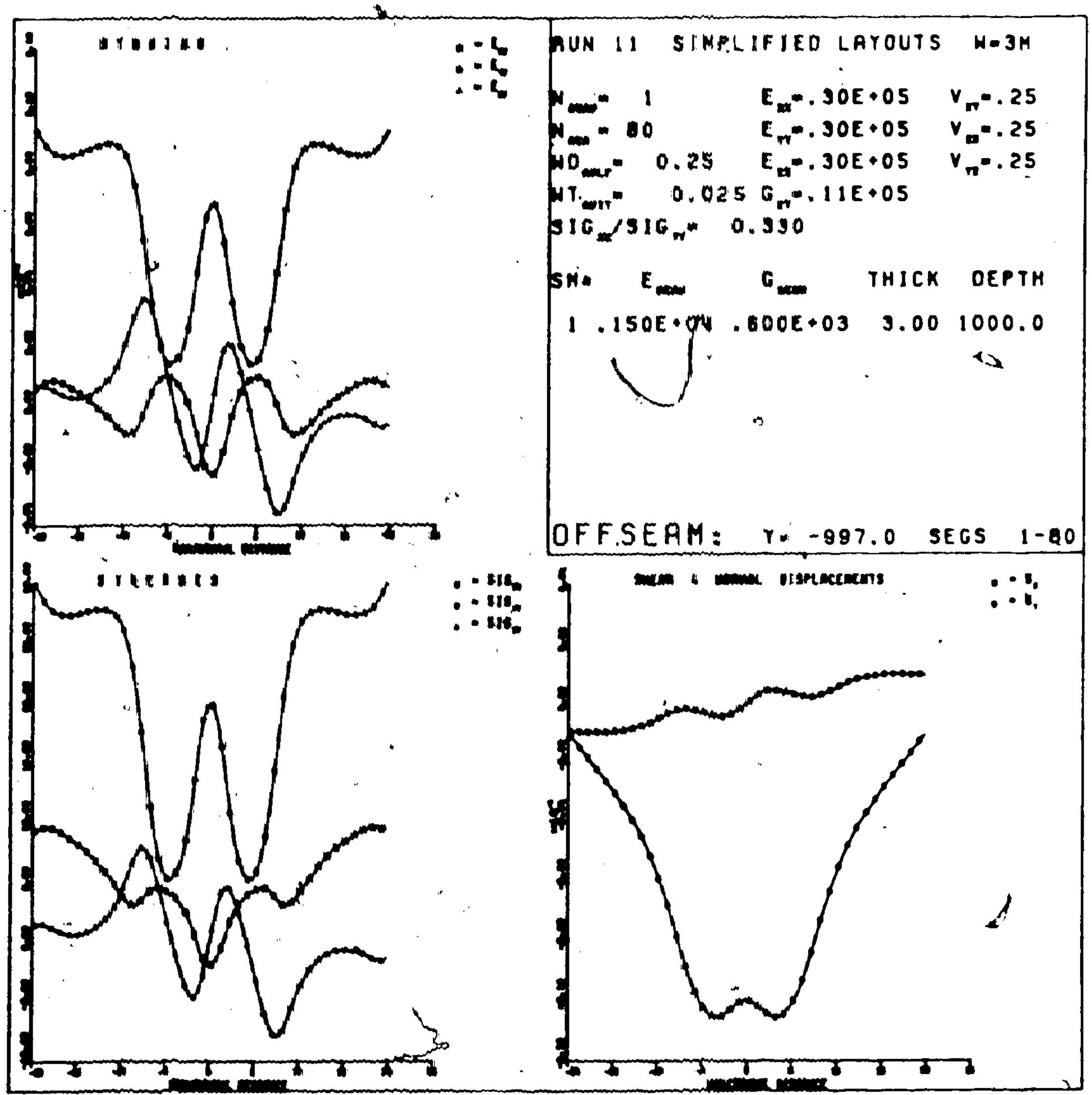

```
RUN 11   SIMPLIFIED LAYOUTS   W=3M

N_seam=  1          E_xx=.30E+05   V_xy=.25
N_segs= 80          E_yy=.30E+05   V_xz=.25
WD_ANLT=   0.25     E_zz=.30E+05   V_yz=.25
WT_UNIT=    0.025 G_xy=.11E+05
SIG_xx/SIG_yy=  0.330

SN*    E_seam        G_seam     THICK   DEPTH

 1  .150E+04  .600E+03   3.00 1000.0

OFF.SEAM:   Y= -997.0   SEGS  1-80
```

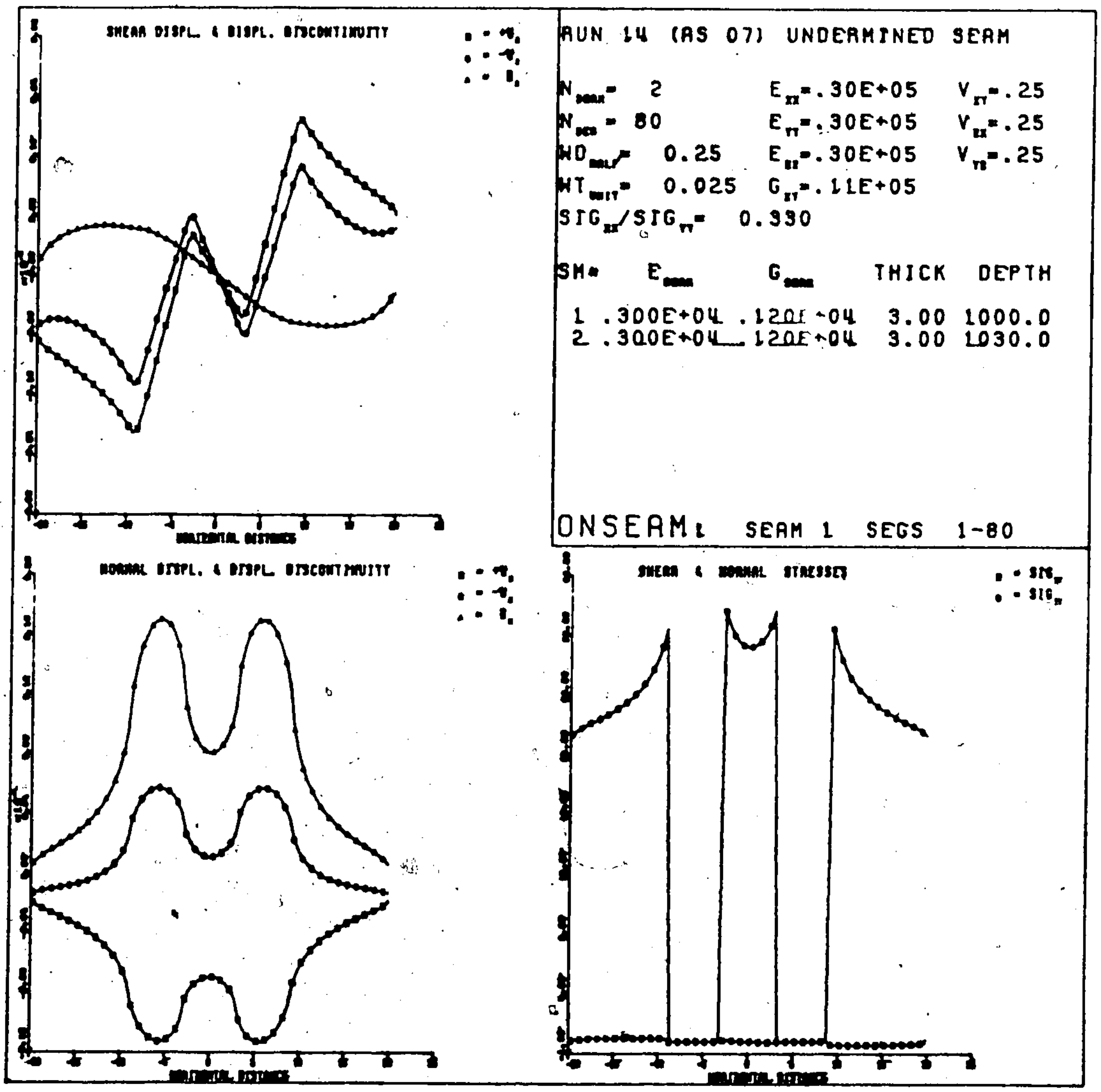

RUN 14 (AS 07) UNDERMINED SEAM

N_{SEAM}= 2 E_{XX}=.30E+05 V_{XY}=.25
N_{SEG}= 80 E_{YY}=.30E+05 V_{ZX}=.25
WD_{WALL}= 0.25 E_{ZZ}=.30E+05 V_{YZ}=.25
WT_{UNIT}= 0.025 G_{XY}=.11E+05
SIG_{XX}/SIG_{YY}= 0.330

SM#	E_{SEAM}	G_{SEAM}	THICK	DEPTH
1	.300E+04	.120E+04	3.00	1000.0
2	.300E+04	.120E+04	3.00	1030.0

ONSEAM: SEAM 1 SEGS 1-80

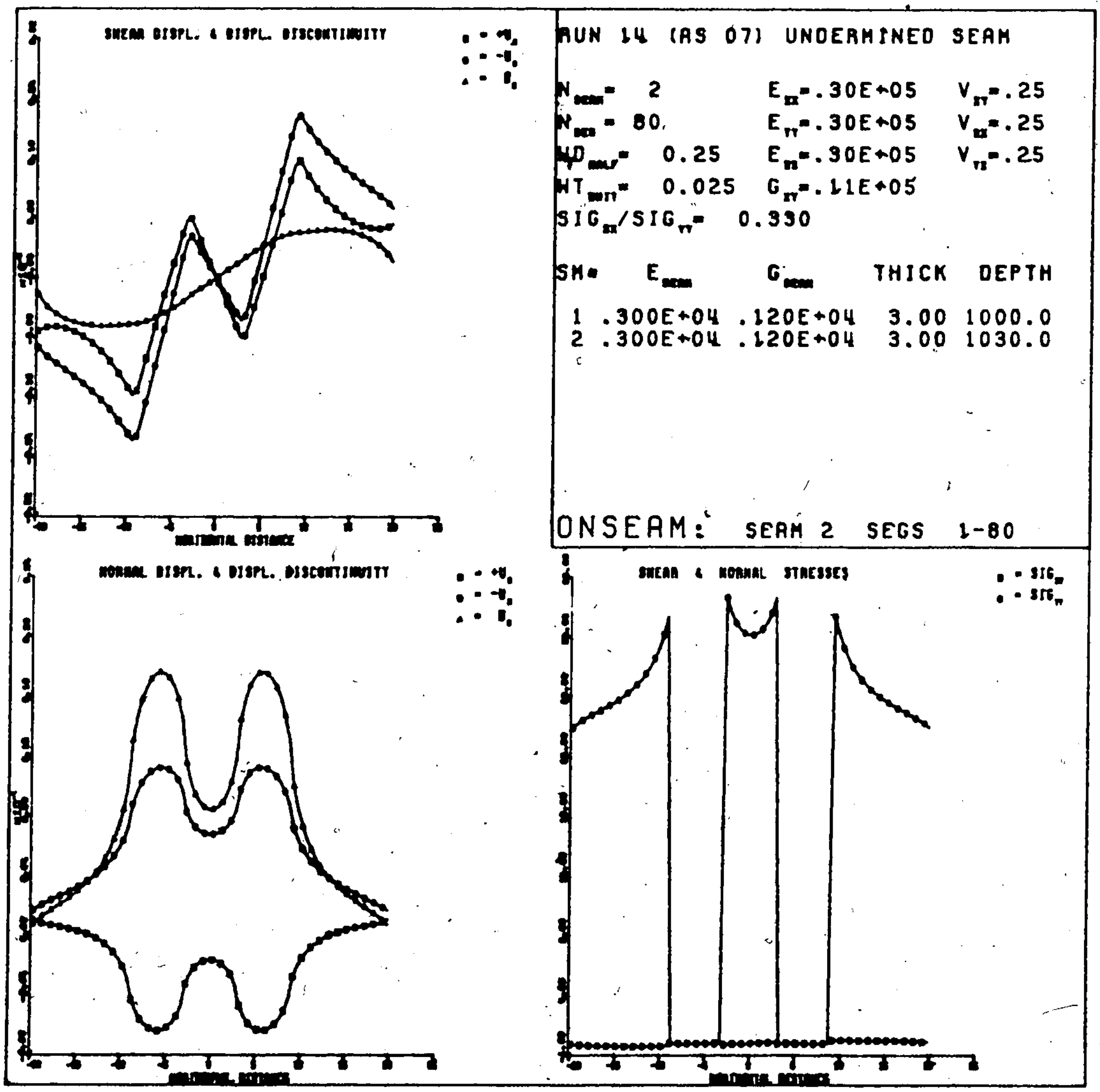

RUN 14 (AS 07) UNDERMINED SEAM

N_{SEAM}= 2 E_{XX}=.30E+05 V_{XY}=.25
N_{SEG}= 80 E_{YY}=.30E+05 V_{ZX}=.25
WD_{HALF}= 0.25 E_{ZZ}=.30E+05 V_{YZ}=.25
WT_{BUTT}= 0.025 G_{XY}=.11E+05
SIG_{XX}/SIG_{YY}= 0.330

SM#	E_{SEAM}	G_{SEAM}	THICK	DEPTH
1	.300E+04	.120E+04	3.00	1000.0
2	.300E+04	.120E+04	3.00	1030.0

ONSEAM: SEAM 2 SEGS 1-80

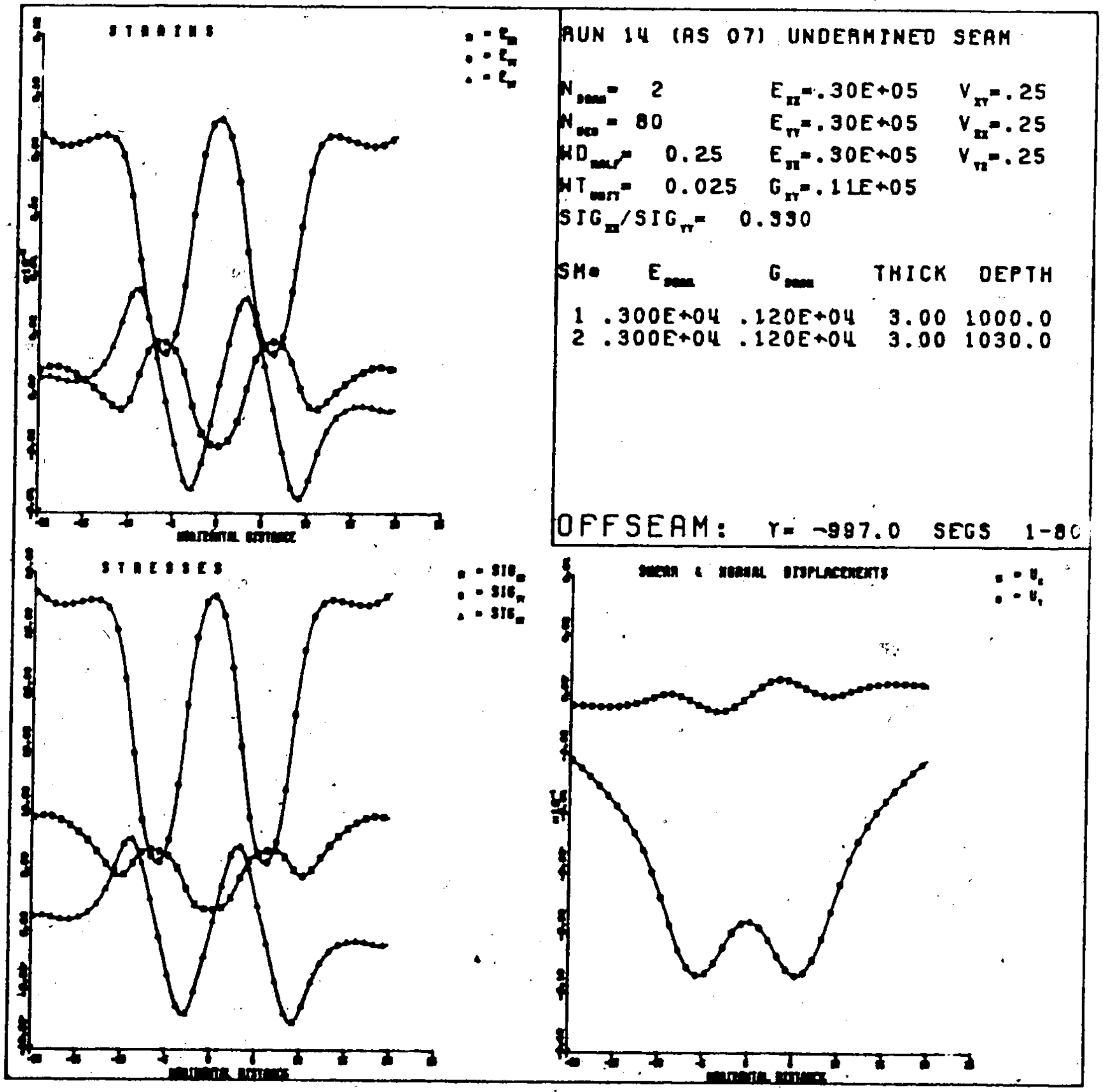

```
RUN 14 (AS 07) UNDERMINED SEAM

N_SEAM=  2          E_XX=.30E+05   V_XY=.25
N_SEG = 80          E_YY=.30E+05   V_XZ=.25
WD_HALF=  0.25      E_ZZ=.30E+05   V_YZ=.25
WT_UNIT=  0.025     G_XY=.11E+05
SIG_XX/SIG_YY=  0.330

SM#    E_SEAM      G_SEAM     THICK  DEPTH

 1 .300E+04 .120E+04   3.00 1000.0
 2 .300E+04 .120E+04   3.00 1030.0

OFFSEAM:  Y= -997.0  SEGS  1-80
```

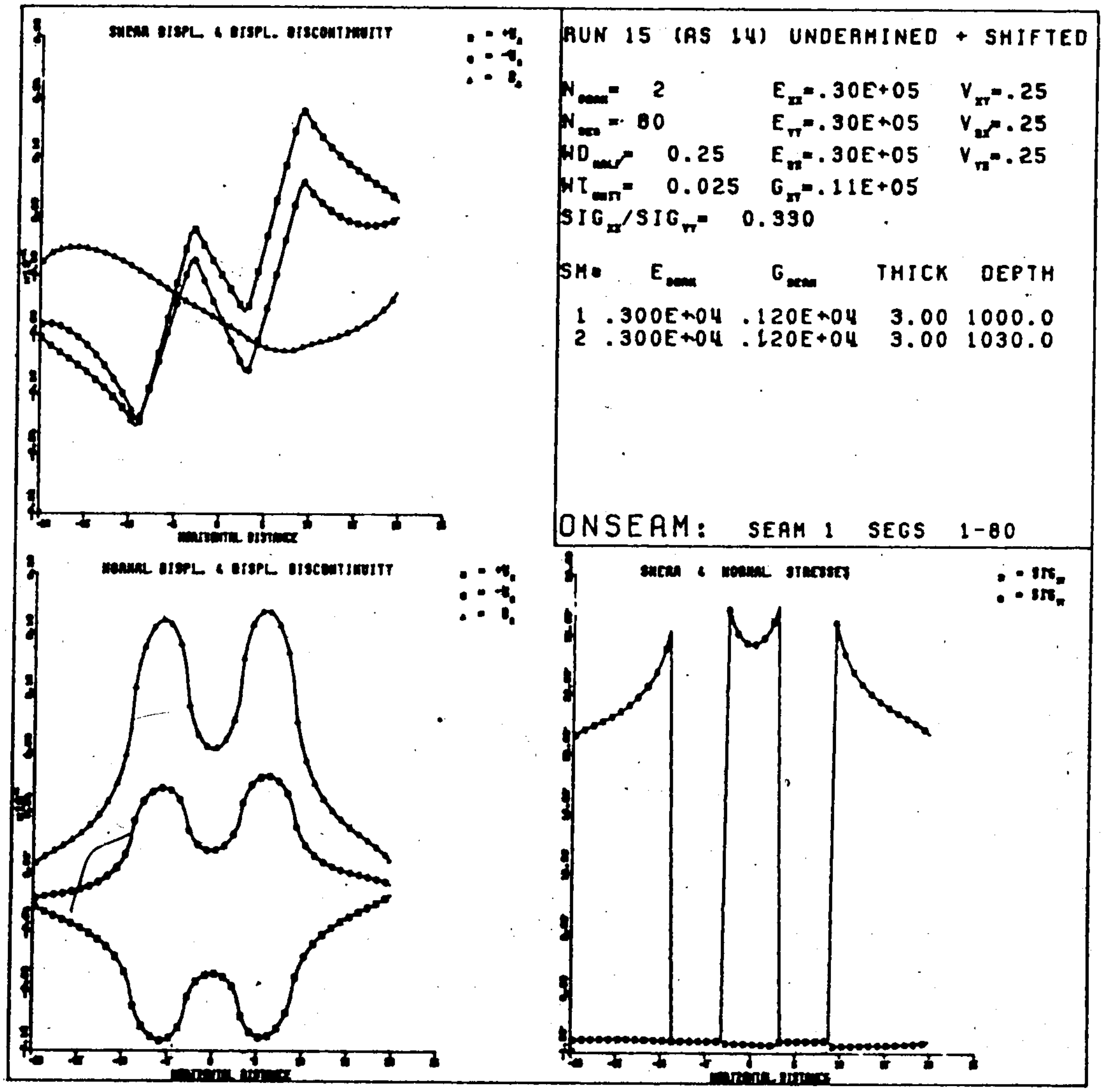

RUN 15 (AS 14) UNDERMINED + SHIFTED

N_{SEAM}= 2 E_{XX}=.30E+05 V_{XY}=.25
N_{SEG} = 80 E_{YY}=.30E+05 V_{ZX}=.25
WD_{HALF}= 0.25 E_{ZZ}=.30E+05 V_{YZ}=.25
WT_{UNIT}= 0.025 G_{XY}=.11E+05
SIG_{XX}/SIG_{YY}= 0.330

SM#	E_{SEAM}	G_{SEAM}	THICK	DEPTH
1	.300E+04	.120E+04	3.00	1000.0
2	.300E+04	.120E+04	3.00	1030.0

ONSEAM: SEAM 1 SEGS 1-80

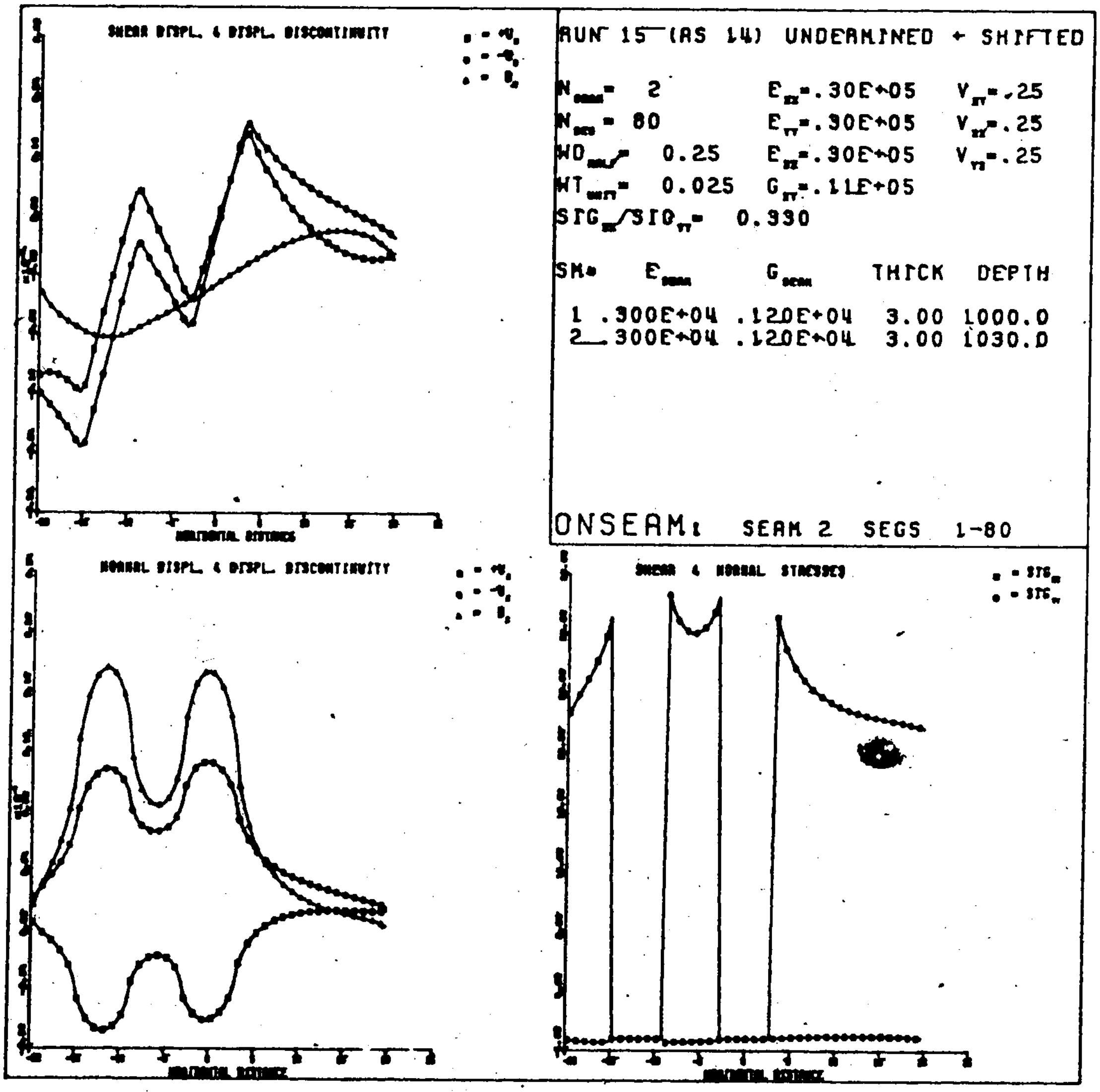

RUN 15 (AS 14) UNDERMINED + SHIFTED

N_{SEAM}= 2 E_{XX}=.30E+05 V_{XY}=.25
N_{SEG}= 80 E_{YY}=.30E+05 V_{XZ}=.25
WD_{HALF}= 0.25 E_{ZZ}=.30E+05 V_{YZ}=.25
WT_{UNIT}= 0.025 G_{XY}=.11E+05
SIG_{XX}/SIG_{YY}= 0.330

SM#	E_{SEAM}	G_{SEAM}	THICK	DEPTH
1	.300E+04	.120E+04	3.00	1000.0
2	.300E+04	.120E+04	3.00	1030.0

ONSEAM: SEAM 2 SEGS 1-80

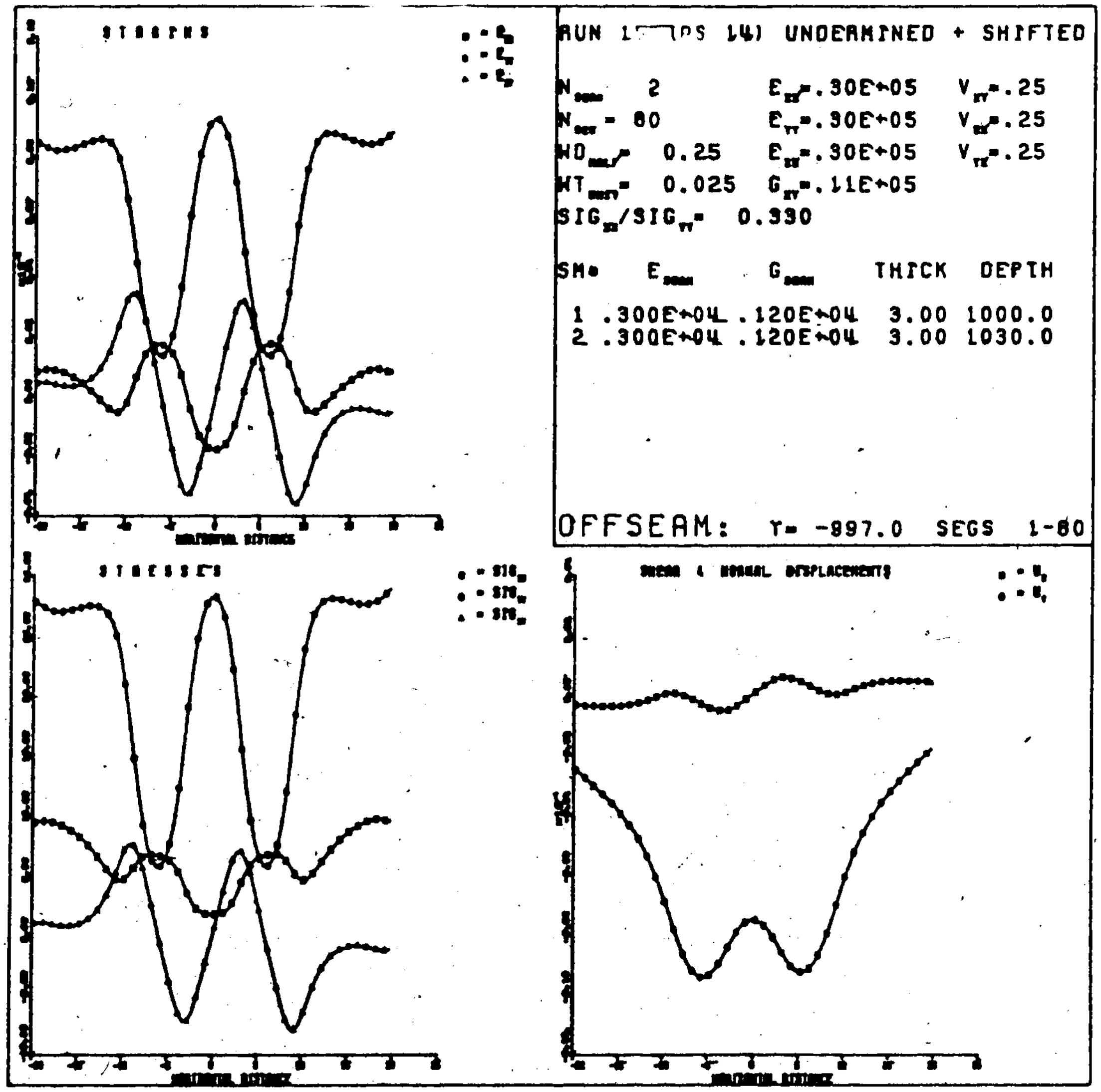

```
RUN 1[illegible]PS 14) UNDERMINED + SHIFTED

NSEAM   2           EXX=.30E+05   VXY=.25
NSEG= 80            EYY=.30E+05   VZX=.25
WDANAL=   0.25      EZZ=.30E+05   VYZ=.25
WTANAL=   0.025     GXY=.11E+05
SIGXX/SIGYY=   0.330

SM#    ESEAM       GSEAM      THICK   DEPTH

 1 .300E+04 .120E+04   3.00 1000.0
 2 .300E+04 .120E+04   3.00 1030.0

OFFSEAM:   Y= -997.0   SEGS   1-80
```

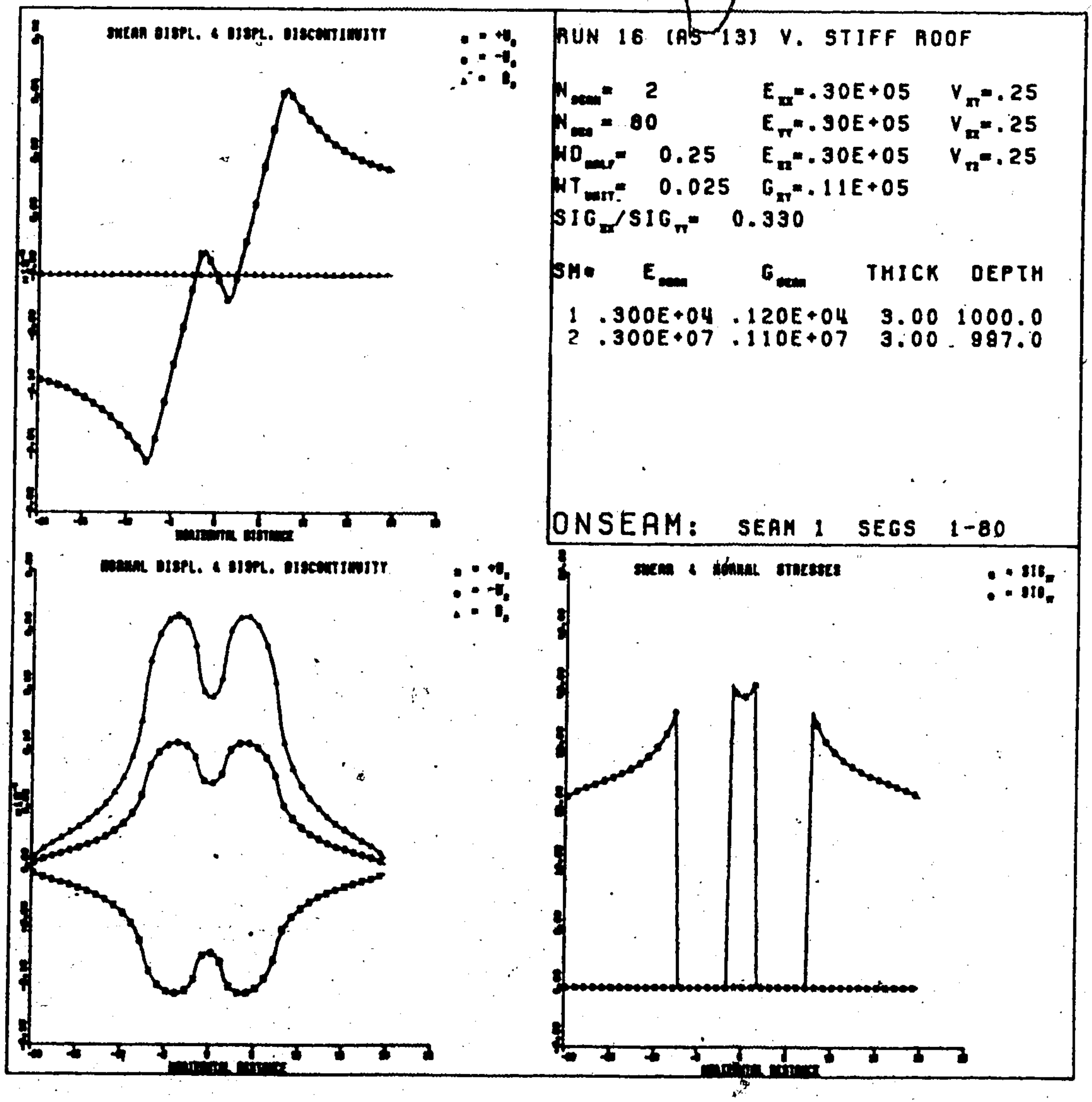

```
RUN 16 (AS 13) V. STIFF ROOF

N_SEAM=  2           E_XX=.30E+05   V_XY=.25
N_SEG = 80           E_YY=.30E+05   V_ZX=.25
WD_HALF=  0.25       E_ZZ=.30E+05   V_YZ=.25
WT_UNIT=  0.025      G_XY=.11E+05
SIG_XX/SIG_YY=  0.330

SM#    E_SEAM       G_SEAM      THICK  DEPTH

 1 .300E+04 .120E+04   3.00 1000.0
 2 .300E+07 .110E+07   3.00  997.0

ONSEAM:  SEAM 1  SEGS  1-80
```

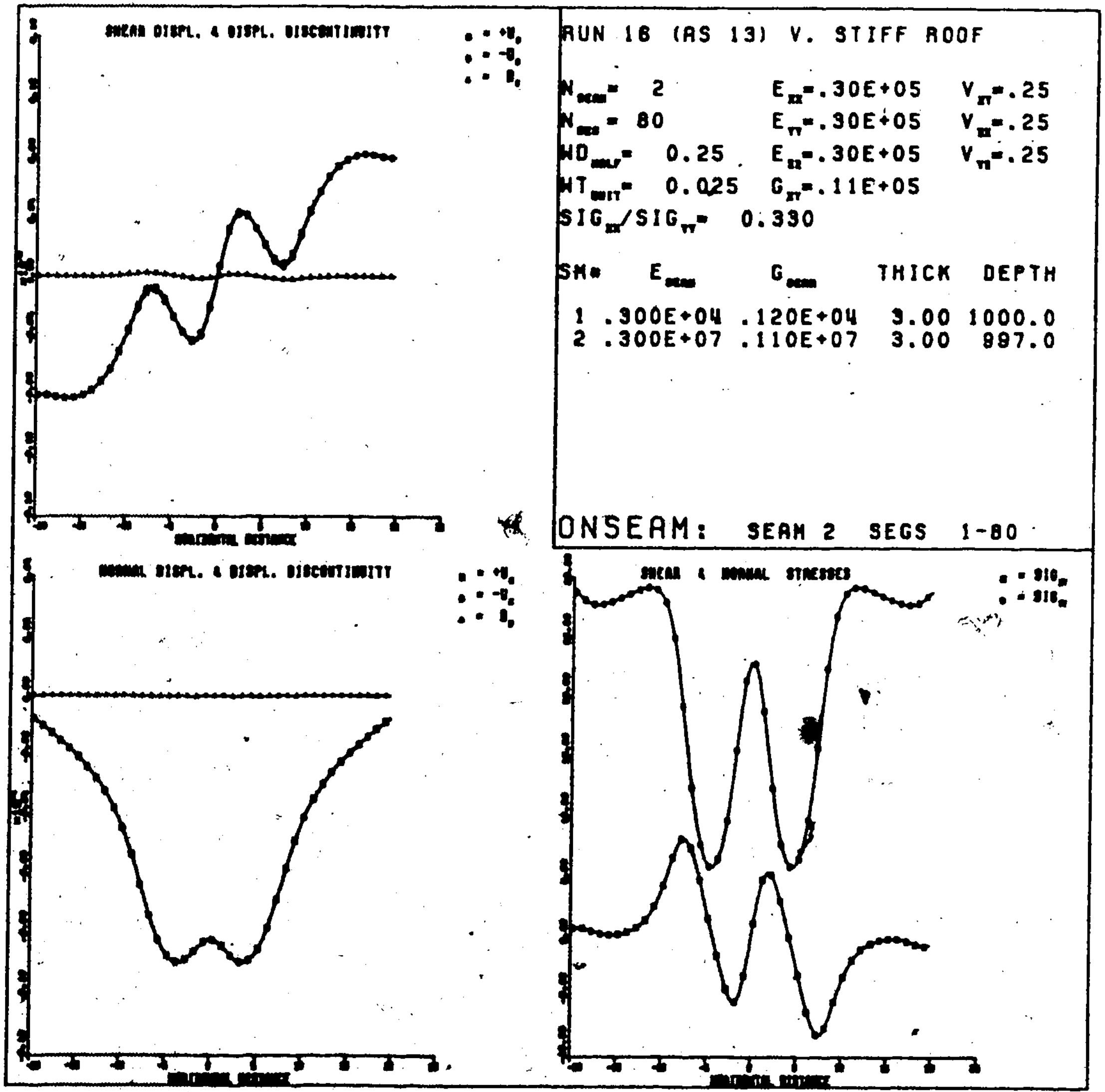

RUN 16 (AS 13) V. STIFF ROOF

N_{SEAM}= 2 E_{XX}=.30E+05 V_{XY}=.25
N_{SEG}= 80 E_{YY}=.30E+05 V_{XZ}=.25
WD_{HALF}= 0.25 E_{ZZ}=.30E+05 V_{YZ}=.25
WT_{UNIT}= 0.025 G_{XY}=.11E+05
SIG_{XX}/SIG_{YY}= 0.330

SM#	E_{SEAM}	G_{SEAM}	THICK	DEPTH
1	.300E+04	.120E+04	3.00	1000.0
2	.300E+07	.110E+07	3.00	997.0

ONSEAM: SEAM 2 SEGS 1-80

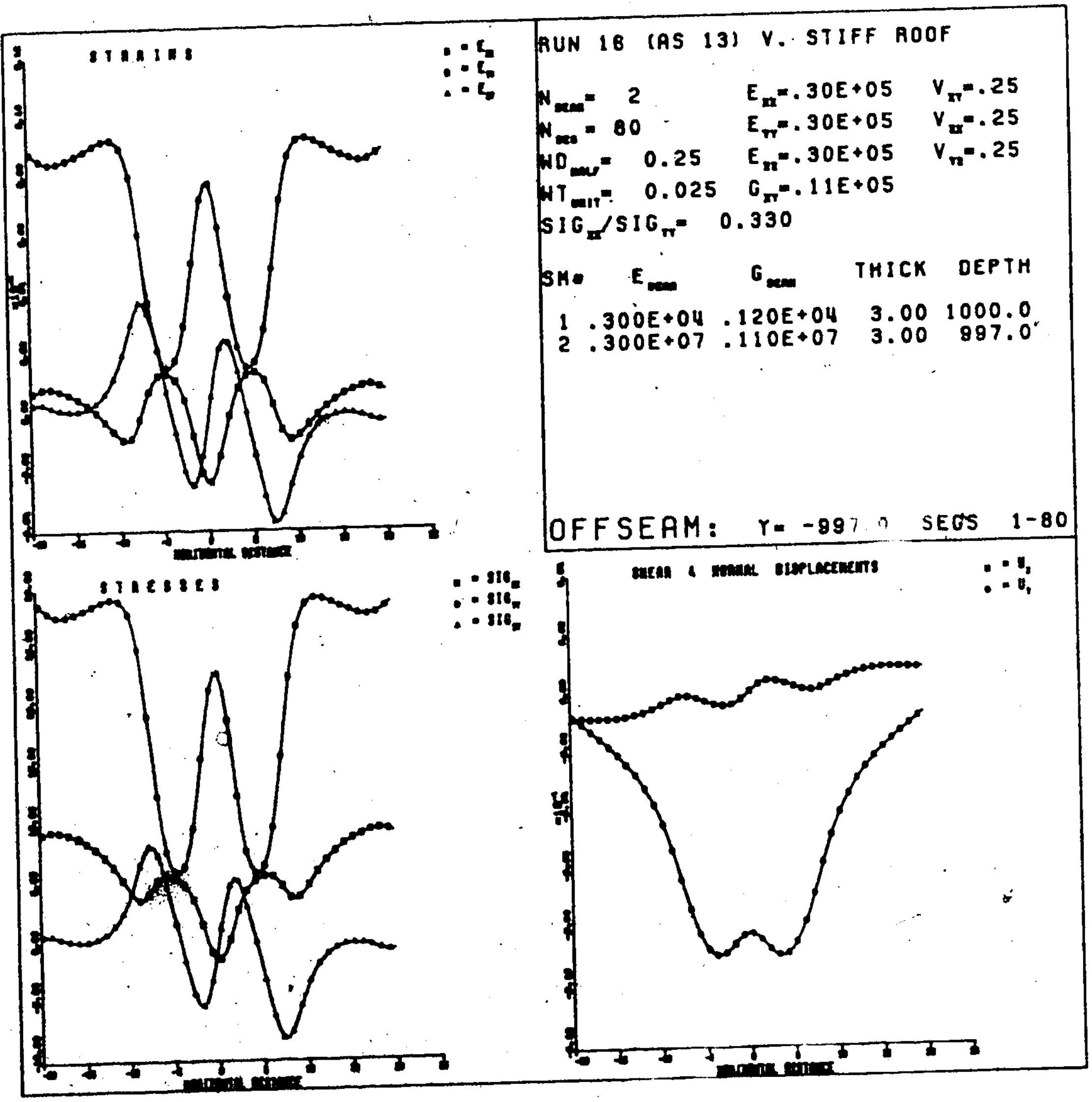

RUN 18 (AS 13) V. STIFF ROOF

N_{SEAM}= 2 E_{XX}=.30E+05 V_{XY}=.25
N_{SEG}= 80 E_{YY}=.30E+05 V_{ZX}=.25
WD_{HALF}= 0.25 E_{ZZ}=.30E+05 V_{YZ}=.25
WT_{UNIT}= 0.025 G_{XY}=.11E+05
SIG_{XX}/SIG_{YY}= 0.330

SM#	E_{SEAM}	G_{SEAM}	THICK	DEPTH
1	.300E+04	.120E+04	3.00	1000.0
2	.300E+07	.110E+07	3.00	997.0

OFFSEAM: Y= -997.0 SEGS 1-80

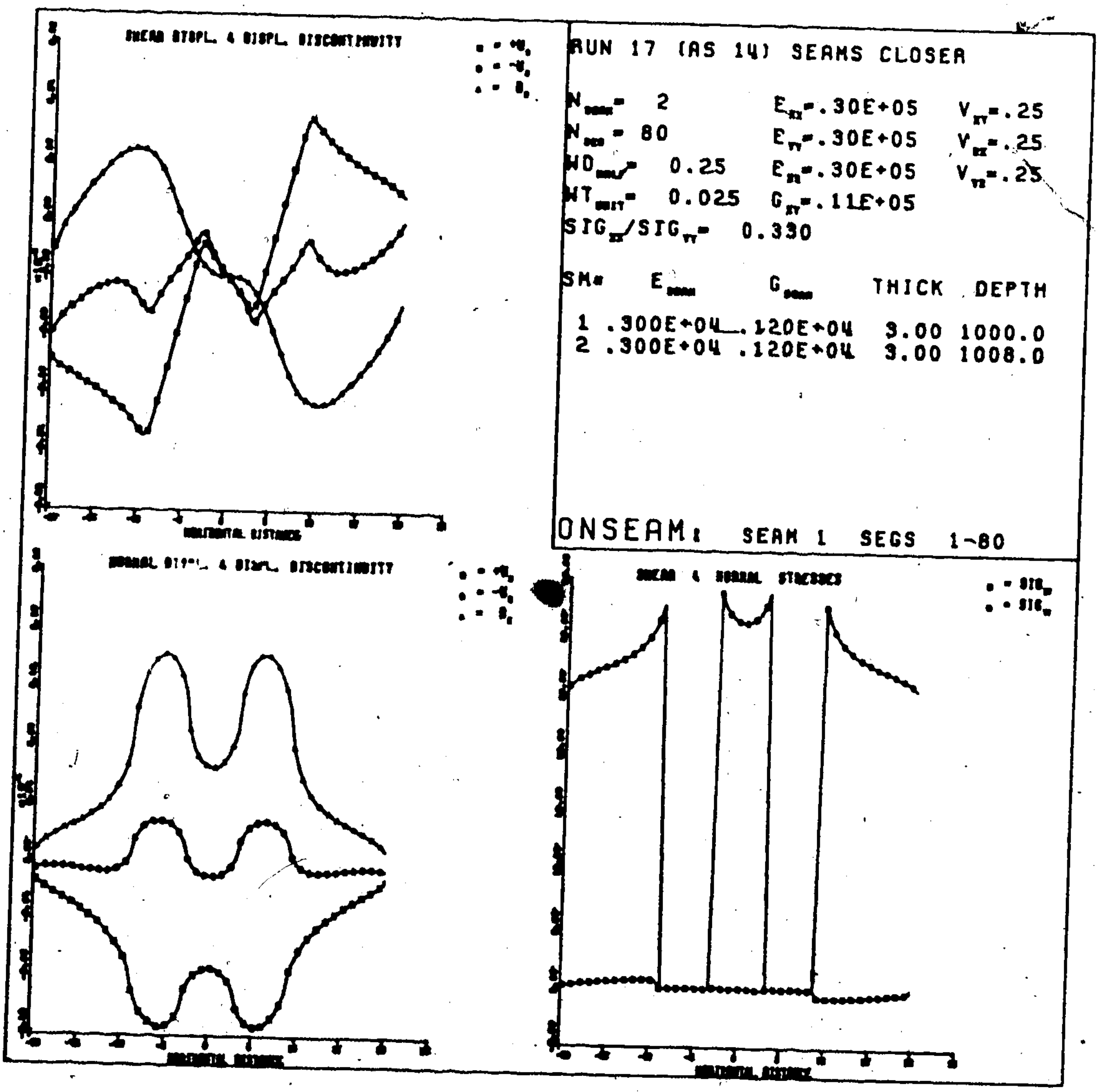

RUN 17 (AS 14) SEAMS CLOSER

N_{SEAM}= 2 E_{XX}=.30E+05 V_{XY}=.25
N_{SEG} = 80 E_{YY}=.30E+05 V_{XZ}=.25
WD_{SEAM}= 0.25 E_{ZZ}=.30E+05 V_{YZ}=.25
WT_{UNIT}= 0.025 G_{XY}=.11E+05
SIG_{XX}/SIG_{YY}= 0.330

SM# E_{SEAM} G_{SEAM} THICK DEPTH
1 .300E+04 .120E+04 3.00 1000.0
2 .300E+04 .120E+04 3.00 1008.0

ONSEAM: SEAM 1 SEGS 1-80

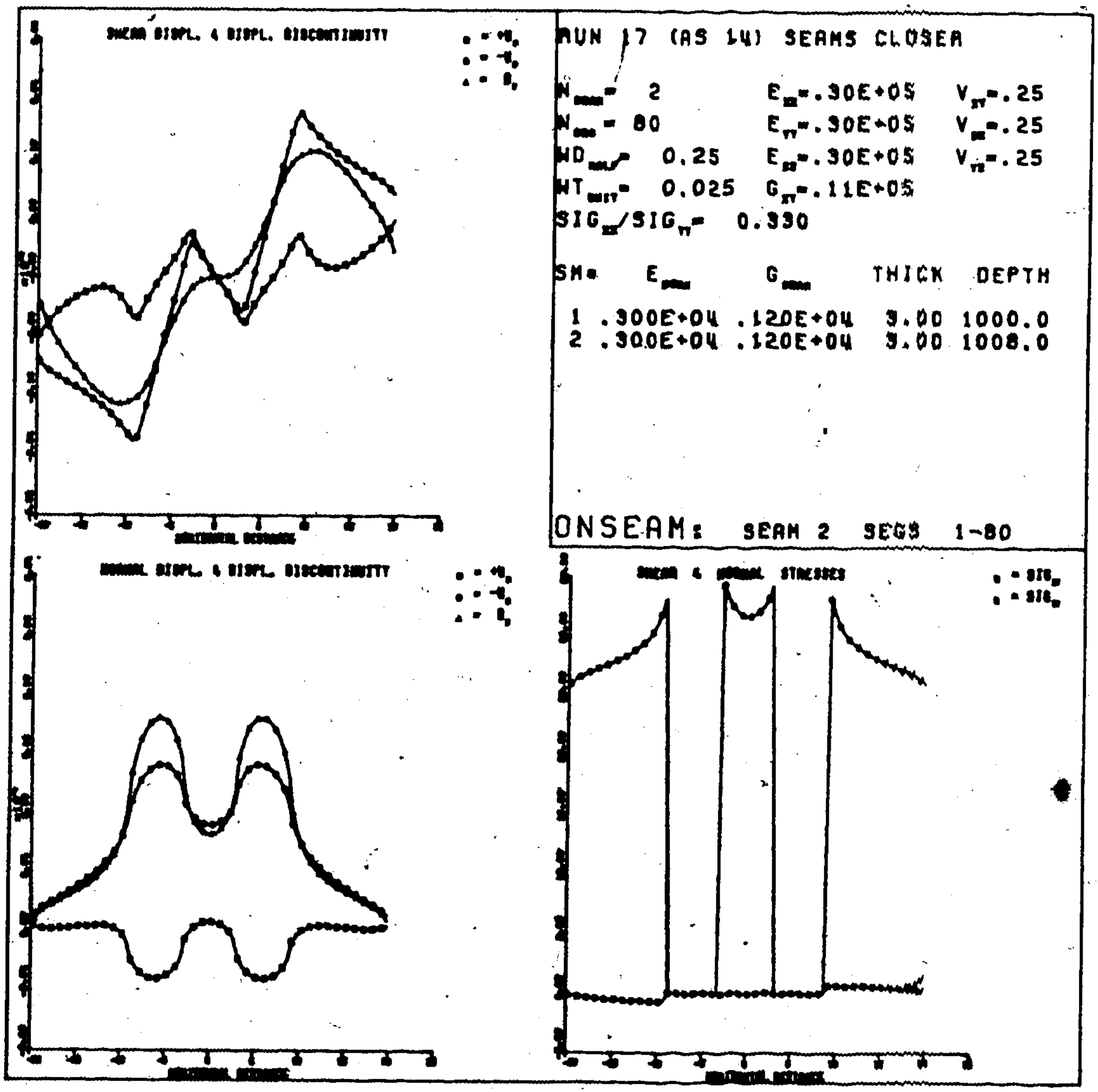

```
RUN 17 (AS 14) SEAMS CLOSER

N[illegible]=  2          EXX=.30E+05   VXY=.25
N[illegible]= 80          EYY=.30E+05   VXZ=.25
WD[illegible]=  0.25      EZZ=.30E+05   VYZ=.25
WT[illegible]=  0.025     GXY=.11E+05
SIGXX/SIGYY=  0.330

SM=    E[illegible]     G[illegible]     THICK  DEPTH

 1 .300E+04 .120E+04   3.00 1000.0
 2 .300E+04 .120E+04   3.00 1008.0

ONSEAM:  SEAM 2  SEGS  1-80
```

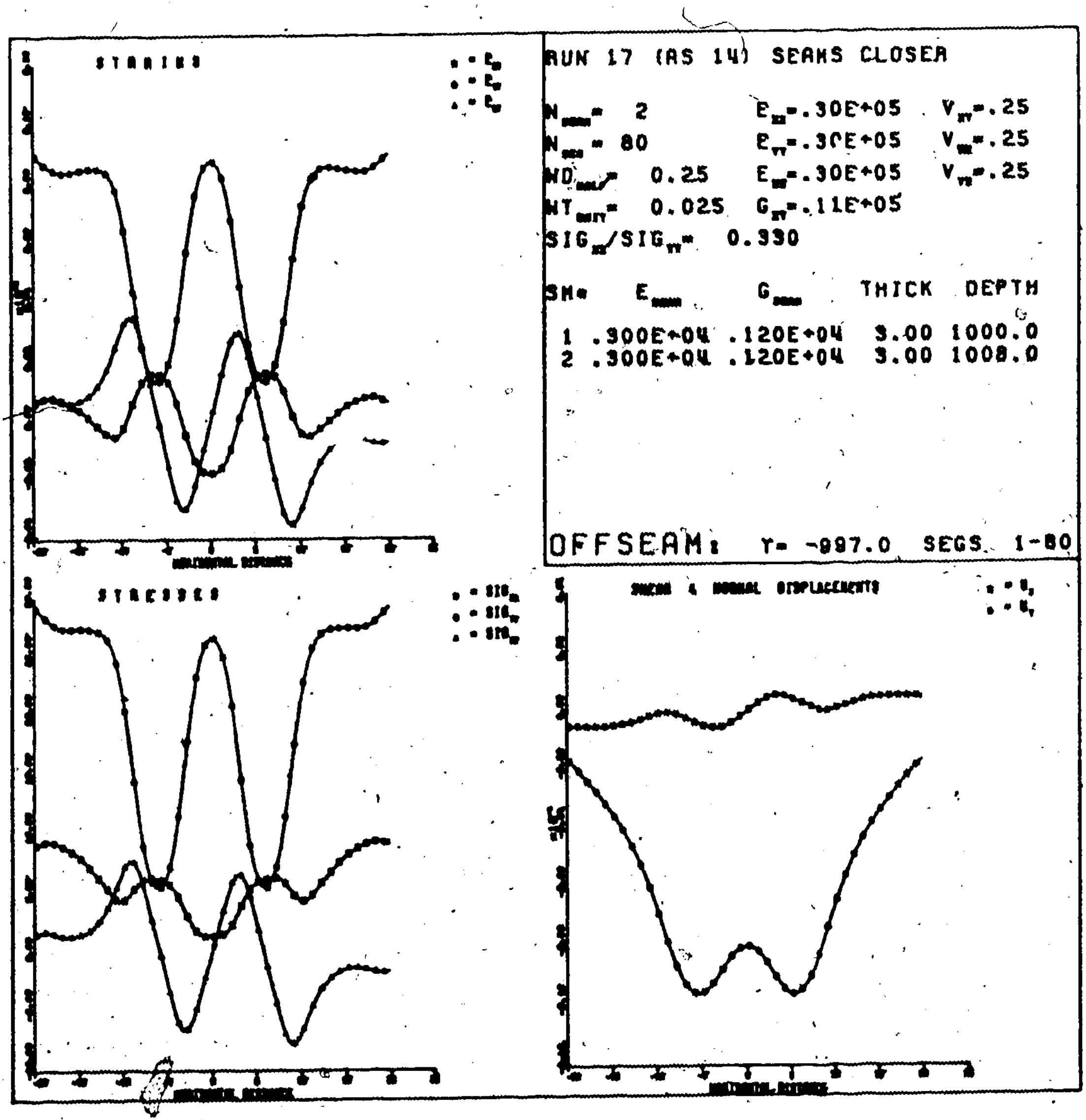

```
RUN 17 (AS 14) SEAMS CLOSER

N_SEAM=  2          E_XX=.30E+05   V_XY=.25
N_SEG = 80          E_YY=.3CE+05   V_XZ=.25
WD_SEAM/=  0.25     E_ZZ=.30E+05   V_YZ=.25
WT_SEAM=  0.025     G_XY=.11E+05
SIG_XX/SIG_YY=  0.330

SM=   E_SEAM      G_SEAM     THICK  DEPTH

 1 .300E+04 .120E+04   3.00 1000.0
 2 .300E+04 .120E+04   3.00 1008.0




OFFSEAM:  Y= -997.0  SEGS 1-80
```

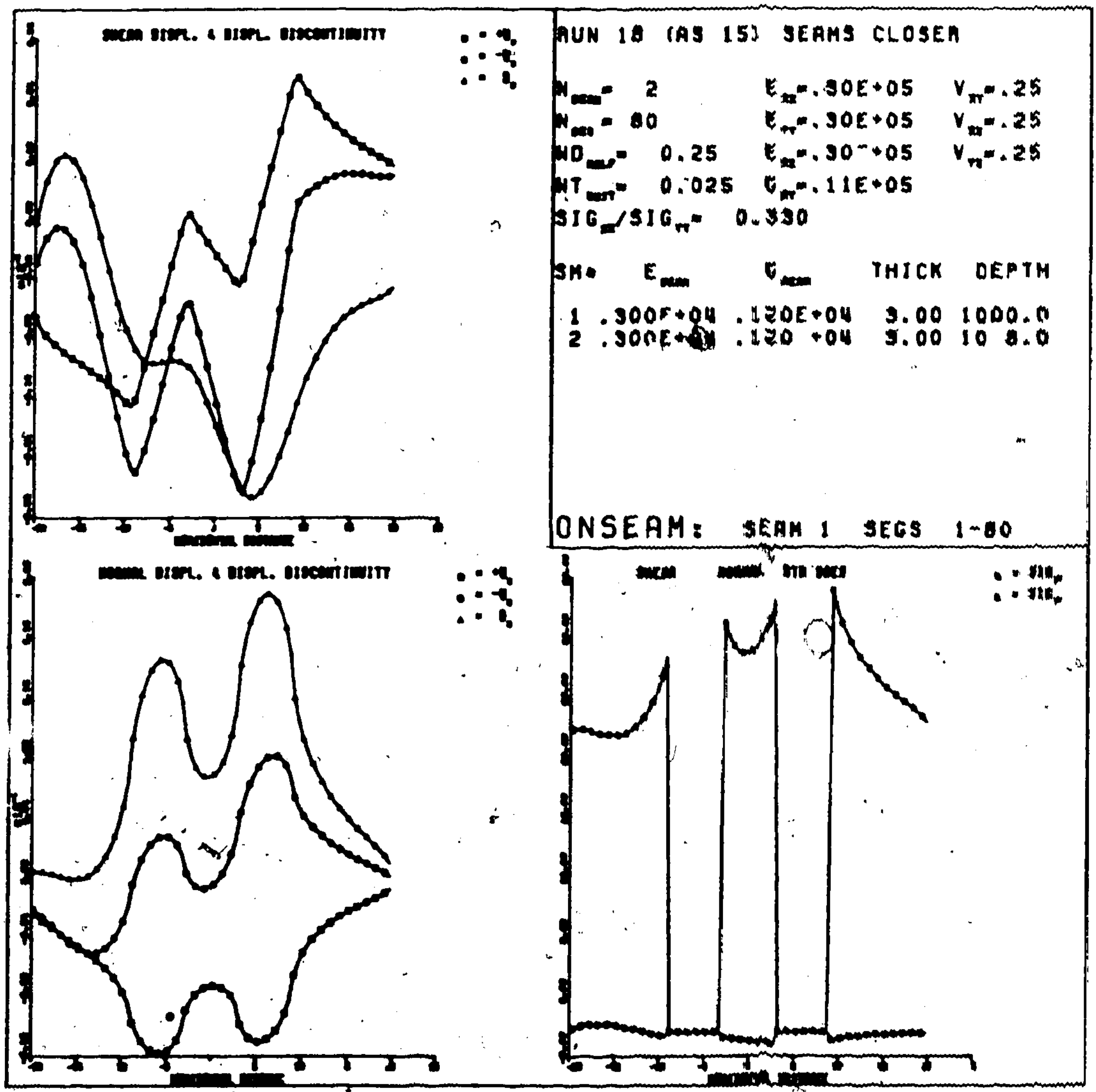

```
RUN 18 (AS 15) SEAMS CLOSER

N    =  2       E  =.30E+05   V  =.25
N   = 80        E  =.30E+05   V  =.25
WD    =  0.25   E  =.30 +05   V  =.25
WT    =  0.025  G  =.11E+05
SIG /SIG  =  0.330

SM#    E           G            THICK   DEPTH

 1 .300F+04  .120E+04   3.00 1000.0
 2 .300E+04  .120 +04   3.00 10 8.0

ONSEAM:  SEAM 1  SEGS  1-80
```

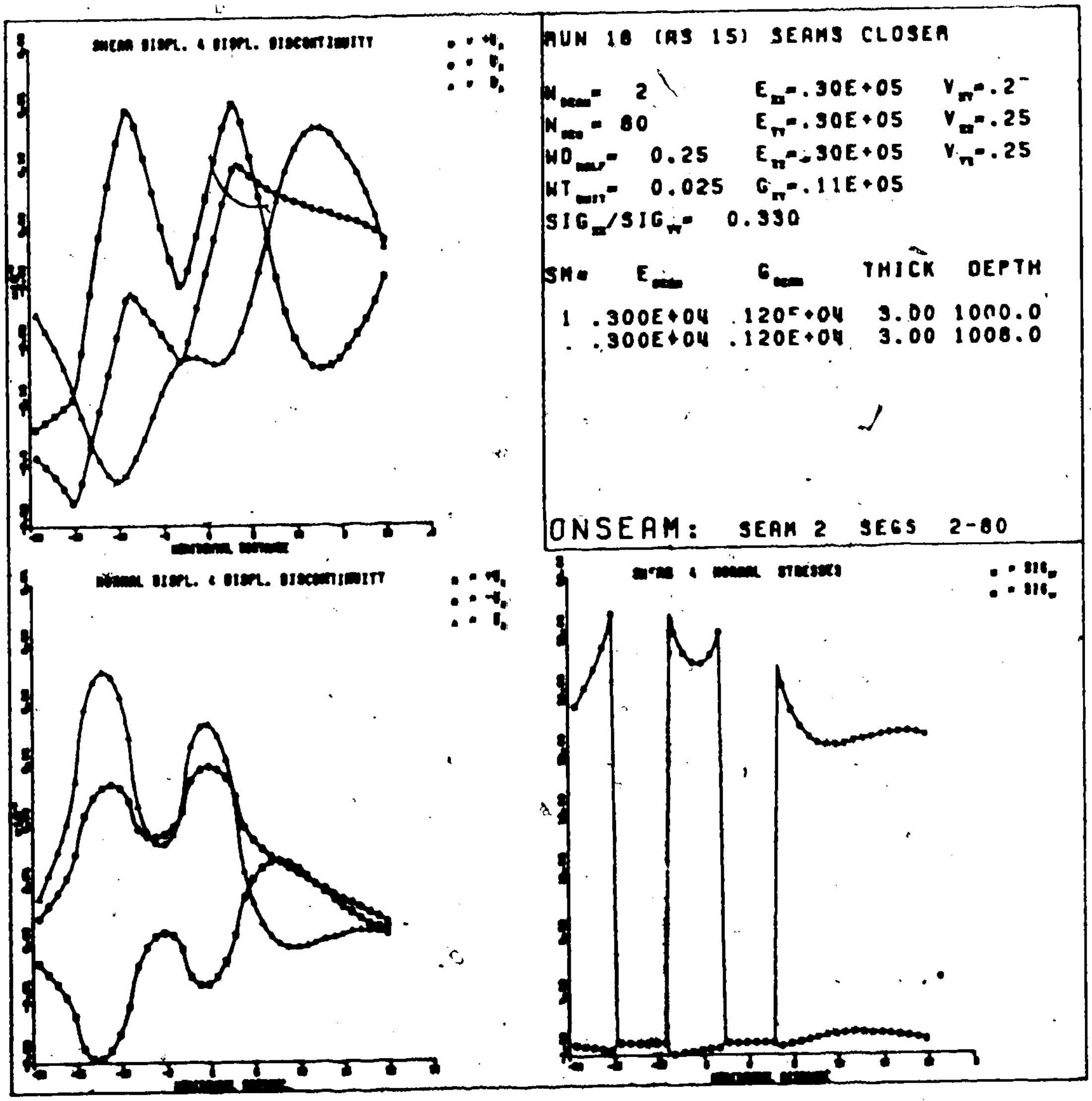

```
RUN 18 (AS 15) SEAMS CLOSER

N    =  2             E  =.30E+05   V  =.2
N    = 80             E  =.30E+05   V  =.25
WD    =  0.25         E  =.30E+05   V  =.25
WT    =  0.025        G  =.11E+05
SIG  /SIG  =  0.330

SM#    E           G          THICK  DEPTH

 1  .300E+04  .120E+04   3.00 1000.0
    .300E+04  .120E+04   3.00 1008.0

ONSEAM:  SEAM 2  SEGS  2-80
```

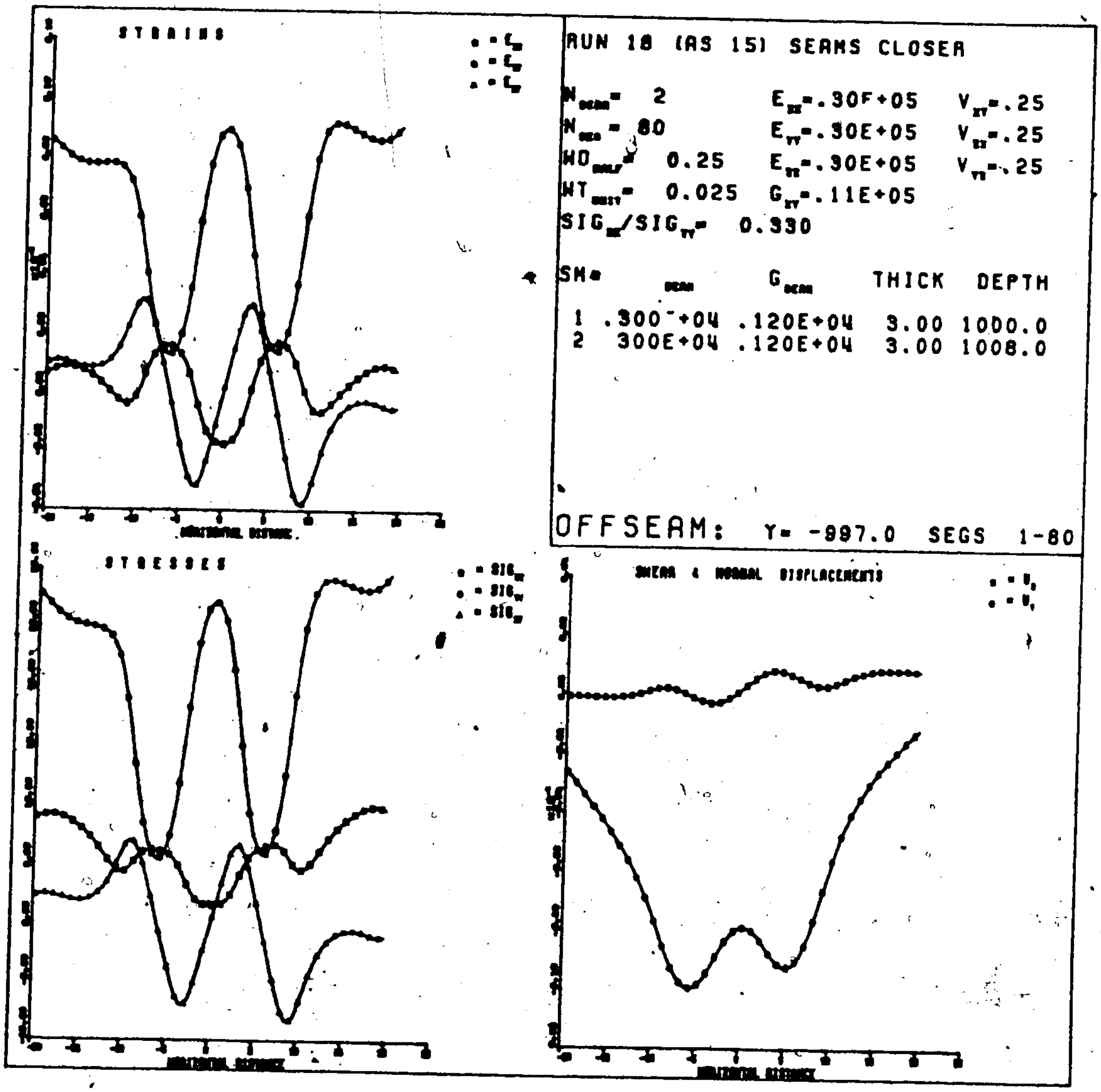

```
RUN 18 (AS 15) SEAMS CLOSER

N_SEAM=  2          E_XX=.30F+05   V_XY=.25
N_SEG =  80         E_YY=.30E+05   V_XZ=.25
WD_HALF=  0.25      E_ZZ=.30E+05   V_YZ=.25
WT_JOINT=  0.025    G_XY=.11E+05
SIG_XX/SIG_YY=  0.330

SM#      E_SEAM      G_SEAM     THICK  DEPTH

 1  .300 +04  .120E+04   3.00 1000.0
 2   300E+04  .120E+04   3.00 1008.0

OFFSEAM:  Y= -997.0  SEGS  1-80
```

APPENDIX 5

GEOTECHNICAL CORE LOGS

MINERAL ENGINEERING DEPARTMENT **UNIVERSITY OF ALBERTA** **GEOTECHNICAL CORE LOG**

PROJECT Siltstone LOCATION ________ E ________ N ELEVATION ________ DIP Vertical BEARING ________ PAGE 1 OF 4 HOLE NO. 2285 (c)

RUN No.	LENGTH OF RUN	LENGTH RECOVERED	% RECOVERY	CLASSIFICATION	LITHOLOGICAL DESCRIPTION type, colour, texture, bedding, structure, hardness, remarks.	DEPTH	SAMPLE	DISCONTINUITIES TYPE	SEPARATION	FILL	ROUGHNESS	DIP TCA	DEFECT FREQ. / ft.	REMARKS
9	6.0	6.0	100		SILTSTONE IRON STAINED IN PLACES	73.0								
						74.0	C18 C17							
						75.0	C16							
						76.0								
						77.0	C15							
					MUDSTONE, DK. GREY CARBONACEOUS AT BASE WITH COAL INCLUSIONS	78.0								SHEARED ZONE
10	7.0	6.2	89		COAL, BRIGHT FRIABLE	79.0								BEDDING 75° TCA.
						80.0								

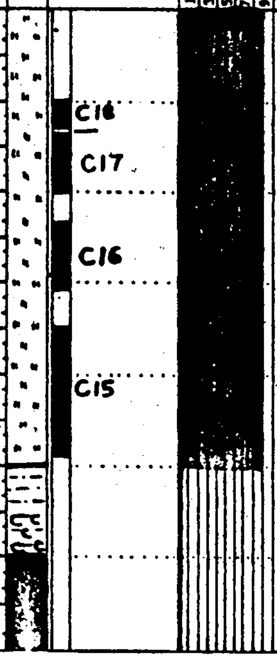

DRILLER K. Frieier DRILL METHOD Water Flush CORE DIAMETER 2 5/8" E. LOGGER R. Adams CORE LOGGER R. Wright

DATE 2/9/80 DRILL RIG ________ BIT USED Diamond DATE ________ DATE 15/12/80

MINERAL ENGINEERING DEPARTMENT

UNIVERSITY OF ALBERTA

GEOTECHNICAL CORE LOG

PROJECT SILKSTONE LOCATION ____ E ____ N ____ ELEVATION ____ DIP VERTICAL BEARING ____ PAGE 2 OF 4 HOLE NO. 2285 (C)

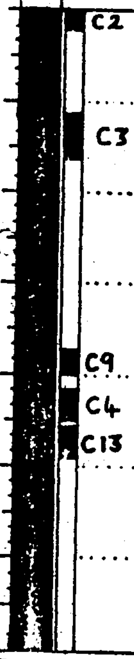

RUN NO.	LENGTH OF RUN	LENGTH RECOVERED	% RECOVERY	CLASSIFICATION	LITHOLOGICAL DESCRIPTION type, colour, texture, bedding, structure, hardness, remarks.	DEPTH	SAMPLE	% RQD 10 30 50 70 90	DISCONTINUITIES TYPE	SEPARATION	FILL	ROUGHNESS	DIP TCA	DEFECT FREQ. / ft.	REMARKS
					COAL, BRIGHT, FRACTURED.	80.0	C2								
						81.0	C3								
						82.0									
						83.0									
						84.0	C9 C4 C13								
						85.0									
11	60	6·5	100			86.0									
						87.0									

DRILLER K. FREIER DRILL METHOD WATER FLUSH * CORE DIAMETER 2 5/8" E. LOGGER R. ADAMS CORE LOGGER R. WRIGHT

DATE 2/9/80 DRILL RIG ____ BIT USED DIAMOND DATE ____ DATE 15/12/80

MINERAL ENGINEERING DEPARTMENT **UNIVERSITY OF ALBERTA** **GEOTECHNICAL CORE LOG**

PROJECT SILKSTONE LOCATION ______ E ______ N ELEVATION ______ DIP VERTICAL BEARING ______ PAGE 3 OF 4 HOLE NO. 2285 (c)

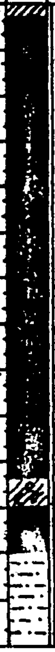

RUN No.	LENGTH OF RUN	LENGTH RECOVERED	% RECOVERY	CLASSIFICATION	LITHOLOGICAL DESCRIPTION type, colour, texture, bedding, structure, hardness, remarks.	DEPTH	SAMPLE	% RQD 10 30 50 70 90	DISCONTINUITIES TYPE	SEPARATION	FILL	ROUGHNESS	DIP TCA	DEFECT FREQ. / ft.	REMARKS
					CLAY, CARBONACEOUS COAL, HARD FRAGMENTED	87.0									
						88.0									NUMEROUS BREAKS ALONG BEDDING
						89.0									
						90.0									
						91.0									
12	70	5.5	79		CLAY/COAL HIGHLY SHEARED	92.0									
					MUDSTONE, MED GREY SOFT	93.0	C7								FRACTURED ALONG BEDDING
						94.0									

DRILLER K. FREIER DRILL METHOD WATER FLUSH CORE DIAMETER 2 5/8" E. LOGGER R. ADAMS CORE LOGGER R. WRIGHT

DATE 2/9/80 DRILL RIG ______ BIT USED DIAMOND DATE ______ DATE 15/12/80

MINERAL ENGINEERING DEPARTMENT **UNIVERSITY OF ALBERTA** **GEOTECHNICAL CORE LOG**

PROJECT SILTSTONE LOCATION ________ E ________ N ELEVATION ________ DIP VERTICAL BEARING ________ PAGE 4 OF 4 HOLE NO. 2285 (c)

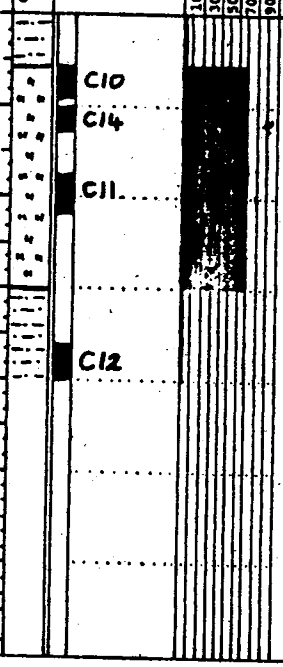

RUN No.	LENGTH OF RUN	LENGTH RECOVERED	% RECOVERY	CLASSIFICATION	LITHOLOGICAL DESCRIPTION type, colour, texture, bedding, structure, hardness, remarks.	DEPTH	GRAPHIC LOG	SAMPLE	% RQD	DISCONTINUITIES TYPE	SEPARATION	FILL	ROUGHNESS	DIP TCA	DEFECT FREQ. / ft.	REMARKS
					SILTSTONE, SHALEY MED GREY, WEAK, FRIABLE	94.0		C10 C14								JOINTING 50° TCA ● 2FT SPACING (perp to dip) PLANAR, CLOSED, MED ROUGH
						95.0										
						96.0		C11								
					MUDSTONE, MED GREY, SOFT, FRIABLE	97.0		C12								
						98.0										
						99.0										

DRILLER K. FREIER DRILL METHOD WATER FLUSH CORE DIAMETER 2 ⅝" E. LOGGER R. ADAMS CORE LOGGER R. WRIGHT

DATE 2/9/80 DRILL RIG ________ BIT USED DIAMOND DATE ________ DATE 15/12/80

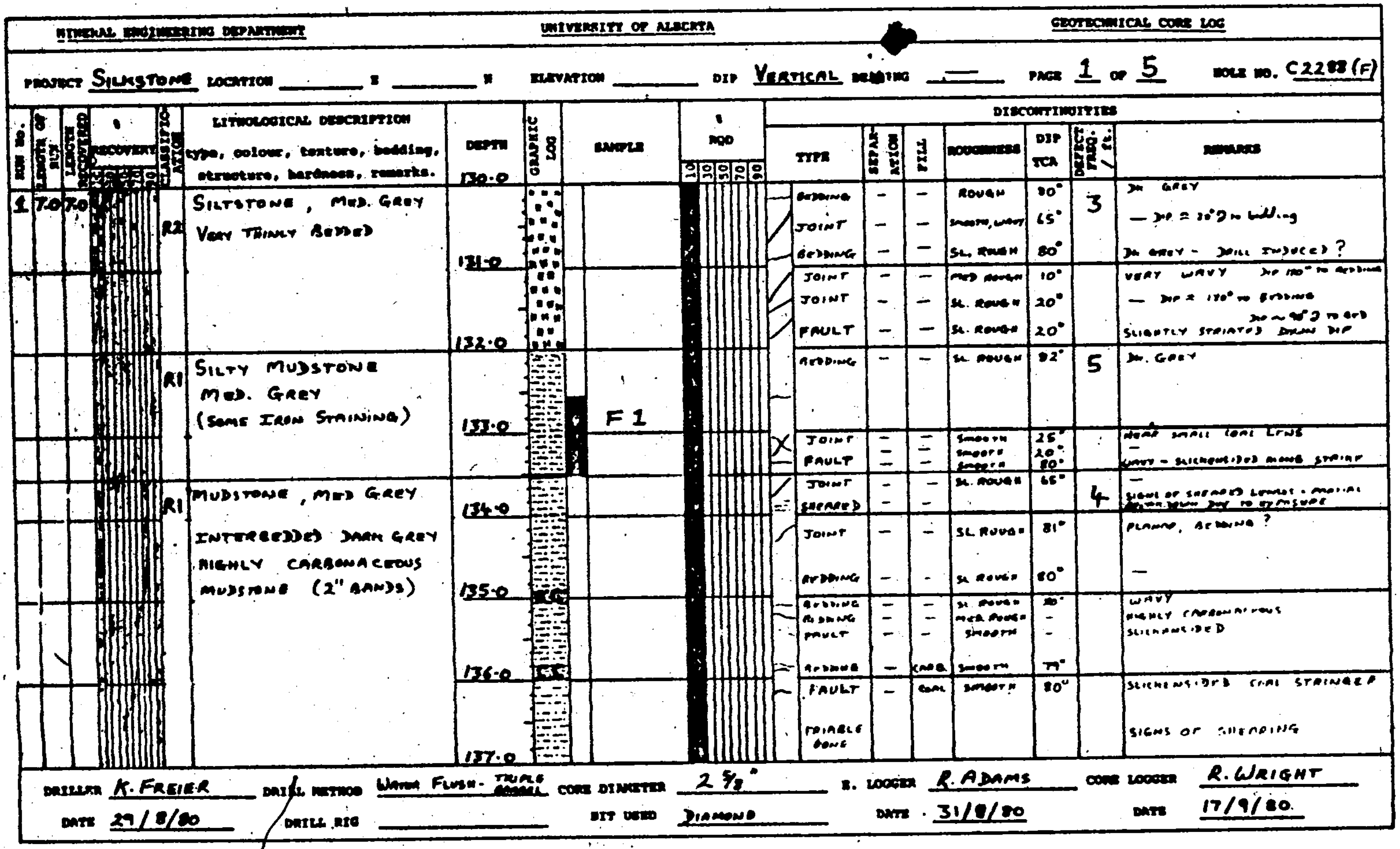

MINERAL ENGINEERING DEPARTMENT UNIVERSITY OF ALBERTA GEOTECHNICAL CORE LOG

PROJECT Silkstone LOCATION ______ E ______ N ELEVATION ______ DIP Vertical BEARING — PAGE 1 OF 5 HOLE NO. C2288(F)

RUN No.	LENGTH OF RUN	LENGTH RECOVERED	% RECOVERY	CLASSIFICATION	LITHOLOGICAL DESCRIPTION type, colour, texture, bedding, structure, hardness, remarks.	DEPTH	GRAPHIC LOG	SAMPLE	% RQD	TYPE	SEPARATION	FILL	ROUGHNESS	DIP TCA	DEFECT FREQ. / ft.	REMARKS
1	7.0	7.0		R2	Siltstone, Med. Grey Very Thinly Bedded	130.0				Bedding	—	—	Rough	80°	3	Dk Grey
										Joint	—	—	Smooth, wavy	65°		— Dip ≈ 30° to bedding
										Bedding	—	—	Sl. Rough	80°		Dk Grey - Drill induced ?
						131.0				Joint	—	—	Med Rough	10°		Very wavy Dip 180° to bedding
										Joint	—	—	Sl. Rough	20°		— Dip ≈ 170° to bedding
										Fault	—	—	Sl. Rough	20°		Dip ~ 90° to bed Slightly striated down dip
				R1	Silty Mudstone Med. Grey (Some Iron Staining)	132.0				Bedding	—	—	Sl. Rough	82°	5	Dk. Grey
						133.0		F1		Joint	— —	— —	Smooth Smooth	25° 20°		Near small coal lens —
										Fault	—	—	Smooth	80°		Wavy - slickensided along strike
				R1	Mudstone, Med Grey Interbedded Dark Grey Highly Carbonaceous Mudstone (2" Bands)	134.0				Joint	—	—	Sl. Rough	65°	4	—
										Sheared	—	—				Signs of sheared layers - partial [illegible] due to exposure
										Joint	—	—	Sl. Rough	81°		Planar, Bedding ?
										Bedding	—	—	Sl. Rough	80°		—
						135.0				Bedding	—	—	Sl. Rough	30°		Wavy
										Bedding	—	—	Med. Rough	-		Highly carbonaceous
										Fault	—	—	Smooth	-		Slickensided
										Bedding	—	Carb.	Smooth	79°		
						136.0				Fault	—	Coal	Smooth	80°		Slickensided coal stringer
										Friable zone						Signs of shearing
						137.0										

DRILLER K. Freier DRILL METHOD Water Flush - Triple Barrel CORE DIAMETER 2 7/8" E. LOGGER R. Adams CORE LOGGER R. Wright

DATE 29/8/80 DRILL RIG ______ BIT USED Diamond DATE 31/8/80 DATE 17/9/80.

Supervised:- D. Tomecek

MINERAL ENGINEERING DEPARTMENT | UNIVERSITY OF ALBERTA | GEOTECHNICAL CORE LOG

PROJECT Silkstone LOCATION ______ E ______ N ELEVATION ______ DIP Vertical BEARING —— PAGE 2 OF 5 HOLE NO. C2288

Run No.	Length of Run	Length Recovered	Classification	Lithological Description type, colour, texture, bedding, structure, hardness, remarks.	Depth	Sample	Type	Separation	Fill	Roughness	Dip TCA	Defect Freq. / ft.	Remarks
					137.0								
2	7.0	7.0	RI	Mudstone, Dark Grey Coal Stringer <1" near top	138.0		Fault Bedding	— —	— —	Smooth Med Rough	30° 85°		Wavy, slickensided down dip Mudstone/coal stringer interface
					139.0		Joint Bedding	— —	— —	Med Rough Sl. Rough	20° 87°		Planar, wavy ~180° to bedding dip —
				Thin coarse sandstone band (iron stained)	140.0							2	
					141.0		Joint Bedding	— —	— —	Rough Sl. Rough	15° 76°		~180° to bedding dip —
				Grading to medium grey mudstone White clay band 1" Bentonite	142.0		Fault Joint	— —	— —	Smooth Sl. Rough	35° 15°		Slickensided Planar
			RI	Mudstone, Dark Grey (Carbonaceous), Broken	143.0		Fault Joint Bedding	— — —	— — Carbon	Smooth Rough Sl. Rough	65° 35° 77°		Slickensided, striated down dip — —
				Mudstone, black, highly carbonaceous, high density Coal, hard, dull	144.0	F2 (T)	Bedding Fault Fault	— — —	Carbon — —	Sl. Rough Smooth Smooth	80° 60° 55°		— Slickensided down dip, 90° to [illegible] no differential [illegible], may be a [illegible] feature

DRILLER K. Freier DRILL METHOD Water Flush - Triple Barrel CORE DIAMETER 2 5/8" E. LOGGER R. Adams CORE LOGGER R. Wright

DATE 29/8/80 DRILL RIG ______ BIT USED Diamond DATE 31/8/80 DATE 17/9/80

SUPPLIED :- [illegible]

MINERAL ENGINEERING DEPARTMENT **UNIVERSITY OF ALBERTA** **GEOTECHNICAL CORE LOG**

PROJECT SILKSTONE LOCATION ______ E ______ N ELEVATION ______ DIP VERTICAL BEARING — PAGE 3 OF 5 HOLE NO. C 2288

RUN No.	LENGTH OF RUN	LENGTH RECOVERED	% RECOVERY	CLASSIFICATION	LITHOLOGICAL DESCRIPTION type, colour, texture, bedding, structure, hardness, remarks.	DEPTH	SAMPLE	TYPE	SEPARATION	FILL	ROUGHNESS	DIP TCA	DEFECT FREQ. / ft.	REMARKS
3	6.075 7.5				COAL, HARD, DULL, FINE WHITE VEINS ALONG MAJOR CLEAT (ARAGONITE FILLING)	144.0		BEDDING JOINT FAULT JOINT	— — — —	— — — —	MED ROUGH SL. ROUGH SMOOTH ROUGH	80° 60° 80° 68°		NO PRONOUNCED CLEAT SHINY SLICKENSIDED — WATER LOSS ~30 GPM
	ERROR IN DRILLER'S LOG, E LOG CORRECTION →					145.0	F6 SAMPLED [illegible] AFTER LOGGING [illegible]							
					COAL MORE FRIABLE, SHINY, CLEAT PRONOUNCED	146.0		JOINT BEDDING	2mm —	$CaCO_3$ —	SL. ROUGH SL ROUGH	12° 73°		MAJOR CLEAT INFILLING —
						147.0	F3. σ_c	BEDDING FAULT BEDDING	— — —	— — —	SMOOTH SMOOTH SMOOTH	80° 80° 70°	—	SHINY SLICKENSIDED, STRIATED —
						148.0	F7 (σ Fc)	FAULT JOINT FAULT	— — —	— — —	SMOOTH SMOOTH SMOOTH	30° 60° 80°		SLICKENSIDED DOWN DIP, DIP DIRN SAME AS BEDDING SHINY STRIATIONS IN APP. DIRECTIONS
						149.0		BEDDING? JOINT FAULT	— — —	— — —	SL. ROUGH MED. ROUGH SHINY	78° 55° 70°		— DIP DIRN ALONG BEDDING SLICKENSIDED, DIRN AS BEDDING
					FINE WHITE FILLING ALONG BEDDING (ARAGONITE) COAL LAMINATED, FRIABLE	150.0 151.0		SHEARED ZONE						SLICKENSIDED PARALLEL PLATES, ALONG BEDDING

DRILLER K. FRIER DRILL METHOD Wire Line - Triple Barrel CORE DIAMETER 2 5/8" E. LOGGER R. ADAMS CORE LOGGER R. WRIGHT

DATE 29/8/80 DRILL RIG ______ BIT USED DIAMOND DATE 31/8/80 DATE 17/9/80

SUPERVISOR :- D. TOMECEK

MINERAL ENGINEERING DEPARTMENT · UNIVERSITY OF ALBERTA · GEOTECHNICAL CORE LOG

PROJECT SILKSTONE LOCATION ________ E ________ N ELEVATION ________ DIP VERTICAL BEARING — PAGE 4 OF 5 HOLE NO. C2288

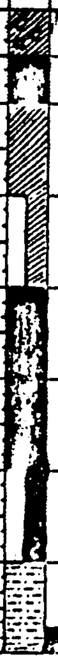

RUN No.	LENGTH OF RUN	LENGTH RECOVERED	% RECOVERY	CLASSIFICATION	LITHOLOGICAL DESCRIPTION type, colour, texture, bedding, structure, hardness, remarks.	DEPTH	SAMPLE	% RQD	DISCONTINUITIES TYPE	SEPARATION	FILL	ROUGHNESS	DIP TCA	DEFECT FREQ. / ft.	REMARKS
						151.0									
					CLAY, SOFT, 'STICKY', BLACK, CARBONACEOUS		F4								
4	70	50			COAL, FRACTURED	152.0									
					CLAY, MEDIUM BROWN, SOFT COAL LENSES (SMALL)	153.0									
						154.0									
					2 FT. CORE LOSS E-LOG INTER-PRETATION COAL, HIGHLY FRAGMENTED	155.0									
						156.0									
						157.0									
					MUDSTONE, MEDIUM GREY, SILTY	158.0	F5 0c								WELL DEFINED PLANAR JOINTS ~30° TCA

DRILLER K. FREIER DRILL METHOD Water Flush, Triple Barrel CORE DIAMETER 2 ½" E. LOGGER R. ADAMS CORE LOGGER R. WRIGHT

DATE 29/8/80 DRILL RIG ________ BIT USED Diamond DATE 31/8/80 DATE 17/9/80

SUPERVISED :- D. Torreck

MINERAL ENGINEERING DEPARTMENT

UNIVERSITY OF ALBERTA

[illegible] CORE LOG

PROJECT Silkstone LOCATION ______ E ______ N ELEVATION ______ DIP Vertical BEARING —— PAGE [illegible] OF 5 HOLE NO. C2288

RUN No.	LENGTH OF RUN	LENGTH RECOVERED	% RECOVERY 10 30 50 70 90	CLASSIFICATION	LITHOLOGICAL DESCRIPTION type, colour, texture, bedding, structure, hardness, remarks.	DEPTH	GRAPHIC LOG	SAMPLE	% RQD 10 30 50 70 90	DISCONTINUITIES TYPE	SEPARATION	FILL	[illegible]	DIP TCA	DEFECT FREQ. / ft.	REMARKS
						158.0		F5 E								
5	4.5	4.5														
					Siltstone, Med. Grey, V. Fine Carbonaceous Banding < 1mm	159.0										Regular planar joints 30° TCA, no infilling
						160.0										
					Grading to V. Fine Grained Siltstone	161.0										
						162.0										Water loss ~ 50 GPM recorded Reason for drill stoppage
					TD 163 FT.	163.0										
						164.0										

DRILLER K. Freier DRILL METHOD Water Flush, Triple Barrel CORE DIAMETER 2 3/8" E. LOGGER R. Adams CORE LOGGER R. Wright

DATE 29/8/80 DRILL RIG ______ BIT USED Diamond DATE 31/8/80 DATE 17/9/80

Supervised D. Tom

MINERAL ENGINEERING DEPARTMENT — **UNIVERSITY OF ALBERTA** — **GEOTECHNICAL CORE LOG**

PROJECT SILTSTONE LOCATION ______ N ______ E ELEVATION ______ DIP VERTICAL BEARING —— PAGE 1 OF 7 HOLE NO. C2289(6)

RUN No.	LENGTH OF RUN	LENGTH RECOVERED	CLASSIFICATION	LITHOLOGICAL DESCRIPTION type, colour, texture, bedding, structure, hardness, remarks.	DEPTH	SAMPLE	DISCONTINUITIES TYPE	SEPARATION	FILL	ROUGHNESS	DIP TCA	DEFECT FREQ. / ft.	REMARKS
1	7.0	5.7	R1	SILTSTONE, DK. GREY/GREEN APHANITIC DARK BANDING (BEDDING)	97.0	G1 (σc)	SHEARED	—	—	MED. ROUGH	90°		WAVY, STRIATIONS
					98.0	G2 τjoint	JOINT	—	—	MED. ROUGH	20°		DIP 180° TO BEDDING DIP
							SHEAR	—	—	MED. ROUGH	85°		STRIATIONS PARR TO DIP
			R1	MUDSTONE, MED GREY/GREEN SILTY, DARK BANDING	99.0		JOINT JOINT JOINT	— — —	— — —	MED. ROUGH SL. ROUGH SL. ROUGH	90° 70° 60°	—	— — —
							JOINT JOINT	—	— CaCO3	SL. ROUGH	20°		DIP 180° TO BEDDING DIP
							JOINT JOINT	— —	— —	MED. ROUGH SL. ROUGH	90° 60°		— DIP 90° D FROM BEDDING DIP
				1" CHERT BAND	100.0	G3 τbed							
1'3" CORE LOST	ASSUMED HERE		R1	OVER DRILLED TRACES OF IRON STAINING LOW RECOVERY 1.3' LOST SMALL COAL LENSES 1mm THICK	101.0 102.0								
			R1	MUDSTONE, MED GREY SILTY (DK. GREY MUDSTONE BAND 2" AT TOP) (MINOR IRON STAINING)	103.0								DRILL INDUCED
						G4 σc	JOINT JOINT	— —	— —	SL. ROUGH SL. ROUGH	90° 90°		SIGNS OF SHEARING
					104.0		JOINT JOINT	— —	— —	SL. ROUGH SL. ROUGH	90° 80°		SIGNS OF SHEARING

DRILLER K. FREIER DRILL METHOD Water Flush, Triple Barrel CORE DIAMETER 2⅞" E. LOGGER ______ CORE LOGGER R. WRIGHT

DATE 2/9/80 DRILL RIG ______ BIT USED DIAMOND DATE ______ DATE 29/9/80

SUPERVISED: D. TOMECEK

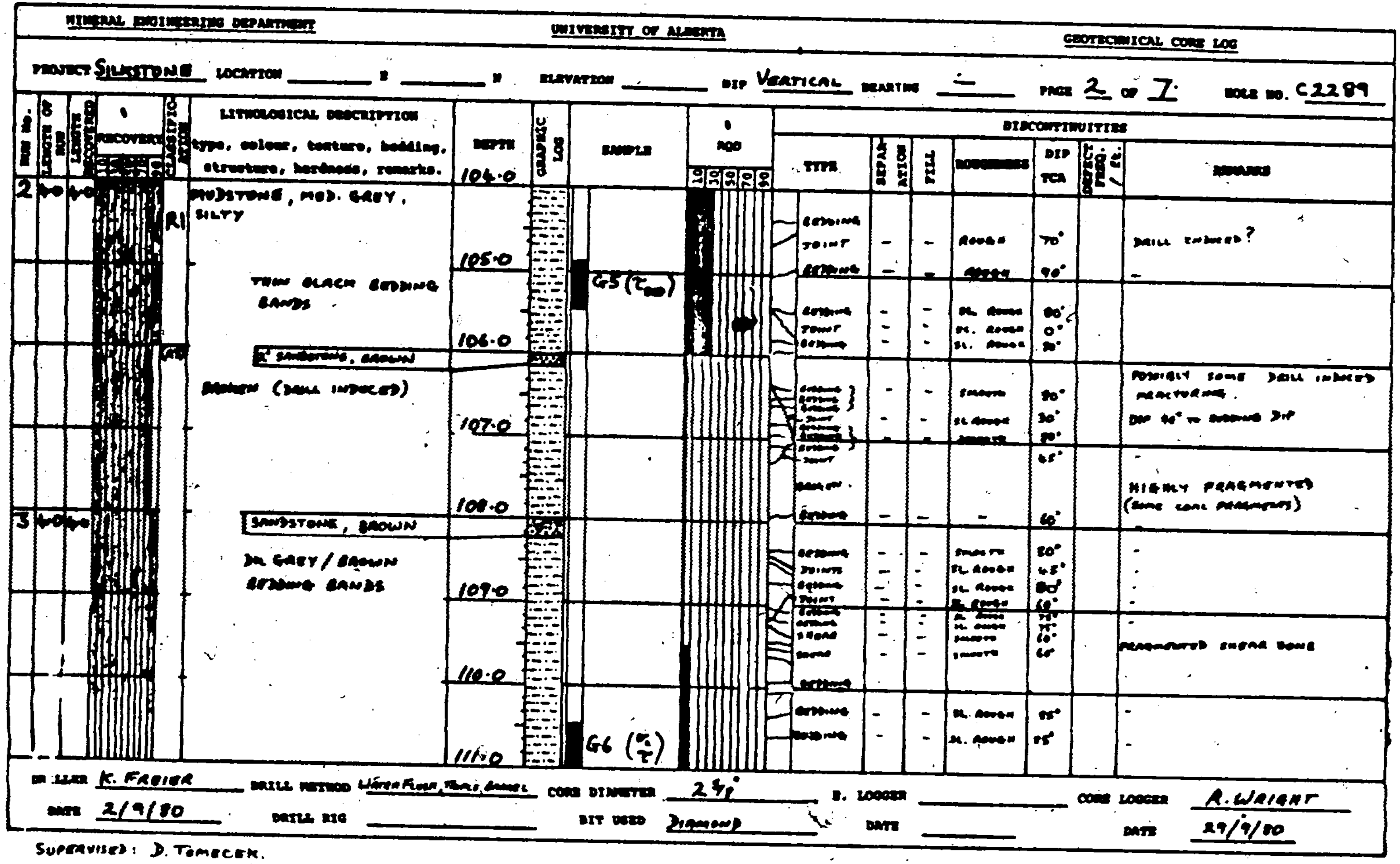

MINERAL ENGINEERING DEPARTMENT — UNIVERSITY OF ALBERTA — GEOTECHNICAL CORE LOG

PROJECT SILTSTONE LOCATION ________ E ________ N ELEVATION ________ DIP VERTICAL BEARING – PAGE 2 OF 7 HOLE NO. C2289

RUN No.	LENGTH OF RUN	LENGTH RECOVERED	CLASSIFICATION	LITHOLOGICAL DESCRIPTION type, colour, texture, bedding, structure, hardness, remarks.	DEPTH	SAMPLE	TYPE	SEPARATION	FILL	ROUGHNESS	DIP TCA	DEFECT FREQ. / ft.	REMARKS
2	[illegible]	[illegible]	R1	MUDSTONE, MED. GREY, SILTY	104.0		BEDDING						
							JOINT	–	–	ROUGH	70°		DRILL INDUCED?
							BEDDING	–	–	ROUGH	90°		–
				THIN BLACK BEDDING BANDS	105.0	G5 (τ_{BD})	BEDDING	–	–	SL. ROUGH	80°		
							JOINT	–	–	SL. ROUGH	0°		
							BEDDING	–	–	SL. ROUGH	90°		
			[illegible]	1" SANDSTONE, BROWN	106.0		BEDDING BEDDING BEDDING	–	–	SMOOTH	90°		POSSIBLY SOME DRILL INDUCED FRACTURING.
				BROKEN (DRILL INDUCED)			JOINT BEDDING BEDDING	–	–	SL. ROUGH	30°		DIP 40° TO BEDDING DIP
							BEDDING	–	–	SMOOTH	90°		
					107.0		JOINT				65°		–
							BROKEN						HIGHLY FRAGMENTED (SOME COAL FRAGMENTS)
							BEDDING	–	–	–	60°		
3	[illegible]	[illegible]		SANDSTONE, BROWN	108.0		BEDDING	–	–	SMOOTH	80°		–
				DK. GREY / BROWN BEDDING BANDS			JOINTS	–	–	SL. ROUGH	45°		–
							BEDDING	–	–	SL. ROUGH	80°		–
							JOINT	–	–	SL. ROUGH	60°		–
					109.0		BEDDING	–	–	SL. ROUGH	75°		–
							BEDDING	–	–	SL. ROUGH	75°		
							SHEAR	–	–	SMOOTH	60°		FRAGMENTED SHEAR ZONE
							SHEAR	–	–	SMOOTH	60°		
							BEDDING						
					110.0		BEDDING	–	–	SL. ROUGH	85°		–
						G6 ($\frac{\%}{\tau}$)	BEDDING	–	–	SL. ROUGH	85°		–
					111.0								

DRILLER K. FRASER DRILL METHOD WATER FLUSH, TRIPLE BARREL CORE DIAMETER 2⅛" E. LOGGER ________ CORE LOGGER R. WRIGHT

DATE 2/9/80 DRILL RIG ________ BIT USED DIAMOND DATE ________ DATE 29/9/80

SUPERVISED: D. TOMECEK.

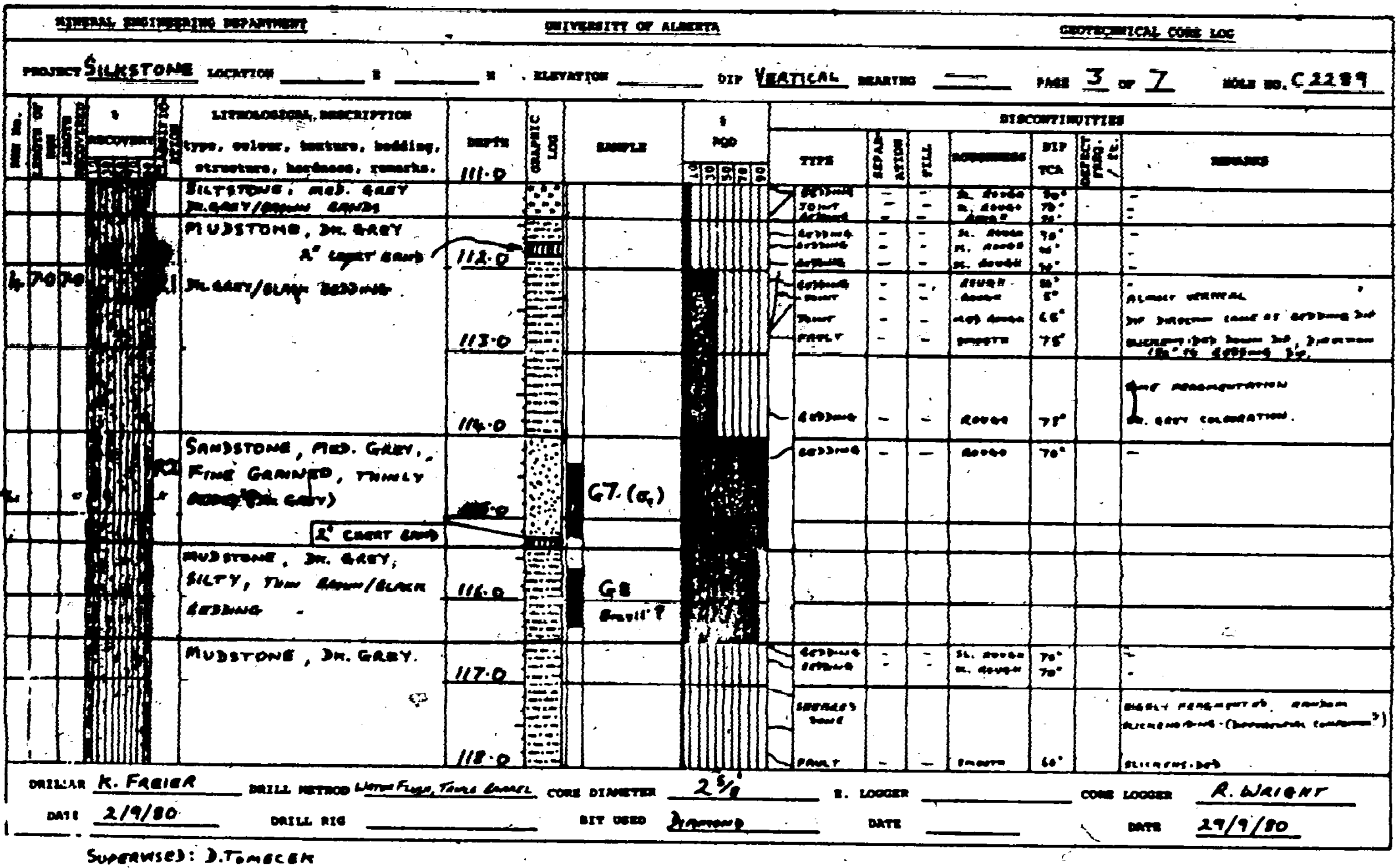

MINERAL ENGINEERING DEPARTMENT — UNIVERSITY OF ALBERTA — GEOTECHNICAL CORE LOG

PROJECT SILKSTONE LOCATION ______ E ______ N . ELEVATION ______ DIP VERTICAL BEARING —— PAGE 3 OF 7 HOLE NO. C2289

RUN No.	LENGTH OF RUN	LENGTH RECOVERED	LITHOLOGICAL DESCRIPTION type, colour, texture, bedding, structure, hardness, remarks.	DEPTH	SAMPLE	DISCONTINUITIES TYPE	SEPARATION	FILL	ROUGHNESS	DIP TCA	DEFECT FREQ. / ft.	REMARKS
				111.0								
			SILTSTONE; MED. GREY DK.GREY/BROWN BANDS			BEDDING JOINT BEDDING	– – –	– – –	SL. ROUGH SL. ROUGH ROUGH?	50° 70° 70°		– – –
			MUDSTONE, DK. GREY 2" LIGHT BAND	112.0		BEDDING BEDDING BEDDING	– – –	– – –	SL. ROUGH M. ROUGH M. ROUGH	70° 60° 70°		– – –
4	70	70	DK.GREY/BLACK BEDDING.	113.0		BEDDING JOINT JOINT FAULT	– – – –	– – – –	ROUGH ROUGH [illegible] ROUGH SMOOTH	80° 5° 66° 75°		– ALMOST VERTICAL DIP DIRECTION SAME AS BEDDING DIP SLICKENSIDED [illegible] (80° TO BEDDING DIP)
				114.0		BEDDING	–	–	ROUGH	75°		[illegible] FRAGMENTATION [illegible]. GREY COLOURATION.
			SANDSTONE, MED. GREY, FINE GRAINED, THINLY BEDDED (DK. GREY) 2" CHERT BAND	115.0	G7 (σ_1)	BEDDING	–	–	ROUGH	70°		–
			MUDSTONE, DK. GREY, SILTY, THIN BROWN/BLACK BEDDING	116.0	G8 BRAZIL'?							
			MUDSTONE, DK. GREY.	117.0		BEDDING BEDDING	– –	– –	SL. ROUGH M. ROUGH	70° 70°		– –
				118.0		SHEARED ZONE FAULT	 –	 –	 SMOOTH	 60°		HIGHLY FRAGMENTED, RANDOM SLICKENSIDES (DIRECTION [illegible]?) SLICKENSIDED

DRILLER K. FREIER DRILL METHOD WATER FLUSH, TRIPLE BARREL CORE DIAMETER 2 5/8" E. LOGGER ______ CORE LOGGER R. WRIGHT

DATE 2/9/80 DRILL RIG ______ BIT USED DIAMOND DATE ______ DATE 29/9/80

SUPERVISED: D.TOMECEK

MINERAL ENGINEERING DEPARTMENT — UNIVERSITY OF ALBERTA — GEOTECHNICAL CORE LOG

PROJECT Silkstone LOCATION ______ E ______ N ELEVATION ______ DIP Vertical BEARING —— PAGE 4 of 7 HOLE NO. C2289

Run No.	Length of Run	Length Recovered	Lithological Description (type, colour, texture, bedding, structure, hardness, remarks)	Depth	Sample	Type	Separation	Fill	Roughness	Dip TCA	Defect Freq. /ft.	Remarks
			MUDSTONE, BLACK, HIGHLY CARBONACEOUS	118.0		FAULT BEDDING FAULT	– – –	– – –	SMOOTH – SMOOTH	60° 80° 45°		SLICKENSIDED SLICKENSIDED
5	7.0	7.0	COAL, DULL, HARD, FRACTURED (FRAGMENTED) MUDSTONE, MED. GREY, SOME MINOR COAL LENSES AND STRINGERS < 1/4" AT TOP	119.0		FRAGMENTED RANDOM BEDDING SHEAR SHEAR (?)	– – –	– – –	SMOOTH SMOOTH SMOOTH	~60° 60° 60°		SLICKENSIDED, 'WAVY' - DEVIATING [illegible]? SLICKENSIDED, WAVY
				120.0		BEDDING				65°		DISCONTINUOUS FRACTURES AROUND COAL LENS, DRILL INDUCED DRILL FRACTURES
				121.0		BEDDING BEDDING BEDDING	– – –	CARB – CARB	SL. ROUGH ROUGH ROUGH			– - BROWNISH STAIN ON WEAKNESS PLANE
				122.0	G9 broken?	BEDDING JOINT	–	–	ROUGH	~10°		ALMOST VERTICAL, DRILL INDUCED?
			MUDSTONE, MED. GREY, SILTY	123.0		BEDDING JOINT	– –	– –	SL. ROUGH ROUGH	70° 30°		WAVY
			MUDSTONE, MED. GREY	124.0	G10	JOINT BEDDING JOINT BEDDING	– – – –	– – – –	SL. ROUGH SL. ROUGH – SL. ROUGH	60° 80° 60° 85°		– – SOME STRIATIONS, WAVY –
				125.0								

DRILLER K. Freier DRILL METHOD Water Flush, Triple Barrel CORE DIAMETER 2 5/8" E. LOGGER ______ CORE LOGGER R. WRIGHT

DATE 2/9/80 DRILL RIG ______ BIT USED Diamond DATE ______ DATE 29/9/80

SUPERVISED: D. TOMECEK

MINERAL ENGINEERING DEPARTMENT **UNIVERSITY OF ALBERTA** **GEOTECHNICAL CORE LOG**

PROJECT SILKSTONE LOCATION ______ E ______ N ______ ELEVATION ______ DIP VERTICAL BEARING — PAGE 5 OF 7 HOLE NO. C2289

RUN No.	LENGTH OF RUN	LENGTH RECOVERED	CLASSIFICATION	LITHOLOGICAL DESCRIPTION type, colour, texture, bedding, structure, hardness, remarks.	DEPTH	SAMPLE
					125.0	
6	60	60		[illegible] CLAY, [illegible], SOFT, [illegible] MUDSTONE, DK. GREY	126.0	G11
					127.0	G12 [illegible]?
				MUDSTONE, BLACK, HIGHLY CARBONACEOUS		
				COAL, DULL, HARD	128.0	
					129.0	G13 σ + ?
				STRONG COAL, SIGNS OF CaCO₃ (ARAGONITE) INFILLING OF CLEAT	130.0	
					131.0	G14 σ + ?
			R2		132.0	

DISCONTINUITIES

TYPE	SEPARATION	FILL	ROUGHNESS	DIP TCA	DEFECT FREQ. / ft.	REMARKS
SHEAR	–	[illegible]	–	70°		THIN, SOFT, CARBONACEOUS LAYER.
JOINT INTERSECTION	– –	– –	– –	30° 5°		~50° BETWEEN JOINT ANGLES (CURVED SHEARING)
RANDOM SHEAR	–	–	–	–		DIFFERENTIAL CONSOLIDATION OR DEWATERING FRACTURES.
JOINT	–	–	SL. ROUGH	50°		–
FAULT	–	–	SL. ROUGH	60°		STRIATED, WAVY ;
BEDDING	–	–	ROUGH	–		–
JOINT	–	–	V. ROUGH	20°		DRILL INDUCED ?
BROKEN BEDDING	–	–	SL. ROUGH			FRAGMENTED DUE TO STIFF FRACTURE OR DRILLING –
BEDDING	–	–	SL. ROUGH			–
FAULT	–	–	SMOOTH	70°		SLICKENSIDED, WAVY
SHEAR	–	–	SMOOTH	70°		FRAGMENTED, SHINY, STRIATED.
BEDDING	–	CaCO₃	ROUGH			–
BEDDING	–	–	ROUGH	70°		(PARTLY SMOOTH)
JOINT	–	–	SL. ROUGH	70°		PARTLY SMOOTH

DRILLER K. FREIER DRILL METHOD WATERFLUSH, TRIPLE BARREL CORE DIAMETER 2 5/8" E. LOGGER ______ CORE LOGGER R. WRIGHT

DATE 2/9/80 DRILL RIG ______ BIT USED DIAMOND DATE ______ DATE 29/9/80

SUPERVISED : D. TOMLESEN

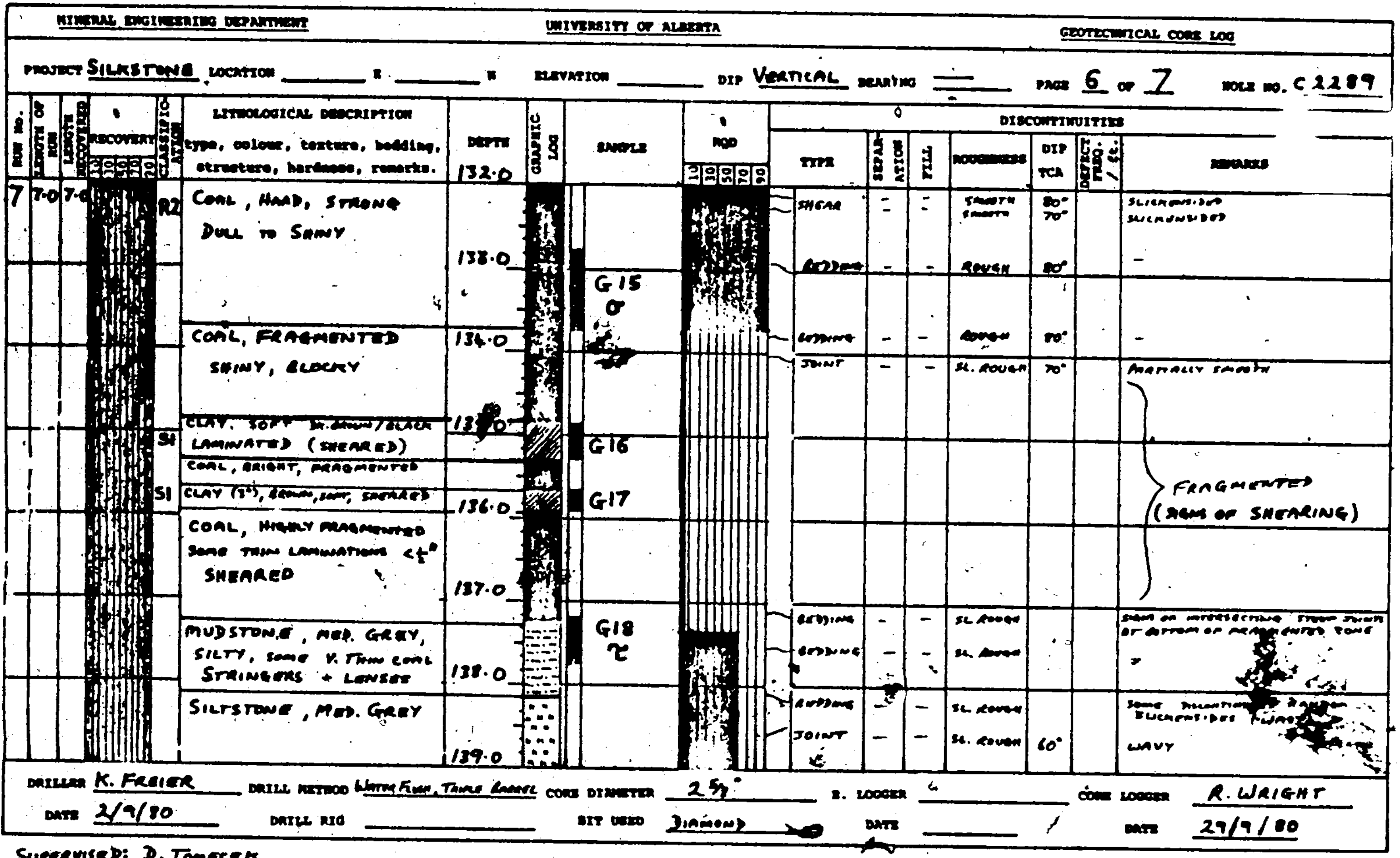

MINERAL ENGINEERING DEPARTMENT **UNIVERSITY OF ALBERTA** **GEOTECHNICAL CORE LOG**

PROJECT SILKSTONE LOCATION ______ E ______ N ELEVATION ______ DIP VERTICAL BEARING ______ PAGE 6 OF 7 HOLE NO. C 2289

RUN No.	LENGTH OF RUN	LENGTH RECOVERED	CLASSIFICATION	LITHOLOGICAL DESCRIPTION type, colour, texture, bedding, structure, hardness, remarks.	DEPTH	SAMPLE
7	7·0	7·0	R2	COAL, HARD, STRONG DULL TO SHINY	132·0 133·0	G15
				COAL, FRAGMENTED SHINY, BLOCKY	134·0	
			SI	CLAY. SOFT DK. BROWN/BLACK LAMINATED (SHEARED)	135·0	G16
				COAL, BRIGHT, FRAGMENTED		
			SI	CLAY (3"), BROWN, SOFT, SHEARED	136·0	G17
				COAL, HIGHLY FRAGMENTED SOME THIN LAMINATIONS <½" SHEARED	137·0	
				MUDSTONE, MED. GREY, SILTY, SOME V. THIN COAL STRINGERS + LENSES	138·0	G18
				SILTSTONE, MED. GREY	139·0	

DISCONTINUITIES

TYPE	SEPARATION	FILL	ROUGHNESS	DIP TCA	DEFECT FREQ. / ft.	REMARKS
SHEAR	– –	– –	SMOOTH SMOOTH	80° 70°		SLICKENSIDED SLICKENSIDED
BEDDING	–	–	ROUGH	80°		–
BEDDING	–	–	ROUGH	70°		–
JOINT	–	–	SL. ROUGH	70°		PARTIALLY SMOOTH
						FRAGMENTED (SIGNS OF SHEARING)
BEDDING	–	–	SL. ROUGH			SIGNS OF INTERSECTING STEEP JOINTS AT BOTTOM OF FRAGMENTED ZONE
BEDDING	–	–	SL. ROUGH			"
BEDDING	–	–	SL. ROUGH			SOME [illegible] RANDOM SLICKENSIDES [illegible]
JOINT	–	–	SL. ROUGH	60°		WAVY

DRILLER K. FREIER DRILL METHOD WATER FLUSH, TRIPLE BARREL CORE DIAMETER 2 5/8" R. LOGGER ______ CORE LOGGER R. WRIGHT

DATE 2/9/80 DRILL RIG ______ BIT USED DIAMOND DATE ______ DATE 29/9/80

SUPERVISED: D. TOMECEK

MINERAL ENGINEERING DEPARTMENT | UNIVERSITY OF ALBERTA | GEOTECHNICAL CORE LOG

PROJECT SILKSTONE LOCATION ________ E ________ N ELEVATION ________ DIP VERTICAL BEARING —— PAGE 7 OF 7 HOLE NO. C2289

RUN No.	LENGTH OF RUN	LENGTH RECOVERED	% RECOVERY	CLASSIFICATION	LITHOLOGICAL DESCRIPTION type, colour, texture, bedding, structure, hardness, remarks.	DEPTH	GRAPHIC LOG	SAMPLE	% RQD	DISCONTINUITIES TYPE	SEPARATION	FILL	ROUGHNESS	DIP TCA	DEFECT FREQ. / ft.	REMARKS
8	70	74		R1	MUDSTONE, MED. GREY, SILTY	139.0 140.0		G19 C?		JOINT BEDDING BEDDING BEDDING	– – – –	– – – –	ROUGH SL. ROUGH SL. ROUGH ROUGH	75° 75° 75° 75°		DIP 180° TO BEDDING DIP. – – –
						141.0				JOINT BEDDING FAULT	1mm – –	COAL – –	SL. ROUGH – –	80° 75° 50°		COAL STRINGER – SLICKENSIDED, DIP SAME AS BEDDING
				R1	SANDSTONE, LIGHT GREY, FINE GRAINED, THIN BLACK BEDDING	142.0				JOINT BEDDING	– –	– –	ROUGH SL. ROUGH	20° 76°		DIP 180° TO BED DIP, WAVY – (STEEP JOINTING APPROX 1' SPACING)
					SOME V. SMALL CARBONACEOUS LENSES	143.0				JOINT FAULT FAULT	– – –	– – –	– – –	30° 60° 70°		– DIP 75° FROM BED DIP, STRIATED, WAVY STRIATIONS, WAVY
				R1	MUDSTONE, MED. GREY, SILTY (SHEARED AT BASE)	144.0				BEDDING BEDDING BEDDING	– – –	– – –	– – –	75° 75° 75°		– – –
				R1	MUDSTONE, DK. GREY, FRAGMENTED	145.0				BEDDING JOINT BEDDING			ROUGH	75° 20°		– – } SHEARED ZONE
				R2	SILTSTONE, MED. GREY	146.0		G20 C		BEDDING	–	–	ROUGH	75°		–

DRILLER K. FRASER DRILL METHOD Water Flush, Triple Barrel CORE DIAMETER 2 5/8" E. LOGGER ________ CORE LOGGER R. WRIGHT

DATE 2/9/80 DRILL RIG ________ BIT USED DIAMOND DATE ________ DATE 29/9/80

SUPERVISED: D. TOMECEK

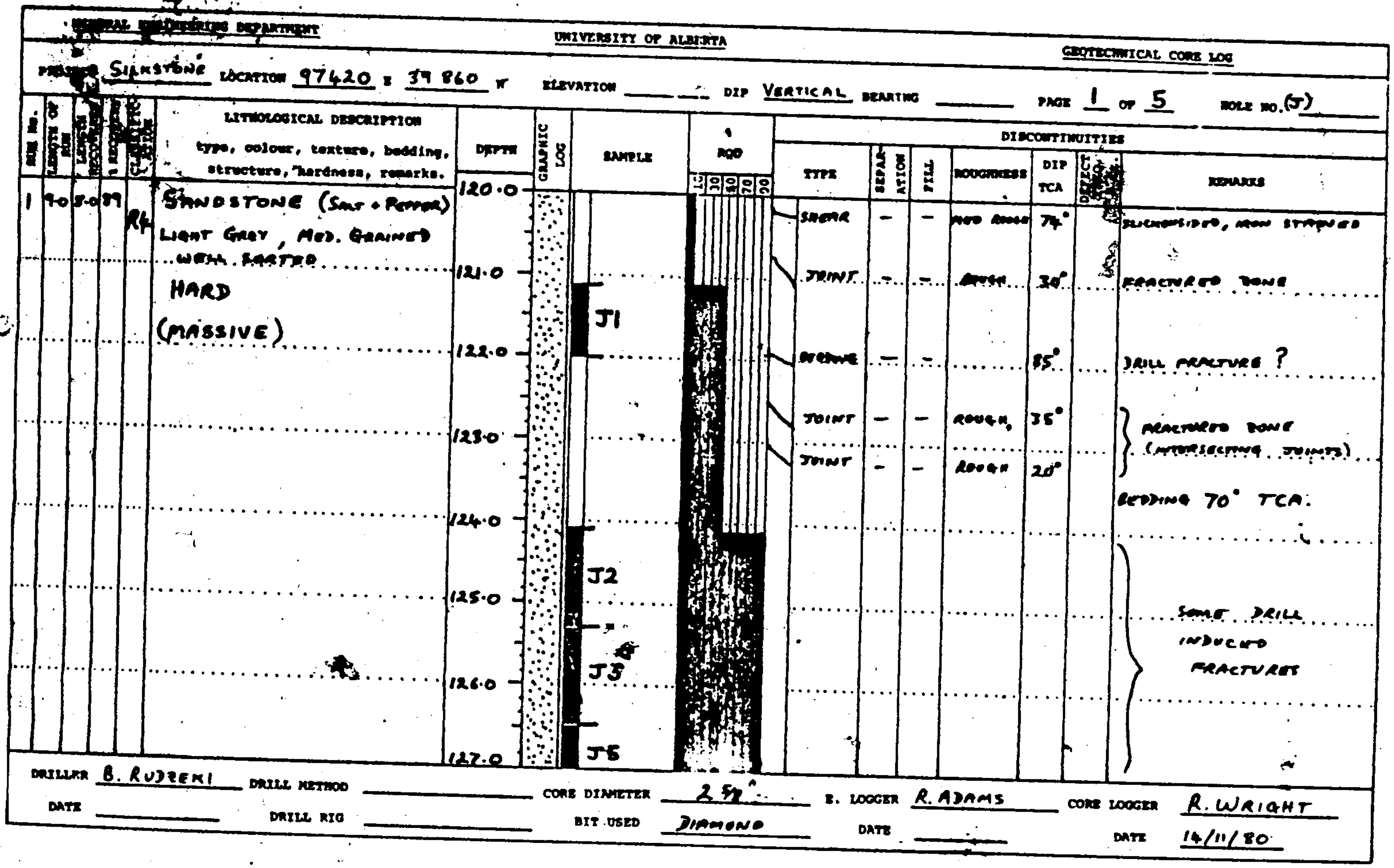

GENERAL ENGINEERING DEPARTMENT

UNIVERSITY OF ALBERTA

GEOTECHNICAL CORE LOG

PROJECT SILKSTONE LOCATION 97420 E 39 860 N ELEVATION ______ DIP VERTICAL BEARING ______ PAGE 1 OF 5 HOLE NO. (J)

RUN No.	LENGTH OF RUN	LENGTH RECOVERED	% RECOVERY	CLASSIFICATION	LITHOLOGICAL DESCRIPTION type, colour, texture, bedding, structure, hardness, remarks.	DEPTH	SAMPLE
1	9.0	8.0	89	R4	SANDSTONE (SALT + PEPPER) LIGHT GREY, MED. GRAINED WELL SORTED HARD (MASSIVE)	120.0 to 127.0	J1 J2 J3 J5

DISCONTINUITIES

TYPE	SEPARATION	FILL	ROUGHNESS	DIP TCA	DEFECT	REMARKS
SHEAR	–	–	MED ROUGH	74°		SLICKENSIDED, IRON STAINED
JOINT	–	–	ROUGH	30°		FRACTURED ZONE
BEDDING	–	–		85°		DRILL FRACTURE ?
JOINT	–	–	ROUGH	35°		FRACTURED ZONE (INTERSECTING JOINTS)
JOINT	–	–	ROUGH	20°		
						BEDDING 70° TCA.
						SOME DRILL INDUCED FRACTURES

DRILLER B. RUDZEKI DRILL METHOD ______ CORE DIAMETER 2 5/8" R. LOGGER R. ADAMS CORE LOGGER R. WRIGHT

DATE ______ DRILL RIG ______ BIT USED DIAMOND DATE ______ DATE 14/11/80

MINERAL ENGINEERING DEPARTMENT **UNIVERSITY OF ALBERTA** **GEOTECHNICAL CORE LOG**

PROJECT SILTSTONE LOCATION 97420 E 39 960 N ELEVATION ______ DIP VERTICAL BEARING ______ PAGE 2 OF 5 HOLE NO. (J)

RUN No.	LENGTH OF RUN	LENGTH RECOVERED	% RECOVERY	CLASSIFICATION	LITHOLOGICAL DESCRIPTION type, colour, texture, bedding, structure, hardness, remarks.	DEPTH	TYPE	SEPARATION	FILL	ROUGHNESS	DIP TCA	DEFECT FREQ. / ft.	REMARKS
1						127.0							
						128.0							
2	8.0	7.25	91			129.0							
					BEDDING 10° TCA	130.0							
					SOME SMALL CARBONACEOUS INCLUSIONS	131.0							
						132.0							
						133.0							} SLIGHTLY FRACTURED ZONE
						134.0							

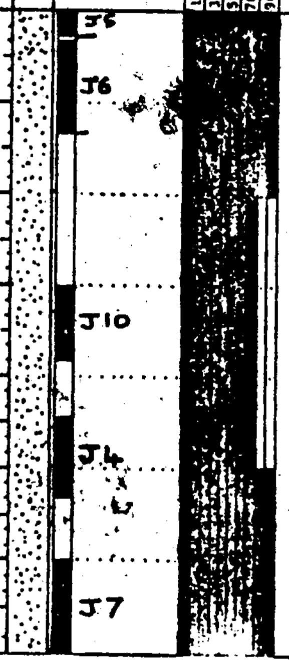

DRILLER E. RUDZEKI DRILL METHOD ______ CORE DIAMETER 2 5/8" E. LOGGER R. ADAMS CORE LOGGER R. WRIGHT

DATE ______ DRILL RIG ______ BIT USED DIAMOND DATE ______ DATE 14/11/80

MINERAL ENGINEERING DEPARTMENT — UNIVERSITY OF ALBERTA — GEOTECHNICAL CORE LOG

PROJECT SILKSTONE LOCATION 97420 E 39860 N ELEVATION ______ DIP VERTICAL BEARING ______ PAGE 3 OF 5 HOLE NO. (J)

RUN No.	LENGTH OF RUN	LENGTH RECOVERED	% RECOVERY	CLASSIFICATION	LITHOLOGICAL DESCRIPTION type, colour, texture, bedding, structure, hardness, remarks.	DEPTH	DISCONTINUITIES TYPE	SEPARATION	FILL	ROUGHNESS	DIP TCA	DEFECT FREQ. / ft.	REMARKS
						134·0							
						135·0							
						136·0							
3	9·0	3·6	40		N.B. MAJORITY OF LITHOLOGY INFERRED FROM E LOGS OF RUN #3	137·0							
						138·0							
					0·45' COAL RECOVERED TO 1·2' BRIGHT, CRUSHED TO CRUMMY (FRIABLE)	139·0							
						140·0							
						141·0							

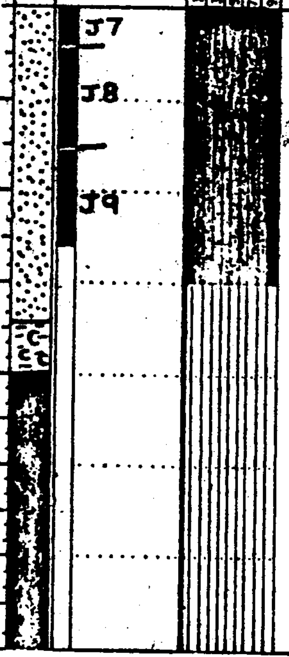

DRILLER B. RUDZEKI DRILL METHOD ______ CORE DIAMETER 2 5/8" E. LOGGER R. ADAMS CORE LOGGER R. WRIGHT

DATE ______ DRILL RIG ______ BIT USED DIAMOND DATE ______ DATE 16/11/80

MINERAL ENGINEERING DEPARTMENT **UNIVERSITY OF ALBERTA** **GEOTECHNICAL CORE LOG**

PROJECT SILKSTONE LOCATION 97 420 E 39860 N ELEVATION ______ DIP VERTICAL BEARING ______ PAGE 4 OF 5 HOLE NO. (J)

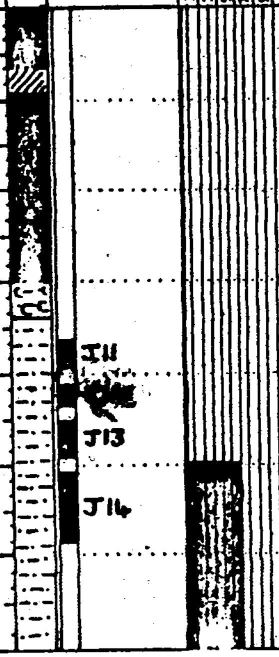

RUN No.	LENGTH OF RUN	LENGTH RECOVERED	% RECOVERY	CLASSIFICATION	LITHOLOGICAL DESCRIPTION type, colour, texture, bedding, structure, hardness, remarks.	DEPTH	SAMPLE	DISCONTINUITIES TYPE	SEPARATION	FILL	ROUGHNESS	DIP TCA	DEFECT FREQ. / ft.	REMARKS
						161.0								
					CLAY, LIGHT TO MED BROWN VERY SOFT. . [illegible] FT. RECOVERED	162.0								
					COAL, BRIGHT, FRIABLE 0.76 FT. RECOVERED	163.0								
					CARBONACEOUS MUDSTONE	164.0								RANDOM SHEARING
					MUDSTONE, DK. GREY, MASSIVE, SILTY		J11	JOINT	–	–	MED ROUGH	50°		
						165.0	[illegible]	JOINT	–	–	MED ROUGH	50°		
							J13	JOINT	–	–	SL. ROUGH	80°		
4	7.0	6.8	97			166.0	J14							SOME DRILL INDUCED FRACTURES
						167.0								
						168.0								

DRILLER B. RUDNICKI DRILL METHOD ______ CORE DIAMETER 2 3/8" E. LOGGER R. ADAMS CORE LOGGER R. WRIGHT

DATE ______ DRILL RIG ______ BIT USED DIAMOND DATE ______ DATE 14/11/80

MINERAL ENGINEERING DEPARTMENT　UNIVERSITY OF ALBERTA　GEOTECHNICAL CORE LOG

PROJECT Silkstone　LOCATION 97420 E 39860 N　ELEVATION ______　DIP Vertical　BEARING ______　PAGE 5 OF 5　HOLE NO. (J)

RUN No.	LENGTH OF RUN	LENGTH RECOVERED	% RECOVERY	CLASSIFICATION	LITHOLOGICAL DESCRIPTION type, colour, texture, bedding, structure, hardness, remarks.

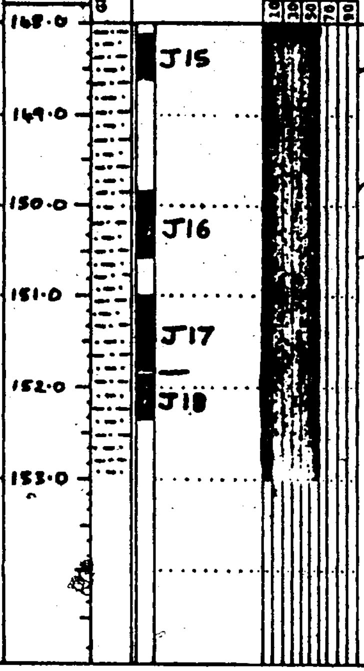

DISCONTINUITIES

TYPE	SEPARATION	FILL	ROUGHNESS	DIP TCA	DEFECT FREQ. / ft.	REMARKS
JOINT	–	–	SL. ROUGH	60°		SLICKENSIDED
						SHEARED ZONE (IRREGULAR)
SHEAR	–	–	SMOOTH	40°		WAVY + STRIATED
BEDDING	–	–	MED ROUGH	70°		CARBONACEOUS

DRILLER B.Rudreri　DRILL METHOD ______　CORE DIAMETER 2⅝"　E. LOGGER R. ADAMS　CORE LOGGER R.WRIGHT

DATE ______　DRILL RIG ______　BIT USED DIAMOND　DATE ______　DATE 14/11/78

APPENDIX 6

GEOTECHNICAL TESTING PROCEDURES

UNIAXIAL COMPRESSION

This test was undertaken on specimens of full core diameter (2.6 inch). The specimens were cut with a diamond saw, then the ends were lapped, using a lapping table with #80 and #220 grit. Specimen width to height ratios between 2.0 and 2.5 were prepared (except for one mudstone specimen with a ratio of 1.6). The ends were lapped so that they were plane and parallel to within 0.002 inch. They were then air dried and electrical resistance strain gauges were attached to each specimen using epoxy cement. Two pairs were placed around the central circumference, one pair for axial strain, and the other for circumferential strai[illegible]

The specimen was placed in an MTS servo controlled stiff testing machine (Plate 2), with a spherical seat on the bottom and the machine spherical seat on the top. Strain indicators were connected to the matched pairs of gauges in a full bridge configuration. The specimen was loaded at a constant machine stroke rate, producing specimen failures within approcimately 10 minutes. Strain readings were taken at load increments of 1000 or 2000 pounds, depending upon the expected failure load.

Axial and lateral strain were plotted against stress (Appendix 7) and the elastic moduli were estimated from these graphs. The Young's Modulus was estimated, by measuring the slope of the axial stress/strain curve, at the stress value equal to 50% of the failure stress. The circumferential strain is negative (geotechnical sign convention) and therefore the sign has been reversed to enable both strains to be plotted on the same graph. The circumferential modulus is estimated by measuring the slope of the circumferential stress/strain curve at 50% of the failure stress. Poisson's Ratio is then calculated from (International Society of Rock Mechanics, Commission on Standardisation of Laboratory and Field Tests, 1979):

Poisson's Ratio = Young's Modulus/Circumferential Modulus

TRIAXIAL COMPRESSION

Specimens for this test were undercored to 1.6 inch diameter using a bench mounted diamond drill with air or water flush (depending upon rock). The undercored specimens were cut with a diamond saw to produce width to height ratios between 2.0 and 2.5. This was not possible for some mudstone and coal samples, as they did not withstand the undercoring process very well. The ends were lapped to be plane and parallel to 0.002 inch. The in situ moisture content was preserved as much as possible by sealing samples in plastic bags prior to testing.

Immediately prior to testing the specimens were unsealed and placed in the triaxial cell. The Hoek-Frank triaxial cell consists of a metal jacket (capable of withstanding internal hydraul~~ic pressures~~ of 10,000 psi), a flexible sleeve (to provide a seal and protect the specimen from the hydraulic fluid), and spherical seats at both ends. The triaxial cell pressure is provided by an intensifier unit that is pressurised from a compressed nitrogen cylinder.

The cell was placed in the MTS servo controlled stiff testing machine (Plate 2) and held in place by a small axial load. The cell was then pressurised to the confining pressure required for the test. For the higher confining pressures this was done in stages, in order to avoid specimen failure as a result of the confining pressure. At each stage the axial load was increased to produce hydrostatic stress conditions. The specimen was then loaded axially at a constant machine stroke rate, producing specimen failures within approximately 10 minutes.

After failure the specimen was removed and weighed, then it was oven dried at 105° Celsius to calculate the moisture content.

BRAZILIAN DISC

Disc specimens were prepared by cutting cylindrical samples perpendicular to the long axis of the core. In situ moisture content was preserved as much as possible by sealing specimens in plastic bags prior to testing.

The specimens were tested in a 5000 Kg stepless compression test machine, with flat platens and a spherical seat at the bottom. Loading was carried out along a diameter, and the load at failure was estimated from the dial gauge reading on a proving ring incorporated into the machine. After failure the specimen was weighed, oven dried at 105° Celsius, and re-weighed to calculate the moisture content.

The tensile strength was obtained from the following equation (International Society for Rock Mechanics, Commission on Standardisation of Laboratory and Field Tests, 1978):

SigT = 0.636(P/D)

SigT = Tensile strength (MN/m²)
P = Maximum load (N)
D = Diameter of specimen (mm)

DIRECT SHEAR

Direct shear specimens, approximately 2cm thick, were prepared by cutting parallel to the discontinuity plane to be tested. During the preparation process the *in situ* moisture content was preserved as much as possible by covering the specimens with a moist cloth. The specimens were mounted into each half of the shear box, using a sulfaset anchorage mix that expands slightly upon setting. The discontinuity plane was arranged so that it was parallel to the plane of shear.

The shear box was mounted into a Farnell direct shear apparatus that could provide a constant shear rate. Normal load was applied by means of a suspended loading platform and assorted weights. Normal and shear displacements were measured by linear variable transducers, and shear load by strain gauges attached to a proving ring. All measurements were continuously recorded on an X-Y plotter.

The specimen was sheared approximately 5mm with a normal load of 300 N, then returned to its intial position with no normal load. This procedure was repeated with normal loads of 1350 N, 2850 N and 4350 N. Peak and residual friction angles were calculated from the shear and normal loads recorded, with adjustment made for the measured dilatancy.

SLAKE DURABILITY

Slake durability tests were carried out using the standard apparatus and procedure (Gyenge & Herget, 1977). The sample was divided into ten pieces with rounded corners, each of approximately 50g weight. These were oven dried at 105° Celsius and weighed. They were then placed in the standard test drum and mounted in the testing apparatus. The drum was partially submerged in tap water at room temperature, and rotated at 20 rpm for 10 minutes. The sample was removed, and oven dried before being re-weighed. This procedure was repeated and the final weight after the second cycle was obtained.

The slake durability index (second cycle) was calculated as the percentage ratio of the final to initial dry sample weights.

SWELLING STRAIN INDEX

Unconfined swelling tests were carried out on cylindrical samples of 1.6 and 2.6 inch diameter. The samples were placed in a metal container with the flat faces horizontal. A dial gauge was positioned on the top surface to measure the vertical expansion. The specimen was submerged in tap water at room temperature, and readings were taken at intervals.

The swelling strain index (unconfined) was calculated from the following equation (Gyenge & Herget, 1977):

$$SSI = 100.d/L$$

SSI = Swelling Strain Index (unconfined %)

d = Maximum vertical expansion (mm)

L = Specimen vertical dimension (mm)

APPENDIX 7

GEOTECHNICAL TEST RESULTS

SILKSTONE GEOTECHNICAL TESTING (CORE SECTIONS + SAMPLING)

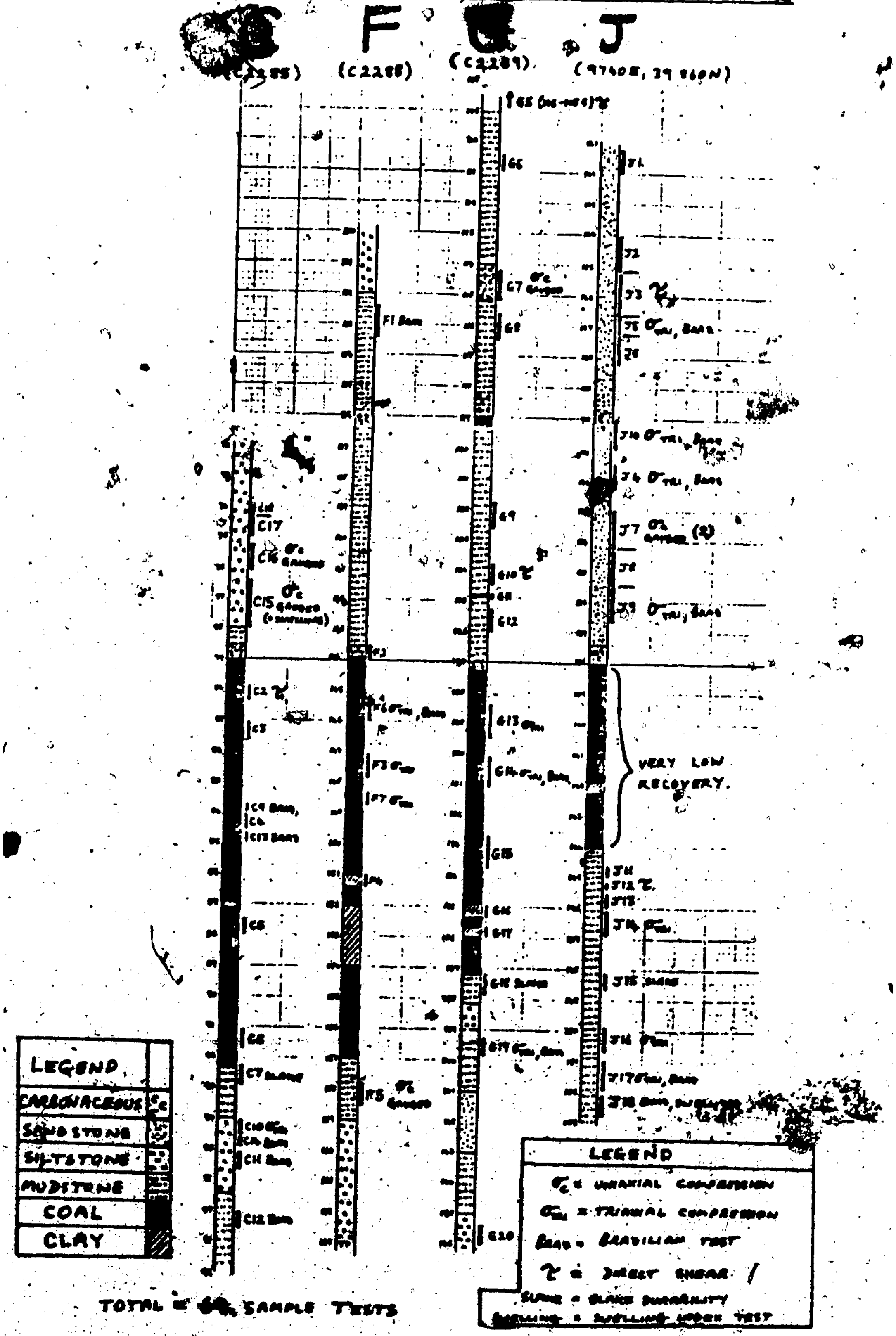
C
F
G
J
(C2285)
(C2288)
(C2289)
(9760E, 39860N)
G5 (in-situ)
G6
G7 σ_c gauged
G8
G9
G10 τ
G11
G12
G13 σ_{tri}
G14 σ_{tri}, Braz
G15
G16
G17
G18 Slake
G19 σ_{tri}, Braz
G20
F1 Braz
F2
F6 σ_{tri}, Braz
F3 σ_{tri}
F7 σ_{tri}
F4
F5 σ_c gauged
J1
J2
J3 τ
J5 σ_{tri}, Braz
J6
J10 σ_{tri}, Braz
J4 σ_{tri}, Braz
J7 σ_c gauged (2)
J8
J9 σ_{tri}, Braz
VERY LOW RECOVERY.
J11
J12 τ
J13
J14 σ_{tri}
J15 Slake
J16 σ_{tri}
J17 σ_{tri}, Braz
J18 Braz, Swelling
C18
C17
C16 σ_c gauged
C15 σ_c gauged (continuous)
C2 τ
C3
C9 Braz,
C4
C13 Braz
C5
C6
C7 Slake
C10 σ_{tri}
C14 Braz
C11 Braz
C12 Braz
LEGEND.
CARBONACEOUS
SANDSTONE
SILTSTONE
MUDSTONE
COAL
CLAY
LEGEND
σ_c = UNIAXIAL COMPRESSION
σ_{tri} = TRIAXIAL COMPRESSION
Braz = BRAZILIAN TEST
τ = DIRECT SHEAR
Slake = SLAKE DURABILITY
Swelling = SWELLING INDEX TEST
TOTAL = 6[illegible] SAMPLE TESTS

SILKSTONE GEOTECHNICAL TESTING - TRIAXIAL

SAMPLE	TYPE	MOISTURE %	σ_1 (psi)	σ_3 (psi)	REMARKS
J5A	SANDSTONE	4.0	10010	500	SHEAR ~ 25° TCA
J5B	SANDSTONE		12700	1000	
J4A	SANDSTONE	-	6150	0	-
J4B	SANDSTONE	-	5600	0	E ~ 0.85x10^{6}psi
J9A	SANDSTONE	2.6	14950	1500	-
J9B	SANDSTONE	2.8	12470	1000	SHEAR ~ 28° TCA
J10A	SANDSTONE	-	16630	2000	-
J10B	SANDSTONE	3.5	17930	3000	SHEAR ~ 33° TCA
J14A	MUDSTONE	5.0	7820	0	COMPLICATED CONE FAILURE
J14B	MUDSTONE	4.8	9420	500	SHEAR ~ 25° TCA
J16A	MUDSTONE	4.2	13040	1500	SHEAR ~ 20° TCA
J17A	MUDSTONE	4.0	15670	2000	COMPLICATED
J17B	MUDSTONE	4.0	11790	1000	SHEAR ~ 20° TCA
C10A	SILTSTONE	3.1	12080	1000	SHEAR ~ 28° TCA
C10B	SILTSTONE	3.4	12040	500	CONE FAILURE
F7	COAL	-	10140	1000	SHEAR ~ 20° TCA
G14A	COAL	-	5350	500	SHEAR ~ 28° TCA
G14B	COAL	-	2270	0	COMPLICATED
G13A	COAL	-	15690	2500	SHEAR ~ 25° TCA
F6B	COAL	-	12820	1500	COMPLICATED
F3	COAL	-	14710	2000	SHEAR ~ 25° TCA

* Samples undercored to 1.6 inch diameter along core axis.
All bedding dips between 10° and 15° TCA (To Core Axis)

SILKSTONE GEOTECHNICAL TESTING - BRAZILIAN DISC

SAMPLE	TYPE	TENSILE STRENGTH (psi)	REMARKS
J4C	Sandstone	295	-
J9C	Sandstone	308	-
J9E	Sandstone	269	-
J9G	Sandstone	290	-
J5D	Sandstone	335	-
J10C	Sandstone	357	-
J10E	Sandstone	355	-
C9	Coal	119	-
G14C	Coal	97	-
C11B	Siltstone	588	-
C14B	Siltstone	389	-
J18B	Siltstone	626	-
C12A	Mudstone	864	Possible bad failure
F1C	Mudstone	282	Weakness plane
J17D	Mudstone	197	-
J1[illegible]	Mudstone	631	-
X[illegible]	Mudstone	1333	Multiple failure
C1[illegible]	Mudstone	891	-
J4D	Sandstone	434	Moisture 3.0%
J9D	Sandstone	305	Moisture 3.3%
J9F	Sandstone	262	-
J5C	Sandstone	471	Moisture 4.7%
J5E	Sandstone	309	-
J10D	Sandstone	289	-
J10F	Sandstone	362	Moisture 4.1%
F6A	Coal	48	-
C13	Coal	263	-
C14A	Siltstone	304	-
G19B	Siltstone	364	-
J18C	Siltstone	745	-
F1B	Mudstone	375	-
J17C	Mudstone	457	-
J17E	Mudstone	171	-
X1B	Mudstone	96	Complex failure
X2B	Mudstone	1043	-

* Axis of discs all parallel to core axis.

* Determination of tensile test plane in relation to bedding was not possible.

SILKSTONE GEOTECHNICAL TESTING - DIRECT SHEAR

SAMPLE	TYPE	AREA cm^2	NORMAL LOAD (N)	FRICTION ANGLE (DEG)	DESCRIPTION
J3A	SANDSTONE	27	950	30.2	SAW CUT PLANE AT 40° TCA. ROCK POWDER LEFT AFTER SHEARING
			1550	31.8	
			2850	32.5	
			3350	33.1	
J12	MUDSTONE	30	1350	20.9	JOINT ~40° TCA MEDIUM ROUGH WITH SOME WAVINESS ALONG STRIKE. FLAKE DEBRIS AFTER SHEAR
			2850	20.0	
			4350	18.7	
G10	MUDSTONE	38	1350	26.5	JOINT ~60° TCA SLIGHTLY ROUGH, WAVY ALONG STRIKE & DIP. MAJOR PORTION FAILED AT 2850N.
			2850	27.7	
G5	MUDSTONE	31	1350	21.7	BEDDING ~75° TCA V. THIN CARBONACEOUS LENSES. ROUGH AND WAVY. MUCH SHEAR DEBRIS AFTER TEST.
			2850	24.8	
			4350	23.3	
C2	COAL	36	1350	23.2	BEDDING ~20° TCA WAVY ALONG STRIKE, ROUGH WITH SOME SMOOTH PATCHES. MUCH SHEAR DEBRIS AFTER TEST.
			2850	22.2	
			4350	25.1	

* Residual values are presented, as there were no significant peak values.

* All shearing was along the discontinuity dip.

SILKSTONE GEOTECHNICAL TESTING - SLAKE DURABILITY INDEX

SAMPLE	TYPE	INDEX	REMARKS
C7	MUDSTONE	78.5	MUCH FINE BLOCKY SEDIMENT
G18	MUDSTONE	16.8	MUCH FINE BLOCKY SEDIMENT
J15	MUDSTONE	95.3	SOME SANDY SEDIMENT

* Second cycle index calculated.

* Tap water at 20° C used.

SILK[illegible] GEOTECHNICAL TESTING - UNCONFINED SWELLING

SAMPLE	TYPE	DURATION HOURS	SSI %	REMARKS
C15B	SILTSTONE	72	2.9	SAMPLE BROKEN ALONG BEDS WITH CARBONACEOUS LENSES
J18A	MUDSTONE	18	2.5	COMPLETE DISINTEGRATION OF SAMPLE AFTER 2 DAYS

* Tap water at 20° C used.

* SSI = Swelling Strain Index (unconfined)

SANDSTONE G7

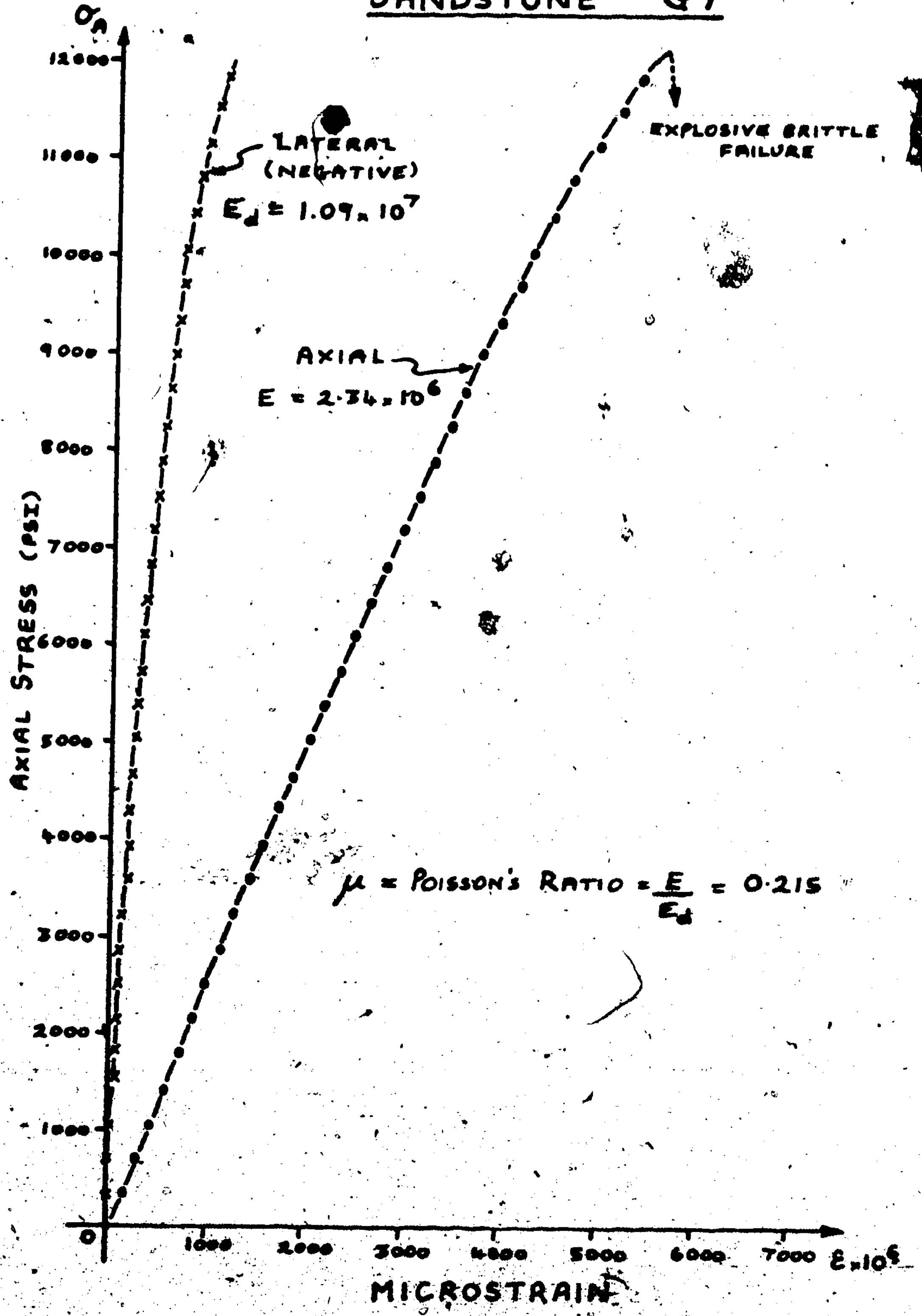

STRAIN GAUGED UNIAXIAL COMPRESSION

SANDSTONE J7A

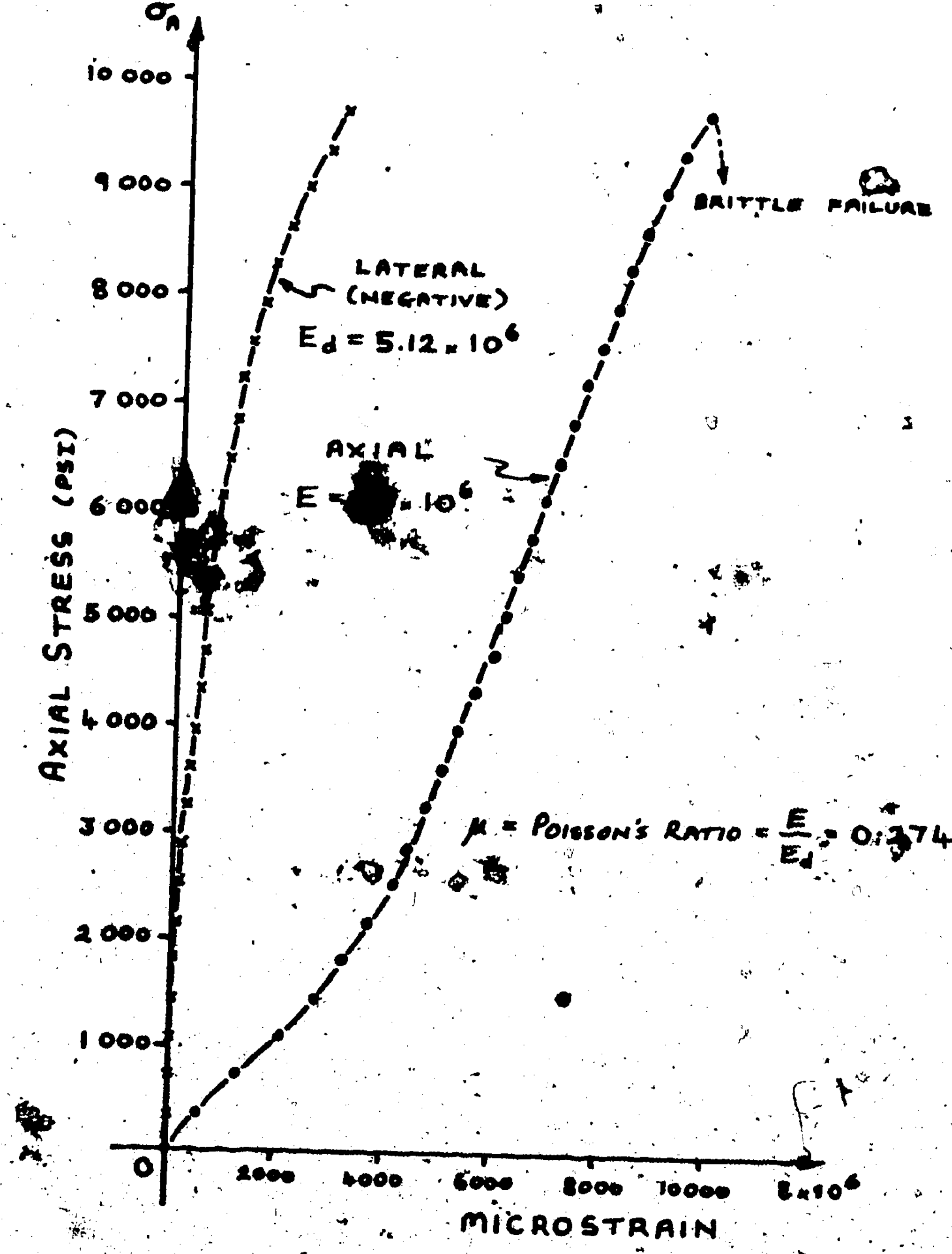

STRAIN GAUGED UNIAXIAL COMPRESSION

SANDSTONE J7B

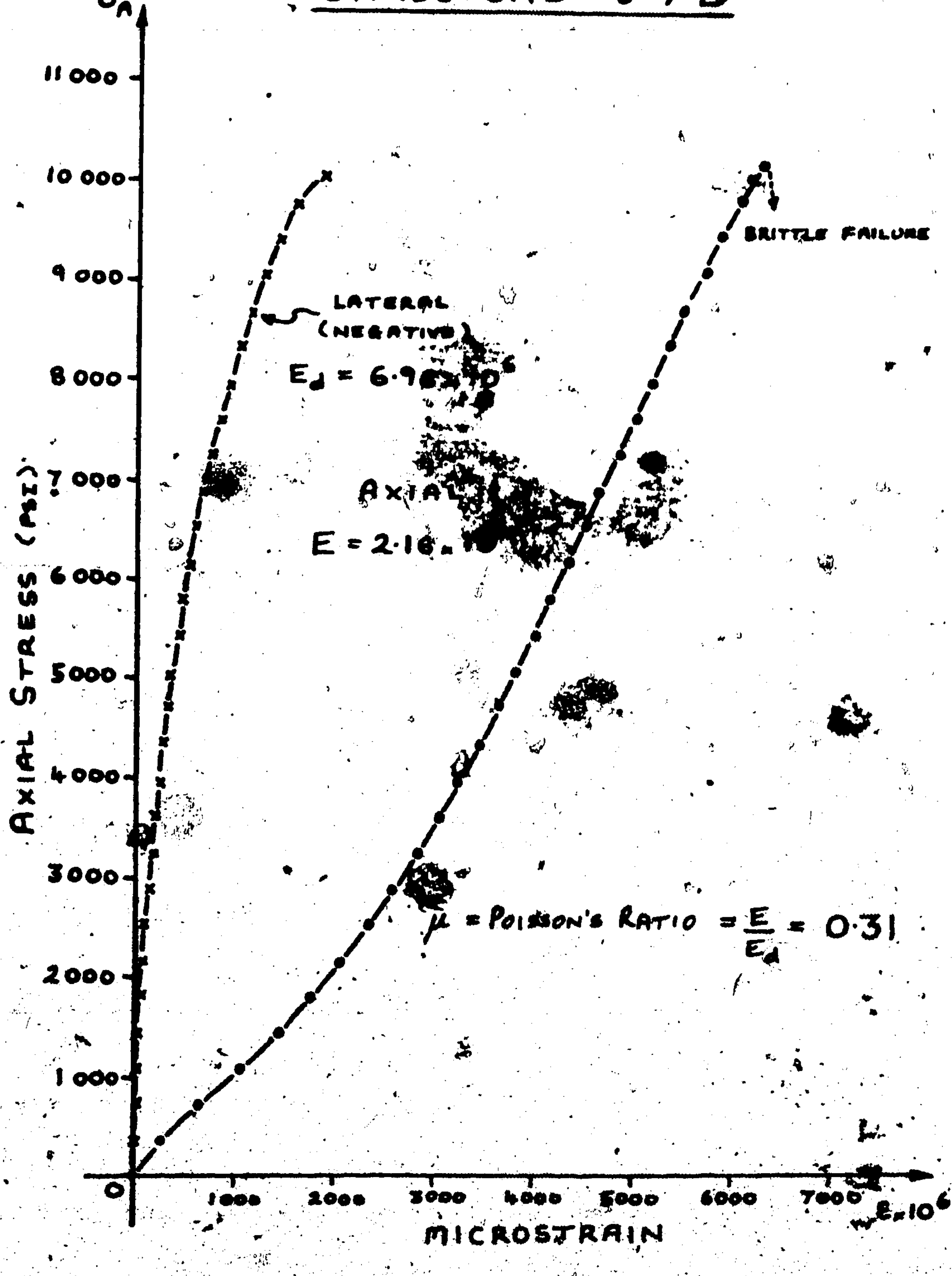

STRAIN GAUGED UNIAXIAL COMPRESSION

SILTSTONE C15A

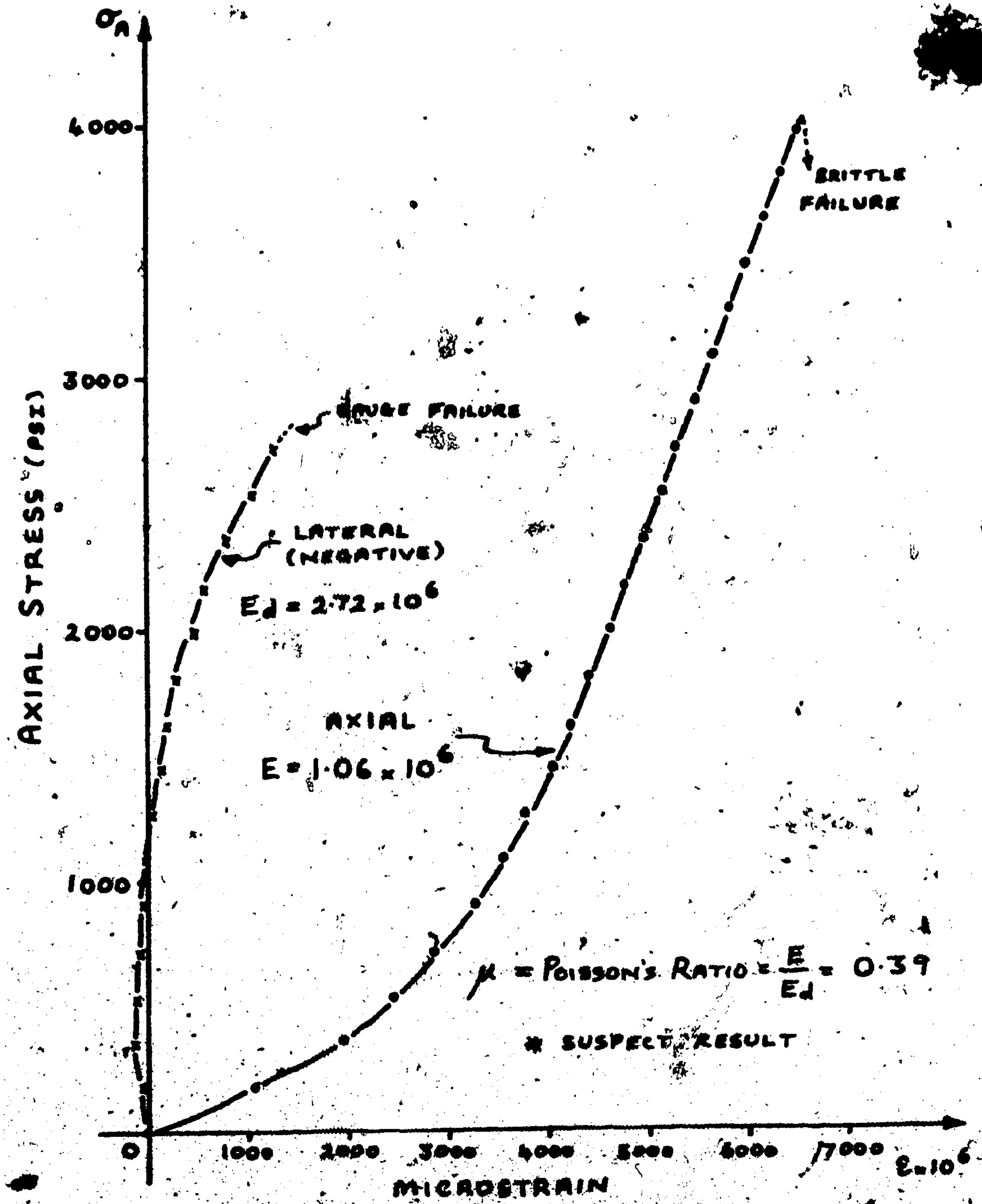

STRAIN GAUGED UNIAXIAL COMPRESSION

SILTSTONE C16

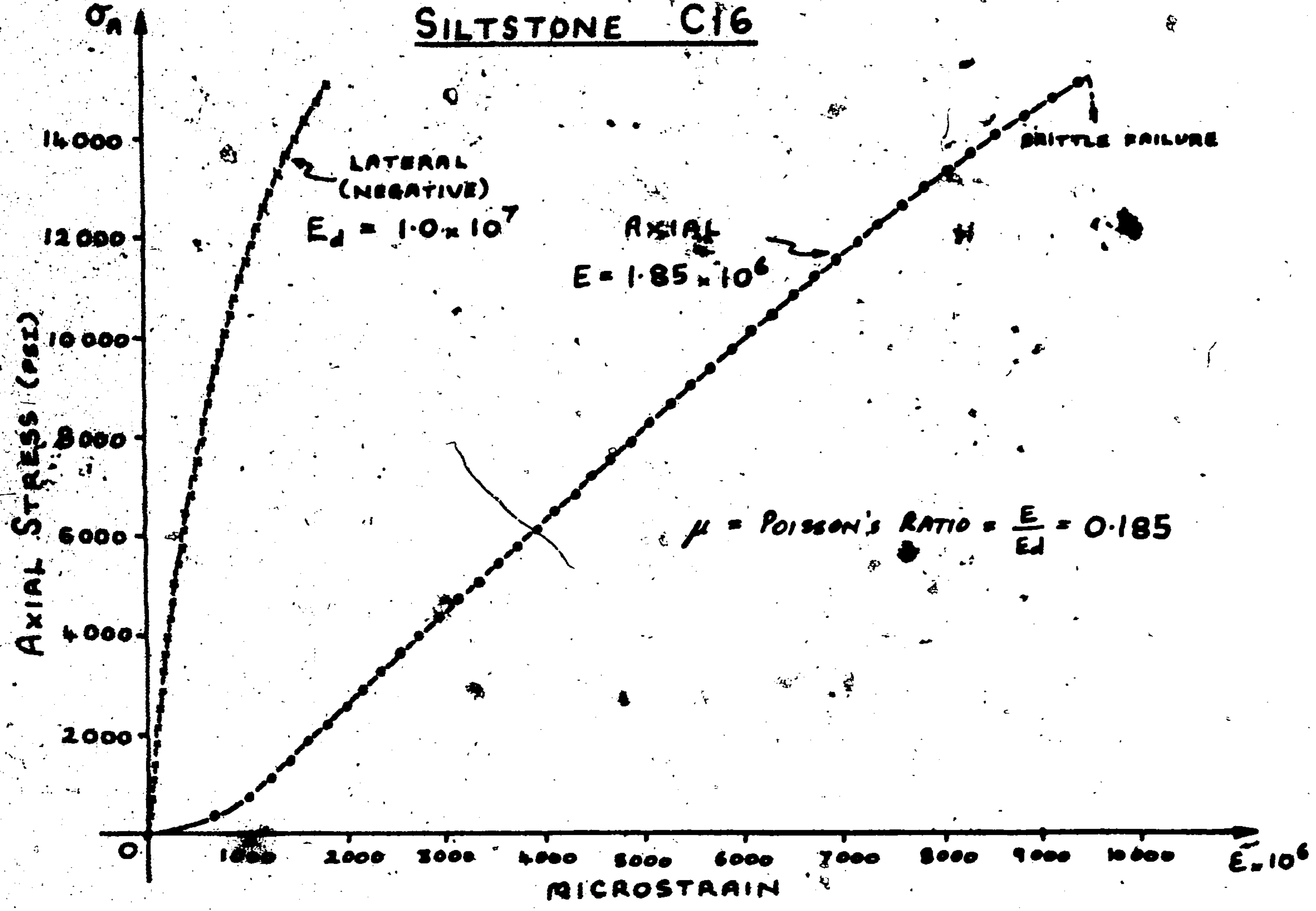

STRAIN GAUGED UNIAXIAL COMPRESSION

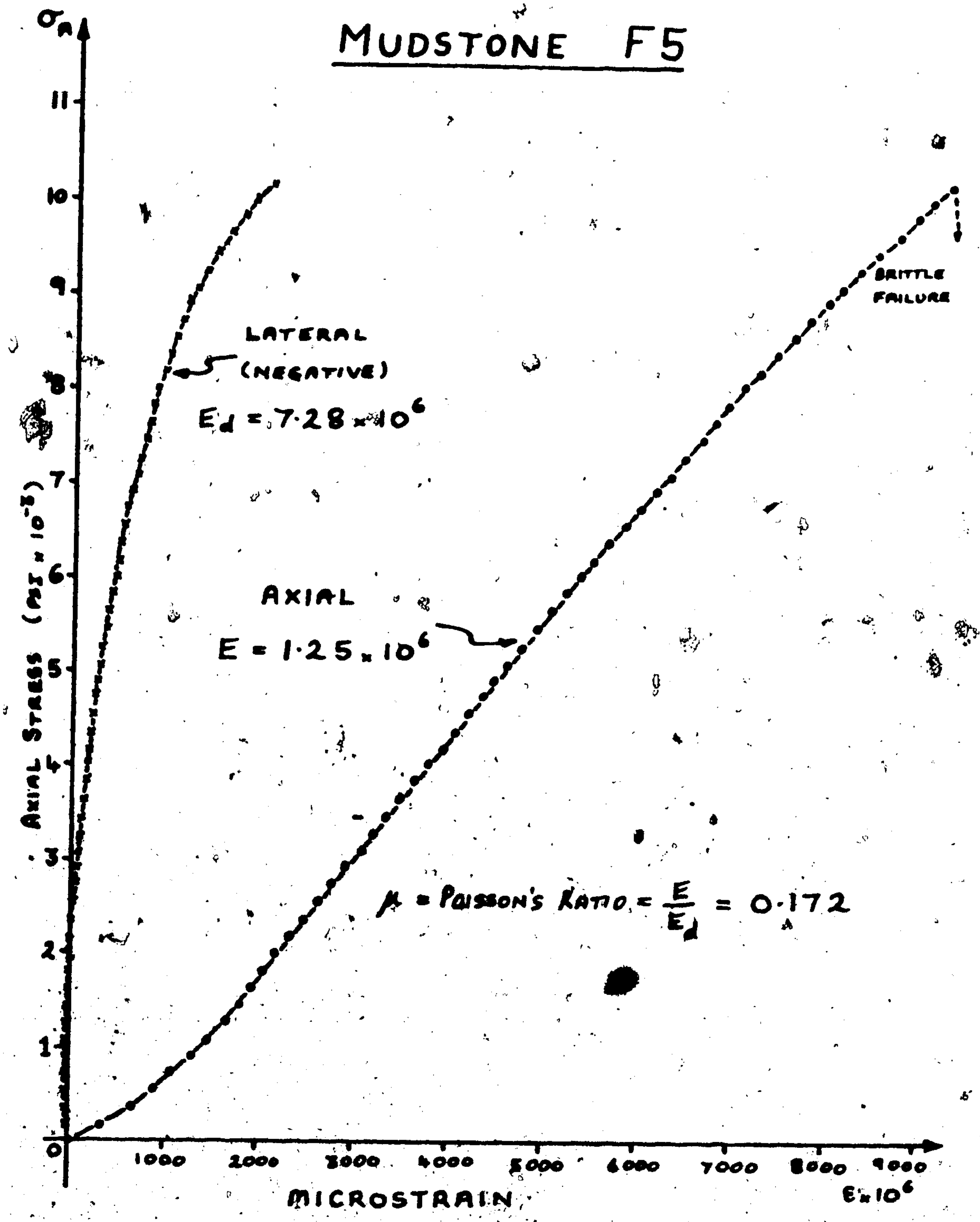

STRAIN GAUGED UNIAXIAL COMPRESSION

APPENDIX 8

MINE SIMULATION RESULTS

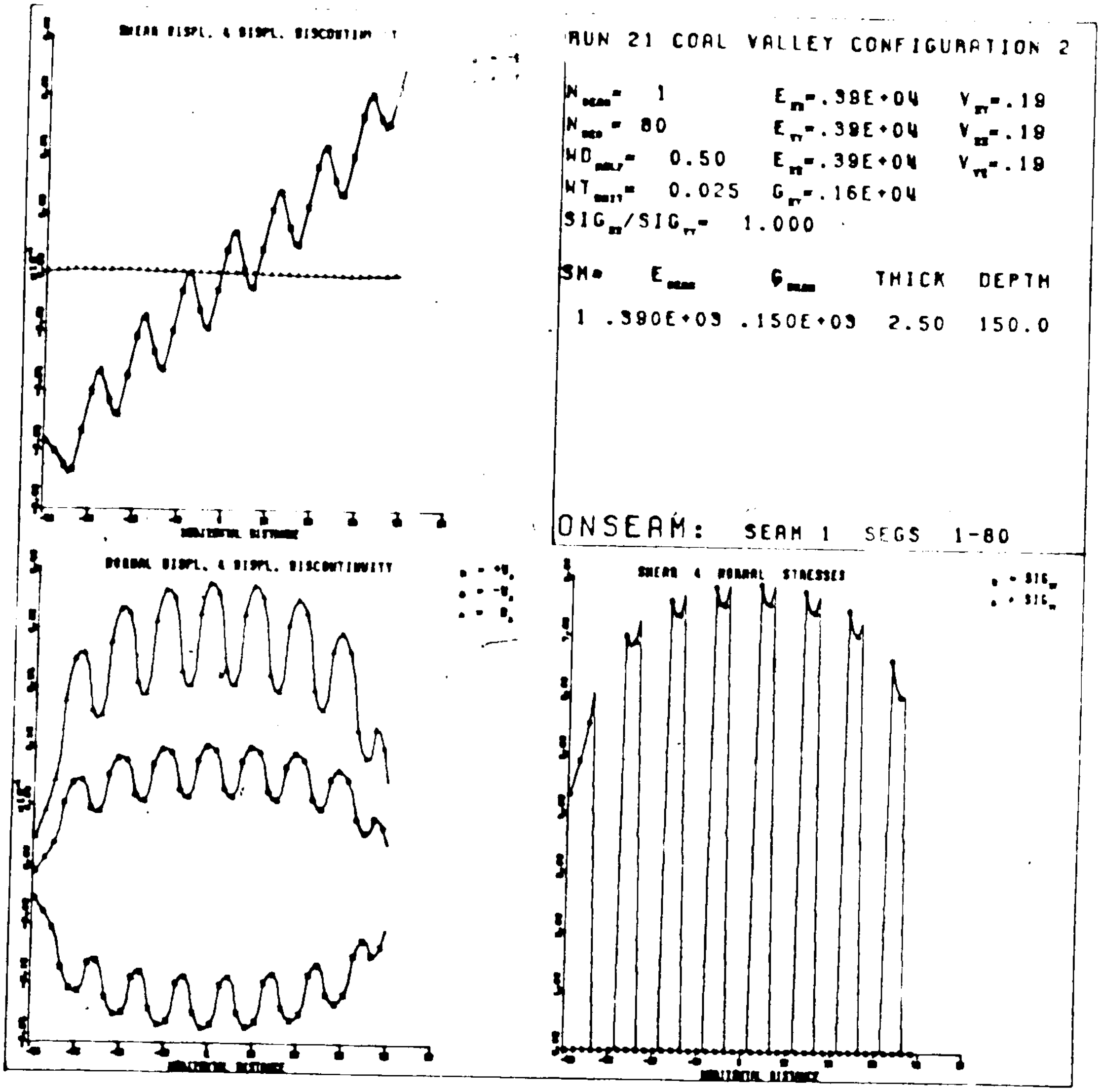

```
RUN 21 COAL VALLEY CONFIGURATION 2

N_SEAM= 1          E_XX=.39E+04   V_XY=.19
N_SEG = 80         E_YY=.39E+04   V_XZ=.19
WD_HALF=  0.50     E_ZZ=.39E+04   V_YZ=.19
WT_UNIT=  0.025    G_XY=.16E+04
SIG_XX/SIG_YY=  1.000

SM#    E_SEAM      G_SEAM     THICK   DEPTH
 1  .390E+03  .150E+03   2.50   150.0

ONSEAM:  SEAM 1  SEGS  1-80
```

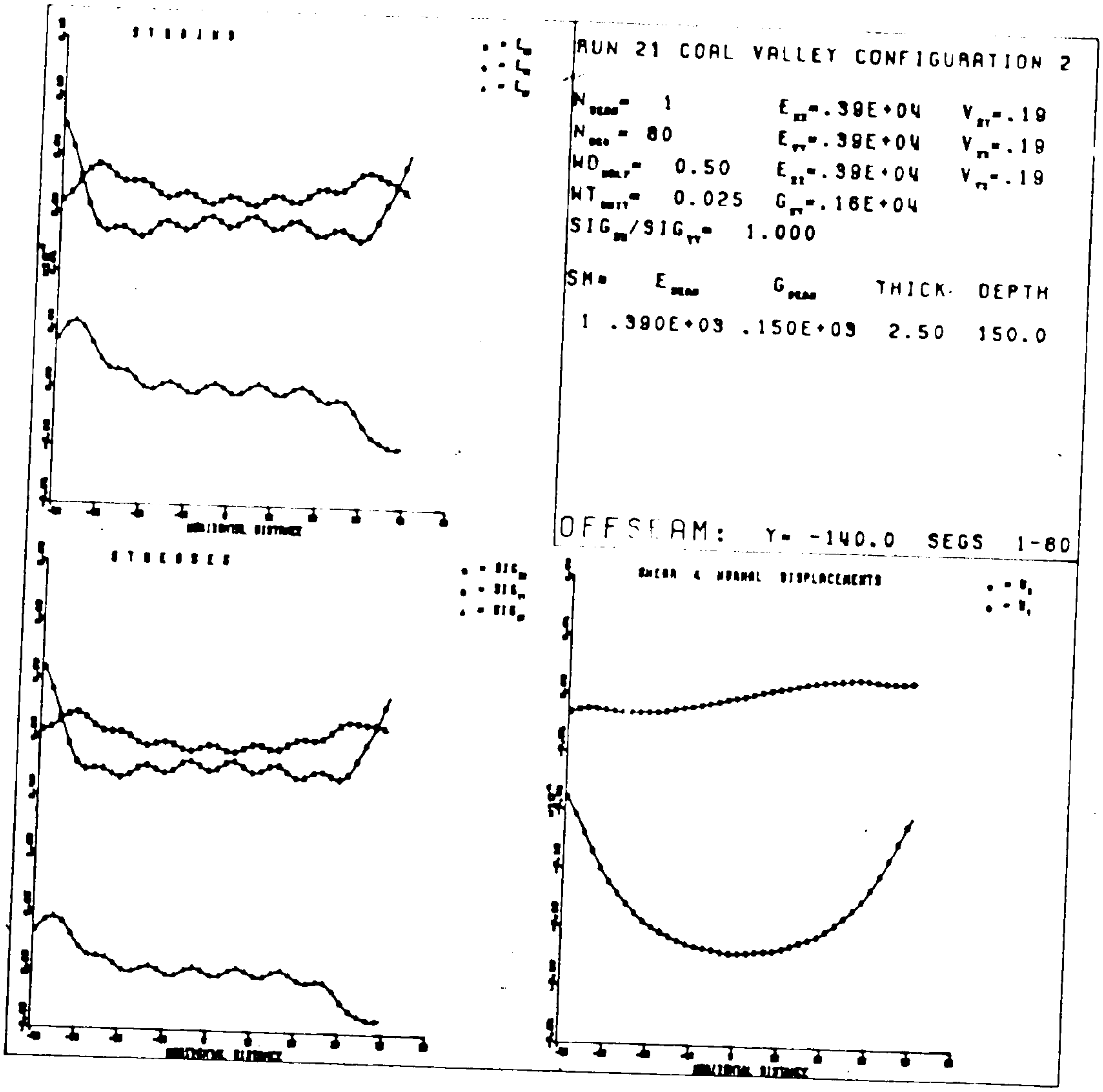

RUN 21 COAL VALLEY CONFIGURATION 2

N_{SEAM}= 1 E_{XX}=.39E+04 V_{XY}=.19

N_{SEG}= 80 E_{YY}=.39E+04 V_{YZ}=.19

WD_{BOLT}= 0.50 E_{ZZ}=.39E+04 V_{XZ}=.19

WT_{BOLT}= 0.025 G_{XY}=.16E+04

SIG_{XX}/SIG_{YY}= 1.000

SM=	E_{SEAM}	G_{SEAM}	THICK.	DEPTH
1	.390E+03	.150E+03	2.50	150.0

OFFSEAM: Y= -140.0 SEGS 1-80

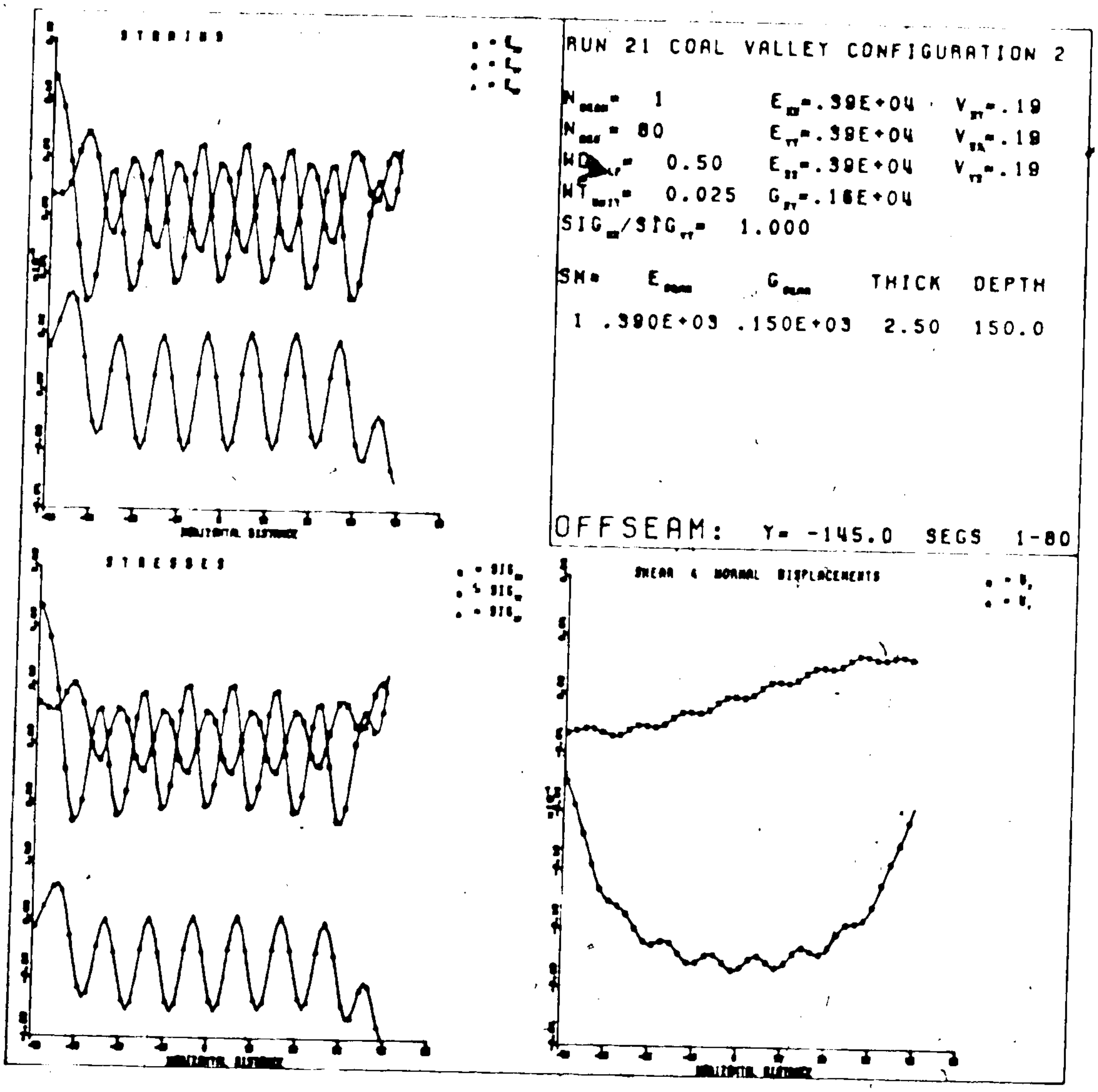

```
RUN 21 COAL VALLEY CONFIGURATION 2

N_SEAM= 1          E_XX=.39E+04   V_XY=.19
N_SEG = 80         E_YY=.39E+04   V_ZX=.19
WD_ELF=  0.50      E_ZZ=.39E+04   V_YZ=.19
WT_UNIT=  0.025    G_XY=.16E+04
SIG_XX/SIG_YY=  1.000

SM=   E_SEAM     G_SEAM     THICK  DEPTH
 1 .390E+03  .150E+03   2.50   150.0

OFFSEAM:  Y= -145.0  SEGS  1-80
```

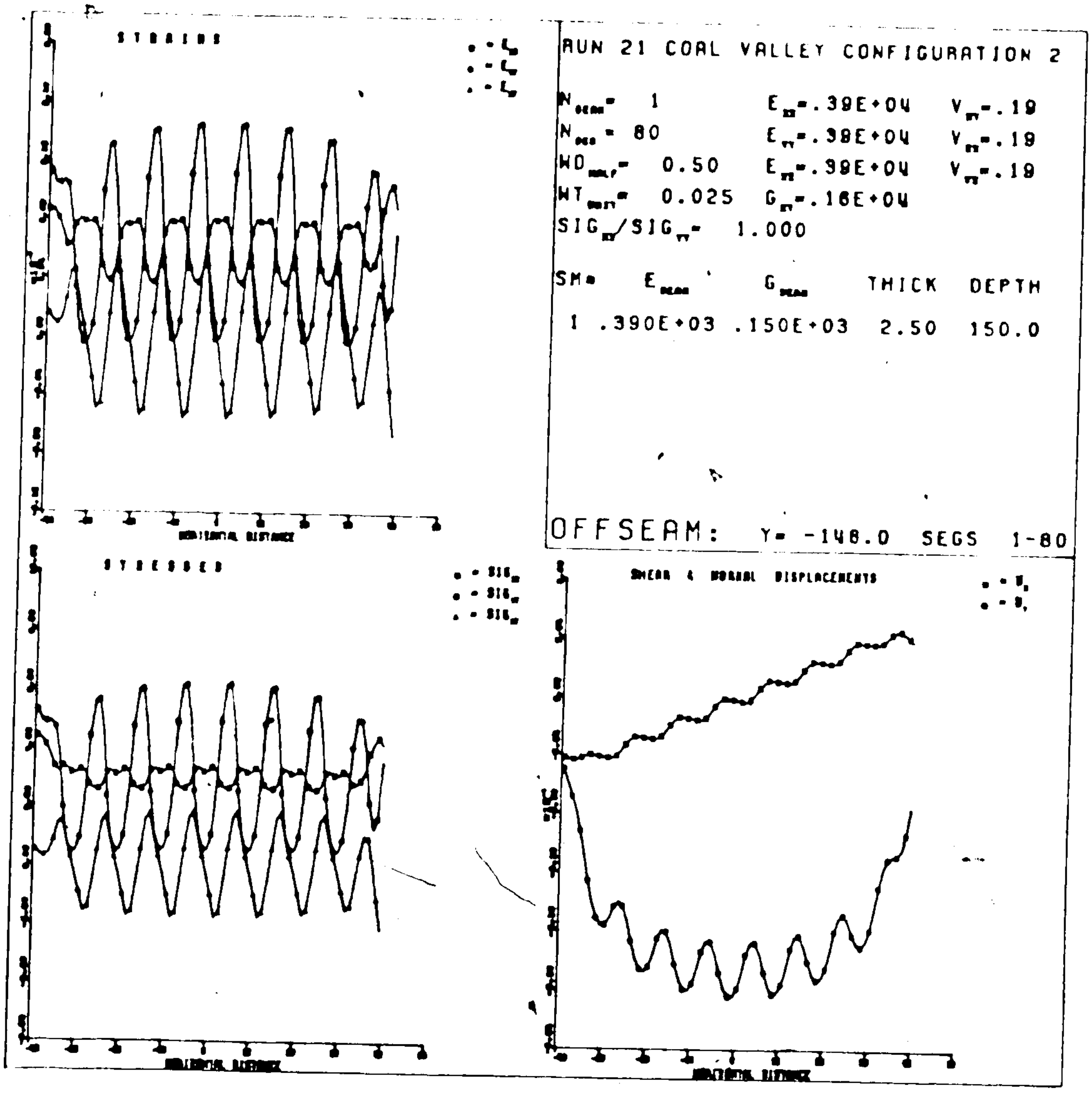

RUN 21 COAL VALLEY CONFIGURATION 2

N_{SEAM}= 1 E_{XX}=.39E+04 V_{XY}=.19

N_{SEG} = 80 E_{YY}=.39E+04 V_{XZ}=.19

WD_{HALF}= 0.50 E_{ZZ}=.39E+04 V_{YZ}=.19

WT_{UNIT}= 0.025 G_{XY}=.16E+04

SIG_{XX}/SIG_{YY}= 1.000

SM=	E_{SEAM}	G_{SEAM}	THICK	DEPTH
1	.390E+03	.150E+03	2.50	150.0

OFFSEAM: Y= -148.0 SEGS 1-80

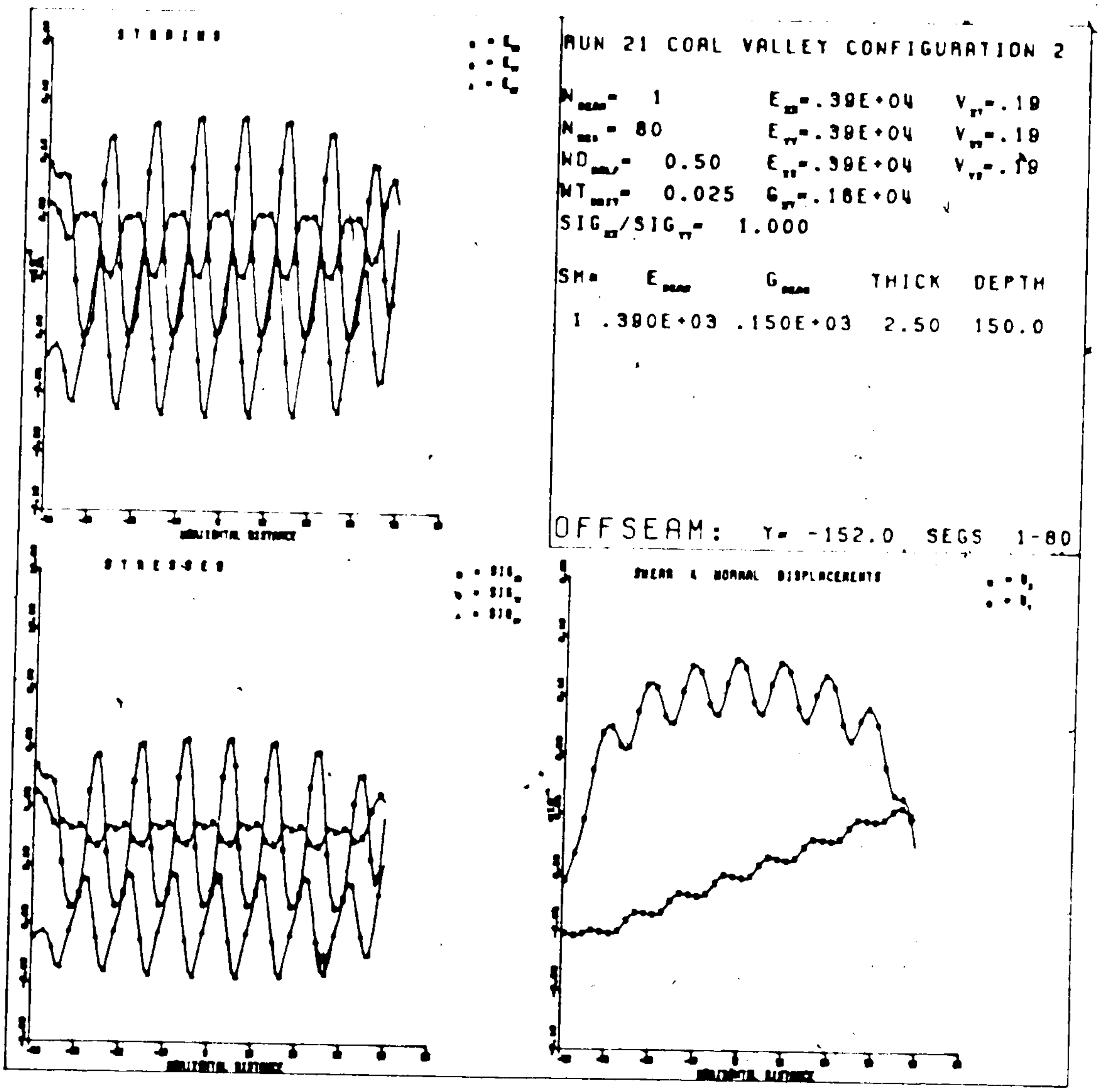

```
RUN 21 COAL VALLEY CONFIGURATION 2

N  =  1          E  =.39E+04   V  =.19
N  = 80          E  =.39E+04   V  =.19
WD  =  0.50      E  =.39E+04   V  =.19
WT  =  0.025     G  =.16E+04
SIG  /SIG  =  1.000

SM=    E         G          THICK  DEPTH

 1 .380E+03 .150E+03  2.50  150.0


OFFSEAM:  Y= -152.0  SEGS  1-80
```

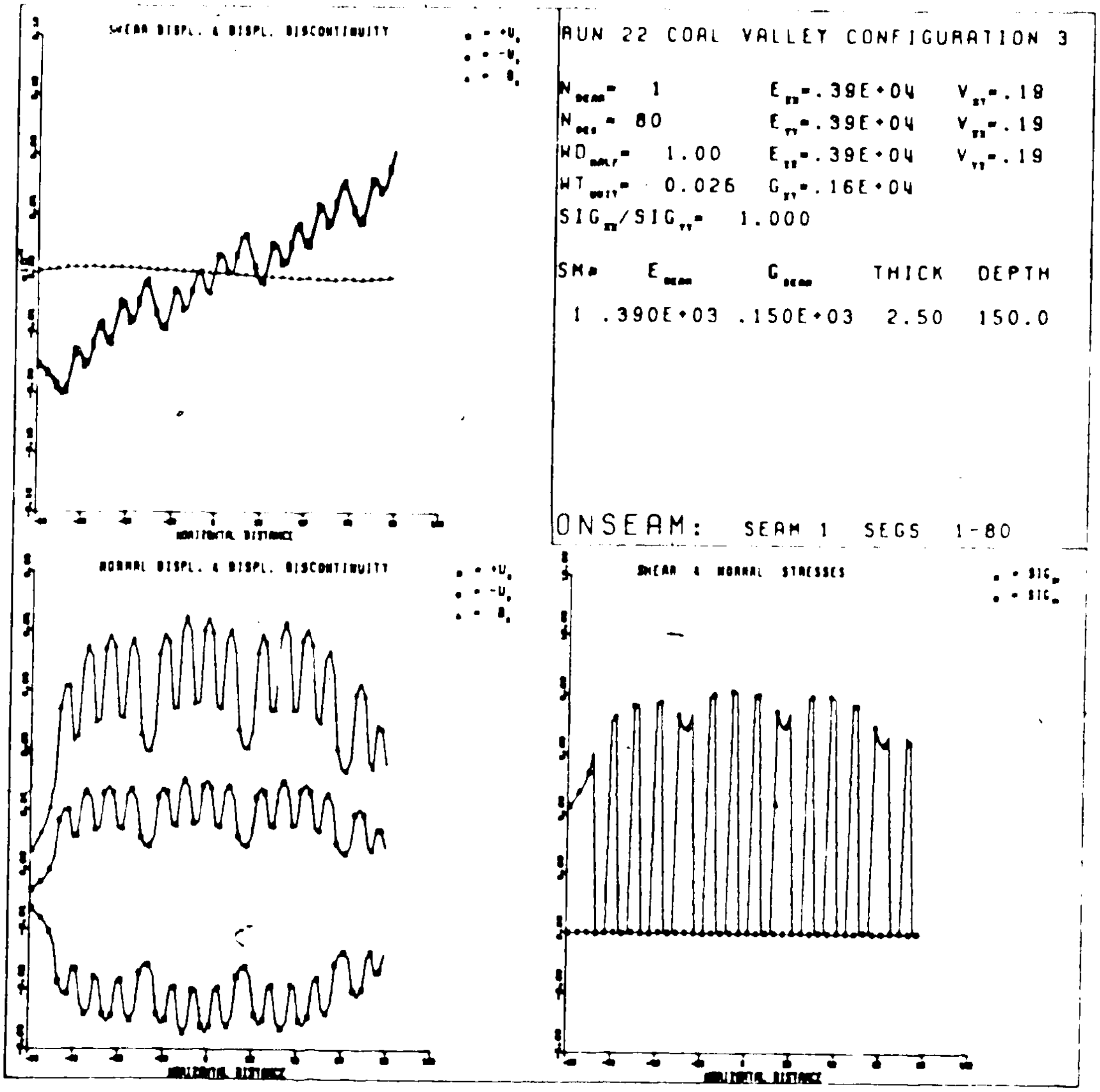

RUN 22 COAL VALLEY CONFIGURATION 3

```
N_SEAM=  1          E_XX=.39E+04   V_XY=.18
N_SEG= 80           E_YY=.39E+04   V_ZX=.19
WD_HALF=  1.00      E_ZZ=.39E+04   V_YZ=.19
WT_UNIT=  0.026     G_XY=.16E+04
SIG_XX/SIG_YY=  1.000

SM#    E_SEAM      G_SEAM     THICK   DEPTH

 1  .390E+03  .150E+03    2.50   150.0
```

ONSEAM: SEAM 1 SEGS 1-80

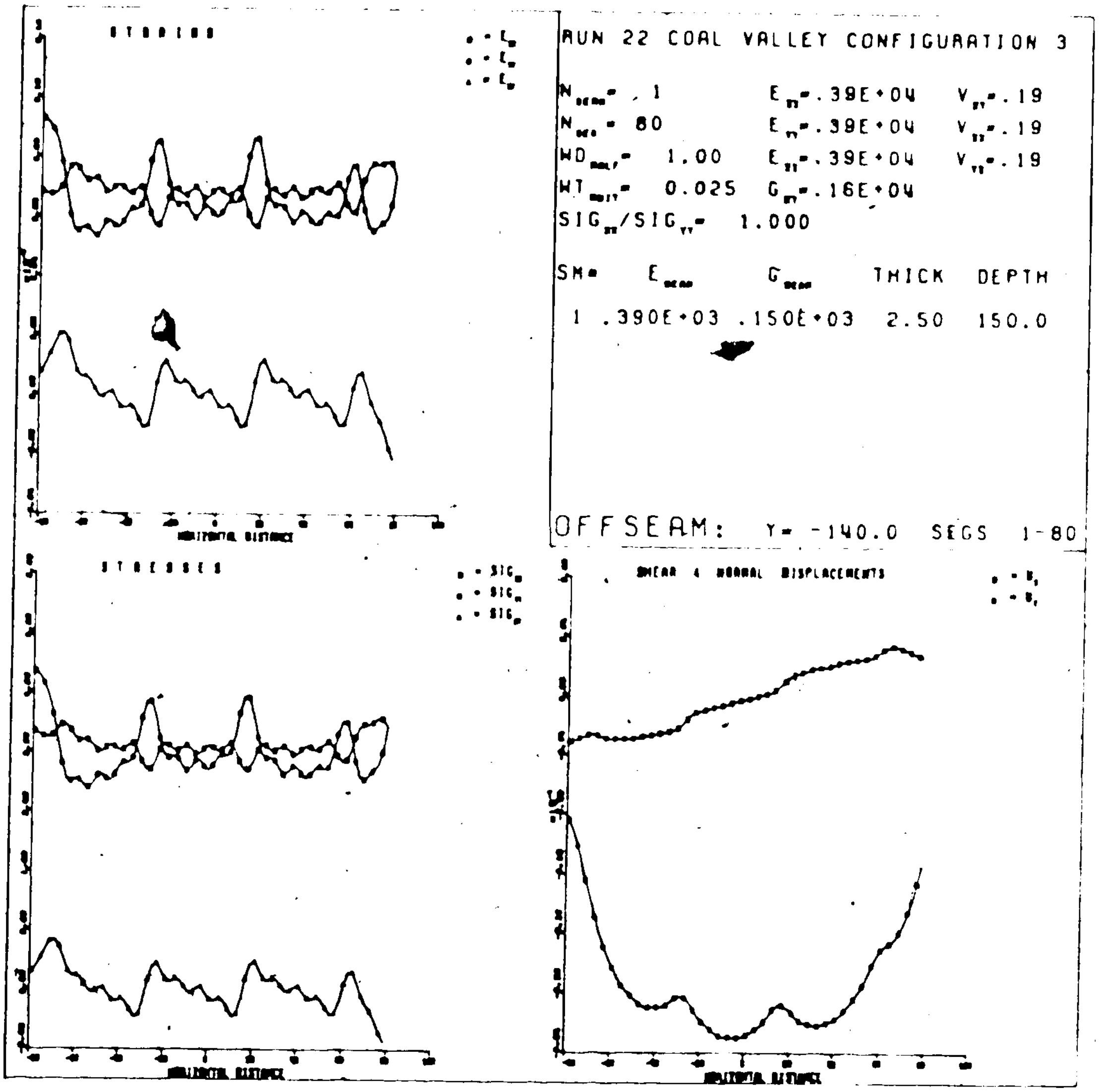

```
RUN 22 COAL VALLEY CONFIGURATION 3

NSEAM= 1          EXX=.39E+04   VXY=.19
NSEG= 80          EYY=.39E+04   VYZ=.19
WDRATIO= 1.00     EZZ=.39E+04   VXZ=.19
WTRATIO= 0.025    GXY=.16E+04
SIGXX/SIGYY= 1.000

SM=    ESEAM      GSEAM      THICK  DEPTH
 1  .390E+03  .150E+03   2.50  150.0

OFFSEAM:  Y= -140.0  SEGS  1-80
```

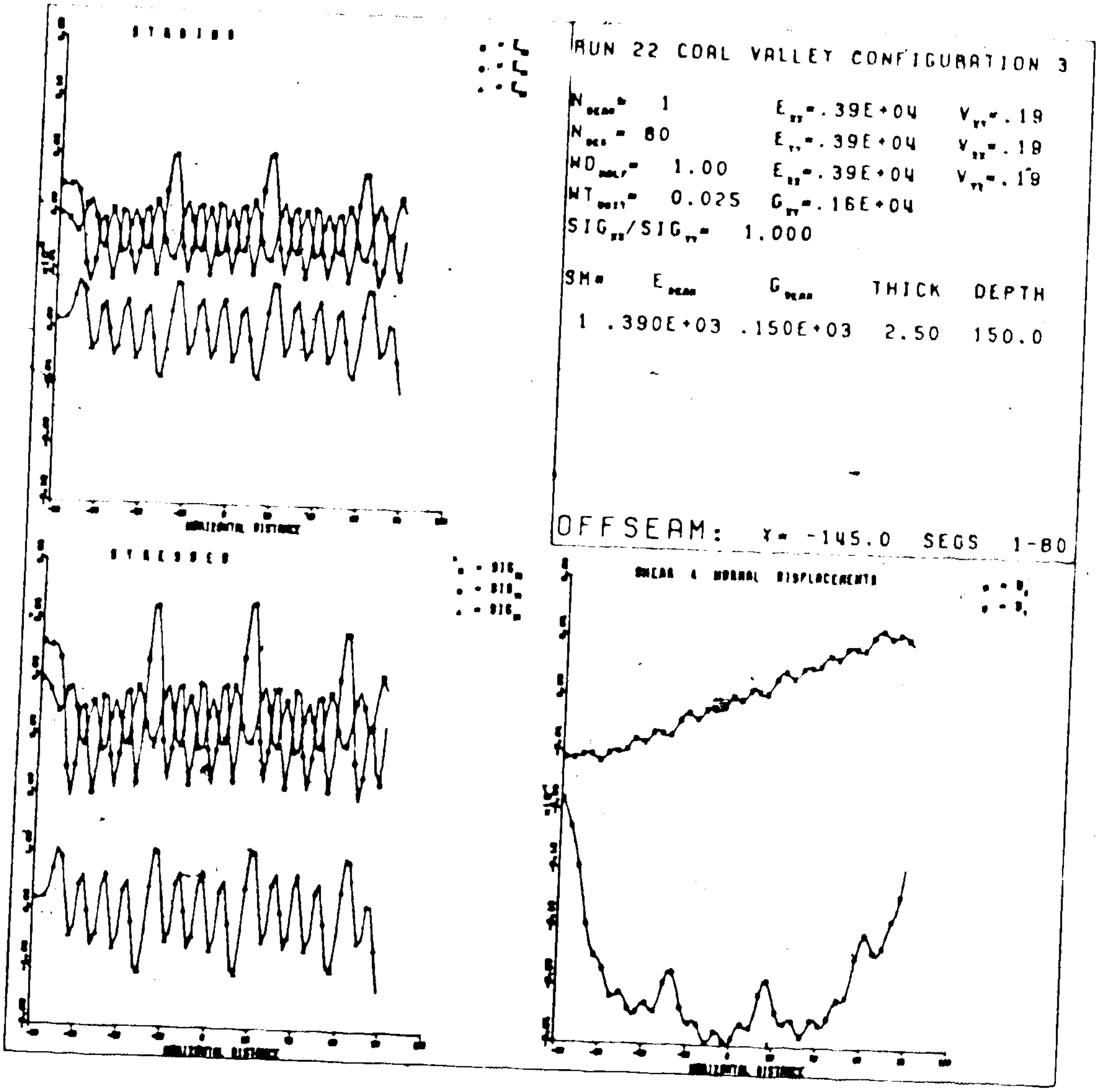

```
RUN 22 COAL VALLEY CONFIGURATION 3

N_SEAM= 1            E_XX=.39E+04   V_XY=.19
N_SEG = 80           E_YY=.39E+04   V_ZX=.19
WD_HALF=  1.00       E_ZZ=.39E+04   V_YZ=.19
WT_UNIT=  0.025      G_XY=.16E+04
SIG_XX/SIG_YY=  1.000

SM=    E_SEAM      G_SEAM     THICK   DEPTH
 1  .390E+03  .150E+03   2.50   150.0

OFFSEAM:  Y= -145.0   SEGS  1-80
```

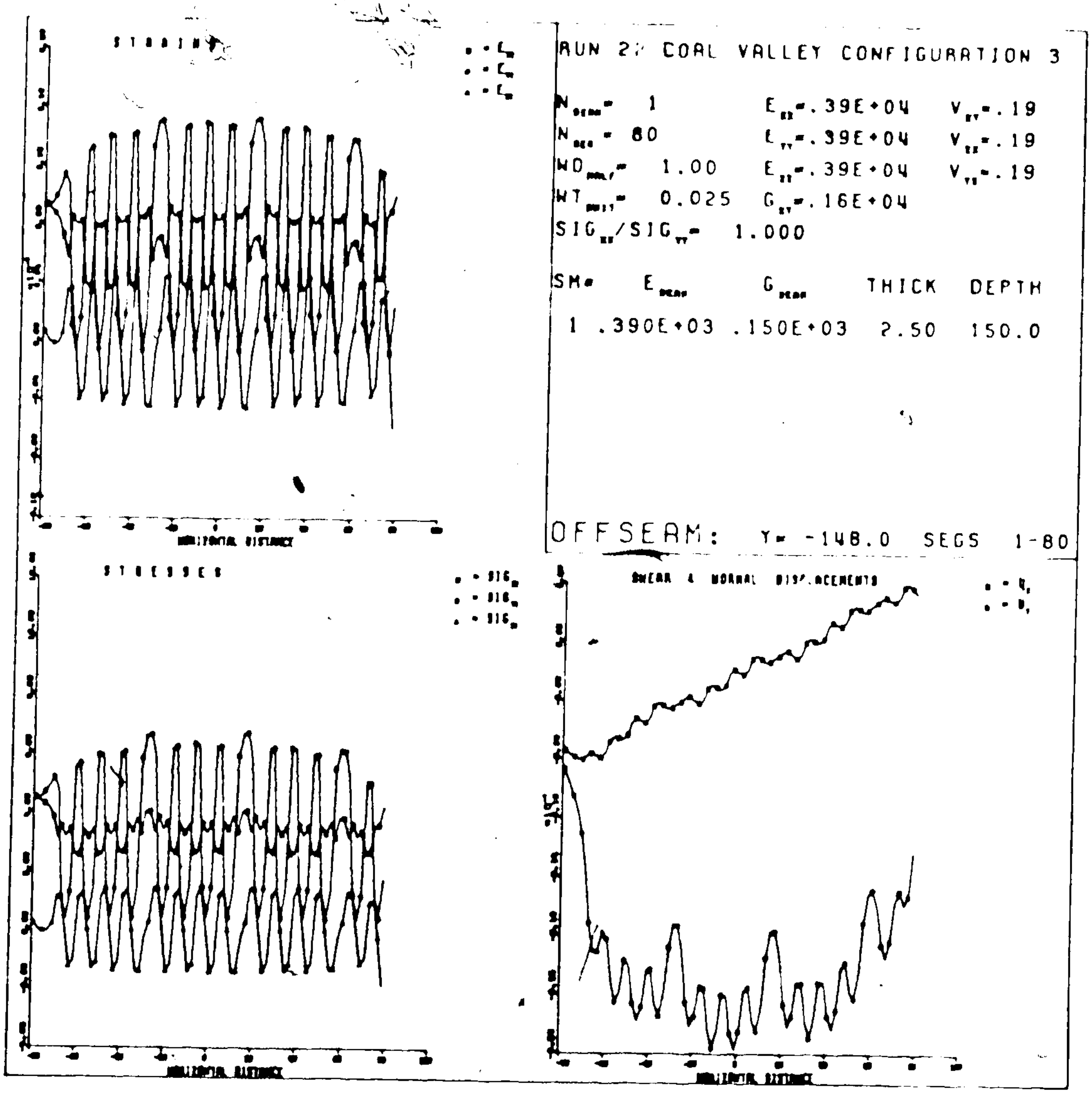

```
RUN 2[illegible] COAL VALLEY CONFIGURATION 3

N_SEAM=  1          E_XX=.39E+04   V_XY=.19
N_SEG = 80          E_YY=.39E+04   V_XZ=.19
WD_MAX=   1.00      E_ZZ=.39E+04   V_YZ=.19
WT_UNIT=  0.025     G_XY=.16E+04
SIG_XX/SIG_YY=  1.000

SM=    E_SEAM      G_SEAM     THICK  DEPTH

 1 .390E+03 .150E+03  2.50  150.0

OFFSEAM:  Y= -148.0  SEGS  1-80
```

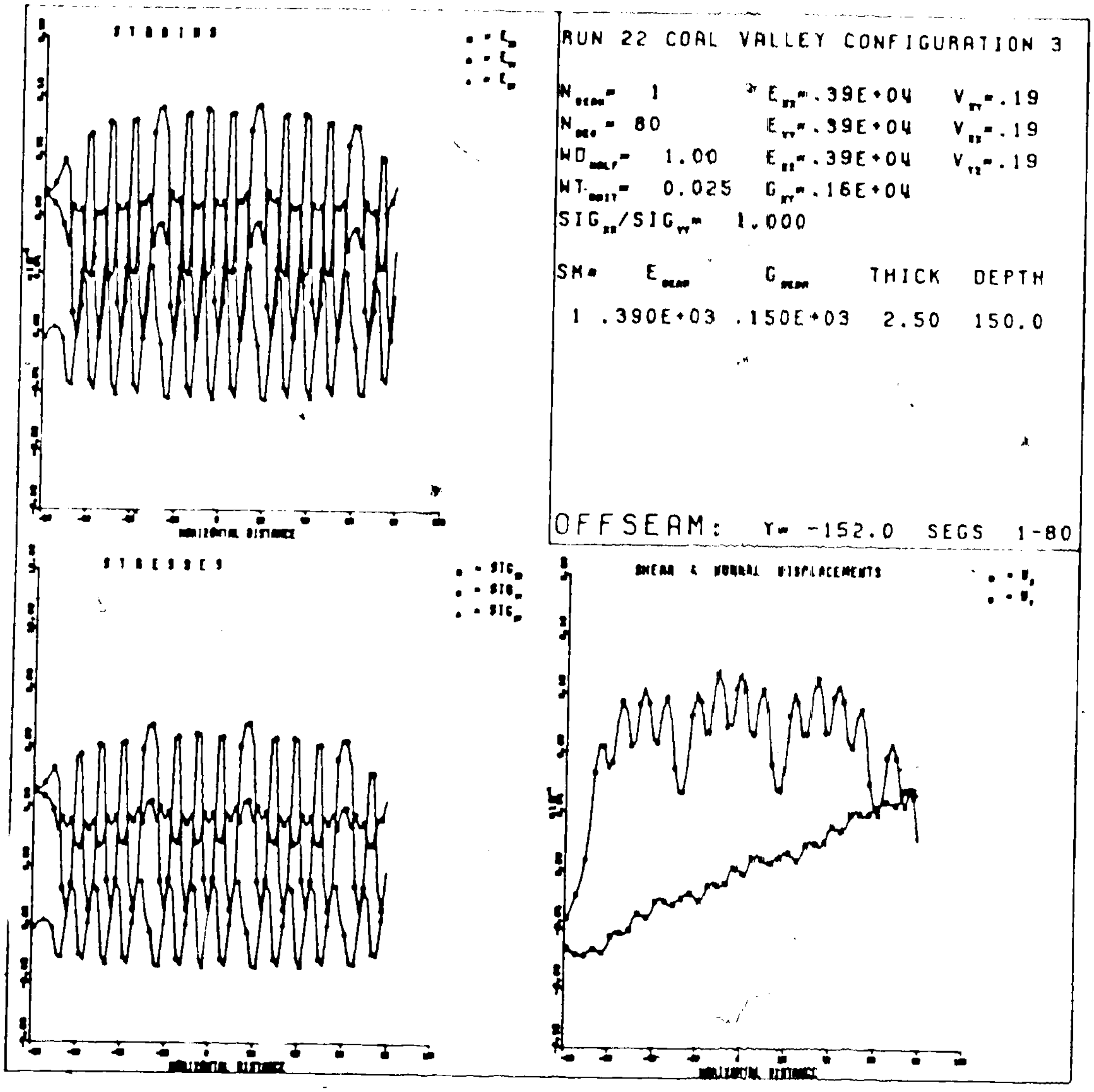

RUN 22 COAL VALLEY CONFIGURATION 3

N_{SEAM}= 1 E_{XX}=.39E+04 V_{XY}=.19
N_{SEG}= 80 E_{YY}=.39E+04 V_{XZ}=.19
WD_{MULT}= 1.00 E_{ZZ}=.39E+04 V_{YZ}=.19
WT_{UNIT}= 0.025 G_{XY}=.16E+04
SIG_{XX}/SIG_{YY}= 1.000

SM=	E_{SEAM}	G_{SEAM}	THICK	DEPTH
1	.390E+03	.150E+03	2.50	150.0

OFFSEAM: Y= -152.0 SEGS 1-80

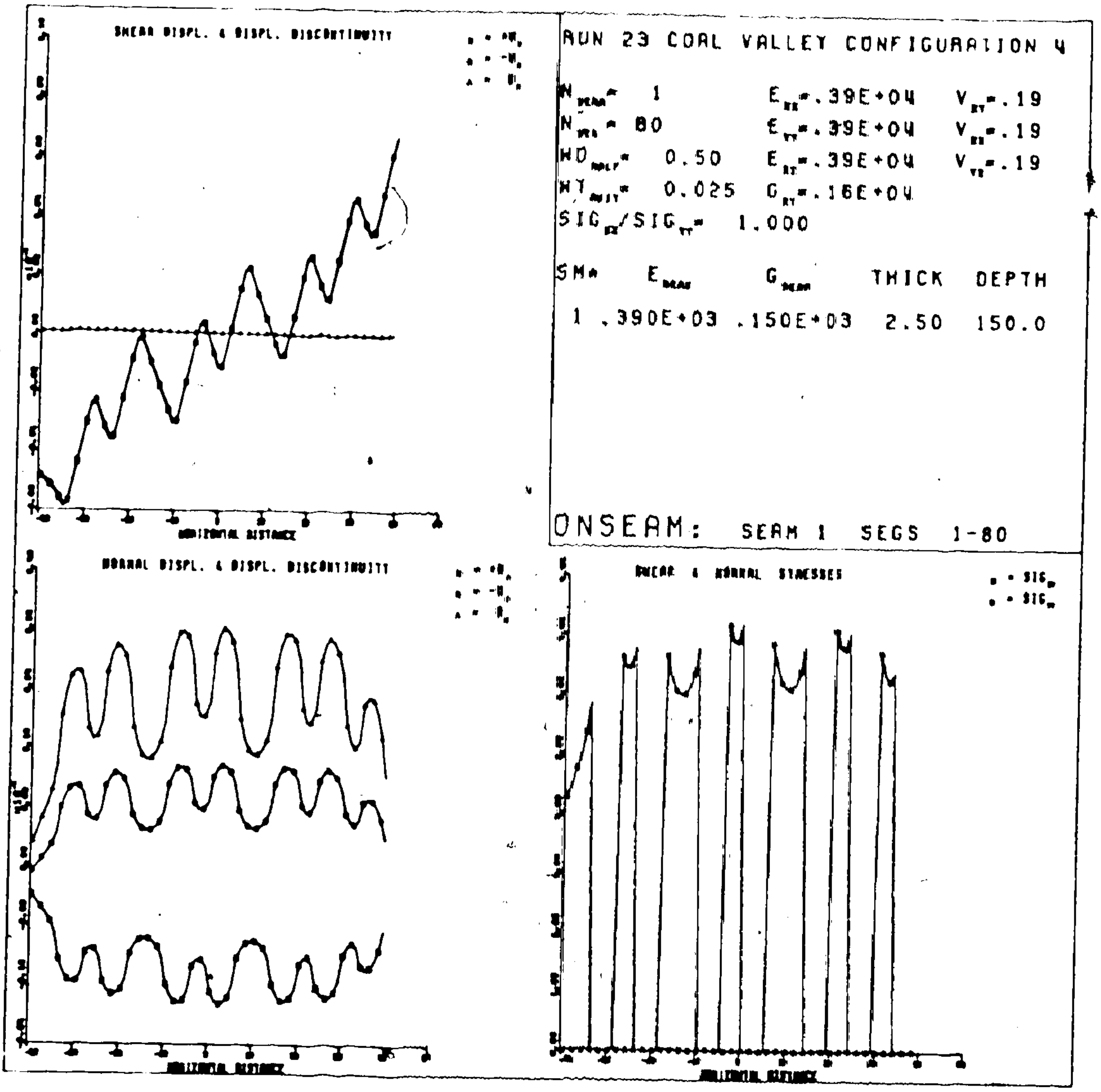

RUN 23 COAL VALLEY CONFIGURATION 4

N_{SEAM}= 1 E_{XX}=.39E+04 V_{XY}=.19
N_{SEG}= 80 E_{YY}=.39E+04 V_{XZ}=.19
WD_{ANLY}= 0.50 E_{ZZ}=.39E+04 V_{YZ}=.19
WT_{ANLY}= 0.025 G_{XY}=.16E+04
SIG_{XX}/SIG_{YY}= 1.000

SM#	E_{SEAM}	G_{SEAM}	THICK	DEPTH
1	.390E+03	.150E+03	2.50	150.0

ONSEAM: SEAM 1 SEGS 1-80

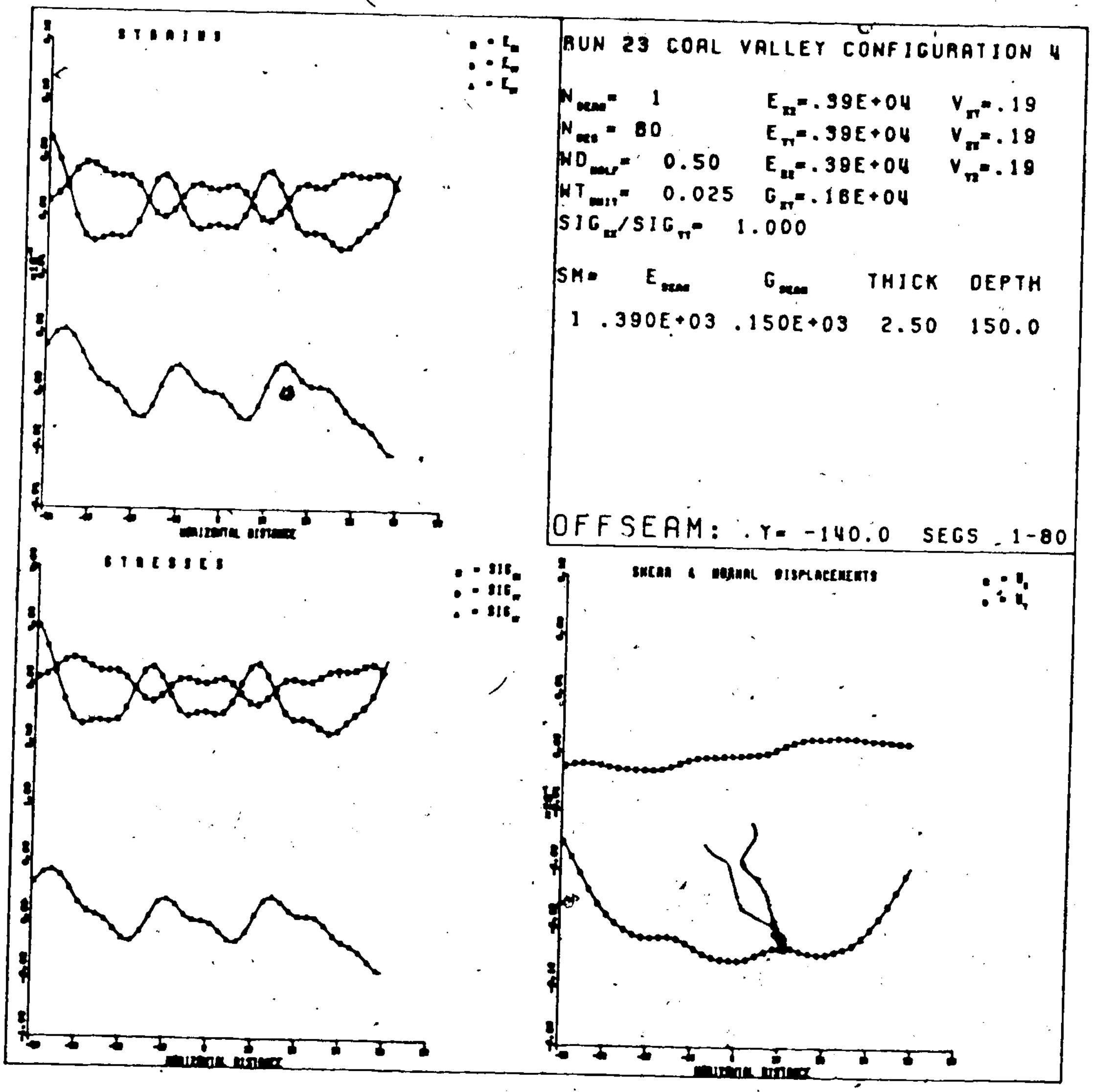

```
RUN 23 COAL VALLEY CONFIGURATION 4

N_SEAM=  1          E_XX=.39E+04   V_XY=.19
N_SEG = 80          E_YY=.39E+04   V_ZX=.19
WD_HALF=  0.50      E_ZZ=.39E+04   V_YZ=.19
WT_UNIT=  0.025     G_XY=.18E+04
SIG_XX/SIG_YY=  1.000

SM=    E_SEAM      G_SEAM      THICK  DEPTH
 1  .390E+03  .150E+03   2.50   150.0

OFFSEAM:  .Y= -140.0  SEGS  1-80
```

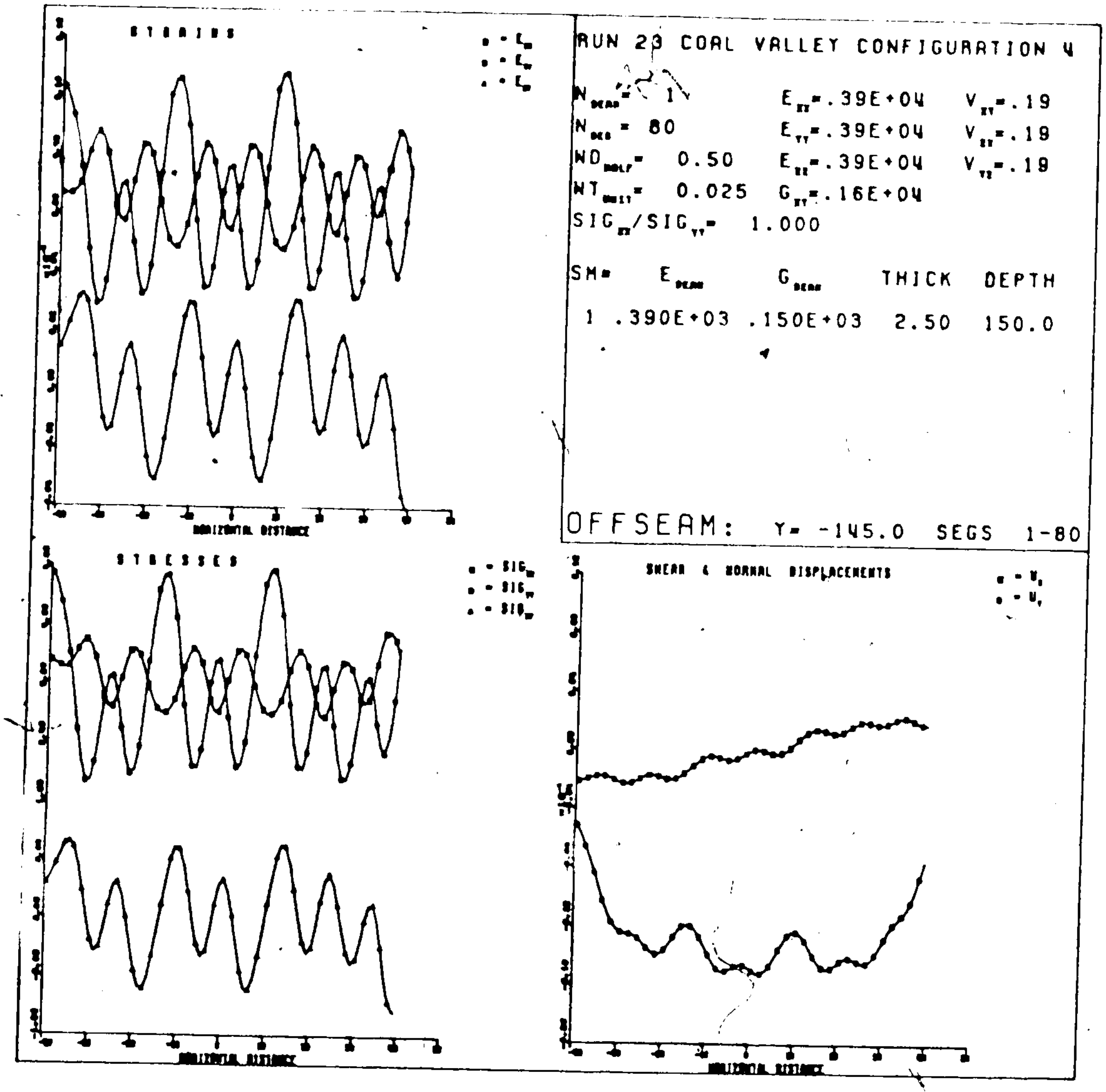

RUN 23 COAL VALLEY CONFIGURATION 4

N_{SEAM}= 1 E_{XX}=.39E+04 V_{XY}=.19

N_{SEG}= 80 E_{YY}=.39E+04 V_{XZ}=.19

WD_{HALF}= 0.50 E_{ZZ}=.39E+04 V_{YZ}=.19

WT_{UNIT}= 0.025 G_{XY}=.16E+04

SIG_{XX}/SIG_{YY}= 1.000

SM=	E_{SEAM}	G_{SEAM}	THICK	DEPTH
1	.390E+03	.150E+03	2.50	150.0

OFFSEAM: Y= -145.0 SEGS 1-80

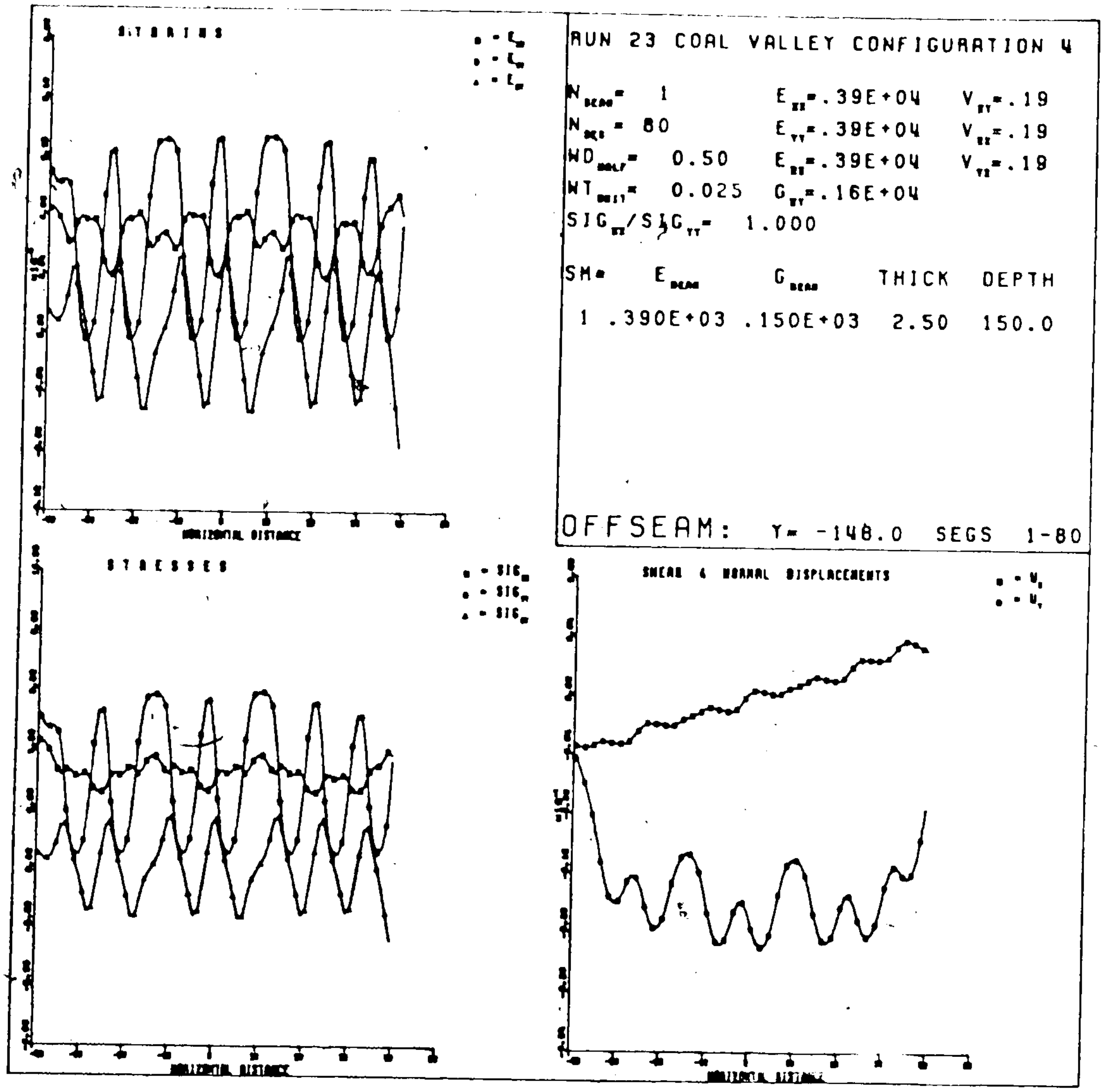

RUN 23 COAL VALLEY CONFIGURATION 4

N_{BEAM}= 1 E_{XX}=.39E+04 V_{XY}=.19
N_{SEG}= 80 E_{YY}=.39E+04 V_{XZ}=.19
WD_{HALF}= 0.50 E_{ZZ}=.39E+04 V_{YZ}=.19
WT_{UNIT}= 0.025 G_{XY}=.16E+04
SIG_{XX}/SIG_{YY}= 1.000

SM=	E_{BEAM}	G_{BEAM}	THICK	DEPTH
1	.390E+03	.150E+03	2.50	150.0

OFFSEAM: Y= -148.0 SEGS 1-80

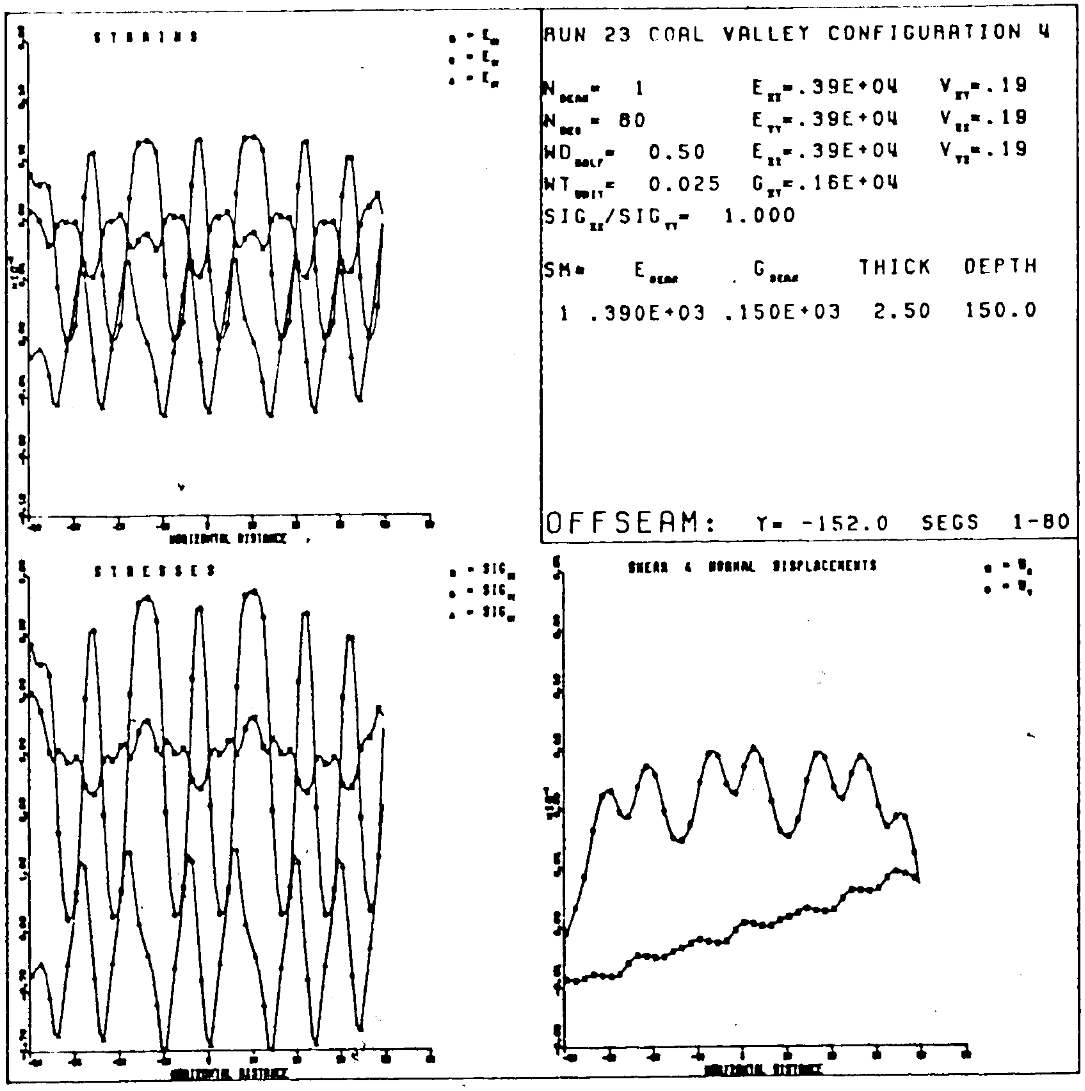

```
RUN 23 COAL VALLEY CONFIGURATION 4

NSEAM=  1          EXX=.39E+04   VXY=.19
NSEG = 80          EYY=.39E+04   VXZ=.19
WDBOLT=  0.50      EZZ=.39E+04   VYZ=.19
WTUNIT=  0.025     GXY=.16E+04
SIGXX/SIGYY=  1.000

SM=    ESEAM     GSEAM     THICK   DEPTH

 1 .390E+03 .150E+03   2.50    150.0

OFFSEAM:  Y= -152.0  SEGS  1-80
```